

# **Reliability of Reinforced Concrete Shear Resistance**

U.A. Huber

13169289



Thesis presented in partial fulfilment of  
the requirements for the degree of  
Master of Science in Engineering (Civil) at the  
University of Stellenbosch

Study Leader: Prof JV Retief

December 2005

## Declaration

I, the undersigned, hereby declare that the work contained in this thesis is my own original work and that I have not previously in its entirety or in part submitted it at any university for a degree.

# Abstract

The lack of a simple rational mechanical model for the shear resistance behaviour of structural concrete members results in the use of simplified empirical methods in codified shear design methods with a limited range of applicability. This may lead on the one hand to insufficient reliability for members on the boundary of the range of applicability and on the other hand to over-conservative designs. Comparison of the provision for shear resistance design of the South African code of practice for the design of concrete structures SANS 10100: 2003 with other related codes shows differences in the design variables taken into account and procedures specified to calculate shear resistance.

The thesis describes a systematic evaluation of the reliability performance of the shear performance of reinforced concrete sections subjected to shear only, and in combination with flexural moments, designed with SANS 10100: 2003. Both sections with and without provision for shear reinforcement are considered. A representative range of parametric conditions are considered in the evaluation. Punching shear is not considered in the present review.

Shear design as specified by SANS 10100 is compared to the provisions of the closely related British code for the structural use of concrete BS 8110, Eurocode 2 for the design of concrete structures EN 1992 and the American bridge design code AASHTO LRFD.

The reliability performance of the shear design method for beams of SANS is considered in terms of a probabilistic shear resistance model, uncertainties in the basic variables such as material properties, geometry and modelling uncertainty. Modelling uncertainty is determined by comparing predicted values with published experimental results.

**Keywords:** structural concrete; shear resistance; shear design; reliability; design codes; code comparison

# Opsomming

Die tekortkoming van eenvoudige rasionele modelle vir skuif gedrag van strukturele gewapende beton lei tot die gebruik van vereenvoudigde empiriese metodes in gekodifiseerde skuif ontwerp met 'n beperkte omvang van gebruik. Dit mag lei tot onvoeldoende betroubaarheid vir ontwerp situasies, maar ook tot oorkonserwatieve ontwerpe. Vergelyking van voorsienings vir skuif weerstand ontwerp in die SANS beton kode, SANS 10100: 2003 en ander verwante kodes toon verskille in ontwerp veranderings en metodes aan vir die berekening van skuifweerstand.

Hierdie tesis beskryf die stelselmatige bepaling van betroubaarheids prestasie van die skuifgedrag van gewapende beton snitte ontwerp volgens SANS. Beide snitte met en sonder skuifbewapening word behandel. 'n Verteenwoordigende bestek van skuif ontwerp parameters word in ag geneem in die beoordeling van die betroubaarheid. Pons skuif word nie hier in ag geneem nie.

Skuif ontwerp soos voorgeskryf deur SANS 10100 word verlyk met die ontwerp methodes van die Britse beton kode, BS 8110, die Europese beton kode, Euronorm Eurocode 2 en die Amerikaanse brug kode AASHTO LRFD.

Die betroubaarheids prestasie van die skuif ontwerp metode vir SANS word bepaal deur middel van 'n probablistiese skuif ontwerp model. Model onsekerheid is vir die doeleindes bepaal deur vergelyking met gepubliseerde eksperimentele resultate.

**Sleutelwoorde:** strukturele beton; skuif weerstand; skuif ontwerp; betroubaarheid; ontwerp kodes; kode vergelyking

# Table of Contents

<b>Abstracts</b>	<b>i</b>
<b>Contents</b>	<b>iii</b>
<b>List of Figures</b>	<b>vii</b>
<b>List of Tables</b>	<b>x</b>
<b>List of Symbols</b>	<b>xii</b>
<b>1. Introduction</b>	<b>1</b>
<b>2. Literature Study: Shear Resistance Theory of Reinforced concrete</b>	<b>5</b>
2.1 Shear Strength of Members without Shear Reinforcement	5
2.1.1 Mechanisms of Shear transfer	6
2.1.2 Shear failure in Members without Shear Reinforcement	9
2.1.3 Factors affecting Shear Strength	13
2.1.4 Historical Development of Shear Design Procedures for Members without Shear Reinforcement	14
2.1.5 Application to Codes	20
2.1.5.1 SANS 10100-1: 2003	
2.1.5.2 EN 1992 Eurocode 2: 2003	21
2.1.5.3 AASHTO LRFD: 2000 and CSA-23.3:1994	22
2.1.5.4 Comparing SANS, Eurocode and AASHTO	24
2.2 Shear Strength of Members with Shear Reinforcement	27
2.2.1 Mechanisms of Shear Transfer	27
2.2.2 Historical Approaches to the Design of Shear Reinforcement in Reinforced Concrete Members	29
2.2.2.1 The 45° Planar Truss Analogy	29
2.2.2.2 The Variable Angle Truss Model	33

2.2.2.3	The Modified Compression Field Theory	40
2.3.3	Application to Codes	47
2.3.3.1	SANS 10100-1: 2003	47
2.3.3.2	EN 1992 Eurocode 2: 2003	48
2.3.3.3	AASHTO LRFD: 2000 and CSA-23.3:1994	51
2.3.3.4	Comparing the SANS, Eurocode and AASHTO	54
<b>3.</b>	<b>Introduction to Reliability analysis of SANS10100-1:2003 and EN 1992 Eurocode: 2003 shear design procedures</b>	<b>59</b>
<b>4.</b>	<b>Determining the Model Factor for SANS 10100-1:2003, EN 1992 Eurocode 2:2003 and AASHTO LRFD 2000</b>	<b>69</b>
4.1	Members without Shear Reinforcement	69
4.1.1	The Experimental Database	70
4.1.1.1	Composition of the Database	71
4.1.1.2	Range and Distribution of Parameters from Database	72
4.1.2	Calculating the Model Factor from SDB_WithoutSR	76
4.1.3	Statistical Properties of the Model Factor	77
4.1.3.1	Basic Statistical Properties	77
4.1.3.2	Trends in the Model Factor: Correlation and Regression Analysis	79
4.1.4	Modelling the Model Factor for the Limit State Functions	84
4.2	Members with Shear Reinforcement	
4.2.1	The Experimental Database	88
4.2.1.1	Composition of the Database	88
4.2.1.2	Shear Resistance Parameters	89
4.2.1.3	Range and Distribution of Shear Parameters	90
4.2.2	Calculation of the Model Factor from SDB_WithSR	94
4.2.2.1	SANS 10100-1: 2003	95

4.2.3	Statistical Properties of the Model Factor	95
4.2.3.1	Basic Statistical Properties	95
4.2.3.2	Trends in the Model Factor: Correlation and Regression Analysis	96
4.2.4	Modelling the Model Factor for the Limit State Function	102
<b>5.</b>	<b>Reliability Analysis of the Limit State Functions for SANS 10100-1: 2003</b>	<b>105</b>
5.1	Members without Shear Reinforcement	105
5.1.1	Choosing a General Probabilistic Model for Shear	105
5.1.1.1	Limit State Equations of SANS	106
5.1.1.2	Statistical Models for Basic Variables	108
5.1.1.3	Reliability analysis of individual examples	109
5.1.1.4	Comparing the probabilistic models of SANS	112
5.1.2	Parametric study	116
5.1.2.1	Scope of the parametric study	116
5.1.2.2	Parametric Study: SANS	117
5.1.2.2.1	Results of Parametric Study	117
5.1.2.2.2	Discussion of the results	119
5.2	Members with Shear Reinforcement	121
5.2.1	Choosing a general probabilistic model for shear	121
5.2.1.1	Limit State Equations of SANS	122
5.2.1.2	Statistical Models for Basic Variables	123
5.2.1.3	Reliability Analysis of Individual Examples	125
5.2.1.4	Probabilistic model for shear resistance for SANS	128
5.2.2	Parametric study	131
5.2.2.1	Scope of the parametric study	132
5.2.2.2	Parametric Study: SANS 10100-1	138
5.2.2.2.1	Results of Parametric Study	138

5.2.2.2.2 Discussion of the results	154
5.2.3 Recommendations for improving the reliability of the SANS shear design procedure	158
<b>6. Conclusion and Recommendations</b>	<b>160</b>
6.1 Members without shear reinforcement	161
6.2 Members with shear reinforcement	162
6.3 Recommendations for further studies	163
<b>7. References</b>	<b>165</b>
<b>Appendix A - Experimental Data</b>	<b>169</b>
<b>Appendix B - Examples: Calculating shear resistance with AASHTO LRFD 2000</b>	<b>175</b>
<b>Appendix C - Example for designing reinforcement for a section in parameter study</b>	<b>186</b>

# List of Figures

## Chapter 2

Fig 2.1: Mechanisms of shear transfer in RC members without shear reinforcement (Kong & Evans, 1980)	7
Fig 2.2: Definition of the shear span to effective depth ratio, $a/d$ (Kong & Evans, 1980)	10
Fig 2.3: Types of cracking in RC beams (Kong & Evans, 1980)	10
Fig 2.4: Variation in shear capacity with $a/d$ for rectangular beams (ASCE-ACI Committee 426, 1973)	12
Fig 2.5: Shear Stress Distribution of cracked RC beam	15
Fig 2.6: Internal forces in RC beam without shear reinforcement (Kani, 1964)	17
Fig 2.7: Shear failure mechanism in RC beam without shear reinforcement (Kani, 1964)	18
Fig 2.8: Relative beam strength, $M_{cr}/M_{fl}$ versus $a/d$ and $\rho$ (Kani, 1966)	18
Fig 2.9: Influence of longitudinal reinforcement on spacing of cracks. (ASCE-ACI Committee on Shear and Torsion, 1998)	23
Fig 2.10: AASHTOO LRFD: 2000 $\theta$ chart for members without shear reinforcement	25
Fig 2.11: AASHTOO LRFD: 2000 $\beta$ chart for members without shear reinforcement	25
Fig 2.12: Planar truss analogy of beam with shear reinforcement (Hsu, 1993)	30
Fig 2.13: Relationship for shear stress ratio vs. reinforcement ratios for the balanced condition (Hsu, 1993)	37
Fig 2.14: Average Stress and strain conditions in a reinforced concrete element (Vecchio & Collins, 1986)	42
Fig 2.15: Stress strain relationships for cracked concrete (Collins et. al., 1996)	44
Fig 2.16: Determination of strain $\epsilon_x$ in non pre-stressed beam (Collins et. al., 1999)	52
Fig 2.17: AASHTO LRFD 2000 $\theta$ Chart for members with shear reinforcement	53
Fig 2.18: AASHTO LRFD 2000 $\beta$ Chart for members with shear reinforcement	53
Fig 2.19: Comparing SANS10100-1 and EN 1992 Eurocode 2	55

Fig 2.20: Applied shear stress vs. amount of shear reinforcement compared for SANS, Eurocode and AASHTO	57
<b>Chapter 3</b>	
Fig 3.1: Probability density function of the limit state equation	59
Fig 3.2: Definition of the characteristic value	63
Fig 3.3: Failure Point of $g(X) = 0$ at $x_i$ *	66
<b>Chapter 4</b>	
Fig 4.1: Distribution of concrete compressive strength for SDB_WithoutSR	73
Fig 4.2: Distribution of aggregate size for SDB_WithoutSR	73
Fig 4.3: Distribution of shear span to depth ratio for SDB_WithoutSR	73
Fig 4.4: Distribution of web width for SDB_WithoutSR	74
Fig 4.5: Distribution of percentage longitudinal tension steel for SDB_WithoutSR	74
Fig 4.6: Distribution of measured shear stress at failure for SDB_WithoutSR	74
Fig 4.7: Distribution of effective member depth of SDB_WithoutSR	75
Fig 4.8: Linear Regression Plot: Model Factor vs. shear span to depth ratio, $a/d$	81
Fig 4.9: Linear Regression Plot for Model Factor: SDB_WithoutSR: Subset 1	83
Fig 4.10: Standardized Residual plots for SANS Model Factor linear regression function	85
Fig 4.11: Normal quantile plot for SANS $MF$	87
Fig 4.12: Distribution of concrete compressive strength for SDB_WithSR	91
Fig 4.13: Distribution of shear span to effective depth ratio for SDB_WithSR	91
Fig 4.14: Distribution of longitudinal tension steel percentage for SDB_WithSR	92
Fig 4.15: Distribution of effective member depth for SDB_WithSR	92
Fig 4.16: Distribution of web width depth for SDB_WithSR	93
Fig 4.17: Distribution of shear reinforcement for SDB_WithSR	93
Fig 4.18: Distribution of measured shear stress at failure for SDB_WithSR	93
Fig 4.19: Linear Regression SANS $MF$ vs. $a/d$ for SDB_WithSR: Complete Database	98
Fig 4.20: Linear Regression SANS $MF$ vs. $a/d$ for SDB_WithSR: Subset 1	99
Fig 4.21: Linear Regression SANS $MF$ vs. $v_s$ for SDB_WithSR: Subset 1	100

Fig 4.22: Scatter plot of concrete contribution vs. shear resistance of SANS for Subset 1	101
Fig 4.23: Residual plots for SANS model factor	103
Fig 4.24: Normal Quantile plot for SANS $MF$	104

## Chapter 5

Fig 5.1: Probabilistic shear resistance model of SANS, no shear reinforcement	115
Fig 5.2: Results from parametric study for members without shear reinforcement	119
Fig 5.3: Probabilistic shear resistance model of SANS	130
Fig 5.4: Representative section for design of shear reinforcement	134
Fig 5.5: Schematic of process for determining probable design situations	136
Fig 5.6: Beams from parameter study with lowest and highest $\beta$ for SANS	141
Fig 5.7: Beam configurations for illustration of effect of concrete contribution on reliability	146
Fig 5.8: SANS Reliability Index vs. shear reinforcement (Set 1)	148
Fig 5.9: SANS Reliability Index vs. percentage longitudinal tension reinforcement (Set 1)	148
Fig 5.10: SANS Reliability vs. amount of shear reinforcement of Set 1 and Set 6 compared	151
Fig 5.11: SANS Reliability vs. amount of longitudinal reinforcement of Set 1 and Set 6 compared	151
Fig 5.12: SANS Reliability vs. amount of concrete contribution of Set 1 and Set 6 compared	152
Fig 5.13: SANS model factor vs. amount of concrete contribution of Set 1 and Set 6 compared	153
Fig 5.14: Band of reliability for SANS for probable design situations	155
Fig 5.15: Effect on reliability of SANS through adjustment of partial material factors	159

# List of Tables

## Chapter 2

Table 2.1: Limits on $\theta$ specified by CEB- <i>fip</i> Model Code and Eurocode	39
--	----

## Chapter 4

Table 4.1: Results of model factors determined from SDB_WithoutSR	78
Table 4.2: Significance of the correlation factor	81
Table 4.3: Linear Regression data for SDB_WithoutSR: <u>Subset 1</u>	82
Table 4.4: Regression and correlation data for members SDB_WithoutSR: <u>Subset 1</u>	82
Table 4.5: Composition of the experimental database for members with shear reinforcement	89
Table 4.6: Results of model factors determined from SDB_WithSR	95
Table 4.7: Correlation data for members SDB_WithSR	96
Table 4.8: Linear Regression data for SDB_WithSR: Subset 1	97

## Chapter 5

Table 5.1: Statistical properties of member dimensions and steel area	108
Table 5.2: Probability moments of basic variables	111
Table 5.3: FOSM Iteration 1 for test case: SANS	111
Table 5.4: FOSM Final Iteration for test case: SANS	112
Table 5.5: General probabilistic model for shear resistance for SANS and Eurocode	114
Table 5.6: Allowable range of design parameters for SANS	116
Table 5.7: Reliability for SANS for various beam configurations with $a/d = 3.0$	118
Table 5.8: Statistical properties of shear steel area and stirrup spacing	124
Table 5.9: Statistical properties of the materials	124
Table 5.10: Design specifications and shear design resistance of test case	125
Table 5.11: Probability moments of basic variables	126
Table 5.12: FOSM Iteration 1 for Test Case: SANS	126

Table 5.13: FOSM Final Iteration for Test Case: SANS	127
Table 5.14: Results of general probabilistic model for SANS	129
Table 5.15: Allowable range of design parameters for SANS	133
Table 5.16: Example design of reinforcement for beams of parameter study	137
Table 5.17: Bias of $MF_{SANS}$ for various configurations of $\rho$ , $v_s$ and $a/d$	139
Table 5.18: FOSM first iteration 1 for Beam A for SANS	141
Table 5.19: FOSM final iteration for Beam A for SANS	142
Table 5.20: FOSM first iteration for Beam A for SANS	142
Table 5.21: FOSM final iteration for Beam A for SANS	143
Table 5.22: Contribution of basic variables to overall bias of performance function	143
Table 5.23: Effect of concrete contribution and bias in $MF$ on reliability of SANS	145

# Chapter 1

## Introduction

Design procedures proposed by national design codes should be safe, conceptually correct, simple to apply and economical in their application with regard to time and money. The most effective design proposals are those that are based on simple conceptual models rather than empirical formulations, as they provide the designer with a rational understanding of the design problem.

Traditionally shear design proposals of reinforced concrete members all over the world have been based on empirical formulations. The complex mechanisms that contribute to the shear resistance of cracked reinforced concrete members were not fully understood resulting in the use of empirical methods. The American Concrete Institute in a state-of-the-art report by the ASCE-ACI Committee 426 of 1973 on the shear strength of reinforced concrete members, expressed the aim for the future that “the design regulations for shear strength can be integrated, simplified, and given physical significance so that designers can approach unusual design problems in a rational manner”. (The Shear Strength of Reinforced Concrete Members by ASCE-ACI Task Committee 426 on Shear and Diagonal Tension, 1973). The report gives a complete overview of theories and practical aspects concerning shear in reinforced concrete that served as a benchmark for many international design codes. Since 1973, much work has been done in developing rational theories that describe the shear behaviour of reinforced concrete, as outlined in the ASCE-ACI Committee 445 Report shear and torsion of 1998. The Canadian concrete design code and the American bridge design code, have answered the call of ASCE – ACI Committee 426 for a unified rational shear design theory by applying one of the shear theories developed since 1973, the modified compression field theory, to their shear design procedures.

The South African concrete design code, SANS 10100-1: 2003 still employs empirical methods for members without shear reinforcement, and the traditional truss approach to design of members with shear reinforcement. The empiricism of SANS limits the range of applicability of the code. For example the SANS shear design procedure originally intended for members made from normal strength concrete, with a cube strength of up to 40 MPa. However, advances in concrete technology have led to the use of high strength concretes with cube strength up to 100 MPa. Higher strength

concretes are more brittle and therefore lead to smoother crack surfaces which results in reduced shear capacity.

The European concrete design code, EN 1992 Eurocode 2, provides shear design procedures that are very similar to those of SANS. For members with shear reinforcement a variation on the traditional truss approach is applied in design.

### **Objectives of the thesis**

The general objective of the thesis is to compare the different approaches to shear design followed by the South African design code, SANS 10100-1:2003, the European code, EN 1992 Eurocode 2 and the American bridge design code, AASHTO LRFD 2000, in order to determine the advantages and disadvantages of the different codes. The current South African code is based on the British code, BS 8110.

The shear design procedure for beams of SANS 10100-1: 2003 was compared to experimental data in this thesis in order to derive a general probabilistic model for shear on the basis of which a reliability analysis of SANS was carried out.

The primary objectives of this thesis are:

- To determine the level of reliability of the SANS shear design procedure over a range of probable design situations.
- To determine design situations where SANS does not achieve the minimum level of reliability and is therefore unsafe.
- To determine whether the level of reliability is consistent over a range of probable design situations.

## **Scope of the Thesis**

The subject of shear design of reinforced concrete members can be divided into two broad categories, known as B regions and D regions, (ASCE-ACI Committee 445 Report, 1998), where B stands for beam or Bernoulli and D stands for discontinuity or disturbed. Strains have a non-linear distribution in D-regions and a linear distribution in B regions. B regions include normally reinforced beams, pre-stressed beams, columns and slabs of constant cross section. D regions include regions with discontinuities in cross section, such as beam to column joints, flat slab to column connections (punching shear), corbels and footings. The shear design of D-regions is usually complex and the region where shear failures are most likely.

This thesis is concerned with B regions only. Design of B-regions for shear is the dominant design situation in practice, compared to design of D-regions and can be reasonably standardized for code design purposes. Moreover the study of B-regions gives insight into the shear resistance mechanisms of RC members. The design of D-regions is more advanced and the determination of shear reliability for such cases is considered to be a topic for future study.

The shear resistance of normally reinforced members made from normal strength concretes is investigated, as these represent the most basic and common design situation in practice. The thesis is further divided into two broad categories:

- Members with shear reinforcement
- Members without shear reinforcement

## **Structure of the thesis**

Chapter 2 provides a summary of shear theory on reinforced concrete members and the design procedures of SANS, Eurocode and AASHTO. The codes are also compared with each other. Chapter 3 deals with general reliability concepts that are required for determining the level of reliability of the SANS shear design procedure for beams. In Chapter 4 SANS is compared to experimental data and the statistical properties of the model factor for SANS is derived. Chapter 5 reports the results of the

reliability analysis for members without and with shear reinforcement, respectively. Chapter 6 gives the conclusions of this thesis.

#### **Note on references to codes**

Whenever reference is made to the South African concrete design code, SANS 10100-1:2003, it is simply referred to as "SANS". The European code, Euronorm 1992 Eurocode 2: 2003 is referred to as "Eurocode" and the American bridge design code, AASTHO LRFD 2000 is referred to as "AASTHO". Graphical representations of Eurocode are referenced as "EN".

# Chapter 2

## Literature Study: Shear Resistance Theory of Reinforced concrete

The literature study is divided into two sections, section 2.1, which is concerned with the shear resistance of members without shear reinforcement, and section 2.2 concerned with members *with* shear reinforcement. The literature study focuses on shear of normally reinforced concrete beams and slabs. The study of shear in disturbed regions, punching shear and shear in pre-stressed members is not covered. A number of shear theories have been developed over the years, but focus is placed on the main approaches which have been applied in major international design codes.

### 2.1 Members without shear reinforcement

Beams without shear reinforcement are not commonly used in design practice. Nonetheless such members are allowed in international design codes under certain conditions. SANS, Eurocode and AASHTO allow reinforced concrete beams to contain no shear reinforcement only if the shear stress applied to the beam is half of the shear resistance of the beam. This rule could be applied in a design situation where a very large beam is required, but the designer wishes to save on shear reinforcing steel. The cross section of the beam could be increased to comply with this rule so that no shear reinforcement would be required. Slabs and footings are other examples of members without shear reinforcement. Neither SANS nor Eurocode require slabs to be supplied with minimum amount of stirrups. In practice designers avoid slabs that require shear reinforcement, for reasons of economy, simply by thickening the slab if shear reinforcement is required. Typically a slab or footing would not fail in a “beam shear” failure mode, but rather a punching shear failure mode. The focus of this thesis is on beam shear failures.

Extensive studies on reinforced concrete beams without shear reinforcement were carried out in Germany (Leonhardt, 1962) and North America (Kani, 1966) to determine the factors that influence the shear resistance of beams. The effect on shear strength was studied by varying a limited set of

parameters thought to affect shear strength. Shear reinforcement was not included in these parameters, for the time being, in order to limit the range of the study. At the time it was thought that beams without shear reinforcement were generally less safe than those with shear reinforcement. The studies yielded insight on the mechanisms that govern shear strength in reinforced concrete beams. These will be discussed shortly in the following section.

### 2.1.1 Mechanisms of shear transfer

Beams are relatively slender members, therefore the shear stress state is a two dimensional situation. There are seven main types of shear transfer mechanisms that contribute to the shear strength of a beam. These are

- (a) Shear stress in uncracked flexural compression zone of the concrete
- (b) Interface shear transfer
- (c) Dowel action
- (d) Arch action
- (e) Shear reinforcement
- (f) Residual tensile stresses

The first five of these mechanisms have been well known for quite some time and have been reported in the ASCE-ACI Task Committee 426 on Shear and Diagonal Tension of 1973. The residual tensile stress mechanism is a more recent discovery and is reported in the Task Committee's report of 1998.

In Figure 2.1 the forces contributing to the shear resistance of a beam at the location of a diagonal tension crack, are shown.  $V_{cz}$  is the shear force carried by the uncracked concrete in the flexural compression zone,  $V_d$  is a dowel force that develops where the longitudinal tension reinforcement crosses the diagonal tension cracks and  $V_{ay}$  is the vertical component of the frictional force that develops along the crack interface.

The total shear resistance is comprised of the sum of these components:

$$V_R = V_{av} + V_{cz} + V_d \quad [2.1]$$

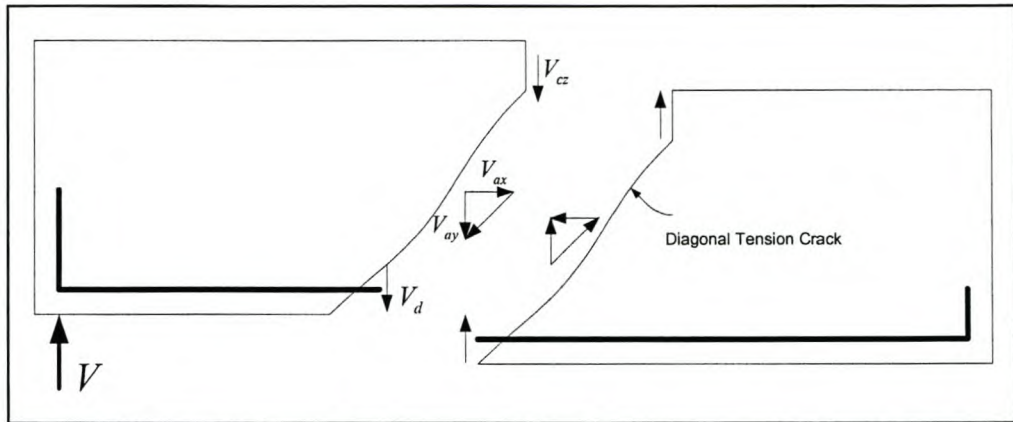


**Figure 2.1: Mechanisms of shear transfer in RC members without shear reinforcement  
(Kong & Evans, 1980)**

**(a) Shear stresses in uncracked concrete,  $V_{cz}$**

Shear stresses in uncracked concrete interact with tensile and compressive forces to form principal tensile and compressive stresses. Principal compressive stresses form at  $45^\circ$  in uncracked concrete. The compression zone is relatively small in slender members; therefore  $V_{cz}$  contributes only a small part to the total shear resistance. In stocky members where the compression zone is deep  $V_{cz}$  becomes more significant.

**(b) Interface shear transfer (or aggregate interlock)**

A diagonal tensile crack forms when the principal tensile stress in the concrete web of the beam exceeds the tensile capacity of the concrete. Shear forces are transferred along the crack by interface shear transfer. Aggregate particles protruding from the diagonal tension crack provides “aggregate interlock”, the vertical component of which contributes to shear resistance. In high strength concretes and in concretes made with light weight aggregates the diagonal tension crack breaks through the aggregate, and shear transfer is then due to a frictional force instead of aggregate interlock, hence the term “interface shear transfer” is preferred in shear literature. However aggregate interlock has a higher shearing capacity than crack friction. The capacity of these two mechanisms depends on the width of the crack, crack slip, aggregate size and the stresses applied to

the crack. Interface shear transfer is the controlling shear mechanism in reinforced members containing no shear reinforcement.

**(c) Dowel action**

If a longitudinal reinforcing bar crosses a diagonal tension crack a dowel force arises in the bar. In addition to this the bar resists the widening of the crack under bending, giving rise to bond stresses along the length of the bar, which may lead to a loss of bond between the bar and the surrounding concrete. When this bond is broken dowel action can no longer carry part of the shear force. In members without shear reinforcement the bond is limited by the tensile strength of the concrete around the bar. As a result of bond loss, dowel action is usually insignificant in such beams. If the longitudinal reinforcement exists in several layers then the splitting is less likely to occur and dowel force may contribute a greater deal to the overall shear resistance.

**(d) Arch action**

In relatively deep beams with short spans, the beam may behave like an arch. Rather than behaving like beams by carrying the applied load through bending and shear, such beams act more like trusses. In such beams the applied load is close to the support and a large part of the load is transferred directly to the support in compression. A concrete “compression strut” forms between the applied load and the support, hence the arch behaviour. The load is therefore transferred by a combination of beam and truss action. A horizontal reaction is required at the support to withstand the horizontal component of the thrust in the concrete strut. This can be provided by anchoring the longitudinal tension reinforcement by means of a bent up end bar. Anchorage failure may be the controlling failure mechanism in such beams, instead of shear failure. Arch action is not a shear transfer mechanism, but beams where this is the dominant load transfer mechanism usually have a higher shear resistance than similar beams which are more slender.

**(e) Residual tensile forces**

Diagonal cracks do not form a clean break. At locations along the crack small uncracked pieces of concrete may transmit tensile forces across the crack, similar to uncracked concrete.

This mechanism is significant in shallow members where crack widths are very small.

The ASCE-ACI Task Committee 426 report lists some numbers on the relative importance of the shear resistance mechanisms in concrete, obtained from experiments on rectangular members without shear reinforcement, near failure load. Percentages are as follows:

20 - 40% Compression zone shear

15 – 20% Dowel Action

25 – 50% Interface shear transfer

At the time the residual tensile stress mechanism was not known, but this component is accounted for in the 25 – 50% interface shear transfer as the two mechanisms are closely related. The dowel action and interface shear transfer mechanism are only activated after initial cracking has occurred. Interface shear transfer is the governing shear resistance mechanism in members without shear reinforcement.

### **2.1.2 Shear failure in members without shear reinforcement**

Beams that fail in shear display some form of distinct diagonal crack that leads to the collapse of the beam. In the 1960's the Canadian researcher Kani defined a shear failure as a failure where a diagonal tension crack caused the failure of a beam, calling it a *diagonal tension failure* (Kani, 1966).

In his study of beams without shear reinforcement Kani set out to identify the factors that affect shear strength of reinforced concrete beams. He found that failure mechanism of a beam is strongly dependent on the shear span to depth ratio,  $a/d$  as defined in figure 2.2. For a simply supported beam loaded with a point load the shear span is the distance between the reactions at the support to applied load. This corresponds to the maximum moment to shear force ratio divided by the effective member depth ( $M/Vd$ ) at the location of the applied load. For a simply supported beam with continuous loading the maximum  $M/Vd$  ratio is not easy to define. For continuous beams with any type of loading the maximum  $M/Vd$  is usually at one of the inner supports, where shear failure is most likely to occur.

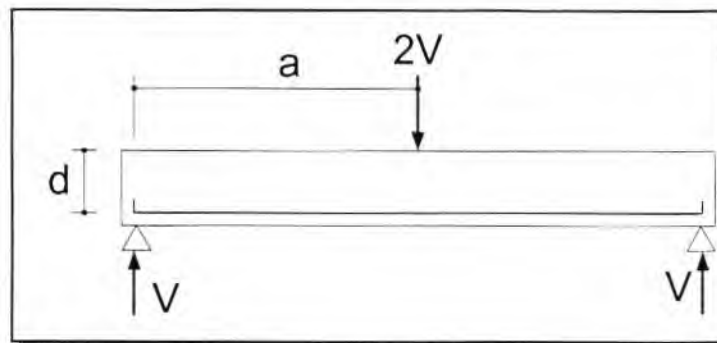


**Figure 2.2: Definition of the shear span to effective depth ratio,  $a/d$  (Kong & Evans, 1980)**

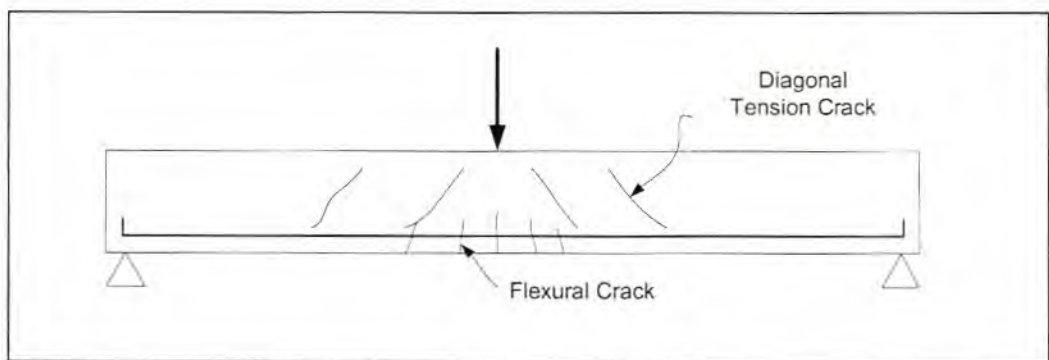


**Figure 2.3: Types of cracking in RC beams (Kong & Evans, 1980)**

A diagonal tension crack forms when the tensile stress in the web of a beam exceeds the tensile strength of the concrete. This crack is known as a web shear crack, or diagonal tension crack, as shown in figure 2.3 for a simply supported beam loaded at mid-span. The crack usually has an inclination of about  $45^\circ$ . For beams with an  $a/d$  above 2.5 the diagonal crack forms at a distance,  $d$ , from the location of the maximum moment. Vertical cracks may form in the region of maximum moment known as flexural cracks. When such a flexural crack joins up with a diagonal shear crack it is known as a flexure-shear crack, which leads to the eventual failure of the beam.

Beams with  $a/d$  ratio larger than about 6.0 usually fail in flexure. Flexural cracks form in the region of the maximum moment. The crack extends to the flexural compression zone and failure occurs when the compression zone fails by crushing.

Beams with  $a/d$  between 2.5 and 6 experience one of two mechanism of failure. For  $a/d$  relatively close to 6 a flexural crack may join up with a diagonal shear crack. With increased loading the crack propagates to the point of loading and failure occurs by splitting of the beam. This type of failure is known as *diagonal tension failure*. For beams with relatively low  $a/d$  ratios (close to 2.5) the diagonal crack will not propagate to the applied load. Instead the bond between the longitudinal reinforcement breaks and the crack propagates toward the support. If the longitudinal reinforcement is not bent up for anchorage, then the beam fails due to anchorage failure. If the reinforcement is bent up the beam behaves as an arch and failure occurs only when the increasing tension force in the longitudinal reinforcement due to increasing load destroys the concrete around the hook. This arch action may lead to a higher shear capacity in the beam. This type of failure is known as *shear tension failure*. The ultimate shear failure load is not much higher than the shear load at initial cracking.

For members with  $a/d$  lower than 2.5 but higher than 1 the diagonal crack forms independently of the flexural crack. A large part of the force is carried by arch action. Failure occurs when the crack penetrates the flexural compression zone, which eventually fails in crushing under the applied load. This failure mode is called *shear compression failure*. Due to the arch action effect failure occurs at as much as twice the cracking load.

Members with an  $a/d$  ratio lower than 1.0 behaves like deep beams. The load is almost directly transferred to the reaction by means of compression. A diagonal crack forms due to the splitting action of the compression force. The crack propagates towards the support and towards the applied load. Failure may occur in several different ways, by anchorage failure, bearing failure at the support or location of the load, or by cracking failure of the arch. Failure may occur at several times the initial cracking load.

Three failure modes have been discussed so far, *diagonal tension*, *shear tension* and *shear compression failure*. Anchorage failure is not regarded as shear failure mode but is often a consequence of shearing action in beams. Another type of failure mode may occur in beams in the form of web crushing. This type of failure mode typically only occurs in thin webbed I beams. Near the neutral axis of the beam the flexural stresses are smaller compared those in rectangular beams, due to the narrow width of the beam (most of the bending stresses are carried in the flanges). As a result the shear stresses present in the web become the principal tensile stresses, if the bending stresses are negligibly small. The principal

tensile stresses are inclined at about  $45^\circ$ . When the principal tensile stress, or shear stress exceeds the tensile capacity of the concrete, a web shear crack forms at an inclination of  $45^\circ$ . With increased load several such parallel cracks form moving toward the support. The concrete isolated between two such cracks forms a compression strut and failure can occur if the compression strength of these struts is exceeded. This is known as *web-crushing* failure.

Most design codes base their shear design provisions on beams with  $a/d$  larger than 2.5, i.e. for beams that fail in diagonal tension. If these provisions are applied to beams with an  $a/d$  between 1.0 and 2.5 they will give very conservative results, because of the increased resistance due to arch action. Figure 2.4 from ASCE-ACI Task Committee 426 of 1973 shows the various shear failure mechanisms as functions of  $a/d$ .

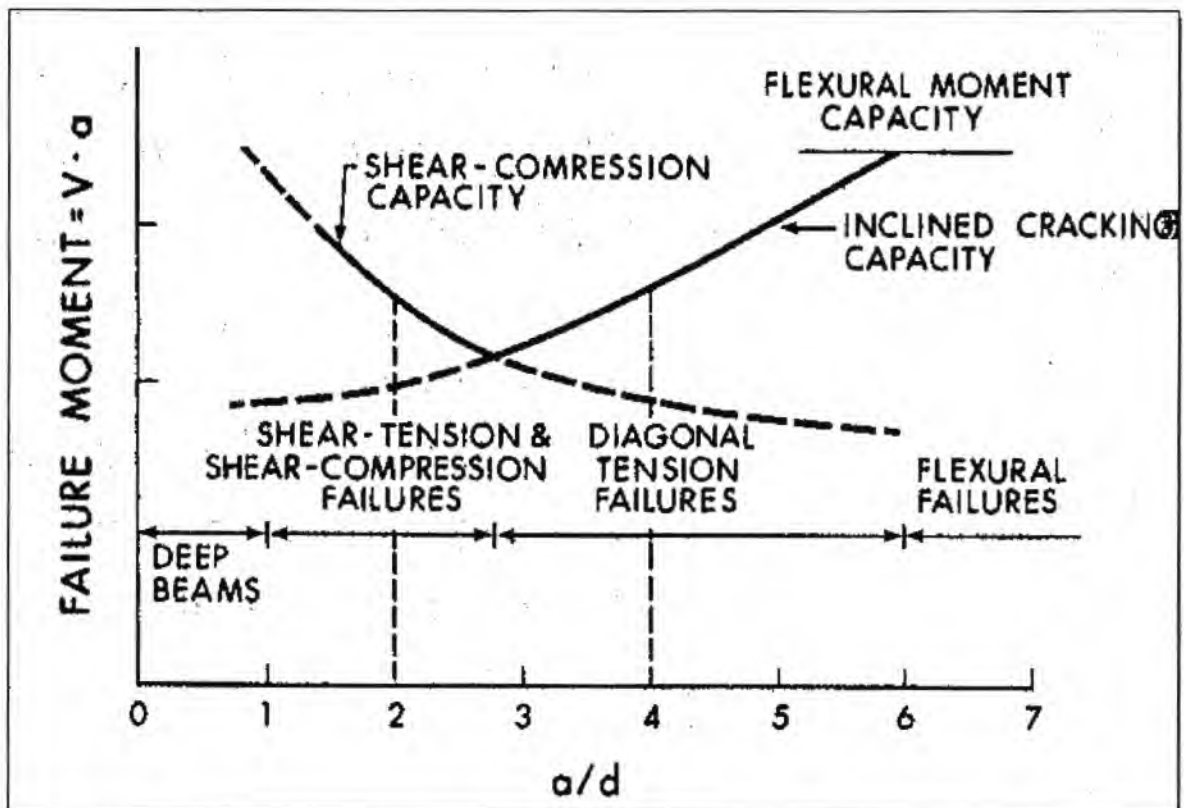


Figure 2.4: Variation in shear capacity with  $a/d$  for rectangular beams.

(ASCE-ACI Committee 426, 1973)

### 2.1.3 Factors affecting shear strength

ASCE-ACI Task Committee 426 identifies characteristics of beams that affect the shear resistance of the beam by affecting the shear transfer mechanisms. These are the shape of the cross section, size of the cross section, amount of longitudinal tension reinforcement, and maximum moment to shear ratio divided by effective member depth ( $M/Vd$ ) or alternatively the  $a/d$  ratio.

#### (a) Effect of Cross section

A beam with the same percentage of longitudinal reinforcement, breadth,  $a/d$  and concrete strength with no web reinforcement as another beam of half the depth, does not have twice the shear strength of the second beam. This is known as the size effect in shear. A deeper beam will develop wider inclined cracks than a similar but shallower beam. As a result the interface shear transfer capacity of the deeper beam is lower than that of the shallower beam, unless the aggregate used to make the concrete was increased proportionally by some factor. On the other hand a beam that has twice the breadth of another similar beam will have twice the shear strength of the smaller beam. This is due to the more or less two-dimensional stress state of the beams, so there is no size effect along the width of the beam. Beams with T and I sections under positive bending have a higher shear strength than rectangular members, due to the larger flexural compressive zone in the flange of the beam. The  $V_{cz}$  component of shear is therefore higher than in rectangular beams. Experimental data, (Placas and Regan, 1973) shows shear strengths of up to 20% higher than for T beams than for rectangular beams. The shear stress is highest in the web of the beam; therefore beams with similar T sections will display proportionally lower shear strength with decreasing web width. T and I beams may fail in web crush as already discussed. Code shear design provisions usually assume that shear resistance is only provided by the web of the beam, therefore giving conservative results for T-beams.

#### (c) Effect of Longitudinal Reinforcement

Shear strength of beams decreases with decreasing percentage of longitudinal tension reinforcement. As the amount of longitudinal tension reinforcement is reduced the dowel action,  $V_d$  is reduced. If the amount of reinforcement is decreased, while the moment is kept constant (provided that the reinforcement does not yield in flexure) the inclined cracks widen and extend further up the web of the

beam, due to the higher strains in the longitudinal reinforcement. As a result both interface shear transfer,  $V_a$  and compression zone shear capacity,  $V_{cz}$  decrease. Yield strength of the longitudinal reinforcement has no effect on the shear capacity of the beam, unless the longitudinal reinforcement has already yielded, during flexural failure. Longitudinal compression reinforcement makes no contribution to shear resistance as there are no flexural cracks in the compression zone, which lead to dowel action where the reinforcement crosses the cracks.

#### **(f) Concrete cylinder strength**

The capacity of the dowel action and the uncracked flexural compression zone increase with increasing concrete strength. The aggregate interlock capacity is dramatically reduced in high strength concrete, as the cracks tend to break through the aggregate rather than around it, as is the case for normal strength concrete.

#### **(e) Effect of $M/Vd$ or $a/d$**

The maximum  $M/Vd$  or  $a/d$  ratio is an important variable that determines not only the shear strength of a beam, but also the manner in which the beam will fail in shear; either by shear compression, diagonal tension or flexural failure. (See figure 2.4)

### **2.1.4 Historical development of shear design procedures for members without shear reinforcement**

The shear stress distribution of an elastic, homogenous rectangular beam is given by:

$$v = \frac{VQ}{Ib} \quad [2.2]$$

$Q$  is the first moment of area of the plane under consideration,  $I$  the second moment of area, and  $b$  the width of the section where the shear stress is to be determined. For a rectangular beam, the shear stress distribution will be parabolic with the maximum shear stress occurring at the location of the neutral axis. However as a result of flexural cracking the stress state in the beam is not elastic and this formula

cannot be applied. In 1902, Mörsch proposed the formulation for shear stress distribution in cracked concrete beams that is still used today:

$$v = \frac{V}{b_w z} \quad [2.3]$$

where  $b_w$  is the web width of the beam and  $z$  is the flexural lever arm. Mörsch assumed when the beam produces flexural cracks at and near the location of maximum moment the normal bending stresses are no longer transferred across the concrete in-between the cracks. As a result the concrete is in a state of pure shear stress. The principal tensile and compressive stresses are zero and the shear stresses are therefore at a maximum. Such a stress state occurs only at the position of the neutral axes (where the bending stresses are zero) in an uncracked beam. Meanwhile the uncracked compression zone is subjected to shear and compression stresses. Shear stresses increase parabolically from zero to the maximum at the location of the neutral axis. Below the neutral axis the shear stress distribution stays constant at the maximum value. Equation 2.3, the average stress distribution over the depth of the beam, is therefore a good approximation of this stress distribution. Figure 2.5 compares the shear stress distribution of a homogenous material with the true stress distribution of cracked concrete and the average distribution assumed by Mörsch. The assumption of zero bending stresses in the concrete between the flexural cracks (these look like the teeth of a comb) is a simplification.

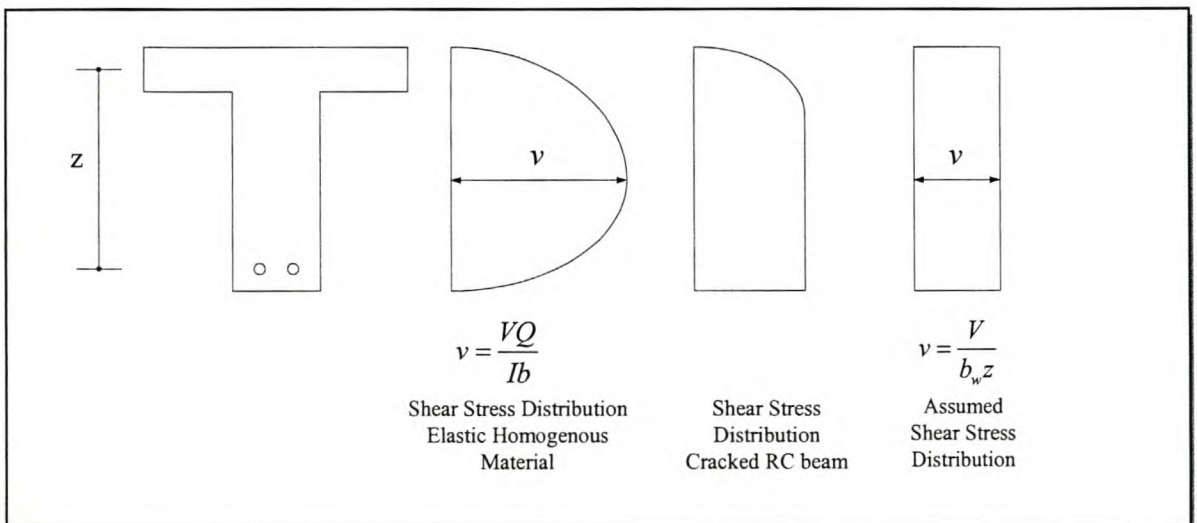


**Figure 2.5: Shear Stress Distribution of cracked RC beam**

The tension in the longitudinal reinforcement at the bottom of the beam causes these concrete “teeth” to bend. Kani (Kani, 1964) developed a model to describe the shear behaviour of beams without shear reinforcement, known as the tooth model. Kani was one of the first to develop a rational theory for shear failure in members without shear reinforcement in an attempt to answer the call of the ACI-ASCE Committee 426 on Shear and Diagonal Tension of 1962, for such a theory.

Kani (Kani, 1964) recognized that shear failure depended on a large number of different parameters, some known and some unknown. To the contrary the design procedure of the American concrete design code (ACI) of the time, which assumed shear capacity to be solely a function of the concrete strength of the RC member. At the time it was not clear what exactly comprised a shear failure. Kani noticed that all beams that did not fail in flexure displayed a diagonal tension crack and proposed that all such failures be defined as diagonal tension failures, recognizing that different diagonal tension failures existed. He carried out an extensive study investigating the effect of concrete compressive strength, percentage of longitudinal tension failure and shear span to depth ratio, recognizing that these parameters were only a few that determined the shear resistance of a beam. Kani recognized that beams without shear reinforcement were not often used in practice but felt that the study of beams without shear reinforcement was the first step in identifying the mechanisms of shear failure.

Kani identified two load carrying mechanisms of shear resistance. For the case where no bond exists between the longitudinal tension reinforcement and the concrete, the tension in the longitudinal reinforcement is transferred to the concrete by the anchorage at the support (force  $T$  in figure 2.6(a)). The applied force,  $P$  is transferred to the support by struts of direct compression as a component of the resultant of  $P$  and the flexural compression resultant. In the case where bond exists between the longitudinal tension reinforcement and the concrete, the tension is transferred to the concrete along the length of the reinforcement bar as a distributed load that increased from zero at the support to a maximum at the centre of the beam. As a result the compression trajectory or thrust line is no longer linear but non linear as shown in figure 2.6(c). The tension force in the longitudinal beam would cause the “teeth” to bend. The teeth would break away from the tension reinforcement when the bending capacity of the teeth was exceeded. Failure of the beam would occur when both the teeth capacity of the beam would be exceeded and the arch formed by the compression trajectory or thrust line, would fail in compression. Kani developed expressions for the capacity of the arch as well as the capacity of the teeth. From his experimental study he found that for beams with an  $a/d$  lower than 2.5 the teeth

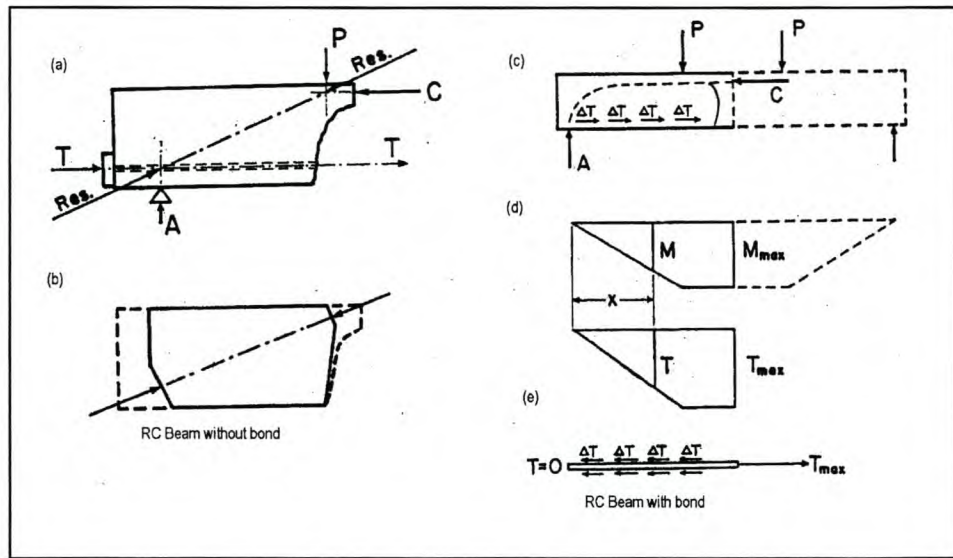


**Figure 2.6: Internal forces in RC beam without shear reinforcement (Kani, 1964)**

capacity would be exceeded before the arch capacity. Failure would occur when the arch capacity is exceeded (i.e. the two mechanisms must fail in parallel for the beam to fail). For beams with an  $a/d$  ratio of higher than 2.5 the teeth capacity is higher than the arch capacity. At failure of the teeth (loss of bond between concrete of the teeth and the longitudinal tension reinforcement) the arch capacity would have already been exceeded and failure would occur by the sudden disintegration of the beam. For an  $a/d$  larger than about 6 the flexural failure due to crushing of the compression zone occurs.

Kani noticed that for  $a/d$  lower than about 6 the full flexural capacity of a beam was not reached due to the premature formation of a diagonal tension crack. The corresponding ultimate moment at shear failure,  $M_{cr}$  would therefore be only a fraction of the moment at the ultimate flexural capacity of the beam,  $M_f$ . He therefore expressed his failure functions for the teeth capacity and the arch capacity as functions of the ratio between  $M_{cr}$  and  $M_f$ . Figure 2.7 shows the failure lines for a beam with 1.88% longitudinal steel and concrete cylinder strength of 26.2 MPa. The shaded area shows the test results obtained from the experiments. Around the value of  $a/d$  of 2.5 the transition occurs from arch action mechanism as the predominant load carrying mechanism to the teeth mechanism as the dominant mechanism. For  $a/d$  larger than 5.6 the beam fails in flexure. Note that for  $a/d$  between 1.0 and 5.6 a “valley” forms, where the flexural capacity of the beam is not reached at the point of shear failure, with

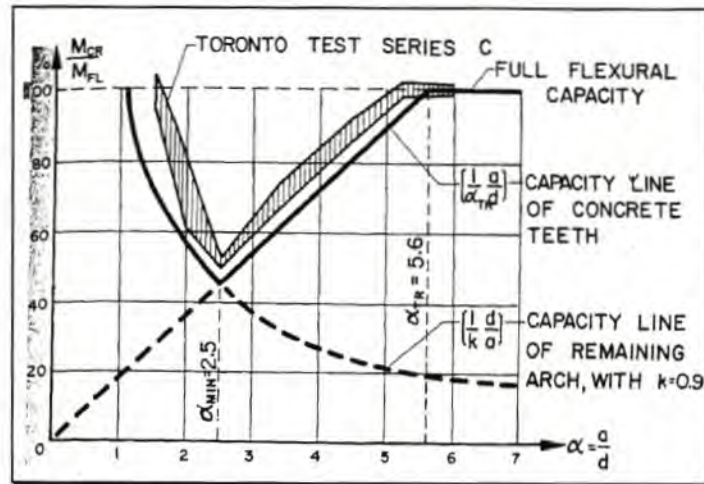


Figure 2.7: Shear failure mechanism in RC beam without shear reinforcement (Kani, 1964)

the minimum value of  $M_{cr}/M_{fl}$  occurring at  $a/d$  2.5. Kani proposed that shear reinforcement be supplied in this range to ensure that full flexural capacity is attained. Kani's investigation was carried out for beams with different percentages of longitudinal reinforcement. The results of  $M_{cr}/M_{fl}$  (here  $M_{cr}$  denoted as  $M_u$ ) are for a 26.8 MPa concrete as a function of  $a/d$  and  $\rho$ , are shown in figure 2.8.

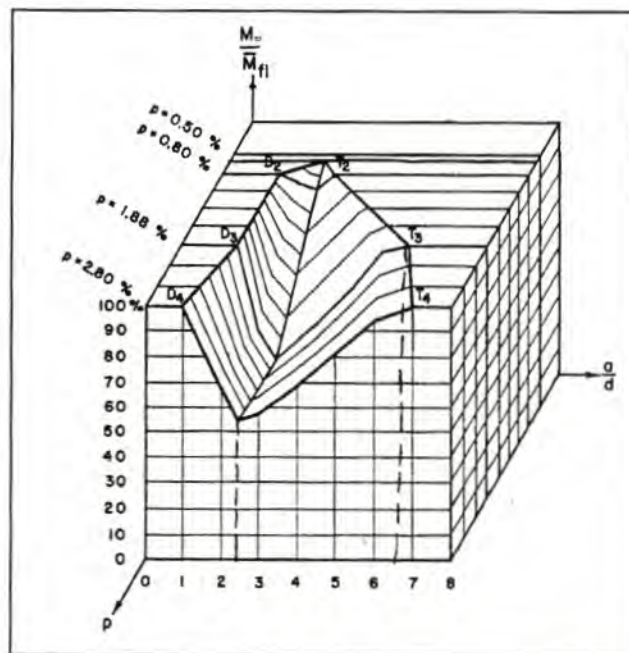


Figure 2.8: Relative beam strength,  $M_{cr}/M_{fl}$  versus  $a/d$  and  $\rho$  (Kani, 1966)

Note the “diagonal tension failure valley” is at its widest for a very heavily reinforced beam with  $\rho = 2.8\%$ , flexural failure occurring at  $a/d$  of 7. For  $\rho$  of 0.8 % diagonal failure occurs within  $a/d$  of 1.5 to 3.5. For  $\rho$  of 0.5% the diagonal failure valley disappears altogether, which means that for a beam so lightly reinforced in bending only flexural failure is possible. For all percentages of steel the transition between failure mechanisms is about  $a/d$  of 2.5.

Kani’s model does not take the important shear resistance mechanisms such as interface shear transfer into account. It does however predict the various shear failure mechanism and was probably the first attempt at a rational explanation of shear resistance. After Kani further research was done on tooth models, particularly taking crack friction into account. Strut and tie models that have been successfully applied for members with shear reinforcement have been adapted for members without shear reinforcement, other approaches have been taken with fracture mechanics. The ASCE-ACI Task Committee 445 Report of 1998 provides an extensive summary on the work done in these fields.

More recently the modified compression field theory, abbreviated as MCFT, (Vecchio and Collins, 1986) has been applied to members without shear reinforcement. The theory provides a general model that describes shear response of cracked reinforced concrete. According to the MCFT shear resistance is governed by the stresses at the crack interface. The modified compression field theory takes a very different approach from the tooth models but both approaches yield similar results. The method will be discussed in detail in section 2.2 for members with shear reinforcement.

While rational approaches such as the tooth model have been in existence for some time, most international codes have used empirical formulations for the shear resistance of members without shear reinforcement. Due to the limited application of beams without shear reinforcement it is perhaps not warranted to use these sophisticated method that require more design effort. Nonetheless these models have improved our understanding on shear in reinforced concrete. In 1994 the modified compression field theory has been applied in the Canadian concrete code, CSA-A23.3 1994, (Rahal and Collins, 1999) and the American Bridge design code (AASHTOO LRFD 2000). Empirical formulations are derived from fitting equations to data from a number of experiments of beams, that are functions of important shear parameters such as  $f_{cu}$ ,  $d$ ,  $\rho$  and  $a/d$ . The advantage of these equations is that they are simple to apply in design. The disadvantage is that they can only be applied to a range of design

situations that correspond to the range of the experiments from which it was derived. One such example is the very simple formulation used in the American concrete design code (ACI 318 1995):

$$v = \frac{V}{bd} = \frac{\sqrt{f_c}}{6} \text{ (MPa)} \quad [2.4]$$

where  $f_c$  is the concrete cylinder strength. The formula is intended as a lower bound on shear resistance of slender beams with at least 1% longitudinal tension reinforcement. It may be unconservative for beams that are very lightly reinforced in bending, very deep members and members made from high strength concrete (ASCE-ACI Task Committee 445, 1998). SANS, which closely based on the British code BS8110, and Eurocode employ more sophisticated empirical formulations. AASHTO LRFD and the Canadian code, CSA 23.3 are exceptions among the international design codes in that they base their design method on the MCFT rather than employing empirical formulations.

## 2.1.5 Applications to codes

### 2.1.5.1 SANS 10100-1: 2003

SANS assumes the shear stress distribution proposed by Mörsh given by equation 2.2, with the flexural lever arm,  $z$ , taken equal to the effective member depth,  $d$ .

$$v = \frac{V}{b_w d} \quad [2.5]$$

$V$  is the maximum design shear force for ultimate limit state and  $b_w$  is the width of the web of the beam. If the web is tapered,  $b_w$  is taken as the average width.

The shear resistance expressed as a stress is then given by the empirical formula:

$$v_c = \frac{0.75}{\gamma_{m,c}} \left( \frac{f_{cu}}{25} \right)^{1/3} \left( \frac{100 A_s}{b_w d} \right)^{1/3} \left( \frac{400}{d} \right)^{1/4} \text{ (MPa)} \quad [2.6]$$

- $\gamma_{m,c}$  is the partial material safety factor for concrete, taken as 1.4 for shear
- $f_{cu}$  is the 5% characteristic concrete *cube* strength for concrete, in MPa
- $\frac{100A_s}{b_w d}$  is the percentage of anchored longitudinal *tension* reinforcement provided for bending.
- $b_w$  is the average width of the web, in mm
- $d$  is the effective member depth in mm

The formula may not be applied to members with

- $f_{cu} > 40$  MPa
- $100A_s/bd > 3\%$

Slabs do not require shear reinforcement as long as  $V_u < V_c$ , where  $V_u$  is the ultimate applied shear force. Beams do not require shear reinforcement as long as  $V_u < 0.5V_c$ .

### 2.1.5.2 EN 1992 Eurocode 2: 2003

The Eurocode's design formulation for members without shear reinforcement was adopted from the CEB-*fip* Model Code 1990. The formula is also empirical in nature. The shear stress is based on the average shear stress distribution from Mörsh, also used in SANS 10100:

$$v = \frac{V}{b_w d} \quad [2.7]$$

$$v_c = \frac{0.18}{\gamma_{c,m}} (f_{ck})^{1/3} \left( \frac{100A_s}{b_w d} \right)^{1/3} \left( 1 + \sqrt{\frac{200}{d}} \right) \geq 0.035 \left( 1 + \sqrt{\frac{200}{d}} \right)^{3/2} f_{ck}^{1/2} \quad [2.8]$$

All variables are defined as for SANS except the 5% concrete characteristic *cylinder* strength is used instead of the cube strength and the partial material factor for concrete is 1.5. The reason for the lower limit on the shear resistance in equation 2.8 is not known.

The empirical limitations to the formula are as follows:

$$f_{ck} \leq 100 \text{ MPa}$$

$$\frac{100 A_s}{b_w d} \leq 2\%$$

$$1 + \sqrt{\frac{200}{d}} \leq 2, \text{ i.e. } d > 200 \text{ mm}$$

The formula appears in the CEB Model Code, but here the concrete material factor has been built in and the term  $0.18/\gamma_{m,c}$  is shown as a single value of 0.12.

### 2.1.5.3 AASHTO LRFD: 2000 and CSA- 23.3: 1994

The AASHTO shear design procedure is known as the General Shear Design method (Collins et. al., 1999) and is based on the modified compression field theory. The method is also applied in the Canadian concrete design code (Rahal and Collins, 1994).

Once again Mörsh's stress distribution is applied, but with the flexural lever arm  $z$  taken as 0.9 times the effective member depth  $d$ . The shear resistance of members without shear reinforcement, expressed as a force, is then given by:

$$V_c = \phi \beta \sqrt{f_c} b_w z \quad [2.9]$$

- $f_c$  is the concrete cylinder strength
- $\phi$  is a resistance factor taken as 0.9

The value  $\beta$  could be called a "crack factor". The modified compression field theory relates the shear resistance of a beam to the extent of cracking it has undergone due to bending. Failure is assumed to occur when the aggregate interlock mechanism fails.  $\beta$  is a function of inclined crack spacing  $s_x$ , the angle of inclination of the cracks  $\theta$  and the average strain  $\epsilon_x$  in the longitudinal direction of the beam.  $\beta$  and  $\theta$  are determined from a graph for a certain strain and crack spacing, shown in Figures 2.10 and 2.11 (from Vecchio and Collins, 1999)

Vecchio and Collins found that the crack spacing  $s_x$  increased with the effective member depth.  $s_x$  is taken as follows:

- For members with no crack control steel along the depth of the beams,  $s_x = 0.9d$
- For members with crack control steel,  $s_x =$  minimum spacing between layers of crack control steel. (see figure 2.9)

Figures 2.10 and 2.11 were developed for a 19 mm aggregate. If a different aggregate is used  $s_{xe}$  and equivalent crack spacing is determined from:

$$s_{xe} = s_x \frac{35}{agg + 16}, \text{ where } agg = \text{aggregate size in mm} \quad [2.10]$$

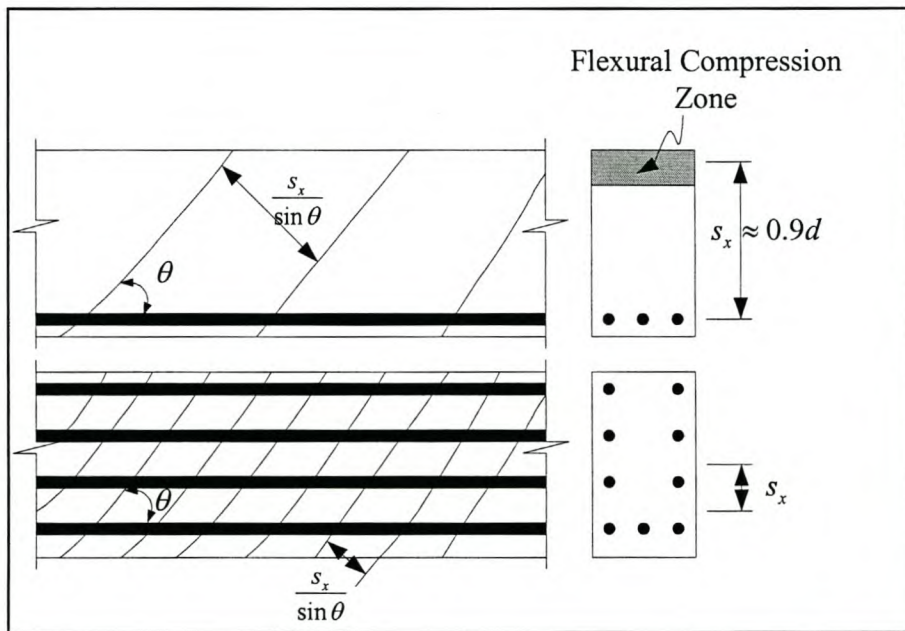


**Figure 2.9: Influence of longitudinal reinforcement on spacing of cracks. (ASCE-ACI Committee on Shear and Torsion, 1998)**

For high strength concrete aggregate size is taken as zero. This increases  $s_x$  and therefore reduces the shear resistance, as high strength concretes have proportionally lower shear strengths as normal strength concretes.

For members without shear reinforcement,  $\epsilon_x$  is taken as  $\epsilon_t$  the average strain at the level of the tension reinforcement, calculated as follows:

$$\varepsilon_t = \frac{M/z + 0.5V \cot \theta - A_p f_{po} + 0.5N}{E_s A_s + E_p A_p}$$

Where,

- $M$  is the moment at the section under consideration. In design the moment at a distance  $0.9d$  from the location of the maximum moment is taken.
- $V$  is the applied shear force at the section under consideration
- $N$  is an applied tensile or compressive force. (A compressive force will have a negative sign)
- $A_p f_{po}$  is the applied pre-stressing force
- $E_s$  and  $E_p$  are the moduli of elasticity for the normal longitudinal tensile reinforcement and the pre-stressing steel respectively.
- $A_s$  and  $A_p$  are respective areas of the normal longitudinal tensile reinforcement and the pre-stressing steel.

In design the value of  $\theta$  must first be estimated when calculating the strain from equation 2.11. Then the corresponding beta value is determined for the strain and  $V_c$  is calculated from equation 2.9. If  $V_c$  is close to the applied shear stress  $V$ , then  $\theta$  has been estimated correctly, if not another  $\theta$  is guessed. Clearly the method requires a few iterations to find the correct solution.

#### 2.1.5.4 Comparing SANS, Eurocode and AASHTO

The shear design procedures of both SANS (equation 2.6) and Eurocode (equation 2.8), for members without shear reinforcement, are completely empirical. The empirical formulas of SANS and Eurocode are very similar. Both have the same terms accounting for concrete strength and longitudinal reinforcement; however the terms containing the effective member depth, which account for the size effect of concrete, are different. The formulas have limitations. Most notably the concrete strength in SANS may not exceed 40 MPa. This does not mean that the shear design procedure may not be applied to beams with concrete strengths higher than 40 MPa, it simply means that when calculating the shear resistance of higher strength concretes,  $f_{cu}$  may not be taken higher than 40 MPa.

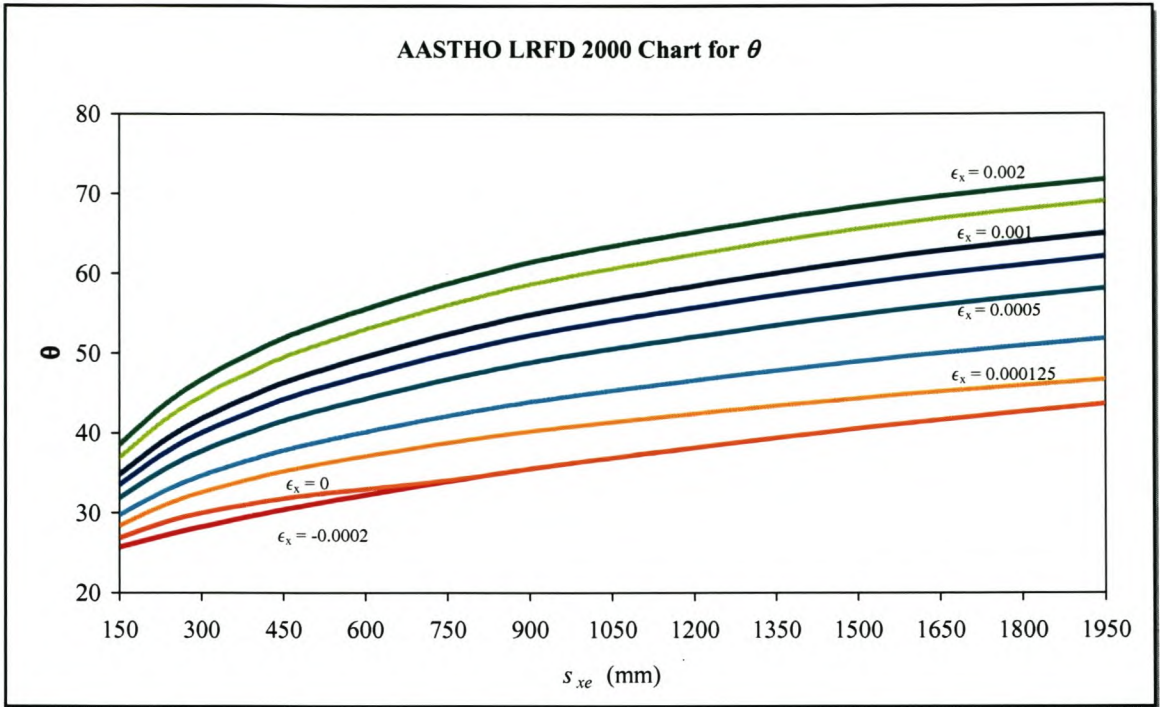


**Figure 2.10: AASHTO LRFD: 2000  $\theta$  chart for members without shear reinforcement**

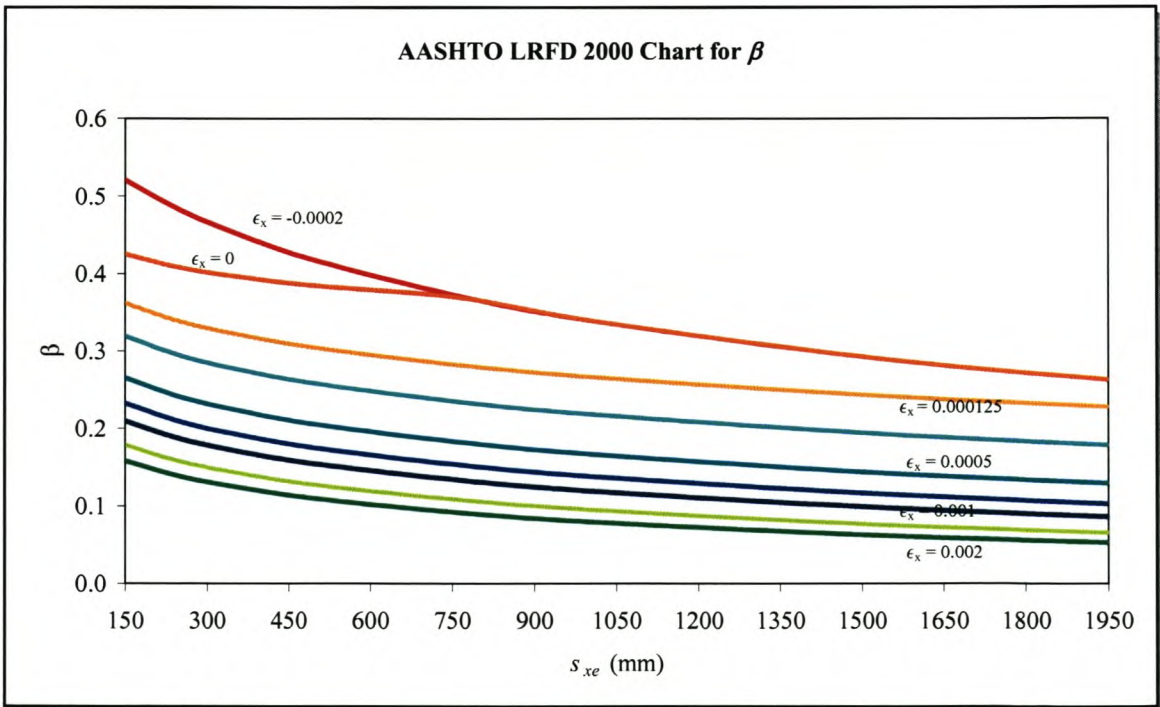


**Figure 2.11: AASHTO LRFD: 2000  $\beta$  chart for members without shear reinforcement**

Therefore factors that are known to affect shear resistance such as the size effect on shear and dowel action are accounted for by including terms for  $d$  and  $\rho$ , however these terms have no rational basis as they were derived empirically. Interestingly  $a/d$  is not included even though it affects shear resistance.

AASHTO offers a more rational approach to shear design. The method predicts that with increased straining of the web due to bending,  $\beta$  decreases (figure 2.11) and hence the shear resistance decreases. As the strain in the web of a beam increases the diagonal tension cracks widen and the aggregate interlock mechanism weakens, and therefore the shear resistance decreases. AASHTO predicts that the shear resistance of a beam also decreases with diagonal crack spacing. However crack spacing increases with increasing member depth. The decrease in shear resistance with increased crack spacing therefore accounts for size effect of shear. Larger beams typically have wider cracks proportional to the aggregate size, than smaller beams, and therefore reduced shearing capacity. However if crack control steel is provided then AASTHO predicts reduced crack spacing, equal to the spacing of the layers of crack control steel. Therefore, according to AASHTO, by providing crack control steel the size effect in shear can be counteracted. Although SANS requires crack control steel for members deeper than 750 mm, it does not allow for an improvement of the shear resistance of such a beam.

The AASHTO shear design procedure can be applied to normally reinforced beams as well as columns and pre-stressed beams, hence the name General Shear Design Method. Pre-stressing and axial forces counteract the straining of the web due to bending (equation 2.11) thereby improving the shear strength of a beam. It is also applicable to high strength concretes. Due to its rational basis, AASHTO has fewer constraints than SANS and Eurocode, however it does contain some empirical elements, such as the formula and assumptions related to the crack spacing. Also the stress-strain relationship for cracked concrete for which the  $\beta$  and  $\theta$  charts (Figures 2.10 and 2.11) have been derived is empirical. The advantage in of the SANS and Eurocode method is that they are much simpler to apply in design than the AASTHO method.

## 2.2 Shear strength of members with shear reinforcement

This section deals with the mechanisms of shear transfer in members with shear reinforcement, which are closely related to those of member without shear reinforcement. The three main historical approaches to shear design of members with shear reinforcement are discussed together with their application in SANS, Eurocode and AASHTO.

### 2.2.1 Mechanisms of shear transfer

Most beams in practice are designed for the purpose of resisting bending moments. In beams with a relatively low slenderness ratio the beam may fail in shear before it reaches its full bending capacity. The purpose of shear reinforcement is to prevent premature shear failure and to ensure that a beam reaches its full bending capacity. In the literature the range of beams for which shear failure is likely to occur is defined in terms of the shear span to depth ratio  $a/d$  as already discussed in section 2.2 for members without shear reinforcement.

The same factors that contribute to the shear resistance of a beam without shear reinforcement also contribute to the shear resistance of a beam with shear reinforcement, but with the added contribution of the shear reinforcement. This thesis is concerned with shear reinforcement in the webs of beams, specifically vertical stirrups since these are most commonly applied in practice. Other forms of shear reinforcement occur in the flanges of T-beams and in shear walls. When shear reinforcement is mentioned, in the remainder of this thesis, then vertical shear reinforcement in the web of beams or slabs is meant.

The shear resistance as given by equation 2.1, including shear reinforcement then becomes:

$$V_R = V_{ay} + V_{cz} + V_d + V_s \quad [2.12]$$

The contribution to shear resistance of the shear reinforcement  $V_s$ , typically supplied in the form of vertical double leg stirrups or alternatively bent up bars,  $V_s$ , is insignificant in uncracked concrete members. Once the member has developed diagonal tension cracks, only the part of the shear

reinforcement crossing a crack contribute to the shear resistance of a beam. A stirrup crossing transfers shear stresses across the crack by developing tension stresses. Failure is assumed to occur when the stress in the stirrups reaches the yield stress of the steel.

Other than supplying an additional component to the shear resistance of a reinforced concrete beam, shear reinforcement improves shear resistance by restraining the widening of the diagonal tension cracks with increased bending, thereby effectively maintaining the interface shear transfer mechanism. Once the stirrups crossing the crack have yielded the inclined crack widens and as a result the interface shear transfer,  $V_{av}$ , decreases. As a result the dowel force,  $V_d$  and the shear in the uncracked compression zone of the beam,  $V_{cz}$ , increase rapidly to carry the shear load. Failure occurs when the compression zone crushes or the splitting of the longitudinal tension reinforcement occurs due to the increased dowel force. Stirrups that cross a diagonal tension crack near the bottom of the beam, close to the longitudinal tension reinforcement may delay splitting by providing restraint to the longitudinal reinforcement. For this mechanism to be effective, stirrups have to be closely spaced to increase the likelihood of a stirrup crossing a crack near the bottom of the beam and to provide adequate restraint the stirrup needs to have a sufficient size. (ASCE-ACI Committee 426, 1973)

Stirrups improve the ductility of a beam by maintaining the crack interface shear transfer and by improving dowel action. Since sudden failures are undesirable, most international codes require that all beams save those of less structural importance to be supplied with a certain minimum (nominal) amount of shear reinforcement, even where the design formulas predict that shear resistance is adequate without shear reinforcement. Most international codes (ACI 318:1995, BS 8110:1987, SANS 10100-1:2003, CSA A23.3: 1994) require that beams where the applied factorized shear load  $V_u$  exceeds half the resistance of the member without shear reinforcement  $V_c$  (equation 2.6 for SANS) be supplied with at least nominal stirrups. Only beams where  $V_u < 0.5V_c$  do not require shear reinforcement. The rule does not apply to slabs, since it is common practice to avoid the use of stirrups in slabs, except near column supports, where punching shear may govern. If the amount of stirrups is less than a certain minimum value, then upon the formation of a diagonal crack the stirrups may fail very suddenly and the beam will then effectively behave like a beam without shear reinforcement.

## 2.2.2 Historical Approaches to the design of shear reinforcement in reinforced concrete members

The traditional approach for designing the shear reinforcement for the web of a beam is by means of a planar truss analogy. All international design codes follow this approach. However the codes differ in the manner that they calculate the so-called concrete contribution to the shear resistance of the beam and the relative importance that they assign to the contribution of steel and concrete to shear resistance. The three main approaches to design of members with shear reinforcement, namely the 45° planar truss analogy (applied in SANS), the plasticity theory (applied in Eurocode) and the modified compression field theory (applied in AASHTO), are discussed in detail in this chapter.

### 2.2.2.1 The 45° Planar Truss Analogy

The traditional approach toward determining the shear resistance of reinforced concrete members with shear reinforcement is the so-called truss analogy, which was first proposed by the Swiss engineer Ritter in 1899. Ritter postulated that after the concrete in the web has cracked due to diagonal tension stresses arising from shear, the beam can be idealized as parallel chord truss as shown in figure 2.12.

The shear reinforcement forms the vertical tension ties of the truss, whereas the diagonal compression struts are formed by the concrete between the diagonal tension cracks. To state this more simply, the compression struts tend to push the top and bottom of the beam apart while the shear reinforcement pulls them together. Ritter assumed that the beam would fail in shear when the shear reinforcement has yielded, or when the inclined concrete struts failed in compression. Therefore from equilibrium either one of the following equations gives shear strength of a beam, expressed as a stress:

$$\text{Shear stress at yielding of stirrups: } v_s = \frac{A_v f_{yv}}{b_w s} \cot \theta \quad [2.13a]$$

$$\text{Shear stress at crushing of struts: } v_d = f_{d,max} \sin \theta \cos \theta \quad [2.13b]$$

These formulas apply to a beam with double leg vertical stirrups of area  $A_v$ , with yield strength  $f_{yv}$  spaced at distance  $s$ .  $f_{d,max}$  is the compressive capacity of the diagonal concrete compression struts.

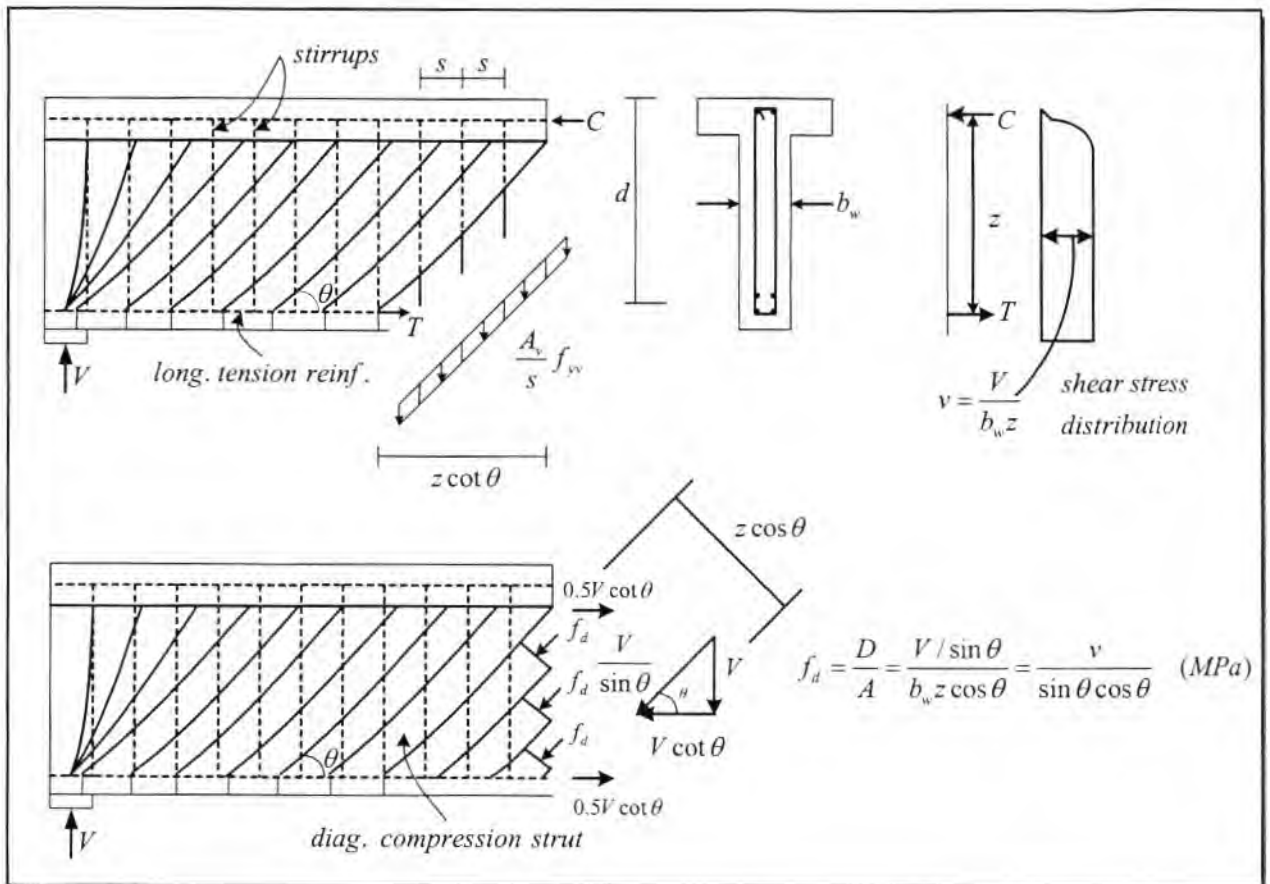


**Figure 2.12: Planar truss analogy of beam with shear reinforcement (Hsu, 1993)**

The angle  $\theta$  is the angle that the diagonal compression struts make with the longitudinal tension reinforcement, assumed to be equal to the angle of the diagonal tension cracks. Note that Ritter's model assumes Mörsc's shear stress distribution of  $V = v/bz$ .

The shear force that is applied to a beam,  $V$ , also causes a component  $V \cot \theta$  in the longitudinal direction. This component causes tensile stresses to develop in the longitudinal reinforcement of the beam, in addition to those caused by bending. The component is divided equally between the longitudinal tension reinforcement and the longitudinal compression reinforcement.

Ritter assumed the angle  $\theta$  to be  $45^\circ$ . The assumption derives from un-reinforced, initially uncracked concrete that cracks at this angle. The assumption is conservative since in most practical beams  $\theta$  is much lower than  $45^\circ$ .

Equations 2.13(a) and 2.13(b) then become,

$$\text{Shear stress at yielding of stirrups: } v_s = \frac{A_v f_{yv}}{b_w s} \quad [2.14a]$$

$$\text{Shear stress at crushing of struts: } v_d = 0.5 f_{d,max} \quad [2.14b]$$

According to Ritter's model, three possible shear failure modes are possible in a beam.

**Shear failure due to the yielding of the stirrups.** If it is assumed that all the stirrups that cross a crack will yield, then the shear resistance is given by equation 2.14a, provided that the stress in the concrete compression struts,  $f_d$  has not reached its maximum value  $f_{d,max}$ . Only the stirrups crossing a diagonal tension crack can contribute to the shear resistance of the beam. Stirrups are only likely to cross a crack if they are spaced at a distance less than the horizontal projection of the crack,  $z \cot \theta$  or in the case of Ritter's 45° model,  $z$ . Maximum stirrup spacing should be taken as  $z$  or less.

**Shear failure due to the crushing of the compression struts.** As indicated by equations 2.13b and 2.14b, there exist compressive stresses in the web of a beam. For members with very thin webs such as I-beams the shear force is distributed over a much smaller area of the web which may lead to the crushing of the web, before the stirrup yield. The stress state in the compression struts is not uni-axial, due to the frictional forces at the location of the diagonal tension cracks. These forces have a softening effect on the concrete and crushing will occur at much lower stress than the cube or cylinder strength of concrete, which represents the principal compressive strength of concrete. Eurocode suggests that  $f_{d,max}$  be taken as 60% of the cylinder strength. Crushing failure is by nature a sudden brittle failure and is therefore not desirable. This type of shear failure is not common, and the approach of most codes is not to explicitly check for crushing failure, but rather to prevent it by defining some upper allowable limit on the shear stress that may be applied to a beam.

**Shear failure initiated by the failure of the longitudinal tension reinforcement.** A typical beam is never subjected to a state of pure shear. The beam is always subjected to both shearing and bending. Bending action affects the shear resistance of the beam and vice versa. The truss model predicts that the shear force,  $V$  has a component  $V \cot \theta$  along the longitudinal axis of the beam. It is assumed that the force is divided equally between the bottom and top longitudinal reinforcement. Under positive

bending the tension reinforcement lies at the bottom of the beam and the compressive reinforcement lies at the top of the beam. Each has to resist half of the tensile force due to shear  $V \cot \theta$  in addition to the force due to bending  $M/z$ , where  $M$  is the moment at the section under consideration. The shear component counteracts the compression due to bending in the longitudinal compression reinforcement. This effect is usually ignored in design codes to be on the conservative side. However, for the tension reinforcement a check must be carried out to ensure that the area of tension steel provided can resist a force of:

$$A_s f_y \geq \frac{M}{d_v} + \frac{V}{2} \cot \theta \quad [2.15]$$

It can be shown that the effect of the shear force on the longitudinal reinforcement can be taken into account by extending the longitudinal tension reinforcement by a distance of  $0.5z \cot \theta$  past the point of where it is no longer needed for bending alone (ASCE ACI Committee 445, 1998). This is because the shear component  $V \cot \theta$  has the effect of shifting the moment diagram by  $z \cot \theta$  away from the supports. Most codes use this approach by specifying a reinforcement detailing rule requiring the longitudinal tension reinforcement to be extended by a distance  $z \cot \theta$  beyond where it is required only for bending, or by some value related to  $z \cot \theta$ .

Ritter's 45° truss model given by equation 2.14a still forms the basis of many international design codes, including SANS 10100-1:2003. Ritter's model assumes that shear strength is only dependent on the amount and properties of the shear reinforcement supplied in the beam. We know that the concrete itself contributes significantly to the shear strength of the beam, by means of various mechanisms of which the most important is interface shear transfer, especially in members with little shear reinforcement. To account for the "concrete contribution" to shear resistance, international codes have supplemented the shear resistance of Ritter's 45° truss model (equation 2.14(a)) with a concrete contribution term,  $v_c$ . This term is usually an empirical formulation used for members without shear reinforcement, such as equation 2.6 of SANS. The shear stress that can be resisted by a reinforced concrete beam with stirrups is then given by:

$$v = v_c + v_s \quad [2.16]$$

Adding the concrete contribution term reduces the conservatism of Ritter's model and improves correlation with experimental data. Another approach at improving Ritter's truss analogy model has been to adjust the angle  $\theta$ . If  $\theta$  is taken less than  $45^\circ$  then  $\cot \theta$  becomes larger than one, thereby reducing the conservatism of Ritter's model. This approach is taken by EN 1992 Eurocode 2 and is known as the variable angle truss model, which is discussed in the following section.

### 2.2.2.2 The Variable Angle Truss Model

A different approach to Ritter's  $45^\circ$  truss model is the variable angle truss model most recently applied in EN 1992 Eurocode 2. The model is also based truss analogy of Ritter's model as derived from equilibrium, except that the inclination of the compression struts,  $\theta$  is allowed to vary within certain limits. The variable angle truss model was first applied in the CEB-FIP Model Code of 1978. The shear design procedure of ENV 1992 Eurocode 2: 1992 and the most recent edition EN 1992 Eurocode 2: 2003 have been adopted from the CEB-*fip* Model Code of 1990. The original Eurocode of 1992 left the designer with a choice between the  $45^\circ$  truss model with concrete contribution very similar to that of SANS 10100-1 and the variable angle truss model. The most recent edition of 2003 has dropped the  $45^\circ$  truss model and only employs the variable angle truss model (Narayanan, 2001).

The variable angle truss model is based on the plasticity theory for reinforced concrete (Hsu, 1993) and is therefore also known as the plasticity truss model. The plasticity truss model assumes that both the longitudinal reinforcement, provided to resist bending and the transverse reinforcement, that is the shear reinforcement, must yield before failure. There are two types of reinforced concrete elements, according to plasticity theory, underreinforced and over-reinforced elements. In an underreinforced element both the longitudinal and the transverse steel yield before crushing of the concrete takes place. In an over-reinforced element the concrete crushes before the steel yields. The underreinforced elements therefore satisfy the plasticity theory but over-reinforced elements do not. The equations that Ritter derived are applied in the plasticity truss model. Note the amount of steel is expressed as a ratio here,

$$\text{Shear stress at yielding of stirrups:} \quad v_s = \rho_v f_{vy} \cot \theta \quad [2.17a]$$

$$\text{Shear stress in concrete struts:} \quad v_d = f_d \sin \theta \cos \theta \quad [2.17b]$$

$$\text{Shear stress at yield of long. reinf.:} \quad v_{sl} = \rho_l f_{yl} \tan \theta \quad [2.17c]$$

Equilibrium of beam shear element (figure 2.12) shows that the shear force has a component in the longitudinal direction of the beam as expressed by equation 2.17(c).

From the plasticity theory's assumption that the longitudinal and transverse reinforcement simultaneously yield at failure, then  $v_s = v_{sl} = v_d$  at failure. Note that the compressive stress in the concrete struts  $f_d$  is not equal to the crushing strength of concrete  $f_{d,max}$ .

Equations 2.17(a) and 2.17(c) can be expressed in terms of  $f_d$  by substituting 2.17(b) into 2.17(a) and 2.17(c), as follows:

$$\rho_v f_{yv} = f_d \cos^2 \theta \quad [2.18a]$$

$$\rho_l f_{yl} = f_d \sin^2 \theta \quad [2.18b]$$

$$v = f_d \sin \theta \cos \theta \quad [2.18c]$$

Now adding 2.17(a) and 2.17(b) and from the identity  $\sin^2 \theta + \cos^2 \theta = 1$ ,

$$\rho_l f_{yl} + \rho_v f_{yv} = f_d \quad [2.19]$$

The equation can be normalized in terms of the crushing strength of the diagonal compression struts,  $f_{d,max}$ .

$$\omega_l + \omega_v = f_d / f_{d,max} \quad [2.20]$$

where,

$$\omega_l = \frac{\rho_l f_{yl}}{f_{d,max}} \quad \text{and} \quad \omega_v = \frac{\rho_v f_{yv}}{f_{d,max}}$$

Note  $\omega_v$  is known as the *shear reinforcement index*.

Three failure conditions exist defined as follows:

$$\text{Underreinforced elements:} \quad \omega_l + \omega_v < 1 \quad [2.21a]$$

$$\text{Overreinforced elements:} \quad \omega_l + \omega_v > 1 \quad [2.21b]$$

$$\text{Balanced condition:} \quad \omega_l + \omega_v = 1 \quad [2.21c]$$

In an underreinforced element the stress in concrete compression struts is less than the stress at crushing of the concrete, at yielding of the reinforcement and vice versa for over-reinforced elements. The balanced condition is the point that separates the two failure modes.

The **underreinforced condition**:  $\omega_t + \omega_l < 1$

Substituting equations 2.18(a) and 2.18(b) into 2.18(c), the shear stress at simultaneous yield of shear and longitudinal reinforcement is then given by:

$v = \sqrt{(\rho_l f_{ly})(\rho_v f_{vy})}$  and dividing both sides by  $f_{d,max}$  :

$$\frac{v}{f_{d,max}} = \sqrt{\omega_l \omega_t} \quad [2.22]$$

Dividing 3.17(b) by 3.17(a),  $\theta$  can be calculated from,

$$\tan \theta = \sqrt{\frac{\omega_t}{\omega_l}} \quad [2.23]$$

The variable angle truss model as applied in EN 1992 is based one of three cases of the balanced condition.

The three cases for the **balanced condition** are,

1.  $\omega_t = \omega_l = 0.5$

The steel in the longitudinal and transverse direction, yield simultaneously with the crushing of the concrete struts at effective stress. From equation 2.22,  $\theta = 45^\circ$  for this case.

2.  $\omega_t < 0.5$

The transverse steel has yielded and is followed by the yielding of the longitudinal steel with simultaneous crushing of the concrete therefore,  $\omega_t = 1 - \omega_l$

$$\frac{v}{f_{d,max}} = \sqrt{\omega_t(1-\omega_t)} \quad [2.24]$$

$$\tan \theta = \sqrt{\frac{\omega_t}{1-\omega_t}} \quad [2.25]$$

$\theta$  is always less than  $45^\circ$ .

3.  $\omega_t < 0.5$

The longitudinal steel has yielded and is followed by the transverse steel yielding simultaneously with concrete crushing

$$\frac{v}{f_{d,max}} = \sqrt{\omega_t(1-\omega_t)} \quad [2.26]$$

$$\tan \theta = \sqrt{\frac{1-\omega_t}{\omega_t}} \quad [2.27]$$

$\theta$  is always more than  $45^\circ$ .

Now by squaring both sides of equation 2.26 and adding  $0.5^2$  on both sides,

$$\left(\frac{v}{f_{d,max}}\right)^2 + (\omega_t - 0.5)^2 = 0.5^2 \quad [2.28]$$

Equation 2.28 of the balanced condition is shown in a graphical form by a semicircle in Figure 2.13. The horizontal axis represents the shear reinforcement index  $\omega_t$  (the amount of shear reinforcement normalized with respect to the capacity of the inclined concrete compression struts). The vertical axis represents the applied shear stress normalized with respect to the capacity of the inclined compression struts. Both  $\omega_t$  and  $v/f_{d,max}$  are dimensionless variables.

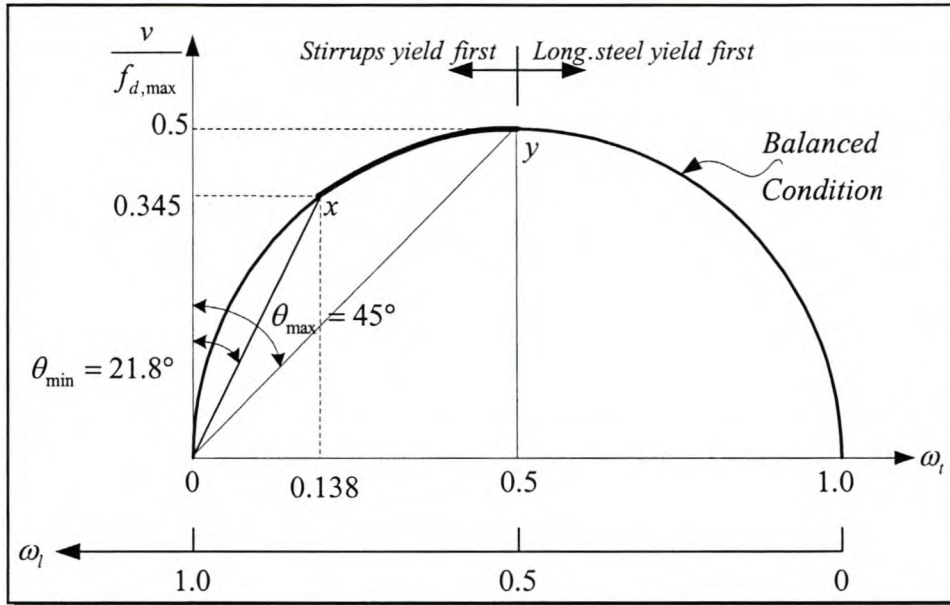


**Figure 2.13: Relationship for shear stress ratio vs. reinforcement ratios for the balanced condition (Hsu, 1993)**

When equation 2.22 is substituted into 2.23 and  $\omega_t$  is eliminated then we get that  $\theta$  can be calculated from:

$$\tan \theta = \frac{\omega_t}{v / f_{d,max}} \quad [2.29]$$

Equations 2.28 and 2.29 can be used to interpret the behaviour of concrete beams reinforced for shear. Equation 2.28 represents the balanced condition, graphically represented as a half circle in figure 2.12. Reinforcement inside the area enclosed by the semi-circle is an underreinforced element and anything outside the semi-circle is an over-reinforced element. EN 1992 requires shear reinforcement to be designed in order to satisfy case 2 of the balanced condition, that is, where the shear reinforcement yields simultaneously with the crushing of the diagonal concrete struts, before the longitudinal reinforcement yields. For case 2,  $\theta$  must be less than  $45^\circ$ . Moreover a lower limit is placed on  $\theta$ , namely  $21.8^\circ$ , which corresponds to  $\omega_t$  of 0.138 as calculated from equation 2.29. From Figure 2.13 one can see that the Eurocode method is actually a hybrid of a constant  $\theta$  method and a variable angle method. For RC members with a shear reinforcement index  $\omega_t$  of between 0 and 0.138, the normalized shear resistance  $v/f_{d,max}$  increases linearly with increasing  $\omega_t$ , due to the constant value of  $\theta$  of  $21.8^\circ$ .

However when  $\omega_t$  exceeds 0.138,  $\theta$  gradually increases from  $21.8^\circ$  to  $45^\circ$  in a non-linear fashion as  $\omega_t$  increases. As a result the shear resistance increases non-linearly with increasing amount of shear reinforcement.

### Assumptions made in applying plasticity theory to Eurocode:

At crushing failure of the concrete, the compressive stress in the diagonal concrete struts is given in Eurocode 2 by:

$$f_{d,max} = \nu f_{cd} \quad [2.30]$$

$f_{cd} = \frac{f_{ck}}{\gamma_c}$ , where  $f_{ck}$  is the 5% characteristic cylinder strength in MPa.

$\nu$  is a constant known as the efficiency factor that allows for the biaxial stress distribution in the diagonal compression struts due to frictional forces at the crack interfaces. In the 1978 CEB Model Code  $\nu$  was simply taken as a constant 0.6. In the 1990 CEB Model Code and the EN 1992 Eurocode 2: 2003 the factor is given as:

$$\nu = 0.60 \left[ 1 - \frac{f_{ck}}{250} \right] \quad [2.31]$$

For normal strength concretes,  $\nu$  is simply taken as 0.6.

The additional factor is to account for high strength concrete ( $f_{ck} > 50$  MPa). The crushing strength of the concrete struts is not constant but actually a function of the tensile strain in the concrete. With increasing tensile strain in the concrete the diagonal cracks become wider and the concrete loses its ability to transfer shear forces by means of friction along the cracks. Tensile strain in turn increases with increasing longitudinal straining of the web due to bending and shear. The crack friction mechanism is not dealt with explicitly in the Plasticity model, but the efficiency factor takes this reduction in crack friction with increased straining into account by reducing the crushing strength of the struts. The efficiency factor given here is a constant but it is conservative and it is usually derived empirically. To determine the crushing strength of a concrete strut accurately one would have to

analyse the strains in the RC member. Since the plasticity truss model does not consider compatibility, it is impossible to determine the strains in the reinforcement and the concrete. Methods like the modified compression field theory are based on compatibility and can determine the strain state of the beam in shear, thus allowing a more accurate calculation of the effective crushing strength.

Table 2.1 below summarizes the limits on  $\theta$  for the model code and Eurocode.

<b>CEB-<i>fip</i> MC: 1978</b> $31^\circ < \theta < 59^\circ$	<b>ENV 1992: 1992</b> $21.8^\circ < \theta < 68^\circ$
<b>CEB-<i>fip</i> MC: 1990</b> $18.4^\circ < \theta < 45^\circ$	<b>EN 1992: 2003</b> $21.8^\circ < \theta < 45^\circ$

**Table 2.1: Limits on  $\theta$  specified by CEB-*fip* Model Code and Eurocode**

The CEB-*fip* model code of 1978 and ENV 1992 allowed values of  $\theta$  greater than  $45^\circ$ . This constitutes the balanced condition case 3. For this case the shear reinforcement is more than 50% of the total required amount of reinforcement ( $\omega_t + \omega_l$ ). Alternatively if  $\theta < 45^\circ$  the shear reinforcement constitutes less than 50% of the total reinforcement. As a result the amount of shear reinforcement is kept low, while the longitudinal reinforcement is increased to compensate. Therefore the upper limit of  $\theta = 45^\circ$  for EN 1992: 2003 ensures that shear reinforcement is designed for the balanced condition case 2. According to equation 2.25 the longitudinal reinforcement index  $\omega_l$  is not required for calculating the shear resistance.

The meaning and origin of the lower limits of  $\theta$  is not entirely clear. Hsu (1993) states that the lower limit is imposed for crack control purposes. This gives the impression that the codes do not allow members to be designed with shear reinforcement indices lower than those corresponding with lower limits of  $\theta$  (For EN 1992:2003 this would be a  $\omega_t$  of 0.138 for  $\theta_{min} = 21.8^\circ$ ) as such members would experience extensive cracking according to the code. However such members are allowed by the codes, just the manner in which the shear resistance is determined (according to constant  $\theta$  or variable  $\theta$  differs).

It is also important to note that the plasticity model does not include a concrete contribution term as is the case for the constant angle method of section 2.2.2.1. The effect of concrete contribution is indirectly considered by the efficiency factor  $v$  of the inclined compression struts (see equation 2.30).

### 2.2.2.3 The Modified Compression Field Theory

The modified compression field theory (MCFT) (Vecchio and Collins, 1986) is reviewed in this section. The MCFT is the most advanced shear theory available to date. Both the 45° truss model and the variable angle truss model are simple conceptual models that are easy to apply in the design practice. They give some insight onto the forces that contribute to the shear resistance of a beam. The variable angle truss model ignores any contribution of tensile forces in the concrete part of the beam that contribute to the shear resistance of a beam. On the other hand, the 45° truss model adds an empirical concrete contribution term to take the contribution of the concrete into account. The addition of the concrete contribution term in the 45° truss model and the variation of the angle  $\theta$  in the variable angle truss model really only serve the purpose of improving the predictions of shear strength compared to experimental results.

The traditional truss models assume that  $\theta$ , the inclination of principal diagonal compression stress, coincides with the direction of the inclined diagonal tension cracks. This is not the case since shear and tensile stresses are transmitted across the cracks so that  $\theta$  is actually lower than the inclination of the diagonal cracks. The variable angle truss model determines  $\theta$  from force equilibrium, but in order to determine the true value of  $\theta$  one would have to consider the forces at the diagonal tension cracks. The ability of the concrete to transfer forces across the cracks is a function of the width of these cracks or the extent of cracking, which in turn depend on how strained the web of the beam is. Morsch recognized this (ACI Committee 445, 1998), but it was believed to be impossible to determine the inclination of the cracks in a mathematical manner. However in 1929, Wagner, a German engineer solved a similar problem of a thin metal sheet loaded in shear (ACI Committee 445, 1998). Wagner assumed that after the sheet had buckled it would continue to carry shear by a diagonal tension field provided that it was stiffened with longitudinal and transverse stringers. He assumed that the angle of inclination of diagonal tension stresses in the buckled sheet would coincide with the direction of principal tensile strain. He then calculated the angle by determination of the deformations in the longitudinal and transverse stringers. This theory is known as tension field theory. A cracked concrete

plate loaded in shear is analogous to this problem, except that instead of buckling diagonal tension cracks form in the plate and the shear is then transmitted by a compression field. With the compression field theory, the angle  $\theta$  is determined considering the strain compatibility of the longitudinal reinforcement, the transverse reinforcement and the diagonally stressed concrete.

Mitchell and Collins (1974) from the University of Toronto first applied the compression field theory to reinforced concrete members subjected to torsion. Further development by Vecchio and Collins (1986) led to the Modified Compression Field Theory (MCFT) for reinforced concrete members subjected to shear.

The MCFT assumes that the direction of principal strain coincides with the direction of principal stress. Experimental investigation has shown that the assumption is reasonable, with principal stress and principal strain direction to be within  $10^\circ$  of each other. The MCFT allows concrete struts at an angle lower than the inclination of the cracks. Therefore, the MCFT recognizes correctly that the direction of principal compressive stress does not coincide with the inclination of the cracks. Because the MCFT allows the compressive stress field to be transmitted across cracks, and since the tensile stress field is perpendicular to the compressive stress field, this implies that tensile stresses also exist in the uncracked concrete between the cracks, that contribute to the shear resistance of the RC member.

The MCFT relates the strains in the cracked concrete to the strains in the reinforcement in terms of average strains that are measured over base lengths greater than the crack spacing. The same is done for equilibrium of the stresses in the concrete and the reinforcement. The MCFT treats cracked reinforced concrete as a new material. The stress strain relationship for cracked reinforced concrete that is required to relate the compatibility conditions to the equilibrium conditions is an empirically fitted relationship. The stress-strain curve obtained from a traditional cylinder test differs from that of the stress-strain curve of cracked reinforced concrete.

The failure of a cracked reinforced concrete element may be governed by local stresses and not average stresses occurring at the location where reinforcement crosses the crack. The MCFT accounts for this effect by limiting the average tensile stress to an upper allowable limit, which depends on the steel stress at the crack and the ability of the crack interface to resist shear stresses.

The stress in the transverse and longitudinal reinforcement are related to the shear stress and tensile stresses in the cracked concrete by means of the Mohr circles of modified compression field theory shown in figure 2.14,

$$\rho_y f_{sy} = f_y + v \tan \theta - f_1 \quad [2.32]$$

$$\rho_x f_{sx} = f_x + v \tan \theta - f_1 \quad [2.33]$$

$$f_2 = v / \sin \theta \cos \theta - f_1 \quad [2.34]$$

$f_1$  is the principal tensile stress in the concrete,  $f_2$  is the principal compressive stress in the concrete,  $v$  is the applied shear stress,  $\theta$  is the inclination of the cracks.

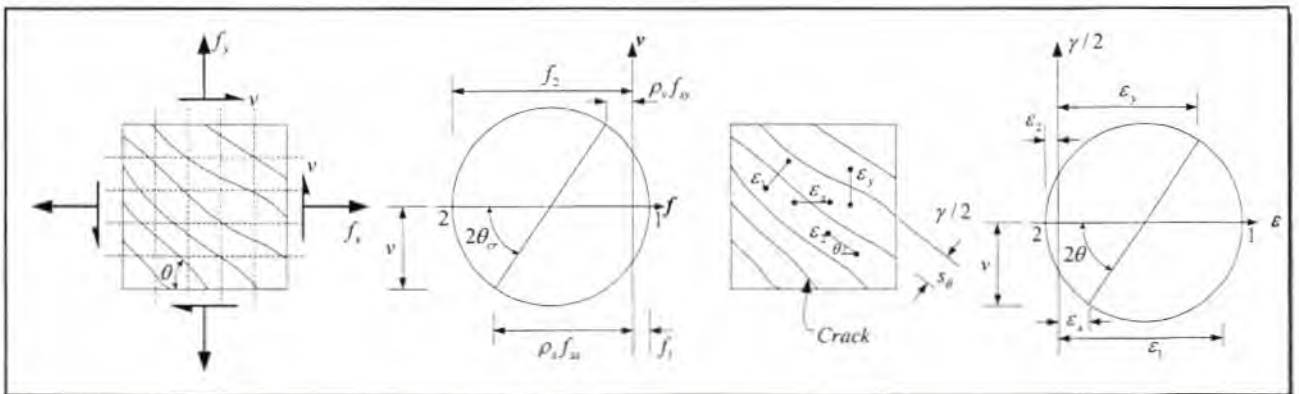


**Figure 2.14: Average Stress and strain conditions in a reinforced concrete element (Vecchio & Collins, 1986)**

To satisfy compatibility conditions strain in the steel reinforcement at a point must always equal the strain the concrete at that point, therefore

Transverse direction:  $\epsilon_{yx} = \epsilon_{sx} = \epsilon_x \quad [2.35]$

Longitudinal direction:  $\epsilon_{xy} = \epsilon_{sx} = \epsilon_x \quad [2.36]$

The subscript 's' denotes steel and the subscript 'c' denotes concrete.

From the Mohr circle, the strains in the transverse and longitudinal directions ( $\epsilon_x$  and  $\epsilon_y$ ) are related to the principal tensile strain  $\epsilon_1$  and the principal compressive strain  $\epsilon_2$  as follows:

$$\varepsilon_x + \varepsilon_y = \varepsilon_1 + \varepsilon_2 \quad [2.37]$$

$$\tan^2 \theta = \frac{\varepsilon_x - \varepsilon_2}{\varepsilon_y - \varepsilon_2} \quad [2.38]$$

The stress-strain relationship for steel and cracked concrete are needed to relate the stresses (equations 2.32 to 2.34) to the strains (equations 2.35 and 2.36).

For steel, the traditional linear relationship is used:

$$f_{sx} = E_s \varepsilon_x \leq f_{x,yield} \quad [2.39]$$

$$f_{sy} = E_s \varepsilon_y \leq f_{y,yield} \quad [2.40]$$

The stress strain relationship for cracked concrete, applied in the MCFT, is given by the following relationships derived from experiments (Collins et. al., 1999):

$$\varepsilon_2 = -0.002 \left( 1 - \sqrt{1 - f_2 / f_{2,max}} \right) \quad [2.41]$$

$$\text{where, } f_{2,max} = f_c / (0.8 + 170\varepsilon_1) \quad [2.42]$$

$$\text{and, } f_1 = \frac{f_{cr}}{1 + \sqrt{500\varepsilon_1}} \quad [2.43]$$

$$\text{but with, } f_1 \leq \frac{0.18\sqrt{f_c} \tan \theta}{0.3 + \frac{24w}{agg + 16}} \quad [2.44]$$

$$\text{where, } w = \frac{s_x}{\sin \theta} \varepsilon_1 \quad [2.45]$$

$f_{cr}$  is the principal compressive stress at initial cracking taken as  $0.33\sqrt{f_c}$  (MPa).

The upper limit on the principal tensile stress,  $f_1$ , as given by equation 2.43 is the limiting stress at which a crack can no longer transfer shear forces due to the slippage of the crack. The limiting stress is

a function of the crack width,  $w$ , which is taken as  $\epsilon_1$  multiplied by the crack spacing in the direction of principal tensile stress,  $s_x/\sin\theta$  and the maximum aggregate size,  $agg$ . The tensile stress  $f_1$  is at a maximum half way between two cracks and zero at the crack location. Figure 2.15 shows how the behaviour of cracked concrete subjected to tensile straining differs from that of the cylinder test where no tensile straining takes place. The peak compressive stress is much reduced compared to the uni-axial compression. Note  $f_{2,max}$  is equivalent to  $f_{d,max}$  used in Eurocode.

The tensile and compressive stress strain relationships for cracked reinforced concrete are shown graphically in Figure 2.15. Note how the peak compressive stress is reduced in cracked concrete due to the tensile straining as compared to the uni-axial compressive test where no tensile straining takes place.

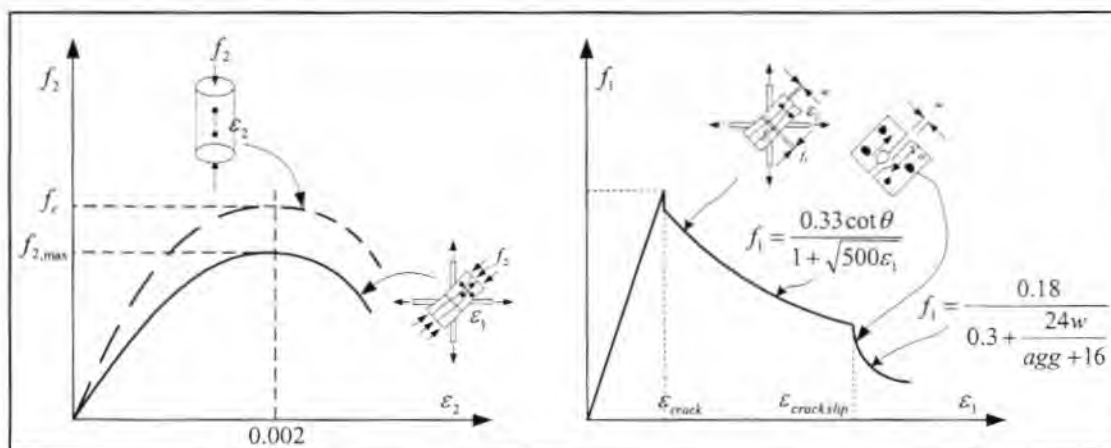


**Figure 2.15: Stress strain relationships for cracked concrete (Collins et. al., 1996)**

The equations on the previous pages can be applied to any type of reinforced concrete element, such as shear walls, slabs, beams and columns. A codified form of the MCFT, known as the General Shear Design Method (Collins et. al., 1996) has been adopted by the Canadian code and the American Bridge Design code (AASHTO LRFD: 2000).

### **The General Shear Design Method (GSDM)**

The General Shear Design method (Collins et. al., 1996) is essentially the MCFT cast into the form of the truss model with concrete contribution similar to that applied in SANS. Concrete contribution is

defined by the GSDM as the vertical component of the principal tensile stress,  $f_l$  in the uncracked concrete between the inclined cracks.

$$v = \frac{V}{b_w z} \quad [2.46]$$

$$v = v_c + v_s = f_l \cot \theta + \frac{A_v f_{yv}}{bs} \cot \theta \quad [2.47]$$

Equation 2.47 is a form of equation 2.32, with  $f_y = 0$ , since no force is applied in the transverse direction of the beam.

The concrete contribution is given as a function of the principal tensile strain from equation 2.43 and 2.44 is then,

$$v_c = \frac{0.33 \cot \theta}{1 + \sqrt{500 \epsilon_1}} \leq \frac{0.18}{0.3 + \frac{24 \epsilon_1 s_x}{(agg + 16) \sin \theta}} \quad [2.48]$$

The upper limit of  $f_l$  is reached when the shear at the crack interface,  $v_{ci}$  can no longer be transmitted across the crack due to the yielding of the stirrups and slipping of the crack.

In order to determine  $f_l$ , the principal tensile strain,  $\epsilon_1$ , has to be calculated.

From equations 2.37 and 2.38 an expression for  $\epsilon_l$  is derived:

$$\epsilon_1 = \epsilon_x + (\epsilon_x - \epsilon_2) \cot^2 \theta \quad [2.49]$$

now substituting for  $\epsilon_2$  from equation 2.41:

$$\epsilon_1 = \epsilon_x + \left( \epsilon_x + 0.002 \left( 1 - \frac{f_2}{f_{2,\max}} \right) \right) \cot^2 \theta \quad [2.50]$$

$f_2$  is given by equation 2.34. Note that equation 2.34 is similar to 2.13(b) the expression for the stress in the compression struts of Ritter's truss model. Ritter's model did not recognize the presence of tensile stresses in the concrete struts. In the general model,  $f_1$  is taken as 0 when calculating  $f_2$  in order to simplify the calculation. The assumption is conservative since the presence of the tensile stresses reduces the compressive stress in the struts, therefore:

$$f_2 = v / \sin \theta \cos \theta \quad [2.51]$$

Then substituting 2.51 in 2.50 for  $f_{2,max}$  the we obtain:

$$\epsilon_1 = \epsilon_x + \left( \epsilon_x + 0.002 \left( 1 - \sqrt{1 - \frac{v}{f_c} \left( \frac{0.8 + 170\epsilon_1}{\sin \theta \cos \theta} \right)} \right) \right) \cot^2 \theta \quad [2.52]$$

Note that  $\epsilon_1$  occurs on both sides of the equation requiring some iteration to find the correct solution for  $\epsilon_1$ . The principal tensile strain is expressed in terms of the strain in the longitudinal direction of the beam, since it is easier to visualize straining in that direction. The main simplification of MCFT in deriving the General shear design method is made in calculating  $\epsilon_x$ . Ideally when applying the MCFT to a reinforced concrete element the element can be divided into a number of slices and the strains can be calculated at each slice, from which the stress distribution through the depth of the element can be determined. (Vecchio and Collins, 1988) This is only possible to do in a software application. For the GSDM the *average* longitudinal strain in the web of the beam is approximated and used to determine the shear resistance. The manner in which the longitudinal strain,  $\epsilon_x$  for the GSDM, is calculated is discussed in the following section 2.3.3.1

The application of the 45° truss model to SANS, the plasticity theory to Eurocode and the MCFT to AASHTO is discussed in the following section.

## 2.3.3 Application to codes

### 2.3.3.1 SANS 10100-1: 2003

SANS 10100 applies the 45° truss model with concrete contribution. SANS 10100 is based on the British code BS8110. The stress distribution is based on the Mörsh formula (equation 2.5).

45° Planar Truss Model with concrete contribution, expressed as a stress:

$$v = v_c + v_s \quad [2.53]$$

$$v = \frac{0.75}{\gamma_{m,c}} \left( \frac{f_{cu}}{25} \right)^{1/3} \left( \frac{100A_s}{b_w d} \right)^{1/3} \left( \frac{400}{d} \right)^{1/4} + \frac{A_v f_{yv}}{\gamma_{m,s} b_w s}$$

Maximum allowable limit on  $v$ :

$$v \leq 0.75 \sqrt{f_{cu}} \leq 4.75 \text{ MPa} \quad [2.54]$$

Minimum amount of shear reinforcement:

- No shear reinforcement is required if  $v < 0.5v_c$
- Nominal shear reinforcement is required for  $0.5v_c < v < v_c$
- Stirrups must be designed according to equation 2.54 for  $v > v_c$

No shear reinforcement is required for slabs unless  $v$  exceeds  $v_c$

Nominal stirrups are as follows:

For mild steel stirrups: 
$$v_s = \frac{A_v f_{yv}}{b_s} \geq 0.0012 f_{yv}$$

For high strength stirrups: 
$$v_s = \frac{A_v f_{yv}}{b_s} \geq 0.002 f_{yv}$$

Where  $b_t$  is the web width at the level of tension reinforcement. Limits are placed on the spacing of stirrups:

Longitudinal spacing of the stirrups:  $s \leq 0.75d$

Spacing of stirrup legs along the breadth of the beam:  $s \leq 0.75d$

To account for the effect of the shear force on the longitudinal reinforcement, SANS requires that the longitudinal tension reinforcement be extended a minimum of the effective member depth,  $d$ , or twelve times the diameter of the smallest bar, beyond the point where it is no longer needed. It is also forbidden to end tension steel in the tension zone of a beam, unless the shear resistance at the section is twice the applied shear force, or alternatively the amount of tension steel area provided is twice the area required.

### 2.3.3.2 EN 1992 Eurocode 2: 2003 (based on CEB-*fip* Model Code 1990)

The design of shear reinforcement is based on the variable angle truss model. For members with vertical stirrups the shear resistance of a beam is taken as the minimum of,

$$v = \left[ \frac{V}{0.9b_w d} \right] = \frac{A_{sv} f_{yd}}{b_w s} \cot \theta \quad [2.55]$$

$$v_{d,\max} = \left[ \frac{V}{0.9b_w d} \right]_{\max} = v f_{cd} \sin \theta \cos \theta \quad [2.56a]$$

$$\text{or } v_{d,\max} = \left[ \frac{V}{0.9b_w d} \right]_{\max} = v f_{cd} / (\cot \theta + \tan \theta) \quad [2.56b]$$

The limiting values of  $\theta$  are as follows:

$$21.8^\circ \geq \theta \geq 45^\circ \quad [2.57]$$

$$1 \leq \cot \theta \leq 2.5$$

When designing the shear reinforcement according to equation 2.56 the concrete contribution is ignored. The expressions for the maximum allowable shear stress, or the stress at which the beam will fail by crushing of the web, is given by equations 2.56(a) and 2.56(b). The two expressions are equivalent; they are often expressed in one or the other form in the literature. It is important to note that the shear stress distribution for Eurocode is different from that of SANS. Eurocode assumes that the flexural lever arm  $z$  is  $0.9d$  instead of  $d$ . This only applies to members with shear reinforcement; for members without shear reinforcement the shear distribution is taken as  $V/b_w d$ .

The material properties  $f_{yd}$  and  $f_{cd}$  represent the design values. They are calculated by dividing the 5% characteristic values of  $f_{yk}$  and  $f_{ck}$  by the respective partial material factors for steel and concrete. This approach is also taken by SANS where  $f_{yv}$  and  $f_{cu}$  are also the 5% characteristic values as defined in SABS 0100-2. The factor  $v$  is taken as 0.6 for normal strength concrete.

The design approach to be taken is as follows. The value of  $\cot \theta$  is calculated for the case where the applied shear stress  $v$ , equals  $v_{max}$  from equation 2.56. If the value of  $\cot \theta$  is greater than the maximum or minimum value as given by 2.57 then the limiting value of  $\theta$  is chosen for design. If the value of  $\cot \theta$  falls within this range, then that value is chosen. The shear reinforcement is then calculated from equation 2.55. This procedure ensures that the minimum possible  $\theta$  (or maximum  $\cot \theta$ ) will be chosen, leading to the most economical design of stirrups possible with the variable angle method. Two basic situations may arise:

1. For members lightly stressed in shear,  $\cot \theta$  may be higher than 2.5 thus enforcing the lower limit on  $\theta$ . In effect the method followed by Eurocode then becomes a *fixed angle truss method* with  $\theta$  constant at  $21.8^\circ$ . This applies to a range of situations where the beams are stressed below some value where the lower limit on  $\theta$  comes into effect.
2. For more highly stressed members  $\cot \theta$  falls within the limits of equation 2.57. Only in this range of applied shear stresses, is the method applied by Eurocode truly a variable angle truss method. It is highly unlikely that  $\cot \theta$  will fall below 1.0 as this will only occur at very high stress levels.

Eurocode follows the same rules as SANS regarding the provisions for minimum shear reinforcement. Similar to SANS no shear reinforcement is required if the applied shear stress is less than half the concrete contribution, where the concrete contribution is calculated from the appropriate Eurocode formula for members without shear reinforcement. Nominal amount of stirrups are provide according to the following rule (Moss and Webster, 2000):

$$v_{s,\min} = \frac{A_{sv}f_{yk}}{b_w s} \geq 0.08\sqrt{f_{ck}} \quad [2.58]$$

Stirrup spacing may not exceed 75% of the effective member depth, in any direction as with SANS.

The effect of the shear force on the longitudinal tension reinforcement is accounted for explicitly by Eurocode. The tension steel reinforcement must fulfil the following requirement:

$$A_s f_y \geq \frac{M}{0.9d} + \frac{V}{2} \cot \theta \quad [2.59]$$

Alternatively the moment diagram can be displaced by  $0.5z \cot \theta$ , with  $z = 0.9d$ , when designing the bending reinforcement.

If  $\theta$  is taken as  $45^\circ$  then the tension reinforcement would need to be extended  $0.45d$  past the point where it is no longer needed. If  $\theta$  is  $21.8^\circ$  then the required extension would be  $1.125d$ . SANS requires an extension of  $d$  so this is conservative for most cases compared to Eurocode.

The maximum allowable shear stress from Figure 2.13 derived from plasticity theory is then,

$$\frac{v_u}{v f_{cd}} = 0.5 \quad \text{with} \quad v = \frac{V}{bz} = \frac{V}{0.9bd}$$

From this follows that  $V_u = 0.45v f_{cd} b_w d$ , which is the maximum allowable shear stress given by Eurocode 2003 and the CEB: 1978.

### 2.3.3.3 AASHTO LRFD 2000 and CSA-23.3 1994

The shear resistance of a reinforced concrete beam designed according to AASHTO is given by the following expression, based on the MCFT:

$$v = \frac{V}{0.9b_w d} = v_c + v_s = \beta \sqrt{f_c} + \frac{A_v f_{yv}}{bs} \cot \theta \quad [2.60]$$

The General Shear Design Method as it is applied in the design codes expresses the concrete contribution  $f_c \cot \theta$  (equation 2.47) by an equivalent term  $\beta \sqrt{f_c}$ . The factor  $\beta$  is a 'crack factor' that depends on the longitudinal strain in the web of the beam. Values of  $\beta$  and  $\theta$  can be determined from graphs derived from the MCFT for a certain level of applied shear stress  $v$  and longitudinal strain in the web of the beam  $\epsilon_x$ . The graphs are shown in figures 2.17 and 2.18.

The longitudinal strain is calculated from the following expression:

$$\epsilon_x = 0.5\epsilon_t = \frac{M_u / 0.9d + 0.5V_u \cot \theta + 0.5N_u - A_p f_{po}}{2(A_s E_s + A_p E_p)} \quad [2.61]$$

The strain equation is given here in its general form. It can be applied to pre-stressed beams and members subjected to an axial force  $N_u$  such as beam-columns, hence the name general shear design method. The horizontal component of the pre-stressing force,  $A_p f_{po}$  decreases the tensile strain in the web, therefore improving the shear strength of the beam. An axial force  $N_u$  can be tensile or compressive. Figure 2.16 illustrates the concept of the strain in the web of a cracked RC beam due to shear, bending and axial forces.

The AASHTO LRFD 2000 follows the American approach of applying an overall resistance factor denoted,  $\phi$  instead of partial material factors. The overall resistance of a member is given by:  $v_u \leq \phi v$ , where  $\phi$  has a value of 0.9 and  $v$  was calculated according to equation 2.60.

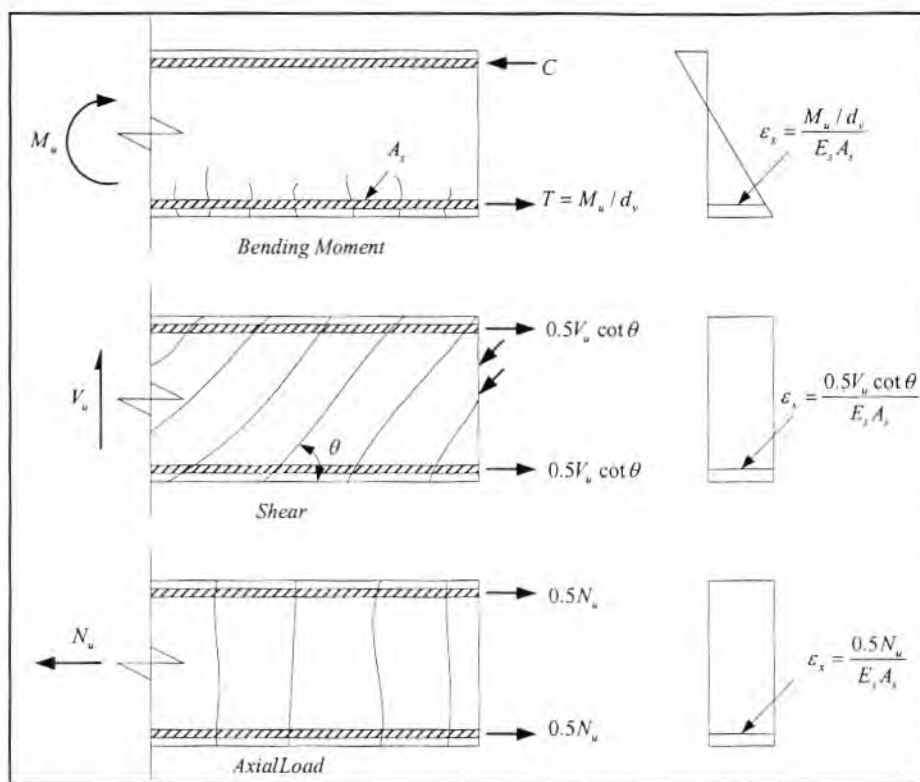


**Figure 2.16: Determination of strain  $\epsilon_x$  in non pre-stressed beam (Collins et. al., 1999)**

Nominal shear reinforcement has to be provided according to the same rules as outlined in SANS and Eurocode. Nominal shear reinforcement is calculated according to the equation 2.60 also applied in the Eurocode, but with 0.08 replaced by 0.083. The amount of longitudinal tension reinforcement must be able to withstand the bending moment as well as the shear force, as given by:

$$A_s f_y \geq \frac{M}{\phi z} + \frac{V}{2} \cot \theta \quad [2.62]$$

The strain on the beam depends on the value of  $\theta$ , as well as the ultimate applied shear force at the section  $V_u$ . When calculating the shear resistance of an existing beam, the applied shear force  $V_u$  equals the shear resistance  $V$  of equation 2.60 which also depends on  $\epsilon_x$ . Some iteration is required to find the correct set of  $\epsilon_x$ ,  $\beta$  and  $\theta$  where  $V = V_u$ .

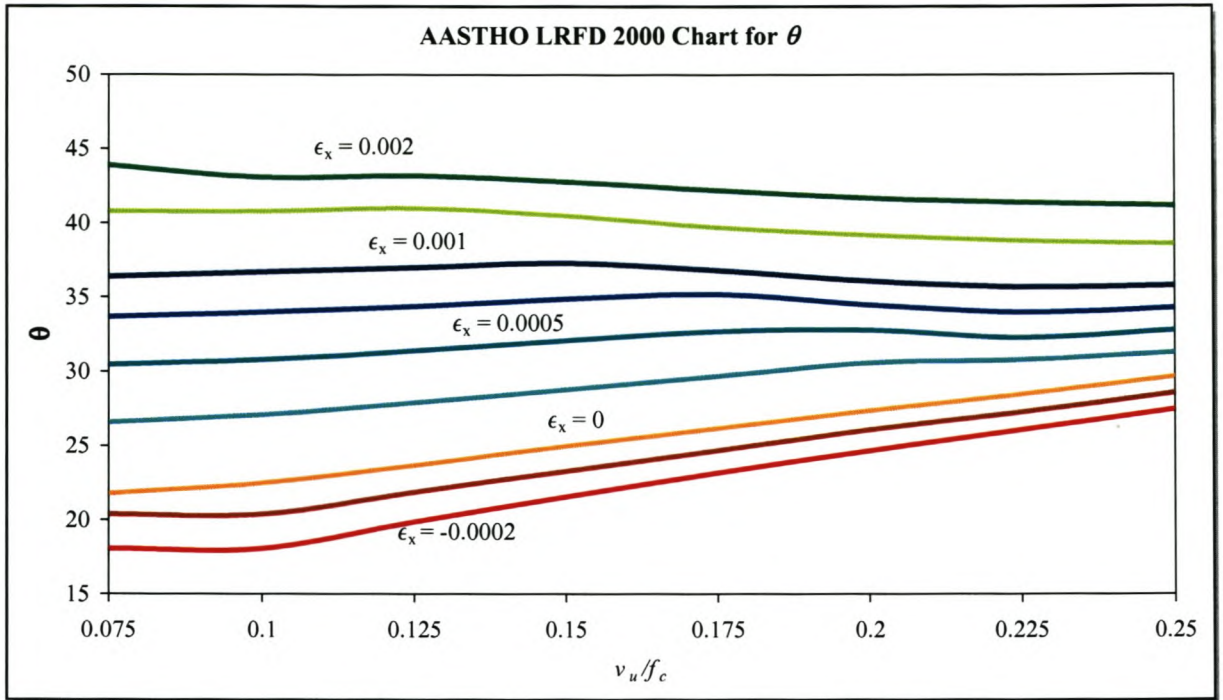


**Figure 2.17: AASHTO LRFD 2000  $\theta$  Chart for members with shear reinforcement**

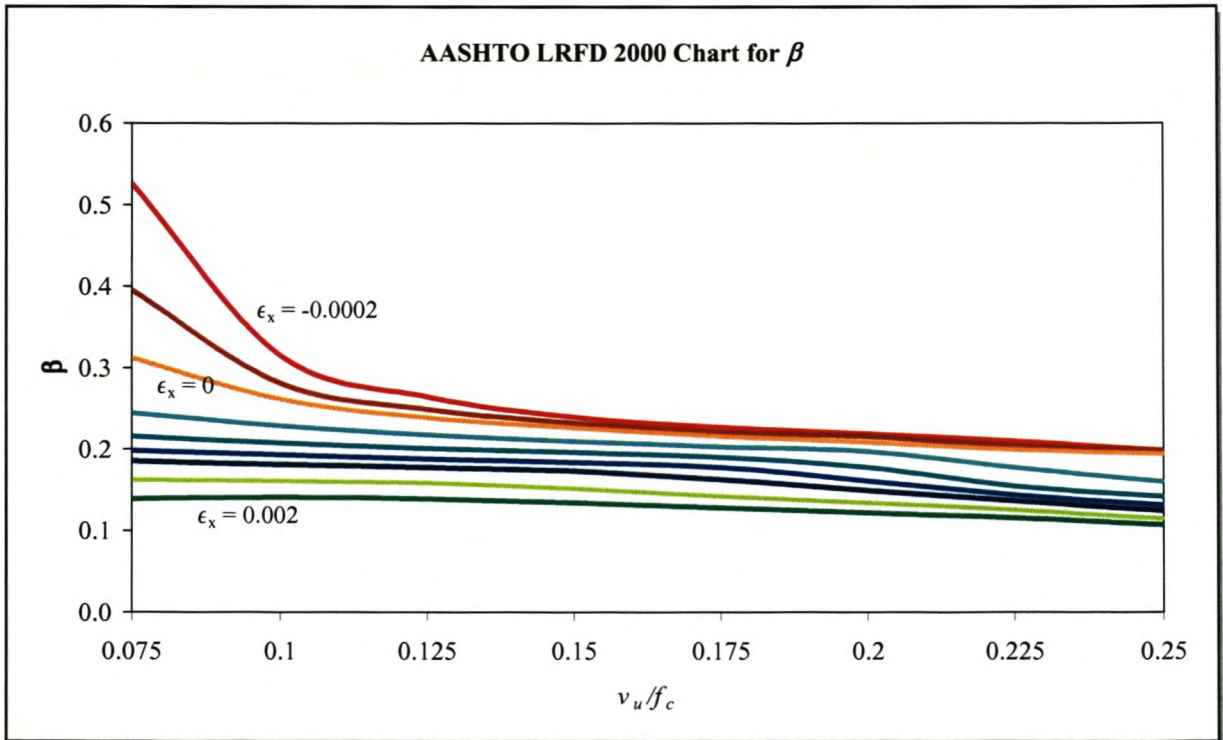


**Figure 2.18: AASHTO LRFD 2000  $\beta$  Chart for members with shear reinforcement**

Figure 2.17 and 2.18 give valuable insight to the behaviour of RC members subjected to shear:

- With increased longitudinal tensile straining in the web of a RC beam (i.e. increasing  $M/Vd$  ratio) the concrete contribution  $(\beta\sqrt{f_c})$  decreases. Increased straining leads to increased crack width which reduces the crack interface shear capacity.
- Concrete contribution decreases with increased applied shear stress.
- The shear resistance of lightly stressed beams can be enhanced with pre-stressing (which may lead to compressive strains of up to 0.0002 mm/mm) which leads to a dramatic increase in concrete contribution. The pre-stressing helps maintain narrow crack widths, thereby maintaining crack interface shear capacity.
- $\theta$  increases with increased straining in the web, but remains fairly constant with increased applied shear stress. According to equation 2.60 an increase in  $\theta$  will lead to a decrease in the contribution of the steel to shear resistance. Therefore for highly strained beams both concrete contribution and steel contribution decreases.

#### 2.3.3.4 Comparing the SANS, Eurocode and AASHTO

In this section SANS, Eurocode and AASHTO are compared to each other. First the design limits of the codes are compared after which SANS and Eurocode are compared conceptually. Finally all three codes are compared by means of a specific example.

##### (a) Design limits of the codes

The SANS, Eurocode and AASHTO design codes all take different approaches to shear design of reinforced concrete beams. The classical approach taken by SANS is simplest and least time consuming method of the three. However SANS is more limited in its range of application than the European and American code, due to its empirical nature. The constraints on the range of applicability of the SANS method derive from the empirical expression of the concrete contribution. Eurocode uses a similar empirical expression to SANS for members without shear reinforcement, but since the

concrete contribution is ignored for members with shear reinforcement the constraints on this expression has no effect.

Eurocode allows a maximum shear strength according of

$$\frac{v_u}{v f_{cd}} = 0.5 \quad [2.63]$$

For a concrete cube strength of 40 MPa, which is an equivalent cylinder strength of about 32 MPa, and a partial material factor for concrete of 1.5 and  $v = 0.6$ , a maximum shear stress of 6.4 MPa is allowed compared to 4.75 MPa for SANS. For higher strength concretes higher stresses are allowed. AASHTO allows a maximum  $v/f_c$  equal to 0.25 (Figure 2.18). Therefore a maximum shear stress of 7.2 MPa for cylinder strength of 32 MPa is allowed taking a resistance factor of 0.9 into account.

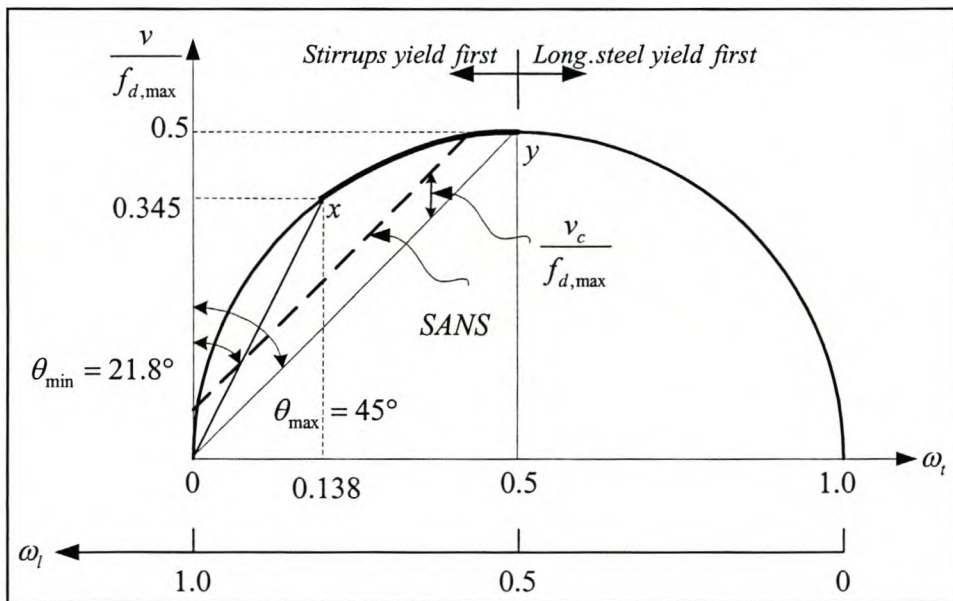


Figure 2.19: Comparing SANS10100-1 and EN 1992 Eurocode 2

**(b) Conceptual comparison of SANS and Eurocode**

Figure 2.19, above, shows the graphical representation of the variable angle truss method applied by Eurocode as compared to the 45° truss model applied by SANS method. Figure 2.19 is identical to Figure 2.13 but with the SANS model added. The horizontal axis represents the amount of shear

reinforcement normalized with respect to the maximum stress in the concrete compression struts  $v f_c$  according to the variable angle strut model:

$$\text{Shear reinforcement index: } \omega_v = \frac{\rho_v}{v f_c} = \frac{A_v f_{yv}}{v f_c b_w s} \quad [2.64]$$

The vertical axis represents the applied shear stress normalized with respect to  $v f_c$ .

The 45° line in figure 2.19 represents the 45° truss model without the concrete contribution. The dashed 45° line represents the SANS 45° truss model with the concrete contribution. It is assumed that the concrete contribution remains constant over the range of shear reinforcement in this comparison, but in reality the concrete contribution will decrease slightly with an increasing shear reinforcement index.

Figure 2.19 shows that for relatively highly reinforced members Eurocode will require less shear reinforcement compared to SANS for the same applied shear stress. For a normalized shear stress ratio of 0.345, Eurocode will require a shear reinforcement index of 0.138. SANS will require roughly 0.25 for the same applied shear stress, depending on the value of concrete contribution. It is difficult to represent the AASHTO method on this graph but from figure 2.16 it can be seen that for a constant strain,  $\theta$  increases with increasing applied stress. The increase in  $\theta$  is not as non-linear as predicted by the variable angle method of Eurocode. This can be seen in figure 2.17 where the AASHTO  $\theta$  remains fairly constant with increasing applied shear stress. SANS and Eurocode will display very different results over a range of applied shear stresses. For very lightly reinforced members Eurocode may require less shear reinforcement than SANS.

### (c) Comparison of SANS, Eurocode and AASHTO by means of a specific example

Figure 2.19 indicates that the difference in the behaviour of SANS and Eurocode is closely related to the amount of shear reinforcement. Differences are also expected for different concrete contribution because Eurocode does not take concrete contribution into account. The factors affecting concrete contribution are numerous and are not closely investigated in the specific example. A section of 300 mm width and 500 mm effective depth, with 2% longitudinal tension steel and  $f_c = 31.6$  MPa ( $f_{cu} = 40$  MPa) was chosen for the example. These parameters which affect the concrete contribution were kept

constant while the amount of shear reinforcement was increased from 0.4 MPa to 4.0 MPa. The  $a/d$  ratio was taken as 2.0, 4.0 and 6.0.

Figure 2.20 shows the plot of shear resistance against shear reinforcement in MPa. Safety factors were included for calculating the shear resistance according to the codes. AASHTO applies an overall resistance factor of 0.9. SANS and Eurocode apply a partial material factor for concrete of 1.4 and 1.5, respectively and a partial material factor of 1.15 for steel.

The following general deductions can be made from figure 2.20:

- The behaviour of SANS and AASHTO with respect to increasing shear reinforcement is very similar, while the behaviour of Eurocode deviates from that of the other two codes.
- SANS and Eurocode are not sensitive to the effect of the  $M/Vd$  (or  $a/d$ ) ratio. AASHTO predicts that shear resistance will decrease with increasing  $a/d$ .

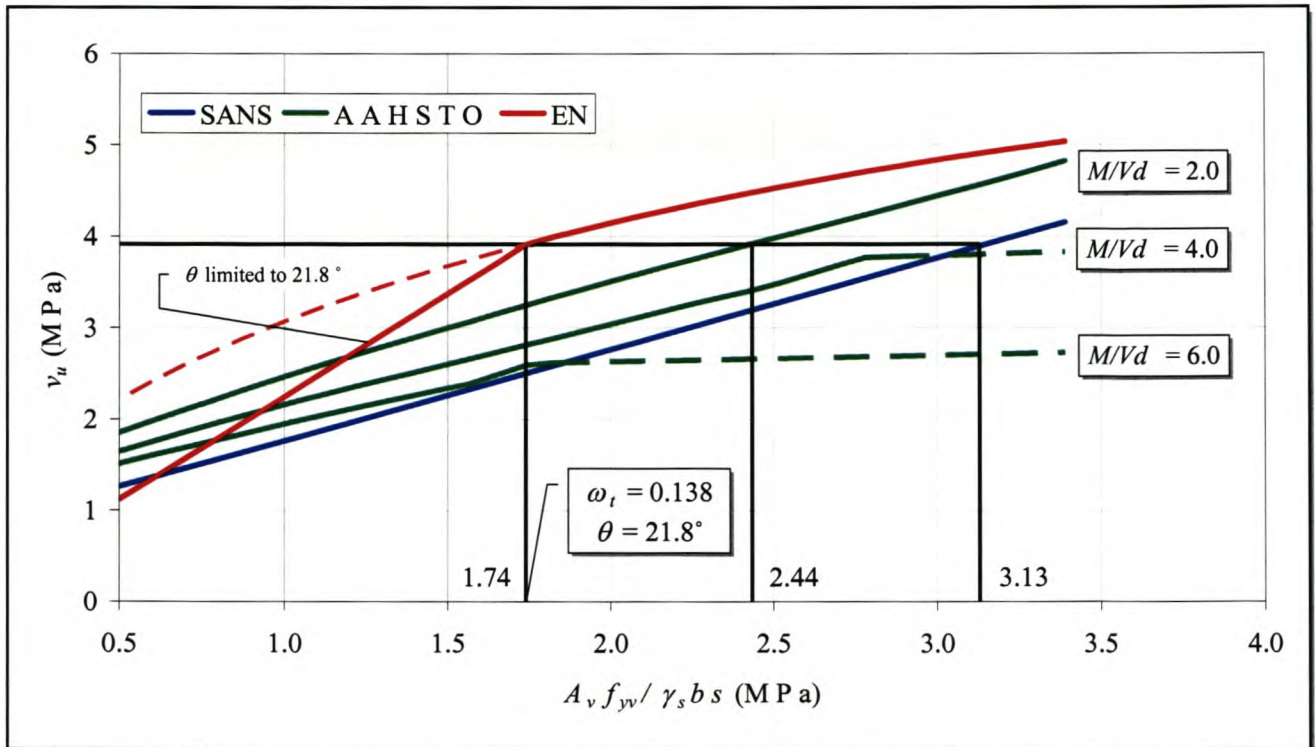


**Figure 2.20: Applied shear stress vs. amount of shear reinforcement compared for SANS, Eurocode and AASHTO**

- SANS is the most conservative of the three codes since it requires more shear reinforcement than the other two codes for the same applied shear stress for almost the entire range of shear reinforcement for this example. Eurocode is the least conservative of the codes; it requires the least shear reinforcement of the three codes.
- In the range where  $\theta$  is constant at  $21.8^\circ$  the required increase in shear reinforcement with increasing applied stress for Eurocode is much more rapid than for the other two codes.
- For very lightly reinforced members Eurocode may actually be more conservative than the other two methods. This conservatism may increase as the concrete contribution increases (for example if the section depth is decreased). This would cause SANS and AASHTO to move upwards.

More specifically for an ultimate shear stress of 3.9 MPa, Eurocode requires a factored amount of shear reinforcement of 1.74 MPa. Incidentally this is the point where Eurocode changes from the constant angle method to the variable angle method. The shear reinforcement index is 0.138 at this point:

$$\omega_t = \frac{A_v f_{yv}}{\gamma_{m,s} b s} / 0.6 f_{ck} = 1.74 / (0.6 \times 31.6 / 1.5) = 0.138$$

The turning point is always at  $\omega_t = 0.138$  regardless of the partial material factors. For the same applied shear stress SANS requires 3.13 MPa of steel, which is significantly more than that required by Eurocode. AASHTO requires 2.44 MPa of steel for  $a/d = 2.0$ . Because AASHTO does not apply a partial material factor for steel of 1.15 the required amount of steel is actually  $2.44 \times 1.15 = 2.81$  MPa. This value is quite close to the value required by SANS. According to AASHTO the beam will fail in bending for  $a/d = 4.0$  and  $6.0$  as indicated by the dashed lines for an applied shear stress of 3.9 MPa.

Although the example does not investigate the effects of concrete contribution it gives a clear indication to the differences in behaviour of the codes. The significant difference in behaviour of the Eurocode compared to the other two codes, especially in the range of shear reinforcement where  $\theta$  is constant and also the omission of a concrete contribution term makes it likely that Eurocode will show a much higher level of uncertainty when compared to experimental data than the other two codes.

## Chapter 3

### Introduction to Reliability analysis of SANS10100-1: 2003 shear design procedure

The fundamental purpose of calibrating loading and resistance codes is to ensure that a certain specified minimum level of reliability is maintained over the entire range of design situations. Other considerations include the economy and user friendliness in applying the codes to design practice. The reliability of a specific failure mechanism such as shear resistance of reinforced concrete beams derives from the difference between the expected values of the resistance and that of the applied loads. However both the resistance and the applied loads are subject to a statistical distribution with a certain mean and standard deviation as shown in figure 3.1.

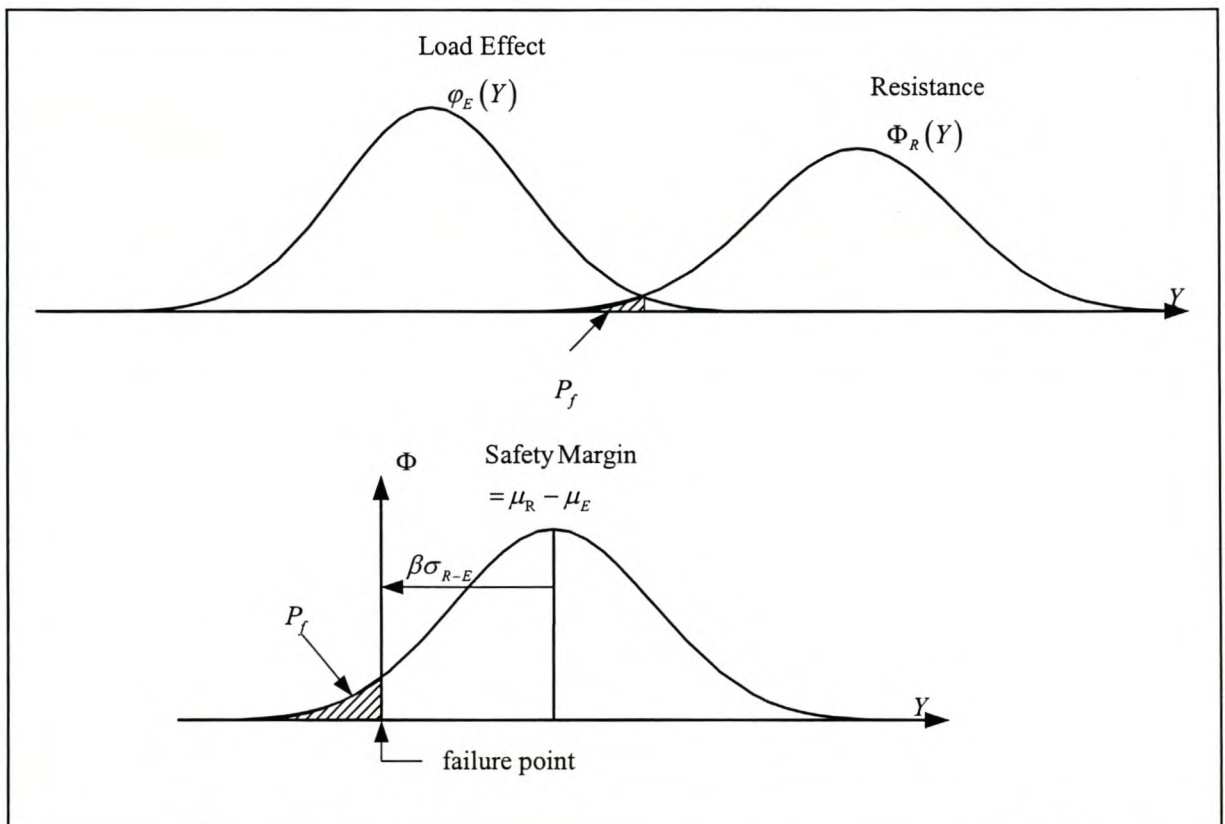


Figure 3.1: Probability density function of the limit state equation.

Failure occurs where the tail ends of the resistance and load distributions overlap. The safety level may be improved by increasing the difference between the expected value of resistance and the expected value of the applied loads. However a greater level of safety comes at the expense of reduced economy. The minimum level of reliability is expressed as the reliability index  $\beta$  which represent the number of standard deviations,  $\sigma_{R-E}$ , that the difference between the expected value of the resistance and the expected value of the loads,  $\mu_{R-E}$ , known as the safety margin, is situated from the failure point.

The reliability of a failure mechanism for a structural element is expressed by a limit state function in the form (Holický and Retief, 2005):

$$g(\mathbf{X}) = R - E \quad [3.1]$$

Where  $R$  is the resistance and  $E$  is the load effect.  $\mathbf{X}$  is a vector of basic variables on which the resistance and loads depend. A structure is safe as long as  $g(\mathbf{X}) > 0$  and will fail if  $g(\mathbf{X}) \leq 0$ . The probability of failure of the element is then given by:

$$P_f = \text{Probability}(g(\mathbf{X}) \leq 0) = \int_{g(\mathbf{X}) \leq 0} \phi_g(\mathbf{X}) d\mathbf{X} \quad [3.2]$$

Where  $\phi_g$  is the joint probability density distribution of the basic variables,  $\mathbf{X}$ . Suppose  $Y$  is a single variable say a shear force that can either be defined as the resistance of a member  $R(Y)$  or the load on a member  $E(Y)$  then probability of failure is expressed as:

$$P_f = \text{Prob}(g(Y) \leq 0) = \int_{-\infty}^{\infty} \phi_E(Y) \Phi_R(Y) dY \quad [3.3]$$

$\phi_R(Y)$  is the probability density function of  $R(Y)$  and  $\phi_E(Y)$  is the probability function of  $E(Y)$ . These probability density functions are often not available due to the lack of data, and even if they are known the solution of the above equation may be costly. Standardised normal distributions are used as an approximation. Often only the first and second moments, i.e. the mean and variance of the variables are known. A technique known as the First Order Second Moment (FOSM) is used to find the failure point of the limits state function.

The probability of failure is then given by,

$$P_f = \Phi(-\beta) \quad [3.4]$$

where  $\Phi$  is the cumulative distribution function of the standardized normal distribution.

The overall minimum value of the reliability index for the ultimate limit state for the European loading code, EN 1990 is  $\beta_t = 3.8$  for a fifty year period and  $\beta_t = 3.0$  for the South African loading code SABS (Reliability Assessment of Alternative Load Combination Schemes for Structural Design, Holický and Retief).

Modern loading codes are divided into material independent loading codes and material based design codes. Ideally the loading codes should be calibrated together with all the material codes. However this is not practical and as a result the calibration of the loading code and the resistance code is separated into two stages (Ter Haar and Retief). First the loading code is calibrated. A set of optimum partial load factors is determined in such a way as to minimize the target and actual reliabilities over all practical load ratios. The resistance is modelled as a single stochastic variable with lognormal distribution. The coefficient of variation of the generic resistance model is varied to represent varying uncertainties of the different failure mechanism in the material codes. The second stage involves the calibration of material codes. Partial material factors as well as resistance factors must be derived that are compatible with the load factors of the loading code.

It is not the purpose of this thesis to calibrate the partial material factors for the shear failure mechanisms of the South African concrete code, SANS 10100-1: 2003, but only to determine the level of reliability as described by the reliability index  $\beta$ . Reliability index for the limit state functions of shear failure mechanisms can be determined independently by expressing the limit state function as follows:

$$g(\mathbf{X}) = R(\mathbf{X}) - R_d \quad [3.5]$$

$R(\mathbf{X})$  is a general probabilistic model for shear representing resistance side of the limit state function.  $R_d$  is the deterministic code design shear resistance for a specific case for which the reliability is to be

determined.  $R_d$  represents the load effect side of the limit state equation. In this manner the reliability inherent to the resistant side of the design process can be determined independent from the load side.

The general probabilistic model for shear represents the true shear resistance which is subject to uncertainties in parameters that affect the shear resistance. These parameters are modelled as basic variables each subject to a statistical distribution. The general probabilistic model is based on an existing shear design model, where the variables of the design model are modelled as basic variables. A major source of uncertainty is the accuracy to which the design procedure is able to predict the true shear resistance. As a result the general probabilistic model for shear includes a model factor as one of the basic variables in order to quantify the uncertainty in the model to predict the true shear resistance. This model factor is obtained by comparing the applied model to experimental data. In theory any shear design procedure can serve as a model. One could use the shear design procedure of SANS, Eurocode or AASHTO; however the general probabilistic model should be based on the design procedure with the least uncertainty in its model factor. The model factor usually contributes significantly to the uncertainty in the general probabilistic model compared to the other basic variables such as material and geometric properties. It is therefore important to model the model factor accurately. In this thesis SANS was used as a basis for the general probabilistic model. The properties of the model factor were derived in Chapter 4. In Chapter 5 the SANS probabilistic model is applied to determine the reliability of the SANS shear design procedure for beams.

The reliability of the limit state function is determined by the safety margin (the mean difference of  $R(X)$  and  $R_d$ ). The safety margin is determined by the bias in the basic variables as well as the value  $R_d$ .

### **Bias of basic variables**

The calculation of resistance and loads are based on characteristic values for the basic variables. Characteristic values of basic variables are lower than the expected values for resistances and higher than the expected values for loads. For the resistance typically only the material properties, such as concrete compressive strength and steel yield strength in the case of shear, are taken as the characteristic values. The use of characteristic values for material properties introduces a conservative bias for these basic variables into the general probabilistic model for shear. This increases the safety margin and thereby increases the reliability. Other variables such as the dimensions and steel areas are taken as their nominal (or design) values when calculating the resistance. These nominal values may be

biased (i.e. the nominal value is either larger or smaller than the expected value) but the bias is generally small for dimensions and steel areas.

SANS 10100-1:2003 requires that the 5% characteristic values of concrete compressive and steel yield strength be used. This means that if a concrete is tested only 5% of the test values may fall below the characteristic value, or alternatively there is a 5% probability that the concrete strength will fall below this value.

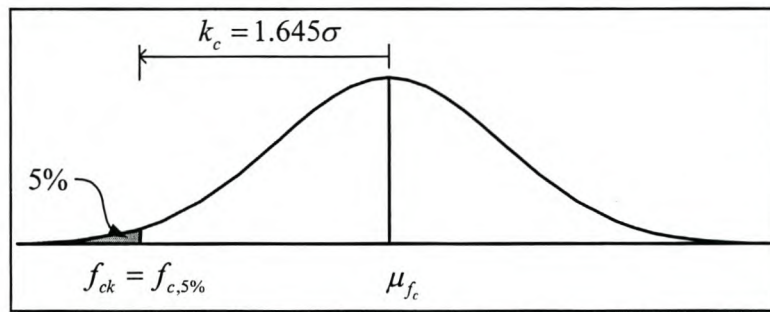


**Figure 3.2: Definition of the characteristic value**

Assuming a normal distribution the mean compressive strength of concrete can be calculated from the 5% characteristic value  $f_{ck}$  as follows:

$$\mu_{f_c} = f_{ck} + 1.645\sigma_{f_c} \quad [3.6]$$

where  $\sigma$  is the standard deviation. Concrete has a higher variability than steel and therefore a higher standard deviation, resulting in a higher conservative bias for concrete.

Variables such as member dimensions and steel area are taken as their nominal (or design) values when calculating shear resistance. However often the nominal value used by the designer does not represent the in-situ (or expected) value. For example, a beam may be slightly wider when cast than specified by

the designer. If the expected value is higher than the nominal value, the variable has a conservative bias that may introduce additional safety to the resistance side of the limit state equation.

$$\text{Bias} = \frac{\text{Expected Value}}{\text{Nominal Value}} = \frac{\text{Mean Value}}{\text{Design Value}} \quad [3.7]$$

The bias has a statically distribution with a certain coefficient of variation. Typically, the bias and coefficient of variation are very small for dimensions and steel area and will have little effect on the reliability of shear resistance. The conservative bias of the concrete compressive strength is calculated by dividing the expected value by the characteristic value.

The use of characteristic values is one way to introduce additional safety into the shear design procedure of the code. Another means of ensuring reliability is the use of safety factors in the design procedure.

### **Partial material factors and resistance factors**

Two possibilities exist to adjust the level of reliability to account for the uncertainty of the basic variables and the model uncertainty. One is to multiply the resistance by a resistance factor smaller than 1.0 and the other is divide the material strengths with partial material factors. Strictly speaking, the resistance factor is meant to account for the model uncertainty and the material factors are supposed to account for the material uncertainty. In the case of the shear resistance equations for members without shear reinforcement for SANS, the partial factor for concrete actually takes on the form of a resistance factor although its symbol, by definition  $\gamma_c$  indicates it to be a partial material factor, because the overall shear resistance is divided by the partial material factor for concrete instead of the concrete compressive strength. The resistance model is a function of the material strengths, therefore the resistance factors are also subjected to the uncertainty of the material properties. Similarly, few structural elements exist where the resistance is only a function of the material strengths. Therefore, the partial material and resistance factor are seldom 'pure' partial material or resistance factors.

The reliability of a failure mechanism is also affected by the mechanics of the resistance function. Some basic variables may dominate the limit state function while others have little effect. In the case of

shear resistance, the model factor dominates the reliability while the other variables have little effect on the reliability. Basic variables with little uncertainty (i.e. variables with a small bias and small coefficient of variation) usually have little effect on the reliability of the failure mechanism. It is important to have accurate statistical data on basic variables that dominate the limit state function as these variables determine the level of reliability. For this reason, some effort was made to assemble a database of shear experiments on beams in order to determine the statistical properties the model factor.

### The first order second moment method (FOSM)

This section briefly explains FOSM method for determination of the reliability index of a limit state equation in the form of equation 3.5. The limit state function for SANS10100 for shear is then given by:

$$g(\mathbf{X}) = v_{gpm}(\mathbf{X}) - v_{code\_design} \quad [3.8]$$

$\mathbf{X}$  is the vector of basic variables that is comprised of the model factor  $MF$ , as well as  $f_c$ ,  $A_s$ ,  $b$ , and  $d$  for members without shear reinforcement. Members with shear reinforcement include additional basic variables in the vector of basic variables namely,  $A_v$ ,  $f_{yv}$  and  $s$ . The FOSM method requires the first two moments of the basic variables namely the expected value and the standard deviation, as well as the statistical distribution to be known. The bias and variation of the model factor introduce the uncertainty of the model into the general probabilistic model for shear  $v_{gpm}(\mathbf{X})$ .

The load side of the limit state function is modelled by a single deterministic variable  $v_{code\_design}$ , which is the shear resistance as would be calculated by the designer using nominal values and characteristic values in the case of material strengths and applying the partial material factors. The use of characteristic values and the application of partial material factors reduce the value of  $v_{code\_design}$ . At the same time, the conservative bias of the basic variables increases the value of  $v_{code\_model}$ . This increases the mean difference,  $v_{code\_model} - v_{code\_design}$  and thereby increasing the reliability index.

The resistance  $v_{gpm}(\mathbf{X})$  is now represented by multiple statistical distributions of the basic variables. The failure point indicated in figure 3.1 is a failure surface in multiple dimensions. The most likely

failure point on the failure surface is the one with the smallest distance to the origin represented by the variable  $\beta$  as shown in figure 3.3.

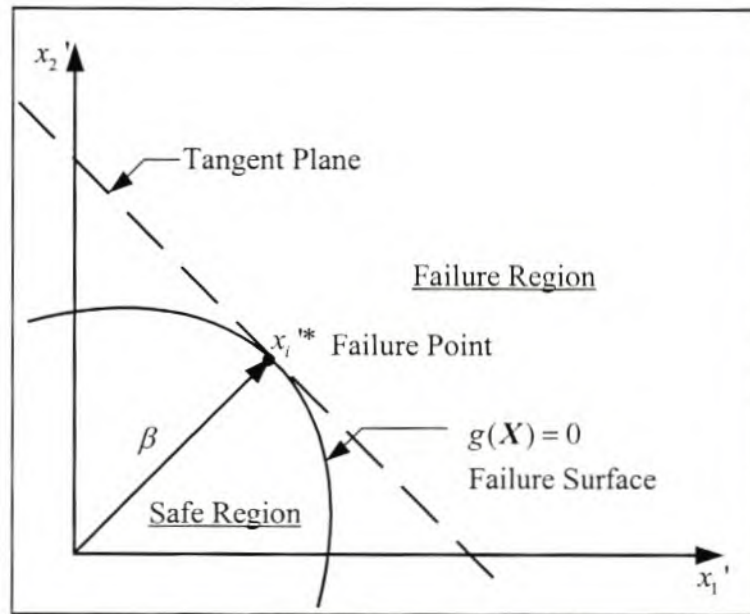


Figure 3.3: Failure Point of  $g(X) = 0$  at  $x_i^*$

The coordinate of the  $i^{\text{th}}$  basic variable at the failure point,  $x_i^*$  is then:

$$x_i^* = -\alpha_i^* \beta \tag{3.9}$$

where  $\alpha_i^*$  is the direction cosine of the  $i^{\text{th}}$  basic variable.

The direction cosines are calculated as follows:

$$\alpha_i^* = \frac{\left( \frac{\partial g}{\partial X_i'} \right)_*}{\sqrt{\sum_i \left( \frac{\partial g}{\partial X_i'} \right)_*^2}} \tag{3.10}$$

where  $\left(\frac{\partial g}{\partial X_i}\right)_*$  is the partial derivative of the limit state function with respect to the variable with respect to the  $i^{\text{th}}$  basic variable,  $X_i$ , multiplied by the standard deviation of  $X_i$  denoted as,  $\sigma_{X_i}$ .

The partial derivatives are then evaluated at the point  $(x_1^*, x_2^*, \dots, x_n^*)$ , where

$$x_i^* = \mu_{X_i} - \alpha_i \sigma_{X_i} \beta \quad [3.11]$$

The solution of the limit state equation  $g(x_1^*, x_2^*, \dots, x_n^*) = 0$  yields the value of  $\beta$ .

The problem is solved by assuming a set of initial  $x_i^*$ , usually by setting them equal to the expected values. The next step is to determine the direction cosines at these values from equation 3.10. The coordinates of the new estimate of the failure point,  $x_i^*$  are functions of the unknown  $\beta$  as shown in equation 3.11. These functions are inserted into the limit state equation and  $\beta$  is found for the case where  $g(x_1^*, x_2^*, \dots, x_n^*) = 0$ . A new estimate of the failure point is calculated from equation 3.11 with the determined  $\beta$ . After this updated direction cosines are calculated from this estimate for the failure point. The process for calculating  $\beta$  is repeated and another estimate of the failure point is determined. Several iterations may be required until  $\beta$  converges. The FOSM solution technique as described above applies to non-linear limit state functions.

### Significance of the direction cosines

The direction cosines of the basic variables,  $\alpha_i^*$ , provide insight to the workings of the limit stage function,  $g(\mathbf{X})$ . The magnitude of the direction cosine of a basic variable is indicative of its contribution to the overall uncertainty of the limit state function. A basic variable with a direction cosine close to  $\pm 1.0$  has a significant effect on the uncertainty of the limit state equation, while a basic variable with a direction cosine close to 0 has little effect. The direction cosines are functions of the partial derivatives as well as the standard deviation. Therefore basic variables with large standard deviations, typically the material strengths and the model factor will have larger direction cosines than basic variables with a low standard deviation such as the dimensions. The partial derivatives are affected by the form the basic variables take. Partial derivatives of basic variables that are denominators or roots are relatively

small and therefore have small direction cosines. The model factor is neither of these and will typically have a relatively high model factor.

Due to the anticipated importance of the model factor some effort was made to gather statistical data on the model factor for SANS by comparing the code to experimental databases, both for reinforced concrete beams with and without shear reinforcement. The general probabilistic model was based on SANS. The reliability of SANS was determined for a large range of design situations. The results are reported in Chapter 5.

# Chapter 4

## Determining the Model Factor for SANS 10100-1:2003

A deterministic model for prediction of the shear resistance of reinforced concrete structural elements can be converted into a probabilistic model by expressing the variables applied in the model probabilistically as so-called basic variables. However, there will still be a residual source of uncertainty related to the degree to which the prediction model reflects the actual resistance behaviour of the structural element. This effect can be provided for through the introduction of a modelling factor into the probabilistic shear resistance model or function. The probabilistic properties of the modelling factor can be obtained statistically by comparing predicted values for shear resistance with “true” values. The true values can be determined experimentally, although experimental error and uncertainty is then an additional source of uncertainty.

In this section modelling factors are derived by comparison to published experimental measurement of shear resistance, using the design procedure of SANS 10100-1:2003 as a basis for a probabilistic shear resistance model. The two cases, members *without* and members *with* shear reinforcement are treated separately in sections 4.1 and 4.2 respectively.

### 4.1 Members without Shear Reinforcement

In practice the majority of members without shear reinforcement are slabs. Most design codes only allow beams to be designed without shear reinforcement if the applied shear stress is half the shear resistance of the member. Slabs can fail in two shear failure mechanisms: beam shear or punching shear. Punching shear is usually the governing failure mechanism. This section deals exclusively with beam shear failure in members without shear reinforcement. Although members without shear reinforcement, where beam shear failure is likely, are not common in practice, it is critical that such members have adequate safety. The failure of such members is sudden and brittle opposed to failure in members with shear reinforcement where sudden failure is prevented by providing at least the minimum amount of stirrups. Experimental data on members without shear reinforcement that failed in

shear is abundant in literature, as the researchers of the past tried to understand shear mechanisms that govern shear resistance by first investigating members without shear reinforcement.

The model factor of a code design method for a single experiment is calculated by dividing the measured shear resistance at failure by the code predicted shear resistance. Partial material factors and resistance factors are ignored as they represent safety elements introduced by the code calibration process to ensure adequate reliability and not safety inherent to the design method itself. The statistical properties of the model factor of a code can be determined from a large number of experiments that comprise an experimental database. The statistical properties of the model factors of code design methods can in itself serve as a valuable means for comparing code design methods. In the context of this thesis the model factor is required to relate the uncertainty in the code design method to the true shear resistance in deriving general probabilistic models for shear resistance required for the reliability analysis. For the purposes of determining the reliability of a code method over the range of design situations that are allowed by the code under investigation, the experimental database should itself cover at least this range. A more extensive database, where available will allow the reliability of the code to be determined if the code design method were to be applied to design situations outside the applicable range of the code, but within the range of the experimental database.

#### **4.1.1. The Experimental Database**

A database of experiments on reinforced concrete beams without shear reinforcement was recently compiled by researchers at the University of Illinois and the Deutsches Institut für Bautechnik for the purpose of code evaluation. The database was published in the American Concrete Institute Structural Journal. (Kuchma et al, 2003). The database was set up to provide experimental data that covers a large range of parameters to enable researchers to test new shear design proposals against. The databank was used by one of the compilers of the database, K. Reineck to compare the empirical equation of the German code DIN 1045-1: 2001 for shear design of members without shear reinforcement. The compilers of the database, all leading researchers of shear in reinforced concrete, felt that available experimental data varied greatly in quality from researcher to researcher. As a result the experiments obtained from various sources underwent a rigorous evaluation process. The ASCE-ACI Committee 445 on Shear and Torsion determined the set of criteria for the acceptance of an experiment to the database called the Evaluation Shear Databank (ESDB). The databank as published contains only

members without shear reinforcement but is being extended to include experiments with shear reinforcement as well. For progress on the databank see: [www.ce.uiuc.edu/kuchma/sheardatabank/home.htm](http://www.ce.uiuc.edu/kuchma/sheardatabank/home.htm)

#### 4.1.1.1 Composition of the Database

The ESBD satisfies the following criteria as determined by the ASCE-ACI Committee 445 on Shear and Torsion:

- Concrete compressive cylinder strength:  $f_c > 12.6$  MPa
- Width of the web of the beam or beam width:  $b_{web}$  or  $b > 50$  mm
- Member depth:  $h > 70$  mm
- Longitudinal reinforcement must be ribbed, to provide adequate bond
- No anchorage failures may occur
- No flexural failures may occur (i.e. experiments must fail in shear)

The first three limitations are related to the scale of the experiments. Experiments below this range do not relate to practice and are therefore not included in the database. Longitudinal reinforcement must be ribbed as smooth reinforcement is not used in practice and pre-mature bond failures associated with such cases are not relevant to practice. Beams with anchorage failures are also excluded as anchorage failure constitutes a shear failure mechanism in its own right that is separate from beam shear failure. Anchorage failures are prevented in practice by bent up bars near the supports.

The database lists concrete cylinder strengths in terms of the concrete cylinder test of diameter 150 mm and height 300 mm as used in North America and Europe. The cylinder test will give about 80% of the strength of the cube test used in South Africa. To determine the equivalent cube strength for evaluating the model factor of SANS the conversion as suggested by the compilers of the database (Kuchma et al, 2003) is used:

$$f_{cu} = 1.267 f_c \quad [4.1a]$$

$$f_c = 0.79 f_{cu} \quad [4.1b]$$

Experiments of beams made with high strength concrete, concrete with cylinder strength of more than 50 MPa, are included in the database. The empirical formula employed by SANS is limited to concrete with cube strength of 40 MPa (cylinder strength 32 MPa). However the formula is probably used in practice for concretes of higher strengths, which do not classify as high strength concretes. For the purposes of the evaluation of the model factor of SANS experiments made of high strength concrete, concrete with cylinder strength of more than 50 MPa (63 MPa cube strength) were further eliminated from the ESBD. The final database used in this thesis contained 231 experiments made from normal strength concrete. The database is called the Shear Databank *without* Shear Reinforcement (SDB\_WithoutSR) for easy reference.

Beams with  $a/d$  ratio below 2.5 are known to carry a large part of the load by arch action rather than shear. Such beams have improved shear capacity. The compilers of the ESDB however suggest that arch action may be significant in beams of  $a/d$  up to 2.9.

The database was split into two subsets because it was felt that the 47 tests of a total of 231 tests with  $a/d$  below 2.9 might unduly increase the conservatism of the code methods by predicting very high shear strengths:

- SDB\_WithoutSR Subset 1: 184 tests with,  $2.9 < a/d < 8.03$
- SDB\_WithoutSR Subset 2: 47 tests with,  $a/d < 2.9$

Beams with  $a/d$  ratio from three to about six fail in a shear failure mode known as diagonal tension failure. Beams with  $a/d$  above six usually fail in flexure, but may fail in shear if they are very heavily reinforced in bending, usually with more than 4% bending steel which is not allowed in practice.

#### 4.1.1.2 Range and Distribution of Shear Parameters

The following figures show the distribution of the important parameters of the complete database of 231 experiments. The details of each experiment are given in Appendix A.1.

Concrete compressive strength		
%	MPa	MPa
0.0	$f_c \leq 12$	$f_{cu} < 15.2$
1.3	$12 < f_c \leq 15$	$15.2 < f_{cu} \leq 19.0$
6.5	$15 < f_c \leq 20$	$19.0 < f_{cu} \leq 25.3$
14.7	$20 < f_c \leq 25$	$25.3 < f_{cu} \leq 31.6$
38.5	$25 < f_c \leq 30$	$31.6 < f_{cu} \leq 38.0$
21.2	$30 < f_c \leq 35$	$38.0 < f_{cu} \leq 44.3$
13.9	$35 < f_c \leq 40$	$44.3 < f_{cu} \leq 50.6$
3.0	$40 < f_c \leq 45$	$50.6 < f_{cu} \leq 57.0$
0.9	$45 < f_c \leq 50$	$57.0 < f_{cu} \leq 63.0$
min	12.6	15.9
max	45.7	57.8

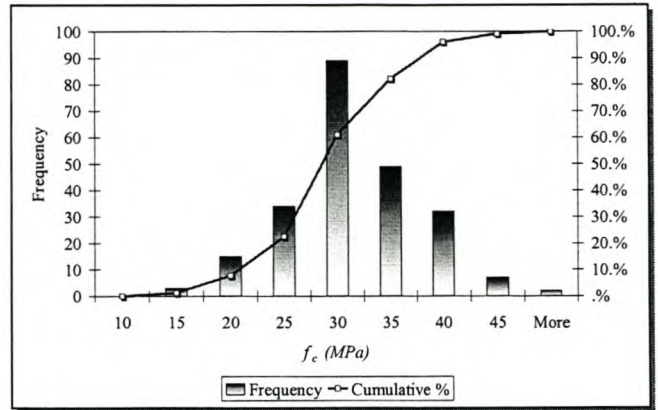


Figure 4.1: Distribution of concrete compressive strength for SDB\_WithoutSR

Maximum Aggregate size	
%	mm
6.9	$agg \leq 6.4$
0.4	$6.40 < agg \leq 9.40$
19.9	$9.40 < agg \leq 13.0$
25.5	$13.0 < agg \leq 19.1$
28.6	$19.1 < agg \leq 25.4$
17.7	$25.4 < agg \leq 30.0$
0.9	$agg > 30$
min	6.4
max	38

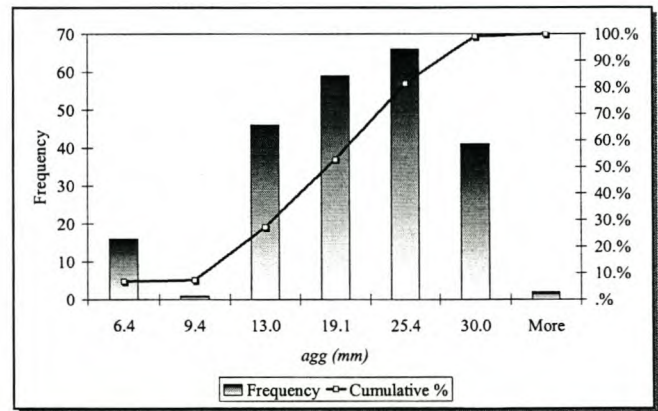


Figure 4.2: Distribution of aggregate size for SDB\_WithoutSR

a/d ratio	
%	mm
0.0	$a/d \leq 2$
39.0	$2 < a/d \leq 3$
36.8	$3 < a/d \leq 4$
14.3	$4 < a/d \leq 5$
5.6	$5 < a/d \leq 6$
3.0	$6 < a/d \leq 7$
0.9	$7 < a/d \leq 8$
0.4	$a/d > 8$
min	2.41
max	8.03

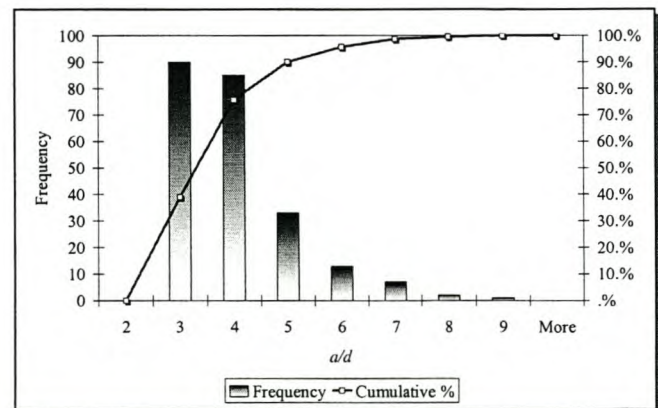


Figure 4.3: Distribution of shear span to depth ratio for SDB\_WithoutSR

Web width	
%	mm
2.6	$b \leq 100$
62.3	$100 < b \leq 200$
19.0	$200 < b \leq 300$
7.4	$300 < b \leq 400$
1.7	$400 < b \leq 500$
1.7	$500 < b \leq 600$
1.3	$600 < b \leq 700$
0.0	$700 < b \leq 800$
0.0	$800 < b \leq 900$
3.9	$900 < b \leq 1000$
min	100
max	1000

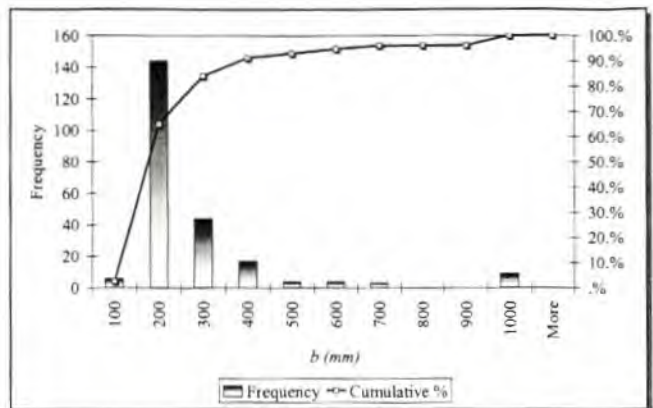


Figure 4.4: Distribution of web width for SDB\_WithoutSR

% Longitudinal Tension Steel	
%	%
0.0	$\rho < 0.1$
4.8	$0.1 < \rho \leq 0.5$
15.2	$0.5 < \rho \leq 1.0$
16.5	$1.0 < \rho \leq 1.5$
19.5	$1.5 < \rho \leq 2.0$
12.6	$2.0 < \rho \leq 2.5$
18.6	$2.5 < \rho < 3.0$
6.5	$3.0 < \rho < 4.0$
0.9	$4.0 < \rho \leq 4.5$
5.6	$4.5 < \rho \leq 5.0$
min	0.14
max	4.73

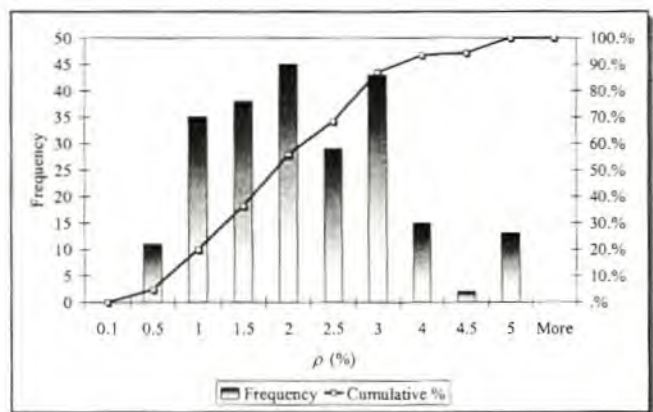


Figure 4.5: Distribution of percentage longitudinal tension steel for SDB\_WithoutSR

Shear Stress at failure	
%	MPa
0.0	$v_u \leq 0.3$
2.2	$0.3 < v_u \leq 0.5$
31.6	$0.5 < v_u \leq 1.0$
48.9	$1.0 < v_u \leq 1.5$
14.3	$1.5 < v_u \leq 2.0$
2.2	$2.0 < v_u \leq 2.5$
0.9	$2.5 < v_u \leq 3.0$
min	0.318
max	2.751

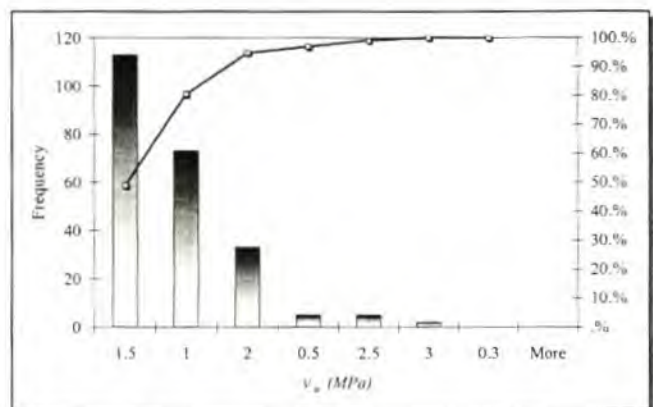
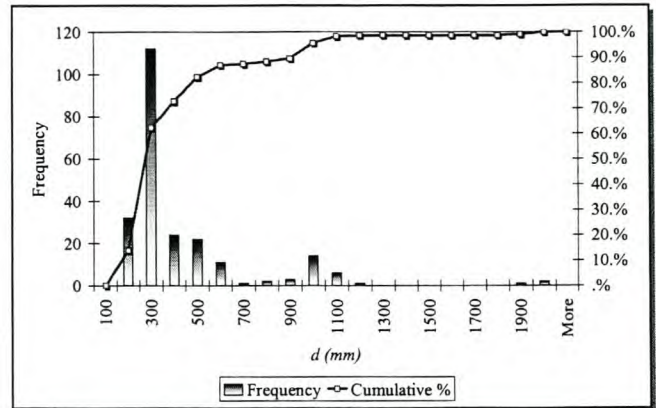


Figure 4.6: Distribution of measured shear stress at failure for SDB\_WithoutSR

Effective member depth	
%	mm
0.0	$d \leq 100$
13.9	$100 < d \leq 200$
48.5	$200 < d \leq 300$
10.4	$300 < d \leq 400$
9.5	$400 < d \leq 500$
4.8	$500 < d \leq 600$
0.4	$600 < d \leq 700$
0.9	$700 < d \leq 800$
1.3	$800 < d \leq 900$
6.1	$900 < d \leq 1000$
2.6	$1000 < d \leq 1100$
0.4	$1100 < d \leq 1200$
0.4	$1200 < d \leq 1900$
0.9	$1900 < d \leq 2000$
min	110
max	2000



**Figure 4.7: Distribution of effective member depth of SDB\_WithoutSR**

Of the experiments 38.5% have concrete cube strength between 32 and 38 MPa. The rest of the experiments are distributed approximately normally about this range. Only about four percent of the experiments have cube strength higher than 50 MPa. The experiments are centered about a cube strength that is common for normal strength concretes. About 54% of the maximum aggregate sizes used in the concrete are between 13 mm and 25 mm. 19 mm aggregate is typically used in practice. Seven percent of the tests had a very small aggregate size of less than 6.4 mm. 64% of the experiments had reinforcement steel between 1 and 2.5 percent, the range commonly used in practice. 31.6% had a reinforcement ratio of above 2.5%, perhaps a range not very applicable to practice.

For the shear span to depth ratio 57% of the tests had a range between three and six. Most building codes base their shear design procedures on this range. 39% had an  $a/d$  ratio between 2.0 and 3.0. A small percentage of experiments had  $a/d$  above 6.0. Usually such slender members will fail in flexure, but since all experiments were verified to have failed in shear, this shows that shear failure is still possible for very slender members, provided they are highly reinforced in the longitudinal direction to prevent flexural failure.

The overwhelming part of the database (73%) had effective member depths between 100 and 400 mm, however 10% of the experiments were very large beams with depths between 900 and 2000 mm.

Most of the beams have a failure shear stress between 0.5 and 2.0 MPa. None of the experiments reached the maximum allowable stress allowed by SANS 10100, namely the smaller of  $0.75\sqrt{f_{cu}}$  or 4.75 MPa. However, such high stresses typically only occur in members with shear reinforcement. The database is probably the most extensive database for reinforced concrete members without shear reinforcement compiled to date and covers a very large range of variables affecting the shear strength of concrete beams.

#### 4.1.2 Calculating the Model Factor from SDB\_WithoutSR

A model factor is calculated for each experiment by dividing the shear stress at failure of the beam as measured in the experiment by the characteristic (i.e. unfactored) shear stress predicted by the code:

$$MF = \frac{V_{\text{experiment}}}{V_{\text{code\_model}}} \quad [4.2]$$

A model factor greater than one for an experiment indicates that the code method predicted a lower strength than was measured and the code was therefore conservative. A model factor calculated as lower than one indicates that the code prediction for the experiment is unconservative.

The shear design procedures for reinforced concrete beams and slabs without shear reinforcement and pre-stressing for SANS is given by the following empirical formula:

$$\text{SANS: } v_c = \frac{0.75}{\gamma_{m,c}} \left( \frac{f_{cu}}{25} \right)^{1/3} \left( \frac{100A_s}{b_w d} \right)^{1/3} \left( \frac{400}{d} \right)^{1/4} \leq 0.75\sqrt{f_{cu}} \leq 4.75 \text{ MPa} \quad [2.5]$$

The code model is used as a basis for the probabilistic model in the reliability analysis. The partial material factors as well as the use of characteristic concrete strengths are applied in the code method to provide the necessary bias in order to increase the reliability of the characteristic value predicted by the unfactored code expression for shear resistance. The model factor is supposed to reflect the inherent bias (if any) of the unfactored expression and for this reason the partial material factors for concrete are taken as one, when calculating the model factor. The code method applies 5% characteristic strength

for concrete, which introduces an additional conservative bias into the code method. The concrete strengths as well as the dimensions and steel areas, are simply taken as the experimentally measured values when calculating the model factor.

The concrete strength in the experimental database used to determine the model factor of SANS was in most instances reported by the cylinder strength, used in Europe and North America, where SANS applies the cube strength as a measure of concrete strength. In order to determine the model factor from experimental data the SANS concrete strength is then expressed in terms of the equivalent cylinder strength. The value of  $v_{code\_model}$  in equation 4.2 is then calculated from:

$$v_{SANS\_MODEL} = 0.75 \left( \frac{1.266 f_{c,measured}}{25} \right)^{1/3} \left( \frac{100 A_s}{b_w d} \right)^{1/3} \left( \frac{400}{d} \right)^{1/4} \leq 0.75 \sqrt{1.266 f_{c,measured}} \leq 4.75 MPa \quad [4.3]$$

### 4.1.3 Statistical properties of the model factor

#### 4.1.3.1 Basic Statistical Properties

A model factor was calculated for each experiment. Statistical properties of the model factor were determined for the complete database SDB\_WithoutSR and for SDB\_WithoutSR: Subset 1 and SDB\_WithoutSR: Subset 2. The following statistical properties were determined:

- Expected value (mean),  $\mu$
- Standard Deviation,  $\sigma$
- Coefficient of variation,  $\Omega$

The distribution of the model factor was assumed to be normal and a check was carried out to verify the validity of this assumption. Table 4.1 shows the mean model factor calculated for SDB\_WithoutSR and for the subsets of the database. The standard deviation and coefficient of variation are also shown. The tabulated model factors for all the experiments are shown in Appendix A.1.

<b>SANS Model Factor: SDB WithoutSR</b>			
	<b>Total Database: 231 Tests</b> $2.41 < a/d < 8.03$	<b>Subset 1: 184 Tests</b> $2.9 < a/d < 8.03$	<b>Subset 2: 47 Tests</b> $2.41 < a/d < 2.9$
mean	1.08	<b>1.03</b>	1.27
std. dev.	0.185	0.129	0.239
c.o.v. (%)	17	<b>12</b>	19

**Table 4.1: Results of model factors determined from SDB\_WithoutSR**

For the total database the SANS model factor has a conservative bias of 8% and a coefficient of variation of 17%. For Subset 1 both the conservative bias and the coefficient of variation decreases by 5%. This is expected due to the presence of beams with an  $a/d$  ratio of less than 2.9 that have been included in the total database. The shear strength of such beams is likely to be underestimated by the code method, because the positive contribution of arch action to shear strength is ignored, resulting in large model factors for these experiments. The inclusion of these beams is also the reason for the higher coefficient of variation for the total database.

Subset 2 contains only stocky beams. Here the conservative bias is 24% higher. The coefficient of variation is 7% higher than for subset 1. This indicates clearly that the increase in the conservative bias and deviation in the total database can be attributed to the presence of stocky beams with  $a/d$  less than 2.9, confirming that the shear resistance is systematically underestimated for such members. The increase in variance is an additional indicator that the code is not capable of predicting shear resistance with arch action. It is likely that some members in Subset 2 experienced arch action and some did not, which resulted in the increase in c.o.v. The conclusion is subsequently that only Subset 1 needs to be considered henceforth.

SANS applies a partial material safety factor for concrete in shear of 1.4. When the model factor is simply multiplied by the partial material factor a “performance factor” is obtained of 1.44. The conservative bias is now increased by 41%. The conservative bias in the model factor of the code therefore reflects the inherent safety of the code model, while the performance factor includes the additional safety introduced by the partial material factor.

### 4.1.3.2 Trends in the Model Factor: Correlation and Regression Analysis

A single expected value for the model factor accompanied by a coefficient of variation does not provide any information on trends in the model factor with other shear parameters. The fact that the model factor is higher for beams with  $a/d$  lower than 2.9 than for  $a/d$  higher than 2.9 is an example of such a trend. However the arch action effect has a relatively clear boundary. Other trends may be more gradual over a wide range of a certain shear parameter. A trend in the model factor with a shear parameter indicates that the code method does not fully take the effect of the parameter on shear resistance into account. If a trend is strong enough it may be necessary to reflect this trend in the model factor of the general probabilistic model for shear resistance applied in the reliability analysis. Trends in the model factor of a code with a shear parameter are identified by determining the correlation between the model factor and the shear parameter. The Pearson’s correlation coefficient is a useful indicator of a relationship between two variables:

$$r = \frac{\sum(x_i - \bar{x})(y_i - \bar{y})}{\sqrt{\sum(x_i - \bar{x})^2} \sqrt{\sum(y_i - \bar{y})^2}}$$

$$-1 \leq r \leq 1$$

$x_i$  = parameter  $x$  of  $i^{\text{th}}$  experimental observation  
 $\bar{x}$  = mean of all  $x$ 's of all experimental observations  
 $y_i$  = parameter  $y$  of  $i^{\text{th}}$  experimental observation  
 $\bar{y}$  = mean of all  $y$ 's of all experimental observations

[4.4]

Significance of Correlation factor:	
±0-0.2	Weak Correlation
±0.2-0.5	Moderately Weak Correlation
±0.5-0.8	Moderate Correlation
±0.8-1.0	Strong Correlation

**Table 4.2: Significance of the correlation factor**

Table 4.2 shows the significance of ranges of the correlation factor. Literature on Pearson’s correlation factor defines a moderate correlation in the range of 0.5 – 0.8. However trends in the model factor are likely to be “weak” by these standards. Correlation factors of greater than 0.2 were considered as significant trends in the model factor warranting closer inspection Table 4.3 summarizes the correlation

and regression data for the model factor vs. the shear parameters,  $a/d$ ,  $d$ ,  $f_c$ ,  $\rho$ ,  $f_y$  and aggregate size for the complete database and for Subset 1. In addition to determining the correlation linear regression functions where fitted to scatter plots of the model factor vs. the shear parameters which showed a significant correlation for Subset 1 of the database. The coefficient of determination  $R^2$  is a measure of the linear relationship that exists between the model factor and the shear parameter. A combination of a relatively strong correlation coefficient and a relatively strong coefficient of determination indicate that a strong linear relationship exists between the model factor and the shear parameter. If the correlation coefficient is strong but  $R^2$  is relatively weak this indicates that the relationship between the model factor and the shear parameter is not linear. A non-linear regression may be a better fit; this would be reflected by a stronger  $R^2$  for such a fit.

#### Trends with $a/d$

Table 4.3 indicates that a strong decreasing trend exists between the model factor of SANS with increasing  $a/d$  by a relatively strong correlation coefficient of -0.45. The influence of experiments that experience arch action is once again demonstrated by the decrease in the correlation in Subset 1 where experiments with  $a/d$  lower than 2.9 are excluded. Nonetheless the correlation coefficient remains relatively strong at -0.33. This is a clear indication that the negative effect of bending on shear is not taken into account by the SANS method.

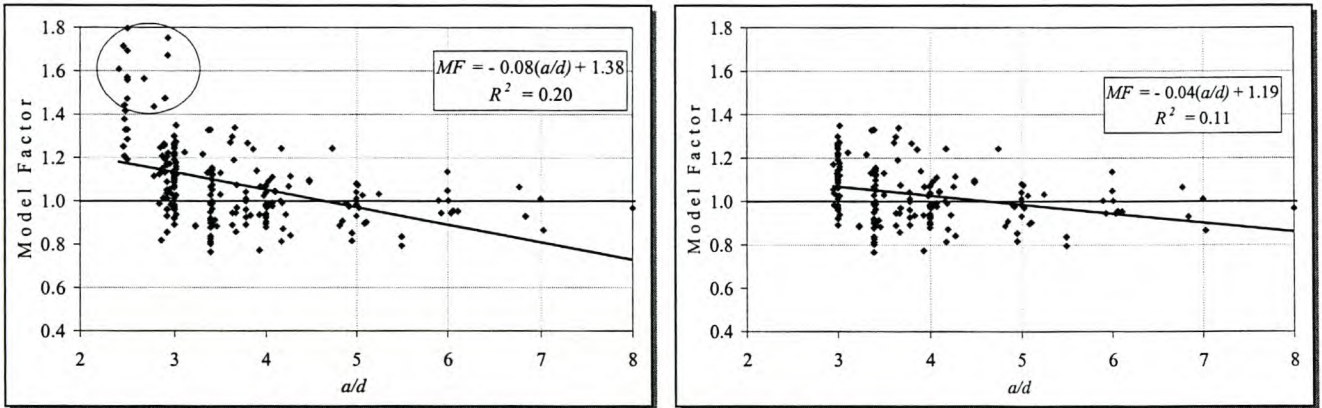
Variable	Complete Set	Subset 1
$a/d$	<b>-0.45</b>	<b>-0.33</b>
$d$ (mm)	-0.13	0
$f_c$ (MPa)	-0.13	0.09
$\rho$ (%)	-0.08	-0.17
$agg$ (mm)	0.14	0.11
$f_y$ (MPa)	-0.03	0.04

**Table 4.3: Linear Regression data for SDB\_WithoutSR**

Variable	gradient	intercept	$R^2$	$r$
$a/d$	-0.04	1.19	0.11	<b>-0.33</b>
$d$ (mm)	0.0002	1.03	0.12	<b>-0.001</b>
$f_c$ (MPa)	0.002	0.98	0.01	<b>0.09</b>
$\rho$ (%)	-0.02	1.07	0.03	<b>0.31</b>
$agg$ (mm)	0.0006	0.03	0.002	<b>0.11</b>

**Table 4.4: Regression and correlation data for members SDB\_WithoutSR: Subset 1**

Figure 4.8 below show the linear regression plots for the complete database and Subset 1 for the SANS model factors. The regression functions from tables 4.3 and 4.4 are also shown.



**(a) SANS: SDB\_WithoutSR: Complete Database**

**(b) SANS: SDB\_WithoutSR: Subset 1**

**Figure 4.8: Linear Regression Plot: Model Factor vs. shear span to depth ratio,  $a/d$**

Figure 4.8(a) represents the complete database. The circled experiments with very high model factors above 1.4 are those that are likely to have experienced arch action. The removal of experiments with  $a/d$  of less than 2.9 in Subset 1 eliminates these high model factors, resulting in a linear regression in the model factor with a much shallower gradient. The decreasing trend in the model factor with increasing  $a/d$  is now much more gradual. This is a clear indication that the inclusion of members with arch action gives an undue impression of a rapid decreasing trend in the model factor with increasing  $a/d$ . The model factor for the reliability analysis should therefore be exclusively modelled on the experiments of Subset 1.

### Trends with $d$

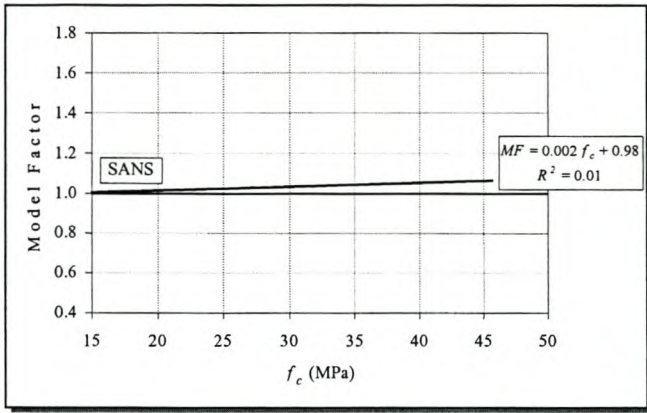
The SANS method perfectly accounts for the size effect on shear resistance with no correlation between its model factor and the effective member depth. The SANS method is an empirically fitted function (equation 2.5). The lack of a trend with effective member depth indicates that the set of data on to which the function was fitted must have included a large number of members of different effective depths resulting in a good fit that reflects the size effect accurately.

Figure 4.9(a) shows the linear regression plot for the SANS Model factor vs. effective member depth for Subset 1. The scatter plot of experimental observations is not shown for clarity. The bias SANS model factor remains consistent at 3% for all effective member depths.

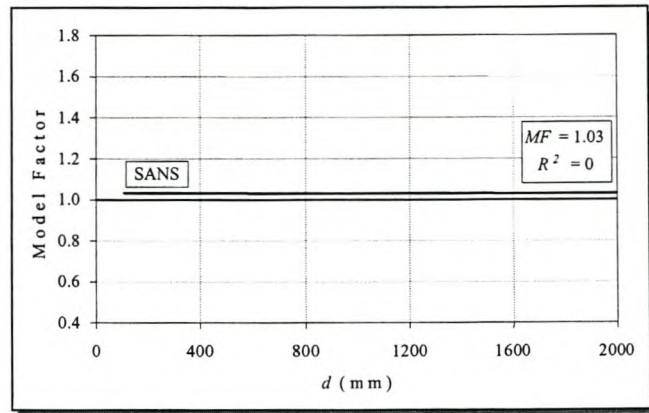
### Trends with $f_c$ , $\rho$ , $f_y$ and $agg$

SANS did not display any significant trends with  $f_c$ . From table 4.4 the correlation coefficient with the model factor to be about 0.1. Similarly there was almost no trend in the model factor with the yield strength of the longitudinal reinforcement,  $f_y$ . This is to be expected as  $f_y$  is known to have no effect on the shear resistance and is therefore not a shear parameter. However  $f_y$  can determine whether a beam fails in shear or bending, by determining the flexural yield point of a beam.

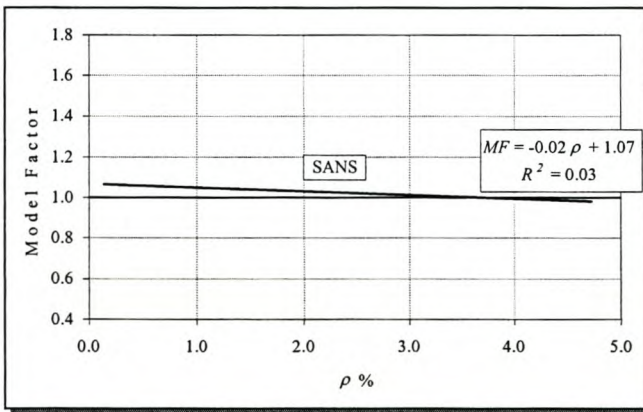
The trends in the model factor with the amount of longitudinal reinforcement was also insignificant for Subset 1 of the database of experiments, with a weak correlation coefficients of 0.17. Similarly SANS did not display any significant trends with aggregate size Figures 4.9 (a) to (d) show the linear regression plots versus the shear parameters  $d$ ,  $f_c$ ,  $\rho$  and aggregate size for SDB\_WithoutSR: Subset 1. Comparison of these plots shows that SANS is not subject to any significant trends for all of these parameters.



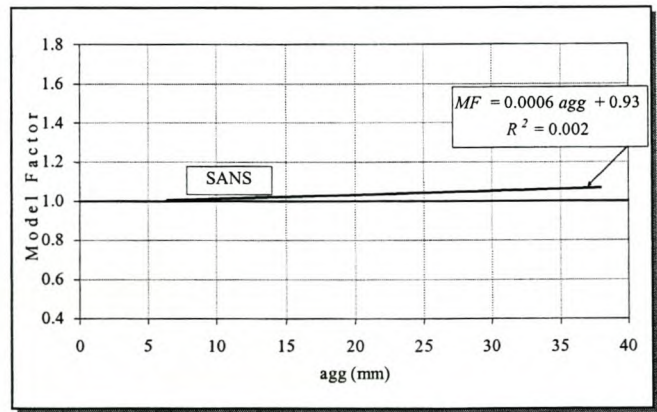
(a) *MF vs. d* (mm)



(b) *MF vs. f\_c* (mm)



(c) *MF vs. rho* (mm)



(d) *MF vs. agg* (mm)

**Figure 4.9: Linear Regression Plot for Model Factor: SDB\_WithoutSR: Subset 1**

To summarize, the experimental study with regard to the database SDB\_WithoutSR: Subset 1 yielded the following results:

- The SANS model factor is subject to a strong decreasing trend with increasing  $a/d$ . The SANS model factor is not sensitive to  $f_c$ ,  $d$  or  $\rho$  or aggregate size.

This means that SANS is a code that is capable of predicting the influence of most shear parameters on shear resistance with accuracy. This makes the SANS model a suitable candidate for a probabilistic model for shear resistance. In the following section an accurate model for the model factor of SANS was derived from the experimental database for the general probabilistic model for shear.

#### 4.1.4 Modelling the Model Factor for the Limit State Function

A simple linear regression model is proposed to model the model factor for a SANS based general probabilistic resistance model.

The model assumes that the experimental observations are scattered normally about the linear regression line, with a constant standard deviation  $\sigma$ . The simple linear regression model is based on Subset 1 of SDB\_WithoutSR, in order to eliminate any undue negative trend due to the inclusion of experiments experiencing arch action.

For the purposes of reliability analysis the mean model factor (which also serves for determining the bias in the model factor) for SANS and is then determined from the linear regression formula from table 4.4:

$$\text{SANS: } \mu_{MF} = -0.042 \left( \frac{a}{d} \right) + 1.19 \quad [4.5]$$

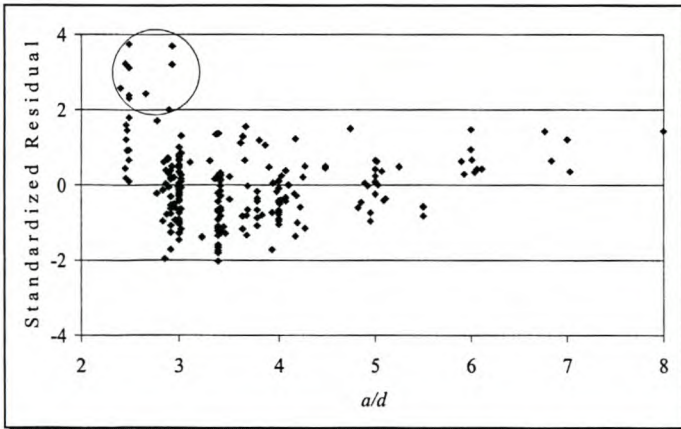
The coefficient of determination of 11% indicates the extent of a linear relationship between  $MF$  and  $a/d$ . Polynomial, exponential and logarithmic regression functions were found to behave nearly linearly and did not provide a better fit. The other parameters  $f_c$ ,  $\rho$ ,  $f_y$  and aggregate size did not show significant trends and are therefore not included in the linear regression.

Assuming that the observed values of the  $MF$  deviate from the predicted values of the  $MF$  (as given by the regression equation) with a standard deviation of  $\sigma$  that is constant over the entire range of  $a/d$ , the standard deviation is then given by:

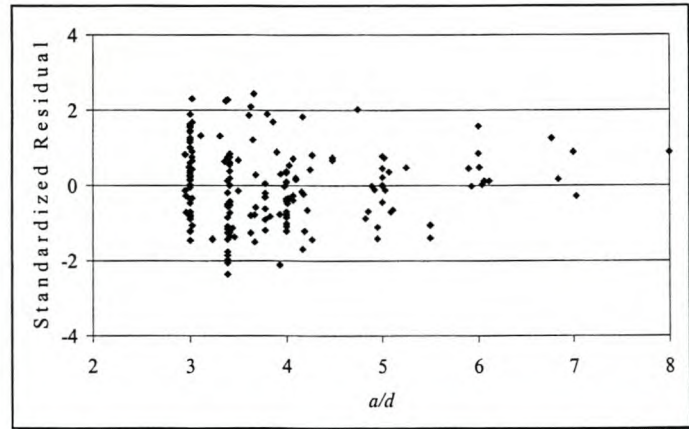
$$\sigma = s_e = \sqrt{\frac{\sum (y_i - \hat{y}_i)^2}{n-2}} \quad [4.6]$$

$y_i$  = Observed Value of *MF*  
 $\hat{y}_i$  = *MF* as predicted by linear regression  
 $n$  = number of observations

Values of the standard deviation for Subset 1 was calculated equal to be 0.122 for SANS. The value is slightly less than that from table 4.1 of 0.129. A further assumption of the simple linear regression model is that the observed values of *MF* are scattered about the regression line with a constant standard deviation. One way to check the assumption of a constant standard deviation over the entire range of *a/d* is to plot the standardized residual (the difference between the observed *MF* and the *MF* predicted by the regression formula standardized with respect to the average standard deviation over the entire range) versus the model factor predicted by the linear regression function. The standardized residual is therefore an indication of how much a data point deviates from the linear regression line. This is shown in figure 4.10(a) and (c) for SANS for the complete database and figure 4.10(b) and (d) for Subset 1.

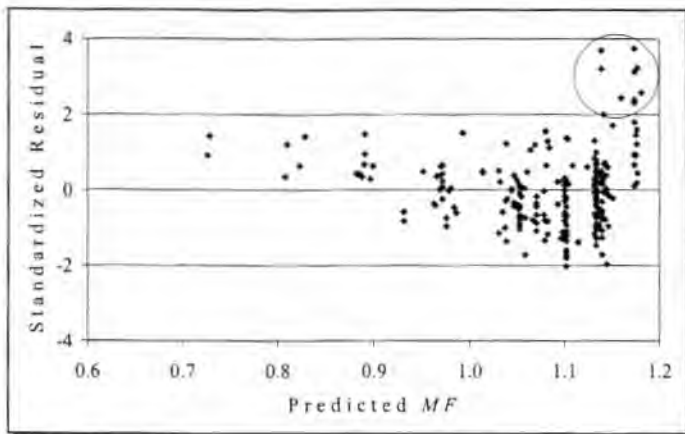


(a) SDB\_WithoutSR: Complete Database  
Standardised Residual vs. *a/d*

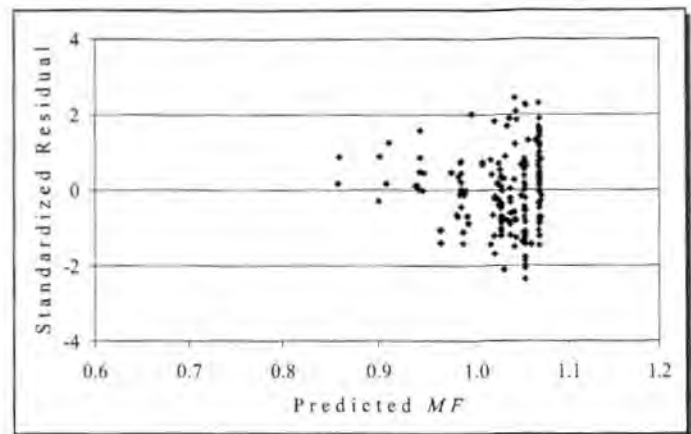


(b) SDB\_WithoutSR: Subset 1  
Standardised Residual vs. *a/d*

**Figure 4.10: Standardised residual plots for SANS Model Factor linear regression function**



(c) SDB\_WithoutSR: Complete Database:  
Standardized Residual vs.  $MF$



(d) SDB\_WithoutSR: Subset 1  
Standardized Residual vs.  $MF$

**Figure 4.10: Standardized Residual plots for SANS Model Factor linear regression function**

If the residuals seem to be randomly placed about the zero residual line with a more or less constant deviation then the constant  $\sigma$  is a reasonable assumption. For the entire dataset some of the residuals for  $a/d$  lower than 2.9, are much higher than two (see figure 4.10(a)), showing considerable deviation from the rest of the data. These are the model factors of more than about 1.15 to the far right of figure 4.10(c), where the standardized residual is plotted against the model factor predicted by the linear regression line. Figures 4.10(a) and (c) indicate that the model factors with the highest residuals are those with  $a/d$  between 2 and 3. These outliers lie on the conservative side, i.e. the residuals for these outliers are all positive. Negative residuals much greater than 2.0 do not occur. The presence of these outliers make the assumption of a constant standard deviation about the linear regression line (i.e. the line with zero residual) unrealistic since the standard deviation is much higher for observations with  $a/d$  between 2 and 3.

Figures 4.10(b) and (d) show standardized residual plots for SANS for subset 1. The extreme outliers are now eliminated. The deviation of experimental data about the zero residual for  $a/d$  values between about 3 and 4.5 seems to be higher than for 4.5 and upward. Therefore the assumption of a constant standard deviation over the entire range of  $a/d$  is not entirely accurate, yet it is a conservative assumption for observations with a high  $a/d$ . Also the weight of experimental data lies toward the lower  $a/d$  values making this a reasonable assumption. However, its application to situations with high  $a/d$

values is more uncertain. The trend is for the deviation to be positive for higher  $a/d$ , i.e. model factors less than 1.0 or over-prediction of the shear resistance.

It was assumed that the observed model factors will be distributed normally about the least squares regression line with a constant standard deviation,  $\sigma$ . Alternatively it can be said that the residuals ( the difference between an observed value of  $MF$  and the value of  $MF$  predicted by the least squares line) is distributed normally. In order to test this assumption a normal quantile plot is constructed with the standardized residuals. The idea behind such a plot is that if the plot is based on the assumption of a normal distribution then the points on the plot will fall close to a straight line on normal graph paper. The standardized residuals are ranked from smallest to largest. A quantile probability is assigned to each residual. The smallest sample will be assigned the  $(0.5/n)^{\text{th}}$  sample quantile, the second smallest the  $(1.5/n)^{\text{th}}$ , ..., and the largest observation is assigned to the  $[(n-0.5)/n]^{\text{th}}$ , where  $n$  is the number of observations. A quantile is the coordinate along the  $z$  axis of a normal distribution that corresponds to a certain probability of exceedance. For example the 95% quantile means that 95% of all observed values with a normal distribution will fall below that value. Figure 4.11 shows the normal quantile plots for SANS. Correlation of the residuals is 99.6% with the normal so it is reasonable to assume a normal distribution of the observations about the linear regression function.

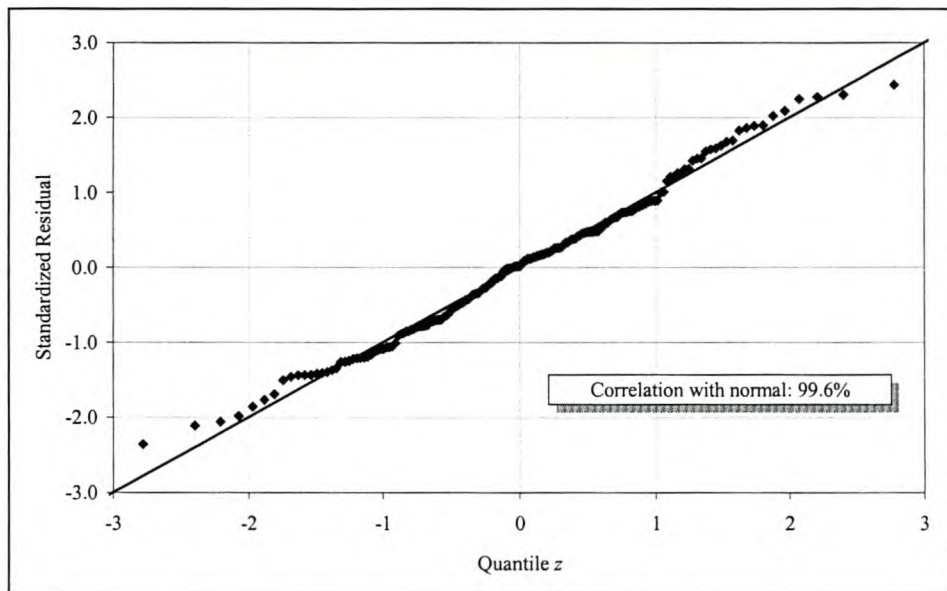


**Figure 4.11: Normal quantile plot for SANS  $MF$**

## 4.2 Members with Shear Reinforcement

The same principles apply to determining the model factor for members with shear reinforcement as for members without shear reinforcement. A database of experiments with shear reinforcement was compiled against which the statistical properties of the SANS model factor was determined. Although members with shear reinforcement are by far more common in practice than those without shear reinforcement experimental data for such members is relatively scarce in shear literature.

### 4.2.1 The Experimental Database

A published experimental database of RC members with shear reinforcement similar to the one for RC members without shear reinforcement (Kuchma et al, 2003), is not yet available. It is the intention of the compilers of this database to extend it to members with shear reinforcement. As a result a database was compiled from papers presented in the American Concrete Institute Structural Journal over the past 50 years. Many of the experimental studies on shear as obtained from the ACI Structural Journal are well known and have served as benchmarks for testing new theories on shear behaviour of RC beams over the years. Experiments were taken from 21 experimental studies on shear, comprising a total of 212 experiments. The database is named SDB\_WithSR for easy reference.

#### 4.2.1.1 Composition of the Database

The composition of the database for members with shear reinforcement is as follows:

- 71 tests had a shear span to depth ratio of less than 2.5. In members with  $a/d$  ratio of less than 2.5 a significant part of the load is carried by arch action, resulting in much higher shear strength.
- 49 tests contained less than minimum required shear reinforcement, according to the AASHTO criterion:

$$v_s = \frac{A_{sv} f_{yv}}{bs} \geq v_{s,min} = 0.083 \sqrt{f_c}$$
 The Eurocode criterion is very similar except the 0.083 is replaced by 0.08. For cases with less than minimum shear reinforcement the shear

reinforcement is ineffective and the shear resistance is best calculated as for a member without shear reinforcement.

- 19 beams where continuous beams with a T-section.
- 27 beams where continuous beams with a rectangular section.
- 25 beams were simply supported beams with a T-section.
- The rest of the experiments (about 70% of the total database) where simply supported beams with rectangular sections.

After eliminating the 49 experiments with less than minimum shear reinforcement, 163 tests remained. All experiments in the database were reported to have failed in one of the two shear failure modes, diagonal-tension failure or shear-compression failure. No experiments were included that had failed in bending or anchorage failure. The overall database complies with the selection criteria applied to the database without shear reinforcement as described in chapter 4.1.1.1. However, it was impossible to verify if the longitudinal reinforcement for all experiments was ribbed. The overall database was then further split into two subsets, Subset 1:  $a/d > 2.5$ , Subset 2:  $a/d < 2.5$ . The database was split into two since beams with an  $a/d$  ratio less than 2.5 may experience arch action and the shear strength may therefore be significantly underestimated by the code methods. Note the limit of 2.9 for members without shear reinforcement was suggested by the compilers of the database, however for members with shear reinforcement the limit is generally accepted as 2.5 in shear literature.

<b>Experimental Database of members with shear reinforcement: SDB WithSR</b>	
Total Database: 163 Experiments	At least minimum shear reinforcement
Subset 1: 99 Experiments	At least minimum shear reinforcement $a/d > 2.5$
Subset 2: 64 Experiments	At least minimum shear reinforcement $a/d < 2.5$

**Table 4.5: Composition of the experimental database for members with shear reinforcement**

#### 4.2.1.2 Shear Resistance Parameters

For each experiment the following parameters were recorded in the database from the sources:

- Width of the beam web,  $b_w$
- Effective member depth,  $d$
- Concrete cylinder strength,  $f_c$
- Percentage tension reinforcement,  $100A_s/bd$
- Yield strength of the longitudinal reinforcement,  $f_y$
- Amount of vertical shear reinforcement,  $A_v f_{yv}/b_w s$  in MPa designated by the symbol  $\rho_w$

The yield strength of the longitudinal reinforcement is required to predict flexural failure in the AASHTO LRFD method but not by SANS; however it does not affect the shear strength of RC members. Note the aggregate size of the concrete used is not included, since this parameter was not well documented in most sources. The aggregate size does not play an important role in members with shear reinforcement, according to the modified compression field theory.

Most experimental sources report the amount of shear reinforcement in terms of a stress,  $A_v f_{yv}/b_w s$ . Separate information on the area of shear reinforcement  $A_v$ , the yield strength of the steel  $f_{yv}$  and the spacing of the stirrups is not available in most sources. The ASCE-ACI Task committee 426 on Shear and Diagonal Tension (ASCE-ACI Committee 426, 1973) found that the amount of shear reinforcement expressed as a stress affects the shear strength, but the individual parameters do not affect the shear strength. Therefore a beam with a steel area  $A_v$  at spacing  $s$ , will have the same shear strength as a beam with steel area  $2A_v$  at double the spacing  $s$ . This is a reasonable assumption as long as the spacing  $s$  is less than the effective member depth  $d$ , in order to ensure that a least one stirrup is likely to cross a diagonal crack.

#### 4.2.1.3 Range and distribution of parameters of database

The range of values should ideally correspond to design situations found in practical structures in order for the modelling factors determined from the database to be representative of conditions for which the codes are applied. The distribution of the parameters should similarly be evenly distributed across the range. The following figures show histograms and tables of the distribution of parameters.

Concrete compressive strength		
%	Cylinder (MPa)	Cube (MPa)
6.1	$15 < f_c \leq 20$	$19 < f_c \leq 25.3$
23.3	$20 < f_c \leq 25$	$25.3 < f_c \leq 31.6$
33.7	$25 < f_c \leq 30$	$31.6 < f_c \leq 38$
20.9	$30 < f_c \leq 35$	$38 < f_c \leq 44.3$
4.9	$35 < f_c \leq 40$	$44.3 < f_c \leq 50.6$
7.4	$40 < f_c \leq 45$	$50.6 < f_c \leq 57$
3.1	$45 < f_c \leq 50$	$57 < f_c \leq 63.3$
0.0	$50 < f_c \leq 55$	$63.3 < f_c \leq 69.6$
0.6	$f_c > 55$	$f_c > 69.6$
min	12	15.2
max	57	72.2

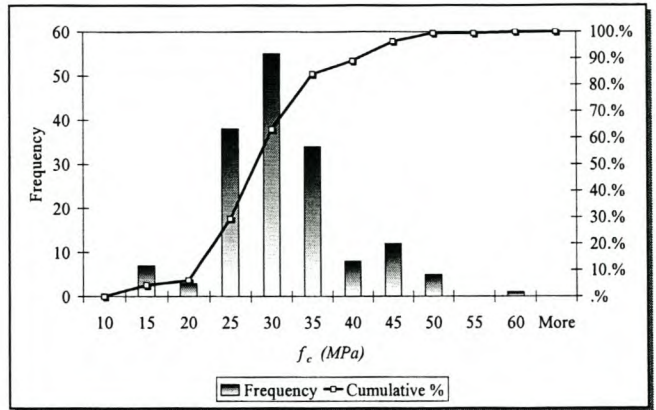


Figure 4.12: Distribution of concrete compressive strength for SDB\_WithSR

a/d ratio	
%	
23.9	$1 < a/d \leq 2$
31.3	$2 < a/d \leq 3$
31.9	$3 < a/d \leq 4$
8.0	$4 < a/d \leq 5$
3.7	$5 < a/d \leq 6$
0.0	$6 < a/d \leq 7$
1.2	$7 < a/d \leq 8$
0.0	$a/d > 8$
min	1
max	7.2

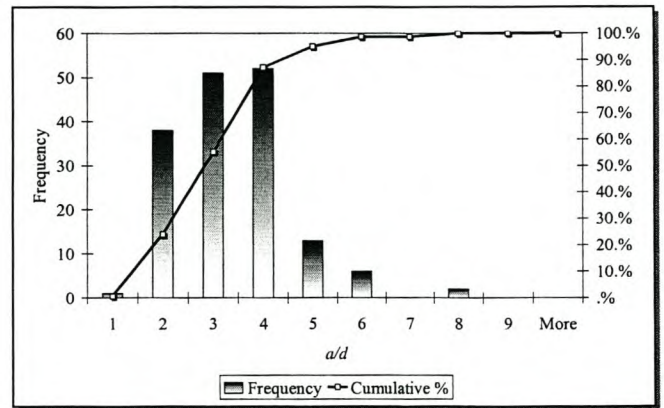


Figure 4.13: Distribution of shear span to effective depth ratio for SDB\_WithSR

% Longitudinal Tension Steel	
%	%
0	$\rho < 0.1$
0.6	$0.1 < \rho \leq 0.5$
3.7	$0.5 < \rho \leq 1.0$
13.5	$1.0 < \rho \leq 1.5$
9.8	$1.5 < \rho \leq 2.0$
21.5	$2.0 < \rho \leq 2.5$
9.2	$2.5 < \rho < 3.0$
23.3	$3.0 < \rho < 4.0$
14.7	$4.0 < \rho \leq 4.5$
3.7	$4.5 < \rho \leq 5.0$
min	0.48
max	4.76

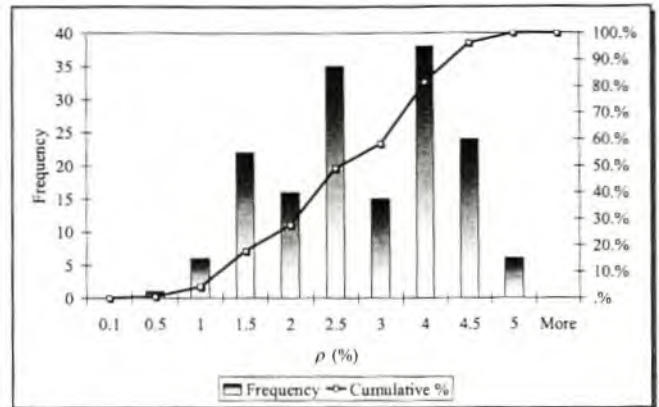


Figure 4.14: Distribution of longitudinal tension steel percentage for SDB\_WithSR

Effective member depth	
%	mm
39.3	$200 < d \leq 300$
40.5	$300 < d \leq 400$
16.6	$400 < d \leq 500$
1.2	$500 < d \leq 600$
1.2	$600 < d \leq 700$
0	$700 < d \leq 800$
0.6	$800 < d \leq 900$
0	$900 < d \leq 1000$
0	$1000 < d \leq 1100$
0.6	$1100 < d \leq 1200$
min	203
max	1200

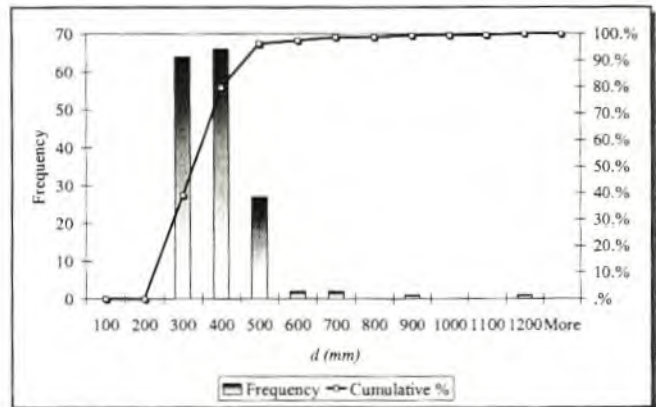


Figure 4.15: Distribution of effective member depth for SDB\_WithSR

Web width	
%	mm
0	$b \leq 100$
59.5	$100 < b \leq 200$
38	$200 < b \leq 300$
0.6	$300 < b \leq 400$
1.84	$400 < b \leq 500$
min	127
max	406

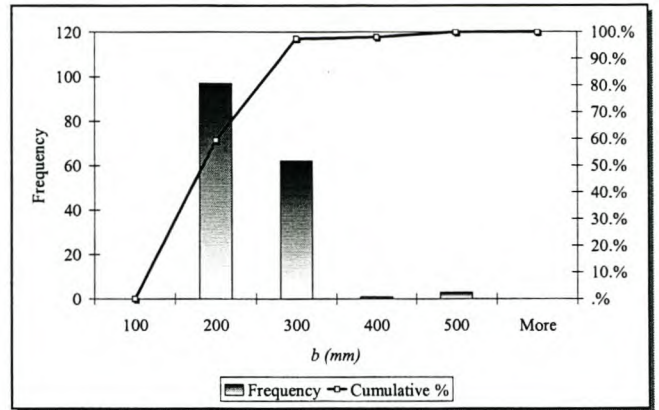


Figure 4.16: Distribution of web width depth for SDB\_WithSR

Shear reinforcement	
%	MPa
4.9	$0.2 < v_s \leq 0.5$
31.9	$0.5 < v_s \leq 1.0$
42.9	$1.0 < v_s \leq 2.0$
19.6	$2.0 < v_s \leq 3.0$
0.6	$3.0 < v_s \leq 4.0$
min	0.28
max	3.05

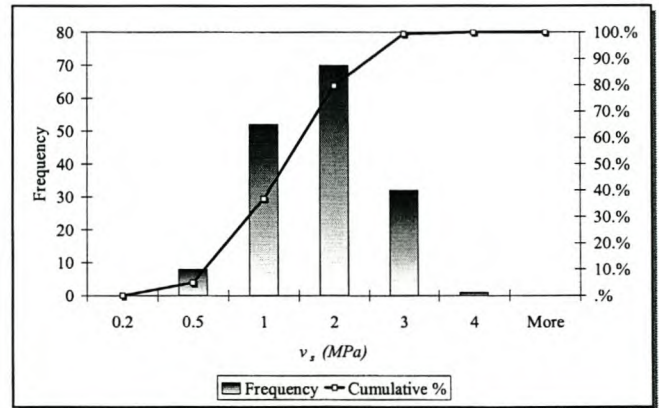


Figure 4.17: Distribution of shear reinforcement for SDB\_WithSR

Shear Stress at failure	
%	MPa
20.9	$1.0 < v_u \leq 2.0$
17.2	$2.0 < v_u \leq 3.0$
22.7	$3.0 < v_u \leq 4.0$
28.2	$4.0 < v_u \leq 5.0$
6.7	$5.0 < v_u \leq 6.0$
3.7	$v_u > 6.0$
min	1.05
max	9.57

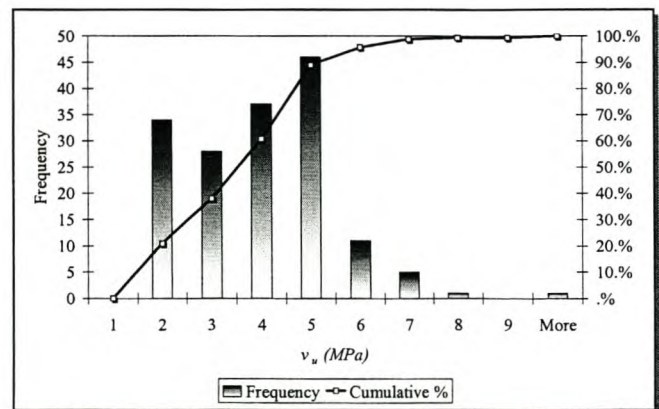


Figure 4.18: Distribution of measured shear stress at failure for SDB\_WithSR

The experiments of the database are centred normally about concrete cylinder strength of about 30 MPa (figure 4.12), which corresponds to normal strength concrete. The majority of experiments (about 40%) had  $a/d$  ratios between 3 and 5. Only 5% of experiments had  $a/d$  greater than 5.0. About 18% of experiments had more than 4% of longitudinal reinforcement. SANS does not allow more than 4% longitudinal tension reinforcement, so these experiments are probably not relevant to practice. Researches tend to provide high percentages of longitudinal tension reinforcement to ensure that experimental beams fail in shear rather than flexure. About 65% of experiments had shear reinforcement of less than 2 MPa. Experiments with very high amounts of shear reinforcement are very scarce in literature. There were only two beams in the database with very deep sections (greater than 800 mm). Beams with relatively shallow sections that are lightly reinforced in shear and bending, which are most common in practice, are well represented in the database.

#### 4.2.2 Calculation of the Model Factor from SDB\_WithSR

The model factor of a single experiment containing shear reinforcement is calculated by dividing the characteristic (i.e. unfactored) code predicted shear resistance by the experimentally measured shear resistance in the same manner as for members without shear reinforcement as described in section 4.1.1. The unfactored code shear resistance is calculated as follows:

The shear resistance, expressed as a force is calculated from

$$V_{SANS\_MODEL} = \left[ 0.75 \left( \frac{1.267 f_{c,measured}}{25} \right)^{1/3} \left( \frac{A_s}{bd} \right)^{1/3} \left( \frac{400}{d} \right)^{1/4} + \frac{A_{sv} f_w}{b_w s} \right] b_w d \quad [4.7]$$

The partial material factors for concrete and steel are taken as unity and the characteristic concrete cube strength is taken as the experimentally measured concrete strength expressed in terms of the equivalent cylinder strength.

The maximum allowable shear stress, which translates into a maximum allowable amount of shear reinforcement, is given by:

$$V_u \leq V_{u,max} = 0.75 \sqrt{f_{cu}} b_w d \leq 4.75 b_w d \quad [4.8]$$

For some of the experiments in the database, the calculated (unfactored) shear stress exceeds the maximum allowable design shear stress. In a design situation this would require an increase in the dimensions of the section. In this case  $V_{u,max}$  was taken as the code predicted shear resistance.

## 4.2.3 Statistical Properties of the Model Factor

### 4.2.3.1 Basic Statistical Properties

A model factor was calculated for each experiment of the database. Statistical properties of the model factor were determined for the complete database SDB\_WithSR and for SDB\_WithSR: Subset 1 and SDB\_WithoutSR: Subset 2. The following statistical properties were determined:

- Expected value (mean),  $\mu$
- Standard Deviation,  $\sigma$
- Coefficient of variation,  $\Omega$

The distribution of the model factor was assumed to be normal and a check was carried out to verify the validity of this assumption. Table 4.6 shows the mean model factor calculated for SANS for SDB\_WithoutSR and for the subsets of the database. The standard deviation and coefficient of variation are also shown. The tabulated model factors and specifications for all the experiments are shown in Appendix A.2.

<b>SANS Model Factor: SDB_WithSR</b>			
	Total Database: 163 Tests $1.00 < a/d < 7.02$	<b>Subset 1: 99 Tests</b> $2.65 < a/d < 7.2$	Subset 2: 64 Tests $1 < a/d < 2.5$
mean	1.37	<b>1.23</b>	1.60
std dev	0.32	0.20	0.35
c.o.v. %	24	<b>16</b>	22

**Table 4.6: Results of SANS model factor determined from SDB\_WithSR**

The SANS method has a coefficient of variation of 24% and a conservative bias of 37% for the entire

database of experiments. Comparing the mean model factors of Subset 1 and 2 it becomes clear that the inclusion of members with an  $a/d$  ratio lower than 2.5 is the main factor contributing to the large conservative bias for the SANS method. If these tests are excluded, then the conservative bias of SANS decreases by 14 percentage points and the coefficient of variation decreases by 8 percentage points. Overall the uncertainty in the model factor has increased for members with shear reinforcement compared to members without shear reinforcement. The c.o.v. has increased from 12% to 16%.

#### 4.2.3.2 Trends in the Model Factor: Correlation and Regression Analysis

This section investigates trend in the model factor with important shear parameters. Trends are identified by correlating the model factor with the shear parameters. Pearson's correlation coefficient,  $r$  from equation 4.4 is employed as the measure of correlation. Linear regression functions were fitted to scatter plots of the model factor vs. shear parameters where a strong relatively strong correlation coefficient was determined, to investigate the extent to which the model factor is linear related to these parameters. The relative importance of correlation coefficients was judged according to table 4.2. A correlation of 0.2 between the model factor and a shear parameter was considered significant.

The correlation was determined for the following shear parameters:  $a/d$ ,  $d$ ,  $f_c$ ,  $\rho$  and  $v_s$ . Correlation with aggregate size was not possible as this data was generally not available for most of the experiments. The results for both the complete database of experiments and for Subset 1 are shown in the table 4.7 below. Significant correlations are highlighted in bold. The linear regression data for the parameters with significant correlations are shown in table 4.8 for SDB\_WithSR: Subset 1. The gradient and intercept of the linear regression functions are shown as well as the coefficient of determination,  $R^2$ .

Variable	Complete Set	Subset 1
$a/d$	<b>-0.58</b>	<b>-0.23</b>
$d$ (mm)	0.02	-0.10
$f_c$ (MPa)	0.12	0.00
$\rho$ (%)	0.11	<b>0.26</b>
$A_{fv}/bs$ (MPa)	0.14	<b>0.33</b>

**Table 4.7: Correlation data for members SDB\_WithSR**

Variable	gradient	intercept	$R^2$	$r$
$a/d$	-0.054	1.43	0.05	-0.23
$\rho$	0.042	1.12	0.07	0.26
$A_{sv}f_{yv}/bs$	0.098	1.13	0.11	0.33

**Table 4.8: Linear Regression data for SDB\_WithSR: Subset 1**

According to table 4.7 the following can be concluded:

- Significant trends with  $a/d$ ,  $\rho$  and amount of shear reinforcement exist.

### Trends with $a/d$

Similar to the case without shear reinforcement, the SANS model factor with shear reinforcement was found to be subject to a decreasing trend with increasing  $a/d$ . Once again  $a/d$  is not accounted for when calculating the shear resistance with SANS. It could be said that the effect is “inherited” from members without shear reinforcement. According to SANS the shear resistance is a summation of a concrete contribution term and a shear reinforcement contribution term (see equation 4.7). The concrete contribution term is given by the empirical function for shear resistance for members without shear reinforcement. So if this function were to contain a term for  $a/d$ , to account for bending-shear interaction in members without shear reinforcement this would also reduce the trend in  $a/d$  for members with shear reinforcement. The inclusion of experiments with  $a/d$  of less than 2.5 in the complete database, once again resulted in experiments with very high model factors for low  $a/d$  due to arch action. This gives the impression of a strong linear trend in model factor with  $a/d$ , indicated by a correlation of -0.58 in table 4.6. Similar to the case for members without shear reinforcement the removal of these experiments in Subset 1 of the database, results in a strong reduction of the correlation coefficient to -0.23. However the correlation is still significant indicating that a significant part of the trend in the total database is also due to bending-shear interaction which is not accounted for by SANS. In figure 4.19 and 4.20 the respective scatter plots of the SANS model factor against  $a/d$  for the complete database and Subset 1 are shown fitted with linear regression functions. Comparison of the plots shows how the perceived trend in  $a/d$  is reduced for Subset 1. For the complete database the linear regression function predicts that the model factor becomes unconservative for  $a/d$  greater than 5.2 although none of the actual observations with  $a/d$  greater than 5.0 had a model factor lower than 1.0. Subset 1 shows that the model factor will only become unconservative for  $a/d$  greater than 7.

Nonetheless the conservative bias in the model factor decreases by about 25% between  $a/d$  of 2.5 and  $a/d$  of 7.0. The reduction in a linear relationship between  $MF$  and  $a/d$  through the elimination of experiments with arch action, is confirmed by the reduction in  $R^2$  from 33% to 5%.

Compared to the correlation of -0.33 for SANS for members *without* shear reinforcement for SDB\_WithoutSR: Subset 1 (see table 4.3) the effect of bending-shear interaction is much reduced in members *with* shear reinforcement. The likely cause of this is that the shear reinforcement provides some crack control to flexural cracks thereby counteracting the effect of bending on shear resistance somewhat.

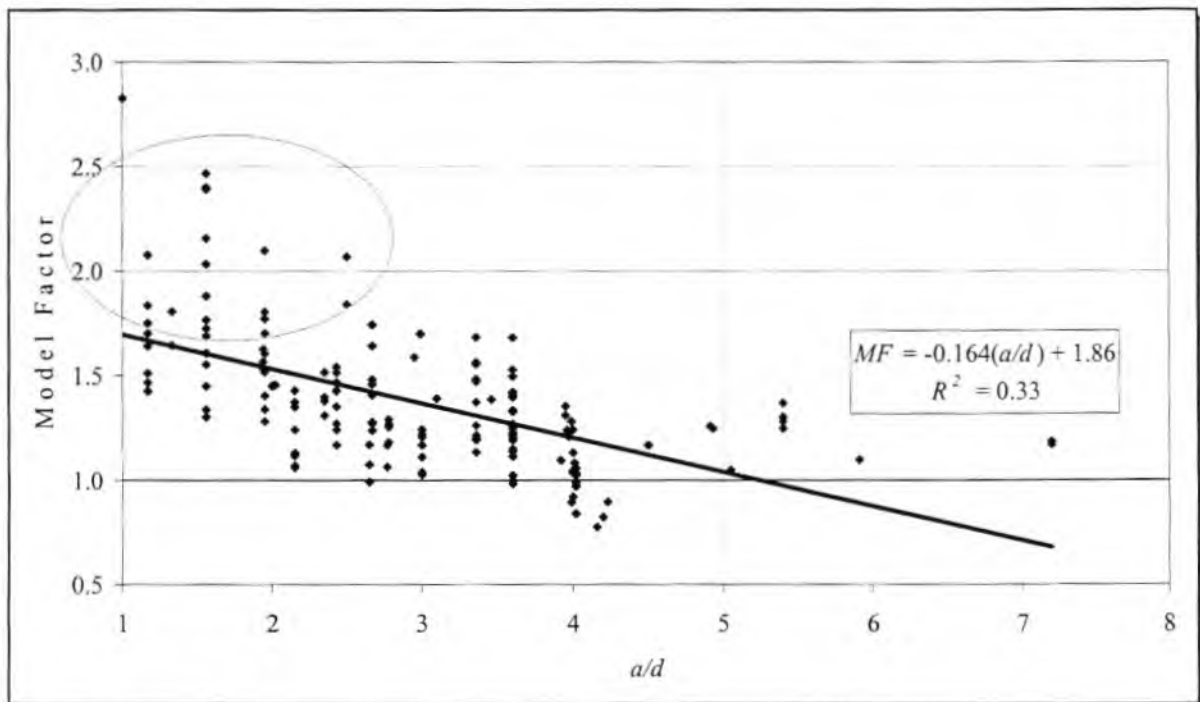
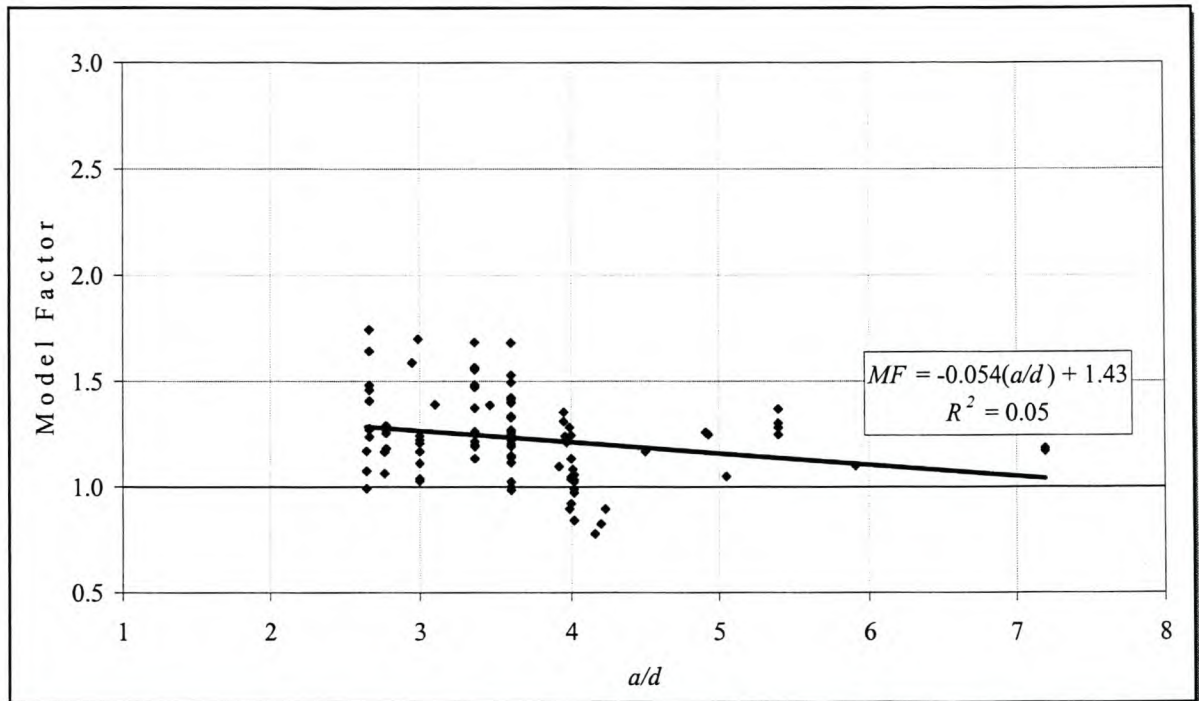


Figure 4.19: Linear Regression SANS  $MF$  vs.  $a/d$  for SDB\_WithSR: Complete Database



**Figure 4.20: Linear Regression SANS  $MF$  vs.  $a/d$  for SDB\_WithSR: Subset 1**

### **Trends with effective member depth**

The correlation between SANS  $MF$  and  $d$  is very weak at -0.1 for both the complete database and Subset 1, which is expected since SANS was already shown to predict the size effect very well for members without shear reinforcement in chapter 4.1.

### **Trends with amount of shear reinforcement**

The SANS model factor displays a trend with amount of shear reinforcement for the total database, with a correlation coefficient of 0.14. However when looking at Subset 1 the correlation coefficient increased to 0.33 with  $R^2$  of 10 %. The linear relationship between the model factor and the amount of shear reinforcement is weak, this is the strongest linear trend amongst all the parameters. The positive correlation coefficient indicates that as the amount of shear reinforcement increases the model factor increases too. A possible explanation is that with an increased amount of shear reinforcement present in a beam it becomes more likely for the reinforcement to cross a shear or flexural crack. Since shear reinforcement is only effective where it crosses a crack the shear steel contributes more to the shear strength, the more cracks it crosses. It may be that the SANS does not fully take this effect into account. The correlation coefficient is sufficiently large that it needs to be taken into account to

achieve the best model for the model factor. Figure 4.21 shows the scatter plot of the SANS model factor vs.  $v_s$  for Subset 1 of the database, demonstrating the increase in conservative bias with increasing shear reinforcement. Note that for members that are relatively highly reinforced in shear (above 1 MPa shear reinforcement) model factors for all experimental observations were greater or equal to 1.0.

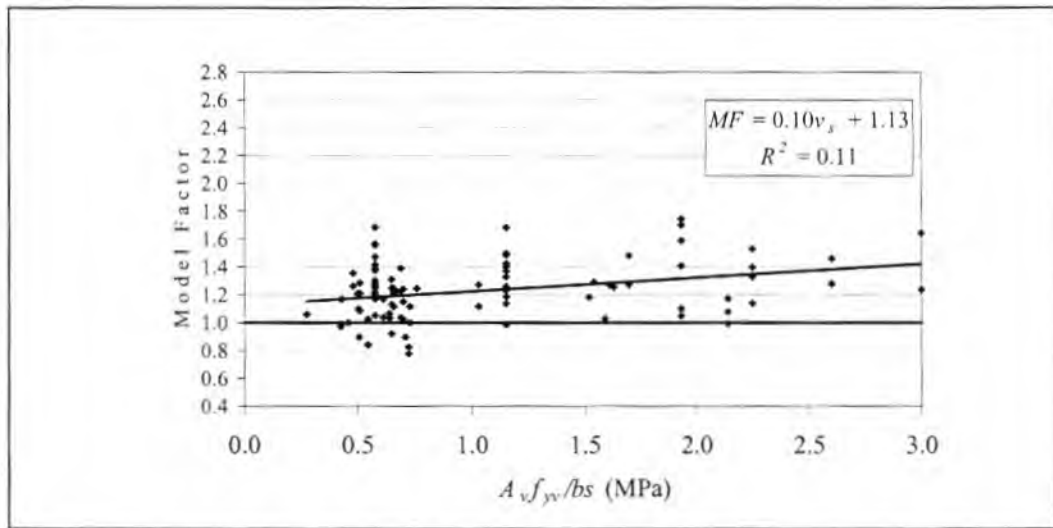


**Figure 4.21: Linear Regression SANS  $MF$  vs.  $v_s$  for SDB\_WithSR: Subset 1**

As the amount of shear reinforcement increases the percentage of concrete contribution to overall shear resistance decreases. Factors that affect concrete contribution such as the effective member therefore have less influence on the shear resistance. SANS is able to capture this effect and the variability in the model factors of the codes remain relatively unchanged with changing concrete contribution.

The decrease in concrete contribution to overall shear resistance ( $100v_c/v_u$  in %) with increasing shear reinforcement is demonstrated in figure 4.22. A linear regression line was fitted to help visualize the trend.

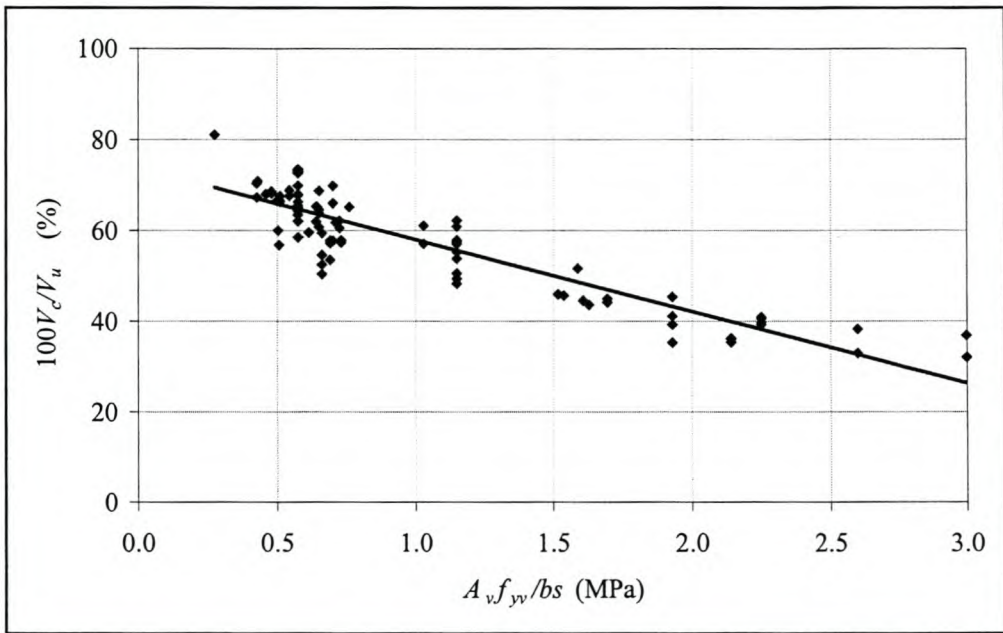


**Figure 4.22: Scatter plot of concrete contribution vs. shear resistance of SANS for Subset 1**

#### Trends with $f_c$ and $\rho$

Similar to members without shear reinforcement the model factor for members with shear reinforcement did not show any significant trend with the concrete cylinder strength. It is interesting to note that the database only contained members of normal strength concrete. If experiments with high strength concrete were included it is likely there would be a trend since the SANS method was not developed and is not intended for the design of high strength concrete beams.

SANS shows an increase in the model factor with increasing percentage of longitudinal tension steel, with a correlation coefficient of 0.26. This trend should be taken into account when modelling the model factor for reliability analysis. Such trends were not observed in members without shear reinforcement. The majority of experiments in the database are simply supported beams. In such beams longitudinal reinforcement increases proportionally with increased shear reinforcement, as shear at mid span increases proportionally with increased applied moment at mid-span, hence the correlation between  $\rho$  and  $v_s$ . It is therefore likely that the trend is due to a correlation between  $\rho$  with  $v_s$  of 0.42 in the database. Therefore the bias in the model factor increases both with  $\rho$  and  $v_s$ , but  $\rho$  also tends to increase with increasing  $v_s$ .

### Suitability of SANS model for reliability analysis

The trends in the SANS model factor with  $a/d$ ,  $\rho$  and  $v_s$  must taken into account in the general probabilistic model through correct modelling of the model factor. Modelling should be based on SDB\_WithSR: Subset 1 to eliminate the effect of arch action on the model factor.

## 4.2.4 Modelling the Model Factor for the Limit State Function

In this section an accurate model is derived for the SANS model factor to be applied in the general probabilistic model for shear required for the reliability analysis.

A multi-parameter linear regression model was fitted to the experimental data of SDB\_WithSR: Subset 1 for mean model resulting in the following equation:

$$MF_{SANS} = 1.279 - 0.052(a/d) + 0.040(\rho) + 0.035(v_s) \quad [4.9]$$

$$R^2 = 0.15$$

$$SSResid = 3.241$$

The coefficient of determination  $R^2$  of 0.15 indicates that 15% of the variation in the model factor is attributable to a linear relationship to  $a/d$ ,  $\rho$  and  $v_s$ . Longitudinal steel  $\rho$  is taken as a percentage, and  $v_s$  in MPa. Both are taken as their unfactored nominal value, when calculating the mean model factor for a specific design situation. The residual sum of squares,  $SSResid$ , which is the sum of the squares of the differences between the observed model factor and the model factor predicted by the linear regression, can be used to determine the standard deviation of the observations of the model factor about the linear regression plane, as follows:

$$\sigma = \sqrt{\frac{SSResid}{n-2}}, \text{ where } n \text{ is the number of observations}$$

Therefore for 99 observations in the experimental database, the standard deviation is 0.183. The residual plots for the parameters of the linear regression are shown in the figure 4.23. The predicted model factors are spread randomly about the zero residual line, indicating that a linear model is

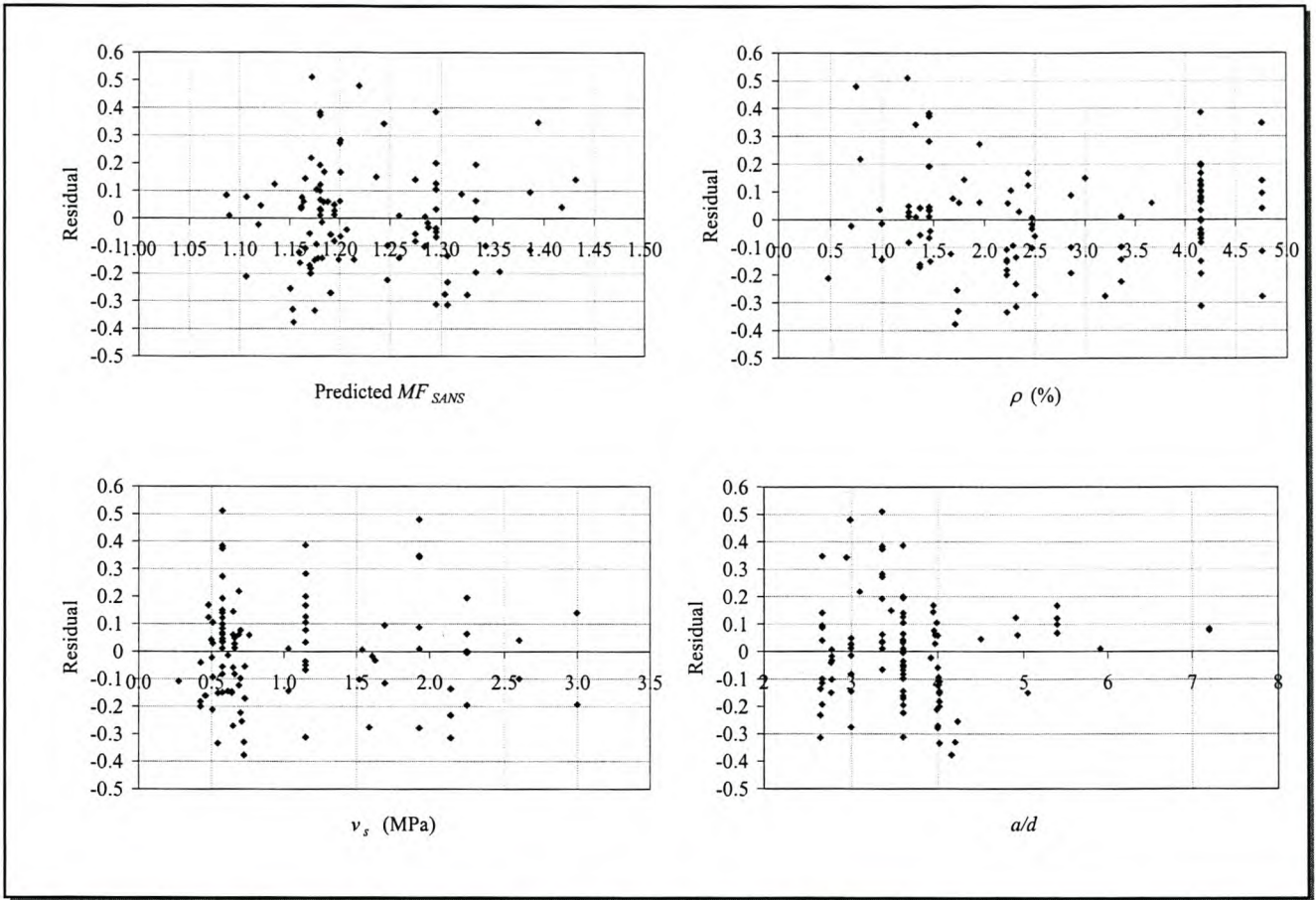


**Figure 4.23: Residual plots for SANS model factor**

appropriate. A trend in the residuals would have indicated that a non-linear model is more appropriate. It is therefore reasonable to assume a constant standard deviation of 0.183 over the entire range of data. For high  $a/d$  values the standard deviation seems to reduce, however the data in this region is very scarce. For the reliability analysis the bias in the model factor for a specific design case can be determined from the linear regression equation. The standard deviation is assumed constant at 0.183. The normal quantile plot of the standardised residual shown in figure 4.24 shows that the residuals are scattered about the linear regression plane (where the residual is zero) with a normal distribution. The simple linear regression model for the model factor of SANS general probabilistic model is summarised below:

$$MF_{SANS} = 1.279 - 0.052(a/d) + 0.040(\rho) + 0.035(v_s)$$

Constant standard deviation about mean  $MF$ :  $\sigma = 0.183$

Normal distribution

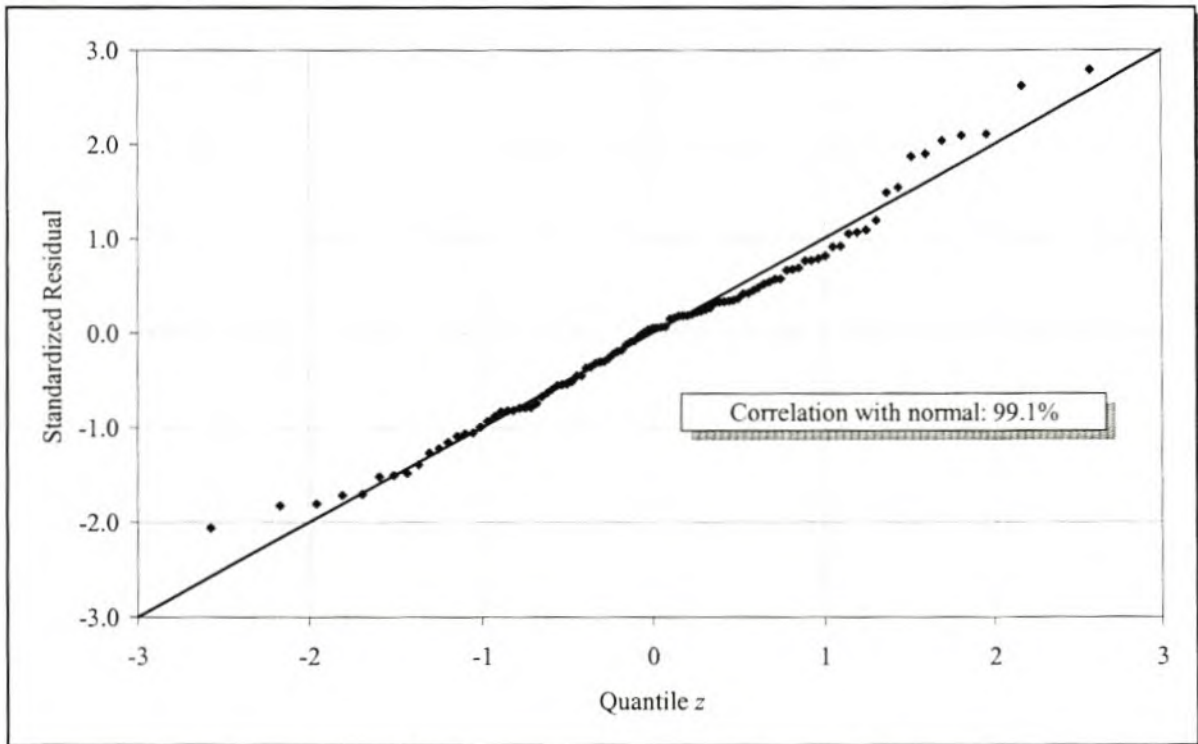


Figure 4.24: Normal Quantile plot for SANS  $MF$

# Chapter 5

## Reliability Analysis of the SANS 10100-1:2003 shear design procedure

In this chapter the reliability of the shear design procedure for SANS and for members with and without shear reinforcement is determined. Chapter 5.1 deals with members without shear reinforcement while Chapter 5.2 deals with members with shear reinforcement. The following procedure was followed:

- The general probabilistic model for shear as based on SANS is discussed.
- The modelling of the model factor of the general probabilistic model to be used in the reliability analysis is based on the results from Chapter 4.
- The reliability of SANS is determined over a range of probable design situations defined within a parameter study.
- The results are reported and evaluated.

### 5.1 Members without Shear Reinforcement

#### 5.1.1 Choosing a general probabilistic model for shear

A general probabilistic model for shear needs to be chosen against which the reliability of SANS can be determined. The general probabilistic model is a model of the true shear resistance. It reflects the statistical variation in the shear resistance due to the statistical variations in the shear parameters. However a large part of the uncertainty in predicting the true shear resistance is as a result of the uncertainty in the model on which the general probabilistic model for shear is based. In this section the suitability of the empirical SANS formula for members without shear reinforcement, as a general probabilistic model for shear, is investigated. It will be shown that the model uncertainty dominates the

uncertainty in the general probabilistic model for shear. Comparison to experimental data in Chapter 4.1 presents statistical data on the uncertainty of the SANS shear model. The uncertainty of SANS is quantified by the coefficient of variation, which was found to be about 12% from comparison to experimental data in chapter 4.1. SANS had a conservative bias in the model factor of 3%. Chapter 4 showed that the model factor of SANS is fairly insensitive to trends with all of the shear parameters. Because SANS uses an empirical formula that is a function of  $f_{cu}$ ,  $d$  and  $\rho$  it is not surprising that the model factor is not subject to trends with these parameters. However  $a/d$  is not taken into account and therefore the method shows a trend with  $a/d$ . In order for the general probabilistic model to account for the effect of  $a/d$ , the model factor must be derived as a function of  $a/d$ .

In the following section the limit state function required for the general probabilistic model as based on SANS is derived.

### 5.1.1.1 Limit State Equations of SANS for members without shear reinforcement

The limit state function for shear is given in general form by equation 3.5:

$$g(\mathbf{X}) = v_{gpm}(\mathbf{X}) - v_{code\_design} \quad [3.5]$$

The supply side of the limit state equation  $v_{gpm}(\mathbf{X})$  represents the general probabilistic model for shear, where  $\mathbf{X}$  is the vector of basic variables, i.e. the vector of shear parameters that contribute to the uncertainty in the general probabilistic model. The demand side of the equation  $v_{code\_design}$  represents a specific code design situation for which the reliability of the code is to be determined. The reliability is expressed in terms of  $\beta$  and represents the reliability inherent to the resistance side of the design case.

#### Limit state equation of SANS based general probabilistic model

The ultimate limit state equation for the SANS based general probabilistic model is as follows:

$$g(\mathbf{X}) = v_{gpm}(\mathbf{X}) - v_{code\_design} \quad [5.1]$$

$$= \left[ MF(0.75) \left( \frac{f_{cu}}{25} \right)^{1/3} \left( \frac{100A_s}{b_w d} \right)^{1/3} \left( \frac{400}{d} \right)^{1/4} \right] - v_{code\_design}$$

The expression for  $v_{gpm}(X)$  is based on the unfactored SANS shear design expression which is multiplied by the model factor  $MF$ . The vector of basic variables  $X$  consists of the model factor  $MF$ , as well as  $f_{cu}$ ,  $A_s$ ,  $b$  and  $d$ . Each basic variable is subject to a statistical distribution and therefore contributes to the uncertainty in the shear resistance. The design resistance  $v_{code\_design}$  for which the reliability is to be determined is calculated from deterministic nominal values for the applicable code while applying the appropriate partial material factors. The  $v_{code\_design}$  is therefore a single deterministic value. For SANS  $v_{code\_design}$  is calculated from the following equation:

$$v_{SANS\_design} = \left( \frac{0.75}{\gamma_{m,c}} \right) \left( \frac{f_{cu}}{25} \right)^{1/3} \left( \frac{100 A_{s,nom}}{b_{w,nom} d_{nom}} \right)^{1/3} \left( \frac{400}{d_{nom}} \right)^{1/4} \quad [2.6]$$

The values of the concrete strength  $f_{cu}$  or  $f_{ck}$  represent the 5% characteristic value. The partial material factor for concrete  $\gamma_{m,c}$  is 1.4 for SANS.

The partial derivatives of the limit state function with respect to the basic variables are as follows:

$$\left( \frac{\partial g}{\partial f_{cu}} \right)^* = (MF)(0.75) \left( \frac{1}{25} \right)^{1/3} \left( \frac{1}{3} \right) (f_{cu}^{-2/3}) \left( \frac{100 A_s}{b_w d} \right)^{1/3} \left( \frac{400}{d} \right)^{1/4} \sigma_{f_{cu}} \quad [5.2a]$$

$$\left( \frac{\partial g}{\partial A_s} \right)^* = (MF)(0.75) \left( \frac{f_{cu}}{25} \right)^{1/3} \left( \frac{100}{bd} \right)^{1/3} \left( \frac{1}{3} A_s^{-2/3} \right) \left( \frac{400}{d} \right)^{1/4} \sigma_{A_s} \quad [5.2b]$$

$$\left( \frac{\partial g}{\partial b_w} \right)^* = (MF)(0.75) \left( \frac{f_{cu}}{25} \right)^{1/3} \left( \frac{100 A_s}{d} \right)^{1/3} \left( -\frac{1}{3} b_w^{-4/3} \right) \left( \frac{400}{d} \right)^{1/4} \sigma_{b_w} \quad [5.2c]$$

$$\left( \frac{\partial g}{\partial d} \right)^* = (MF)(0.75) \left( \frac{f_{cu}}{25} \right)^{1/3} \left( \frac{100 A_s}{b_w} \right)^{1/3} (400)^{1/4} \left( \frac{-7}{12} d^{-10/12} \right) \sigma_d \quad [5.2d]$$

$$\left( \frac{\partial g}{\partial MF} \right)^* = (0.75) \left( \frac{f_{cu}}{25} \right)^{1/3} \left( \frac{100 A_s}{b_w d} \right)^{1/3} \left( \frac{400}{d} \right)^{1/4} \sigma_{MF} \quad [5.2e]$$

There is no partial derivative for  $v_{code\_design}$ , the demand side of the limit state function, because the value is a constant and therefore falls away with differentiation.

## First Order Second Moment (FOSM) Analysis

A First Order Second Moment (FOSM) analysis method was set up in Microsoft Excel for the general probabilistic model based on SANS. The FOSM analysis procedure is included in the attached CD.

### 5.1.1.2 Statistical Models for Basic Variables

The following statistical properties of the basic variables are required for the FOSM method applied to the limit state function to determine the reliability:

- *Bias*: The bias is required to calculate the expected value of the basic variable from its nominal (design) value (equation 3.7).
- *Coefficient of variation*: The coefficient of variation quantifies the variability in the basic variable.
- *Statistical distribution*: Most variables follow the normal distribution.

Available statistical models for the basic variables  $b$ ,  $d$  and  $A_s$  were taken from available literature (Mirza and McGregor, 1979). The statistical model for  $f_{ck}$  and  $f_{cu}$  was taken from Holický (2002).

#### The model factor

The statistical properties of the model factor of SANS as was derived in chapter 4.1 are used in the reliability analysis.

#### Member dimensions

The following models for member dimensions were taken from Mirza and McGregor.

Basic Variable	Bias	c.o.v. (%)	Distribution	Source
$d$	0.99	2-3	Normal	Mirza, McGregor (1979)
$b$	1.01	2	Normal	Mirza, McGregor (1979)
$A_s$	1	2	Normal	Mirza, McGregor (1979)

**Table 5.1: Statistical properties of member dimensions and steel area**

The bias of 0.99 for  $d$  indicates that in practice the expected value of  $d$  is usually slightly lower than the design value. The coefficient of variation of 2% for  $d$ ,  $b$  and  $A_s$  indicate that these parameters vary only slightly from their design values and are therefore unlikely to contribute significantly to the uncertainty in predicting shear resistance.

### Concrete compressive strength

SANS defines the concrete compressive strength used in the codes as the 5% characteristic value of concrete compressive strength. The material model implemented in the ISO standards and used for the calibration of the Eurocodes, is reported by Holický (2002):

$$\mu_{f_c} = f_{ck} + k_c \sigma_{f_c} \quad [5.3a]$$

$$\sigma_{f_c} = 0.10\mu_{f_c} \rightarrow 0.18\mu_{f_c} \quad [5.3b]$$

where  $\mu_{f_c}$  is the mean compressive cylinder strength,  $f_{ck}$  is the characteristic concrete compressive strength (the characteristic design value of the concrete) and  $\sigma_{f_c}$  is the standard deviation of the concrete compressive strength. The factor  $k_c$  depends on the quality control during the testing of concrete. For concrete with a normal distribution,  $k_c$  will take on a value of 1.645 for a 5% characteristic value. However for good testing practice it may occur that the characteristic value is closer to 2%, then  $k_c$  will have a value of 2. Holický suggest  $k_c$  be taken between 1.5 and 2.0.

The use of a characteristic value provides a conservative bias for the concrete compressive strength as shown in figure 3.2 for a 5% characteristic value. The model can be applied equally to cube strength or cylinder strength. Holický suggests a coefficient of variation of 10% for concrete where good quality control is exercised and a c.o.v. of 18% for concrete with poor quality control. This corresponds well to the range of between 10% and 20% based on many test results as reported by Wiley (Melchers, 1999). Holický suggests a lognormal distribution for concrete. Mirza and McGreggor states a normal distribution is applicable to most concrete and lognormal distributions for concretes of poor quality control, however the error is small between the two different distributions. Mirza and McGreggor suggest that a normal or lognormal distribution can be applied.

The model as reported by Holický is applied in this reliability analysis. Substituting 5.3(b) into 5.3(a) the mean concrete compressive strength is given by:

$$\mu_{f_c} = \frac{f_{ck}}{1 - \Omega k_c} \quad [5.4]$$

where  $\Omega$  = coefficient of variation

Assuming that the true characteristic value is 5% for SANS,  $k_c$  is taken equal to 1.645 and for the worst case of quality control concrete with a c.o.v of 18% then,

$$\mu_{f_c} = \frac{f_{ck}}{0.70} \quad [5.5]$$

The bias according to formula 5.5 is therefore 1.43.

### 5.1.1.3 Reliability Analysis of Individual Examples

In this section the reliability of a single design situation is determined for the SANS design procedure based on the SANS general probabilistic model. The purpose is to identify the extent to which each of the basic variables contributes to the overall uncertainty in modelling the shear resistance. The test case has the following design properties:

#### Test case: Member without shear reinforcement

- $b_w = 200$  mm
- $d = 300$  mm
- $100A_s/bd = 1\%$
- $f_{cu} = 20$  MPa
- $a/d = 6$

The statistical properties of the basic variables applied in the FOSM analysis from section 5.1.1.2 are tabulated below. The model factor is modelled as a single basic variable with properties as reported in table 4.1 as a preliminary analysis for SANS. The modelling of the model factor was further refined for the parameter study.

Variable	Bias	C.o.v. (%)	Distribution
$f_{cu}/f_c$	1.43	18	Normal
$A_s$	1.00	2	Normal
$b$	1.01	2	Normal
$d$	0.99	2	Normal
$MF_{SANS}$	1.03	12	Normal

**Table 5.2: Probability moments of basic variables**

Table 5.3 and table 5.4 show the first and final iteration of the FOSM analysis for determining the SANS reliability of the test case. For the limit state function in these tables the general probabilistic model for shear was based on SANS. Note for a first estimate of the failure point, represented by the vector  $\mathbf{X}^*$ , the expected values of the basic variables are used. The value of  $\beta$  is then determined for the new failure point (where  $g(\mathbf{X}) = 0$ ). The Excel sheets are provided in the attached CD filed under the relevant chapter section. For an iteration  $k$ , the initial failure point was taken as the failure point from the previous iteration,  $k - 1$ . Iterations were repeated until  $\beta$  converged.

SANS based probabilistic model: Iteration 1 Test Case , determine reliability for SANS						
Variable $X_i$	Design Value	Expected Value	Std Dev	dg/dX	Direction Cosines	$X^*$
$f_{cu}$ (MPa)	20	29	5.1	0.052	0.44	22
$A_s$ (mm <sup>2</sup> )	600	600	12.0	0.006	0.05	598
$b$ (mm)	200	202	4.0	-0.024	-0.20	205
$d$ (mm)	300	297	5.9	-0.010	-0.08	299
$MF$	1	1.03	0.124	0.104	0.87	0.699
			$\Sigma(dg/dX)$	0.120	$\beta$	3.07
					$g(\mathbf{X})$	0.00

**Table 5.3: FOSM Iteration 1 for test case: SANS**

SANS based probabilistic model: Iteration 10 Test Case , determine reliability for SANS							
Variable $X_i$	Design Value	Expected Value	Std Dev	dg/dX	Direction Cosines	$X^*$	
$f_{cu}$ (MPa)	20	23	5.1	0.041	0.39	23	
$A_s$ (mm <sup>2</sup> )	600	599	12.0	0.004	0.03	599	
$b$ (mm)	200	203	4.0	-0.013	-0.12	203	
$d$ (mm)	300	298	5.9	-0.006	-0.06	298	
$MF$	1	0.69	0.124	0.096	<b>0.91</b>	0.688	
				$\Sigma(dg/dX)$	0.105	$\beta$	3.03
						$g(X)$	0.00

**Table 5.4: FOSM Final Iteration for test case: SANS**

The direction cosines indicate the extent to which a basic variable contributes to the overall uncertainty of the general probabilistic model. The closer the values are to 1.0 the greater the contribution to the overall uncertainty in the model. Clearly the model factor dominates the uncertainty. The dimensional parameters make almost no contribution to overall uncertainty. After the model factor the concrete strength has a relatively weak contribution to the uncertainty. The use of the 5% characteristic however improves reliability by increasing the safety margin (the difference between the supply and demand sides) of the limit state function, by increasing the conservative bias of  $f_{cu}$ . The conservative bias in the general probabilistic model is thereby increased, thus improving the reliability.

In the next section the statistical distribution of the SANS general probabilistic model is derived and represented graphically. Such a distribution can be applied to find the reliability of a number of different design situations for SANS or even other codes.

#### 5.1.1.4 The probabilistic model of SANS

In the previous sections the reliability index was determined for a specific design situation, as defined by  $v_{code\_design}$ , according to the limit state function:

$$g(X) = v_{gpm}(X) - v_{code\_design}$$

The general probabilistic model involves the inverted process. The distribution of the general probabilistic model for the code shear resistance can be determined from the performance function simply by finding the corresponding values of  $v_{code\_design}$  for a set of probabilities of failure:

$$g(\mathbf{X}) = v_{code\_model}(\mathbf{X}) - v$$

for

$$P_f = p(v_{code\_model} < v) \quad [5.6]$$

where  $P_f$  is the probability of failure in percent. A set of values of  $v$ , are found for a range of  $P_f$  ranging from say 0.01% to 75%. The probability of failure,  $P_f$  can be expressed in terms of the reliability index,  $\beta$  and plotted against  $v$ , to obtain a graphical representation of the plot. The demand side of the equation  $v$  represents the design shear resistance. It can be calculated according to any code design method for which the reliability is to be determined. The following statistical data can be obtained from the plot:

*Statistical Distribution:* If the code shear resistance model follows a normal distribution, the plot of  $v$  against  $\beta$  will follow a straight line. The correlation between  $v$  and  $\beta$  should be close to 100% for a normal distribution.

*Mean:* The mean shear resistance is found from the plot where  $\beta = 0$ .

*Standard Deviation:* The standard deviation equals the absolute value of the gradient of the plot.

*Coefficient of Variation:* The coefficient of variation is found by dividing the standard deviation by the mean. The distribution of the general probabilistic model was derived for the design section from section 5.1.1.3. Table 5.5(c) shows the values of  $v$  for various probabilities of failure, for the SANS based probabilistic model, calculated from with the FOSM method.

<b>(a) Design Values</b>	
$f_{cu}/f_c$ (MPa)	20/15.8
$\rho$	1%
$b$ (mm)	200
$d$ (mm)	300
$a/d$	6.0

<b>(b) Probability Moments</b>			
$X_i$	Bias	c.o.v. (%)	Distribution
$f_{cu}/f_c$	1.43	18	Normal
$A_s$	1.00	2	Normal
$b$	1.01	2	Normal
$d$	0.99	2	Normal
$MF_{SANS}$	1.03	12	Normal

<b>(c) General probabilistic model: SANS</b>				
$v$	$P_f$	$\beta$	$\beta$ true normal	std dev
0.492	0.01	3.719	3.582	0.105
0.529	0.05	3.291	3.229	0.105
0.548	0.1	3.090	3.055	0.105
0.596	0.5	2.576	2.594	0.105
0.620	1	2.326	2.364	0.105
0.647	2	2.054	2.106	0.105
0.664	3	1.881	1.940	0.105
0.678	4	1.751	1.813	0.105
0.688	5	1.645	1.709	0.105
0.727	10	1.282	1.344	0.105
0.793	25	0.674	0.710	0.105
0.870	50	0.000	-0.029	0.105
0.951	75	-0.674	-0.804	0.105

<b>(d) Correlation with normal</b>	99.84	%
Mean	0.867	MPa
c.o.v.	12.07	%

**Table 5.5: General probabilistic model for shear resistance for SANS**

The plot results are shown graphically on normal probability paper in figure 5.1. The general model of both SANS shows a correlation with the normal distribution of greater than 99%.

The coefficient of variation for the SANS probabilistic model is 12.07%. This coefficient of variation is nearly identical to that of the model factor derived in Chapter 4.1, reaffirming the dominance of the model factor on the uncertainty of the general probabilistic model. The SANS shear design formula predicts a shear resistance of 0.53 MPa for the test case. According to the SANS based probabilistic

model the reliability is 3.03. This is indicated by the dashed lines in figure 5.1 (also see table 5.6). If the partial material factors were to be reduced in SANS resulting in a prediction of shear resistance of say 0.6 MPa instead of 0.53 for the test case then the reliability would decrease to about 2.6. Similarly a different code's reliability (say Eurocode) could be determined for the test case from the SANS based general probabilistic shear distribution in figure 5.1.

The model factor was modelled simply as a single basic variable in deriving the SANS based general probabilistic distribution for shear in figure 5.1. However SANS shows a trend in the model factor with  $a/d$ . This is not reflected in the general probabilistic models of figure 5.1, therefore this model is not capable of predicting the effect of  $a/d$  on shear.

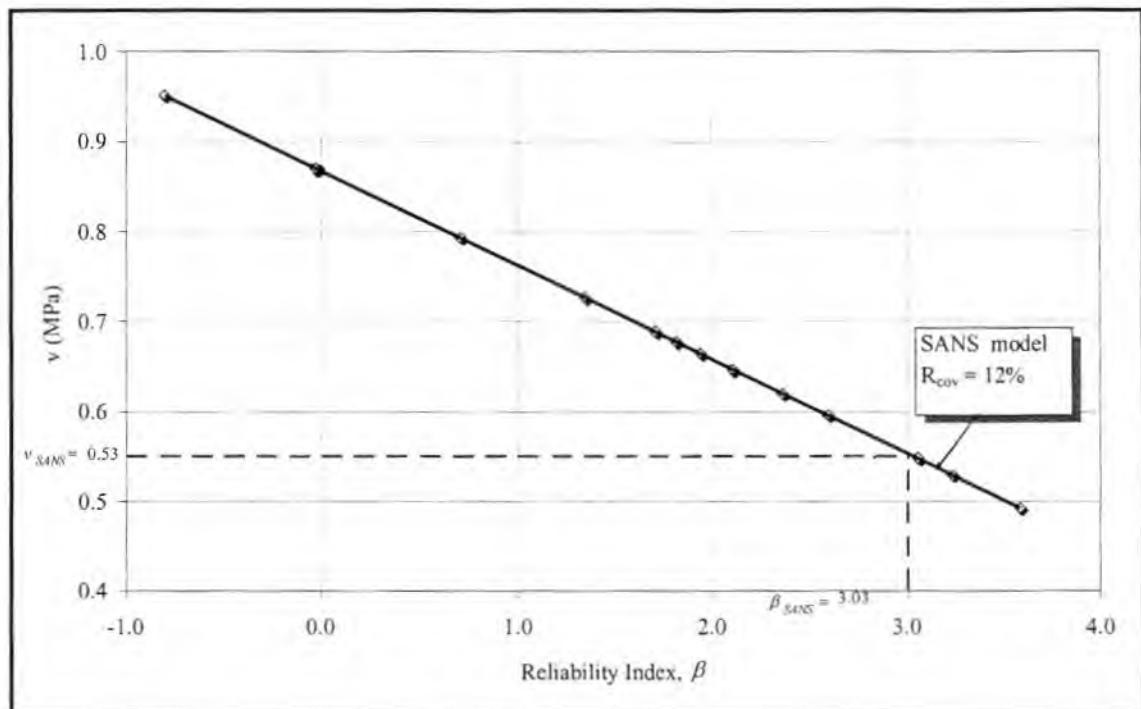


**Figure 5.1: Probabilistic shear resistance model of SANS, no shear reinforcement**

For the purposes of the parameter the modelling of the model factor was improved to reflect the effects of  $a/d$  on the reliability of shear. The bias of the model factor was modelled by the linear regression function derived in section 4.1, table 4.4.

The bias of the model factor of the SANS probabilistic model was modelled by the linear regression function as a function of  $a/d$  fitted to experimental data in chapter 4.1 and summarized in table 4.4:

$$\text{Bias } MF_{SANS} = -0.042(a/d) + 1.19$$

$$\sigma = 0.122$$

When calculating the bias for a specific design situation the deterministic design value of  $a/d$  was taken, i.e.  $a/d$  was not modelled as a basic variable subjected to statistical variation.

## 5.1.2 Parametric study

The purpose of the parametric study is to determine the level of reliability of the SANS shear design method for a range of design situations that fall within the design limits of the code. A design situation is defined as a practical combination of  $f_{cu}$ ,  $d$ ,  $\rho$  and  $a/d$  that makes up a reinforced concrete beam. The parameter study allows us to identify any design cases where the target minimum level of reliability defined as  $\beta = 2.0$  are not achieved. Trends in reliability with any of the shear parameters can be identified from the parameters allowing judgement on the consistency of the reliability of the code.

### 5.1.2.1 Scope of the parametric study

The reliability of the design codes must be determined over a range of design parameters allowed by the code. Table 5.6 shows the limits of SANS for members without shear reinforcement.

Parameter:	min	max	SANS 10100 clause
$f_{cu}(MPa)$	20	40	3.4.2.1.1 Table 1
$\rho$ (%)	0.13	4%	4.11.4.2.1/4.11.5.1
$a/d$ (or $M/Vd$ )	3.0	6	-
$v$ (MPa)	-	$v_u < 4.75$ MPa	4.11.4.5.3/4.3.4.1.1

**Table 5.6: Allowable range of design parameters for SANS**

It is unlikely that a member without shear reinforcement would contain 4% longitudinal bending reinforcement. At such high bending stresses shear reinforcement would be required. The SANS states that  $f_{cu}$  may not be taken greater as 40 MPa when calculating the shear resistance of a beam. This thesis is limited to the study of normal strength concretes. Concrete shear theory predicts that beams generally do not fail in shear for  $a/d$  ratios greater than 6.0. However some of the experimental data in chapter 4.1 showed that shear failure is possible for  $a/d$  ratios as high as 8.0. Such beams are typically highly reinforced in the longitudinal direction to prevent bending failure. There is no limit on the effective member depth allowed by SANS. However SANS requires that crack control steel be provided for members with  $d$  greater than 750 mm. Experiments (ASCE-ACI Task Committee 445, 1998) have shown that crack control steel actually improves shear resistance by countering the size effect. However the general probabilistic model for shear is not capable of predicting this effect and the results are therefore only applicable to beams where no crack control is provided.

For the parametric study a number of practical design examples were set up. Three sections were chosen: a shallow section ( $d = 300$  mm,  $b = 200$  mm), medium ( $d = 600$  mm,  $b = 400$  mm), and very deep section. ( $d = 1200$  mm,  $b = 800$  mm). The values of  $f_{cu}$  and  $\rho$  were varied for the alternative sections within the range of table 5.7, while  $a/d$  was kept constant at 3.0 and the reliability was determined from the SANS limit state function (equation 5.1). After that  $a/d$  was varied between 3 and 8 and the level of reliability determined.

### **5.1.2.2 Parametric Study: SANS**

#### **5.1.2.2.1 Results from the Parametric Study**

The results are categorized into two parts, namely parameters that do not affect the reliability of the code, and parameters that show trends in the reliability of the codes.

#### **Parameters to which SANS reliability is not sensitive**

It was found that the reliability of SANS is not sensitive to changes in  $f_{cu}$  and  $\rho$ .

This means that SANS fully account for the effect of these two parameters on shear resistance. SANS was also insensitive to changes in  $d$ . Both  $f_{cu}$  and  $\rho$  have very small direction cosines as was demonstrated in section 5.1.1.3 and therefore contribute very little to the overall uncertainty of the general probabilistic model. Since the bias of the model factor is not a function of either  $f_{cu}$  or  $\rho$  it was not expected that these parameters should have any significant effect on reliability. The results of 5 beam configurations from the parameter study are shown in table 5.7 to illustrate these results.

Test no:	1	2	3	4	5
$f_{cu}$ (MPa)	20	20	<b>40</b>	20	20
$100A_s/bd$	<b>0.13</b>	<b>4.0</b>	0.13	0.13	0.13
$b$ (mm)	200	200	200	400	800
$d$ (mm)	300	300	300	<b>600</b>	<b>1200</b>
$a/d$	3.0	3.0	3.0	3.0	3.0
$\beta_{SANS}$	3.2	3.3	3.2	3.2	3.2

**Table 5.7: Reliability for SANS for various beam configurations with  $a/d = 3.0$**

The reliability of SANS increases slightly with an increase in  $\rho$ , when comparing test 1 and test 2 in table 5.7. However the increase is negligible. An increase in  $f_{cu}$  had no effect on the reliability of SANS. The reliability of SANS remained unchanged for an increase in  $d$ .

#### **Parameters to which SANS reliability is sensitive**

While SANS reliability was found to be insensitive to  $\rho$ ,  $f_{cu}$  and  $d$  the most significant trend in reliability was found to be with  $a/d$ . It was found that SANS reliability decreased with  $a/d$ . This is because the design procedure does not account for  $a/d$  when calculating shear resistance. However the general probabilistic model as based on SANS was able to predict the effect of  $a/d$  on shear resistance through correct modelling of the model factor, as the bias of the model factor was fitted to experimental data as a function of  $a/d$ .

Figure 5.2 shows the results from reliability of SANS plotted against  $a/d$ . Each point on the graph indicates a test case from the parameter study.

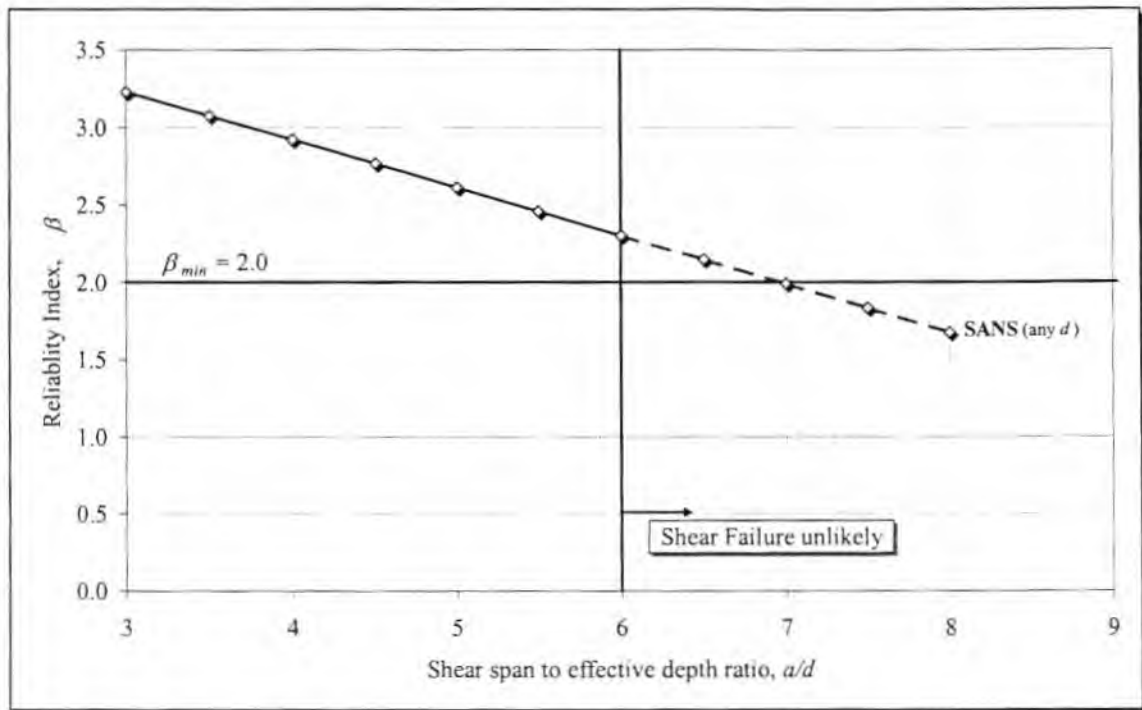


**Figure 5.2: Results from parametric study for members without shear reinforcement**

The line was plotted for tests from the parameter study with  $f_{cu} = 20$  MPa,  $d = 300$  mm and  $\rho = 0.13\%$ . However because the reliability of SANS is insensitive to changes in these parameters the line can be considered representative of any design situation regardless of the values of  $f_{cu}$ ,  $d$  and  $\rho$ . The beam test for  $a/d = 3.0$  for SANS corresponds to beam test 1 of table 5.7.

SANS reliability decreases from a maximum of 3.2 at  $a/d = 3.0$  to a minimum of 2.3 at  $a/d = 6.0$ . Shear reliability further decreases as  $a/d$  increases beyond 6.0 but shear failure is not likely for  $a/d$  greater than 6.0. Therefore the target minimum reliability index of 2.0 is achieved for all probable design situations where shear failure is likely.

#### 5.1.2.2.2 Discussion of the results

The results show that reliability of SANS is consistent with  $f_{cu}$ ,  $d$  and  $\rho$  but inconsistent with  $a/d$ . This means that SANS adequately accounts for the effects of  $f_{cu}$ ,  $d$  and  $\rho$  on shear but not for the negative effect that bending has on the shear resistance. Nevertheless minimum reliability is achieved for all design cases where shear failure is likely. For members with a relatively low  $a/d$  this may lead to

conservative designs in the sense that a shallower section could be used in design for the same shear stress.

SANS only allows beams to be designed without shear reinforcement where the applied shear stress is one half the calculated shear resistance. This rule further improves reliability but is not reflected in the results of the parameters study of figure 5.2. Here it is assumed that the applied shear stress equals the applied shear resistance. Slabs are cases where this rule does not apply. However slabs of effective member depth of 1200 mm are not very likely in practice and punching shear is usually the governing shear failure mechanism in slabs. Economy of design could be improved by decreasing the partial material factor for concrete. This would cause an overall downward shift in the reliability function of figure 5.2. The safety factor could be optimised so that target minimum reliability of 2.0 is met for  $a/d$  equal to 6.0. However because the shear resistance formula for members without shear reinforcement in calculating the shear resistance of members with shear reinforcement the effect of lowering the partial material factor for concrete must be investigated in conjunction for such members.

Consistency in reliability with increasing  $a/d$ , could be improved by deriving an empirical expression for shear resistance in members without shear reinforcement, where  $a/d$  is one of the variables. Because this empirical expression is also the concrete contribution term for members with shear reinforcement this would also improve consistency in reliability with  $a/d$  for members with shear reinforcement.

## 5.2 Members with Shear Reinforcement

### 5.2.1 General probabilistic model for shear

A general probabilistic model for shear needs to be chosen against which the reliability of SANS can be determined. In this thesis SANS is used as the basis for the general probabilistic model. The statistical properties of the model factor of SANS were derived in chapter 4.2 for this purpose. This section briefly investigates the suitability of the SANS method.

The limit state function for determining reliability is represented in the following general form as given by equation 3.5:

$$g(\mathbf{X}) = v_{gpm}(\mathbf{X}) - v_{code\_design} \quad [3.5]$$

The supply side of the limit state equation  $v_{gpm}$  represents the general probabilistic model which can be based either on the SANS or another code shear design procedure. The demand side of the limit state equation represents a code design resistance for which the reliability is to be determined. The resistance is calculated with SANS to determine the reliability of SANS for a particular design situation.

The uncertainty in the shear resistance is characterized by the uncertainty in the probabilistic model for shear. This uncertainty derives from the statistical variation in the shear parameters modelled as basic variables ( $\mathbf{X}$ ), which include geometrical properties, material properties and most importantly the uncertainty of the model itself in predicting shear resistance. The statistical properties of the basic variables are defined by the bias, coefficient of variation and statistical distribution. The statistical data of the geometric properties and material strength are available from published literature (Mirza & McGregor, 1979), while the statistical properties of the SANS model factor was determined in chapter 4. It is expected that the uncertainty in the geometric properties and the material properties will contribute only slightly to the overall uncertainty of the general probabilistic model, while the uncertainty in the model factor will contribute most to the uncertainty in the general probabilistic model. The uncertainty in the model arises because the model factor is not able to perfectly predict shear resistance because it may not account for all parameters that affect shear resistance as is the case

for the  $a/d$  ratio. Another source of uncertainty in the model factor arises from the fact that most code models are based on simplifying assumptions made to facilitate the design process.

Once the probabilistic model for shear resistance has been derived the level of reliability of SANS can be determined for a range of possible design situations. Different combinations of shear design parameters may lead to different levels of reliability. A parametric study will identify the changes in the level of reliability for different design configurations for SANS.

The following procedure was followed in determining the reliability of reinforced concrete beams with shear reinforcement designed with SANS:

- The limit state functions for a probabilistic model based on SANS were derived. The reliability of individual design situations was determined from this probabilistic model, to determine the relative importance of the basic variables on the overall uncertainty of the probabilistic model. The performance functions for SANS and the partial derivatives, required for the reliability analysis are shown in section 5.2.1.1. The statistical properties of the basic variables are given in section 5.2.1.2 and the results of reliability analysis of the individual results are reported in section 5.2.1.3.
- The general probabilistic model for a range of design situations for SANS is derived in section 5.2.1.4.
- The choice and range of the parametric study is discussed in section 5.2.2.1
- The results from the parametric study are reported and evaluated in section 5.2.2.2 for SANS.

### 5.2.1.1 Limit State Equations of SANS

The ultimate limit state equation of SANS as given in the form of equation 5.1 is as follows:

$$\begin{aligned}
 g(\mathbf{X}) &= v_{code\_model}(\mathbf{X}) - v_{code\_design} \\
 &= [v_c + v_s]_{code\_model} - v_{code\_design} \\
 &= MF \left[ (0.75) \left( \frac{f_{cu}}{25} \right)^{1/3} \left( \frac{100A_s}{b_w d} \right)^{1/3} \left( \frac{400}{d} \right)^{1/4} + \left( \frac{A_v f_{yv}}{b_w s} \right) \right] - v_{code\_design} \quad [5.7]
 \end{aligned}$$

The vector of basic variables,  $\mathbf{X}$ , consists of the model factor as well as the other parameters  $f_{cu}$ ,  $A_s$ ,  $b_w$ ,  $d$ ,  $A_v$ ,  $f_{yv}$  and  $s$ . The partial derivatives of the limit state function  $g(\mathbf{X})$ , required for the FOSM method in the reliability analysis are listed below:

$$\left(\frac{\partial g}{\partial f_{cu}}\right)^* = (MF)(0.75)\left(\frac{1}{25}\right)^{1/3}\left(\frac{1}{3}\right)\left(f_{cu}^{-2/3}\right)\left(\frac{100A_s}{b_w d}\right)^{1/3}\left(\frac{400}{d}\right)^{1/4}\sigma_{f_{cu}} \quad [5.8a]$$

$$\left(\frac{\partial g}{\partial A_s}\right)^* = (MF)(0.75)\left(\frac{f_{cu}}{25}\right)^{1/3}\left(\frac{100}{b_w d}\right)^{1/3}\left(\frac{1}{3}A_s^{-2/3}\right)\left(\frac{400}{d}\right)^{1/4}\sigma_{A_s} \quad [5.8b]$$

$$\left(\frac{\partial g}{\partial b_w}\right)^* = (MF)(0.75)\left(\frac{f_{cu}}{25}\right)^{1/3}\left(\frac{100A_s}{d}\right)^{1/3}\left(-\frac{1}{3}b_w^{-4/3}\right)\left(\frac{400}{d}\right)^{1/4}\sigma_{b_w} + (MF)\left(\frac{A_v f_{yv}}{s}\right)\left(-b_w^{-2}\right)\sigma_{b_w} \quad [5.8c]$$

$$\left(\frac{\partial g}{\partial A_v}\right)^* = (MF)\left(\frac{f_{yv}}{b_w s}\right)\sigma_{A_v} \quad [5.8d]$$

$$\left(\frac{\partial g}{\partial f_{yv}}\right)^* = (MF)\left(\frac{A_v}{b_w s}\right)\sigma_{f_{yv}} \quad [5.8e]$$

$$\left(\frac{\partial g}{\partial s}\right)^* = (MF)\left(\frac{A_v f_{yv}}{b_w}\right)\left(-s^{-2}\right)\sigma_s \quad [5.8f]$$

$$\left(\frac{\partial g}{\partial MF}\right)^* = (0.75)\left(\frac{f_{cu}}{25}\right)^{1/3}\left(\frac{100A_s}{b_w d}\right)^{1/3}\left(\frac{400}{d}\right)^{1/4}\sigma_{MF} + \frac{A_v f_{yv}}{b_w s}\sigma_{MF} \quad [5.8g]$$

### 5.2.1.2 Statistical Models for Basic Variables

The statistical properties of the model factor of SANS for members with shear reinforcement were derived in chapter 4.2. For SANS the models of the basic variables of the concrete contribution to overall shear resistance,  $A_s$ ,  $b$ ,  $d$  and  $f_{cu}$  as applied to the limit state function for members without shear reinforcement, are again applied to the limit state function of members with shear reinforcement. The statistical models apply to the entire range of the parametric study.

Statistical models are required for the additional basic variables,  $A_v$ ,  $s$  and  $f_{yv}$ .

### Shear steel area and stirrup spacing

Basic Variable	Bias	c.o.v. (%)	Distribution	Source
$A_v$	1.0	2	Normal	Mirza, McGreggor (1979)
$s$	1.0	3	Normal	Mirza, McGreggor (1979)

**Table 5.8: Statistical properties of shear steel area and stirrup spacing**

### Steel shear reinforcement yield strength

SANS defines the yield strength of shear reinforcing steel as the 5% characteristic value. Holický (2002) suggests the following model to calculate the expected value of steel reinforcing steel, from the characteristic value of steel,  $f_{yvk}$ :

$$\mu_{f_{yv}} = \frac{f_{yvk}}{1 - k\Omega_{f_{yv}}} \quad [5.9]$$

The factor  $k$  depends on the quality control of the steel. If the characteristic value of 5% is defined in the code,  $k$  should be taken as 1.645. Holický suggests a value of two for  $k$  suggesting that the quality control in practice is such that the true characteristic value is actually 2%. For this study  $k$  was taken conservatively as 1.645. Holický suggests a coefficient of variation,  $\Omega$  between 7 and 10% for ordinary structural steel at yield. The coefficient of variation is taken conservatively as 10%.

Basic Variable	Bias	c.o.v. (%)	Distribution	Source
$f_c, f_{cu}$	1.43	18	Normal	Holícký (2002)
$f_{yv}$	1.20	10	Normal	Holícký (2002)

**Table 5.9: Statistical properties of the materials**

The bias, which is the expected value of  $f_{yv}$  divided by the characteristic value, is then found from equation 5.9.

For the purpose of comparing the general probabilistic model for shear, the model factor was modelled as a single basic variable with bias and coefficient of variation as determined for the database of 99 experiments tabulated in table 4.14. The bias of the model factor was modelled more accurately in the parameter study with the regression functions in chapter 4.2.3.

### 5.2.1.3 Reliability Analysis of Individual Examples

In this section the reliability index of a single individual beam section was determined based on the SANS probabilistic shear resistance model. The purpose of these two examples is to demonstrate the dominant effect of the model factor on the uncertainty of the general probabilistic model. The section was taken from the subsequent parametric study. The test case is a highly reinforced shallow section. The nominal values of the design parameters of the test case are shown in table 5.11 below.

Specifications	Test case
$f_{cu}$ (MPa)	40
$\rho$ (%)	3.4
$d$ (mm)	300
$b$ (mm)	200
$v_s (A_s f_{yv} / bs)$	1.74
$v_{SANS\ design}$ (MPa)	2.8

**Table 5.10: Design specifications and shear design resistance of test case**

The following method was followed for determining the reliability index:

- A performance function was set up for SANS and the level of reliability was determined for the specific design situation according to each code.
- The reliability index of SANS was determined by means of the First Order Second Moment method implemented in a Microsoft Excel sheet using the limit state function for SANS (equation 5.7) and the appropriate partial derivatives (equation 5.8). The design shear resistance  $v_{code\ design}$  which represents the demand side of the limit state function was calculated according to SANS (equation 2.53) to determine the reliability for SANS. The design shear resistance is

calculated from *nominal* values and the appropriate partial material factors for SANS ( $\gamma_{m,s} = 1.15$ ,  $\gamma_{m,c} = 1.4$  are applied.

- The SANS model factor was modelled as a single basic variable with mean 1.23 and standard deviation 16% as outlined in table 4.6 of section 4.2.3.

### Results from the reliability analysis

Table 5.12 summarises the statistical data of the basic variables applied in the reliability analysis, from section 5.2.1.2.

Variable	Bias	C.o.v. (%)	Distribution
$f_{cu}/f_c$	1.43	18	Normal
$A_s$	1.00	2	Normal
$b$	1.01	2	Normal
$d$	0.99	2	Normal
$A_v$	1.00	2	Normal
$f_{yv}$	1.20	10	Normal
$s$	1.00	3	Normal
$MF_{SANS}$	1.23	16	Normal

**Table 5.11: Probability moments of basic variables**

Table 5.12 and table 5.13 show the first and final iteration of the test case for the limit state function, where the general probabilistic model is based on SANS. The reliability of the SANS code is evaluated.

SANS based probabilistic model: Iteration 1 Test Case , determine reliability for SANS							
Variable $X_i$	Design Value	Expected Value	Std Dev	dg/dX	Direction Cosines	$X^*$	
$f_{cu}$ (MPa)	40	57	10.3	0.118	0.13	53	
$A_s$ ( $mm^2$ )	2013	2013	40.3	0.013	0.01	2011	
$b$ (mm)	200	202	4.0	-0.195	-0.22	204	
$d$ (mm)	300	297	5.9	-0.023	-0.03	297	
$A_v$ ( $mm^2$ )	101	101	2.0	0.059	0.07	101	
$f_{yv}$ (MPa)	250	300	30.0	0.293	0.34	273	
$s$ (mm)	63	63	1.9	-0.088	-0.10	64	
$MF$	1	1.23	0.197	0.782	0.90	0.75	
				$\Sigma(dg/dX)$	0.873	$\beta$	2.71
						$g(X)$	0.00

**Table 5.12: FOSM Iteration 1 for Test Case: SANS**

SANS based probabilistic model: Iteration 5 Test Case , determine reliability for SANS							
Variable $X_i$	Design Value	Expected Value	Std Dev	dg/dX	Direction Cosines	$X^*$	
$f_{cu}$ (MPa)	40	55	10.3	0.072	0.09	55	
$A_s$ (mm <sup>2</sup> )	2013	2012	40.3	0.008	0.01	2012	
$b$ (mm)	200	204	4.0	-0.109	-0.14	204	
$d$ (mm)	300	297	5.9	-0.013	-0.02	297	
$A_v$ (mm <sup>2</sup> )	101	101	2.0	0.032	0.04	101	
$f_{yv}$ (MPa)	250	282	30.0	0.171	0.22	282	
$s$ (mm)	63	63	1.9	-0.048	-0.06	63	
$MF$	1	0.73	0.197	0.743	<b>0.96</b>	0.73	
				$\Sigma(dg/dX)$	0.776	$\beta$	<b>2.66</b>
						$g(X)$	0.00

**Table 5.13: FOSM Final Iteration for Test Case: SANS**

Note that as an initial estimate of the failure point ( $X^*$ ), the expected values (calculated by multiplying the nominal value of a basic variable with its corresponding bias) of  $X$  are used. The direction cosine of the model factor is very close to 1.0. This indicates that the uncertainty in the shear resistance model is almost exclusively dominated by the uncertainty in the model factor. The direction cosines of the dimensional parameters are negligibly small, indicating that these parameters do not contribute significantly to the overall uncertainty of the shear resistance. The direction cosines of the material properties,  $f_{cu}$  and  $f_{yv}$  are more pronounced at about 0.1 for  $f_{cu}$  and 0.2 for  $f_{yv}$ , but nevertheless weak compared to the model factors.

The direction cosines are a function of the partial derivatives of the basic variables as well as the standard deviation of the basic variables. Partial derivatives of variables that are a function of a root such as in the case of  $f_{cu}$  in the case of SANS, or variables that are denominators of a fraction, such as  $d$ ,  $s$  and  $b$  tend to be much smaller than the variables themselves, hence leading to a small partial derivative. It is therefore not surprising that a variable such as  $b$  which is both a denominator and has a coefficient of variation of only 2% should have a very small direction cosine and therefore little contribution to the overall uncertainty.

### 5.2.1.4 Probabilistic model for shear resistance for SANS

In this section the general probabilistic model distribution of shear resistance of SANS is determined.

The general probabilistic model for the code shear resistance is determined from the performance function by finding the corresponding values of  $v_{code\_design}$  for a set of probabilities of failure, as follows

$$g(\mathbf{X}) = v_{code\_model}(\mathbf{X}) - v$$

$$\text{for } P_f = p(v_{code\_model} < v) \quad [5.10]$$

where  $P_f$  is the probability of failure. A set of values of  $v$ , are found for a probability of failure,  $P_f$  ranging from 0.01% to 75%. The probability of failure,  $P_f$  can be expressed in terms of the reliability index,  $\beta$  (equation 3.4) and plotted against the  $v$ , to obtain a graphical representation of the general probabilistic model.

The results of the general model, based on test case of the previous section are shown in Table 5.16 and plotted in figure 5.3. The following general observations can be made:

- The probabilistic models for SANS has a coefficient of variation of 15%.
- The SANS model correlates with the normal distribution at 99.9%

<b>(a) Shear Resistance Model: SANS</b>				
$V$ (MPa)	$P_f$ (%)	$\beta$	$\beta$ true normal	std dev
2.1711	0.01	3.72	3.63	0.747
2.4568	0.05	3.29	3.25	0.747
2.5960	0.1	3.09	3.06	0.747
2.9561	0.5	2.58	2.58	0.747
3.1309	1	2.33	2.34	0.747
3.3234	2	2.05	2.09	0.747
3.4465	3	1.88	1.92	0.747
3.5400	4	1.75	1.80	0.747
3.6165	5	1.64	1.69	0.747
3.8831	10	1.28	1.34	0.747
4.3452	25	0.67	0.72	0.747
4.8890	50	0.00	-0.01	0.747
5.4708	75	-0.67	-0.79	0.747

(b) Correlation with normal	99.91	%
Mean	4.88	MPa
c.o.v.	15.3	%

**Table 5.14: Results of general probabilistic model for SANS**

Figure 5.3 is a graphical representation of the probabilistic model of shear resistance from table 5.14. A member with a calculated shear resistance of 4.0MPa will have a corresponding reliability index of 1.1 according to the general probabilistic model for SANS.

The model factor completely dominates the uncertainty in the probabilistic model, which results in the coefficient of variation of the shear resistance distribution equalling that of the model factor. It is therefore important to model the model factor as accurately as possible.

The behaviour of the model factor can be defined by the following three criteria:

- The bias and coefficient of variation
- Trends in the model factor with design parameters
- Sensitivity to design parameters.

Based on the first criterion SANS is clearly the better model for describing shear resistance. With a conservative bias of 1.23 it has greater inherent conservatism than for members without shear reinforcement. Also the coefficient of variation is 16% is about 4% greater than for members without shear reinforcement. The ideal model would have a bias of 1.00 and a coefficient of variation of 0%.

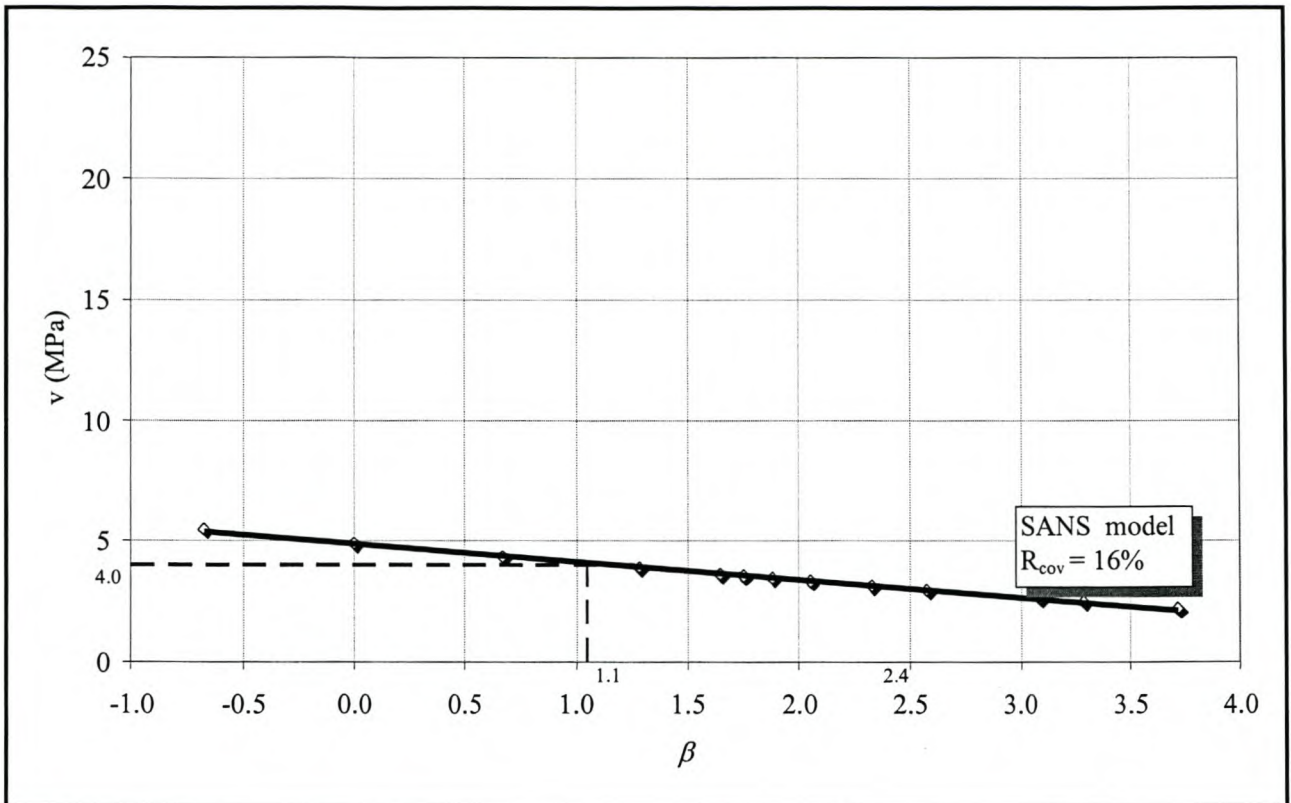


**Figure 5.3: Probabilistic shear resistance model of SANS**

If the model factor of a code shear design model displays trends with any of the shear design parameters, or other parameters, that are not variables of the shear design procedure such as  $a/d$ , it means that the code does not adequately take the effect of this parameter on shear resistance into account.

In table 4.8 the trends of the code model factor with various design variables are summarized. The magnitude of the trends are defined by the coefficient of determination,  $R^2$  which relates the percentage of correlation between the model factor and the variable that can be attributed to a linear relationship between the model factor and that variable. The trends in the SANS model factor were all very weak at less than 10% for all parameters. The absence of any significant trends greatly simplifies the modelling of the model factor in the limit state function.

SANS is sensitive to most of the important shear parameters, and can therefore model a wide range of design situations more accurately.

The performance function is therefore given by equation 5.8. However the prediction in the bias of the SANS model factor is improved by modelling with the linear regression equation derived in chapter 4.2.3:

$$\text{Bias } MF_{SANS} = 1.279 - 0.052(a/d) + 0.040(\rho) + 0.035(v_s)$$

$$R^2 = 0.15$$

$$\sigma = 0.183$$

It is assumed that the model factor is distributed normally about the linear regression line which represents the mean (or bias) with a constant standard deviation of 0.183. The improved modelling also ensures that the general probabilistic model predicts the effects of bending (i.e. the  $a/d$  ratio) on shear.

## 5.2.2 Parametric study

The purpose of the parametric study can be categorized in four main points as follows,

1. To determine the level of structural resistance reliability of SANS over a range of probable design situations. Design situations that do not achieve the minimum level of reliability are identified. As a guide the minimum level of resistance reliability is assumed to be a  $\beta$  of 2.0 in this thesis, but this is generally decided on by a code revision committee. The parameter study gives an idea of the average level of reliability of the codes.
2. To identify any trends in the level of reliability of the code with design parameters. Trends in the level of reliability of the code with specific design parameters indicate that the code design procedure does not sufficiently account for those parameters. The trends help to identify cases where the code may be unconservative or conversely over conservative.

3. To determine the consistency in the reliability of the code. The ideal code design procedure would display the same level of reliability for all probable design situations. Such a design procedure would be perfectly consistent. Three types of consistency can be defined. The first type of consistency is defined as the resilience of the level of reliability of the code with changing shear design parameters. However most codes offer simplified shear design procedures and trends in the reliability with design parameters are to be expected. Another form of consistency is the consistency of the trends themselves. A trend in the reliability with a certain design parameter is consistent if the trend is either increasing or decreasing over the entire probable range of that parameter. If the trend increases for part of the range and decreases for another part it is inconsistent. The third form of inconsistency is defined by sudden discontinuous changes in reliability.
4. Based on the trends in reliability with design parameters remedies can be recommended to improve the consistency of the code method. Typically one would want the level of reliability close to the minimum over the entire range of design situations as this will result in the most economic, yet safe designs. Consistency can be improved in different ways, the most convenient being the adjustment of the safety factors of the code.

### 5.2.2.1 Scope of the parametric study

The parametric study is limited to a range of design situations that are allowed by the design code under investigation. Parameters that may affect the level of reliability of the design code are divided into two categories, namely parameters that affect shear resistance that are taken into account by the shear design procedure and parameters that affect shear resistance that are not taken into account by the design procedure. In the case of SANS, factors that affect the shear resistance are  $f_{cu}$ ,  $\rho$ ,  $d$  and  $v_s$ . The  $a/d$  ratio is a parameter that affects shear resistance but is not taken into account by SANS when calculating the shear resistance. Parameters that are not taken into account by the code design procedure but accounted for by the general probabilistic model for shear used in the reliability analysis are expected to result in trends in level of reliability with that parameter. Therefore SANS is expected to display trends in the reliability with  $a/d$ . Other factors such as  $f_{cu}$ ,  $\rho$ ,  $d$  and  $v_s$  can also display trends if their contribution to shear resistance is not correctly modelled by the shear design procedure, compared to the general probabilistic model used in the reliability analysis.

Table 5.15 summarises the allowable range of design parameters according to SANS. The relevant clauses from the code are included for reference. Note  $f_{cu}$  is limited to a range of normal strength concretes ( $f_{cu} \leq 40$  MPa).

Parameter:	min	max	SANS 10100 clause
$s$ (mm)	practical limit	$0.75d$	4.3.4.1.3
$f_{yv}$ (MPa)	250	450	4.2.4.1.3
$A_v$ (mm <sup>2</sup> )	101 (8 mm stirrups)	226 (12 mm)	-
$f_{cu}$ (MPa)	20	40	3.4.2.1.1 Table 1
$\rho$ (%)	0.13	4%	4.11.4.2.1/4.11.5.1
$a/d$ (or $M/Vd$ )	2.5	6	-
$v$ (MPa)	$v_{s,min} = 0.0012f_{yv}/\gamma_{m,s}$	$v_u < 4.75$ MPa	4.11.4.5.3/4.3.4.1.1

**Table 5.15: Allowable range of design parameters for SANS**

Deep beams ( $a/d < 2.5$ ) are excluded from the investigation. Shear failures are unlikely in beams with  $a/d$  higher than 6.0 and are also excluded from the investigation. Shear stresses higher than 4.75 MPa are not allowed by SANS. A large number of design situations occur in practice where a particular design situation is described by any combination of the parameters listed in table 5.15 that affect the shear resistance according to the SANS probabilistic model.

A probable design situation is characterized by four main characteristics, namely the section, the concrete strength, the moment to shear ratio and the applied shear stress. The effective member depth and concrete compressive strength are important parameters that affect the shear resistance. The moment to shear ratio at the section under consideration determines the relative amount of longitudinal (bending) and transverse (shear) reinforcement. The applied shear stress, determines whether the beam will be lightly or highly reinforced. By constructing various combinations of these four characteristics within the allowable limit of SANS as summarized in table 5.15 a range of probable sections can be determined. The design sections that are derived can represent a number of different design situations. The shear reinforcement of a beam is usually designed for the section where the shear stress is at a maximum. For a two-span continuous beam as shown in figure 5.3, this is at the location of the inner support where the moment to shear ratio is at a maximum. This is where shear failure is most likely to occur. For a simply supported beam with a concentrated load at mid-span the shear force is constant over the entire span. The longitudinal reinforcement is designed for the maximum moment at mid-span.

If the longitudinal reinforcement is extended over the entire span for simplicity then the relative amount of shear and longitudinal reinforcement will remain constant over the entire beam. The reinforcement of this beam was therefore calculated at the section where the moment to shear ratio was a maximum.

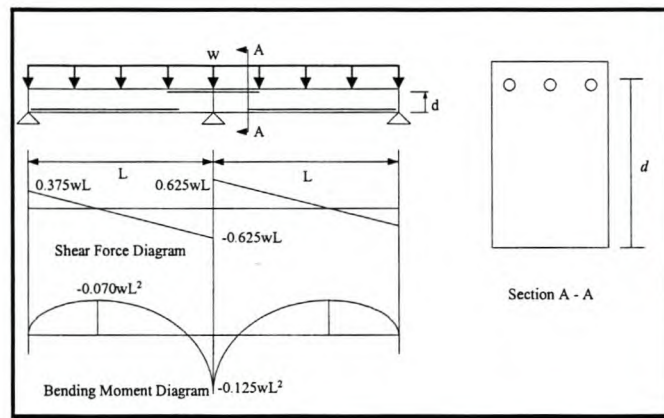


**Figure 5.4: Representative section for design of shear reinforcement.**

Various design situations as defined by probable combinations of design parameters, were determined for the parameter study as follows:

1. *Choose Section:* Three sections were used in the parametric study: a shallow, medium and deep rectangular section with dimensions as shown in figure 5.5. The medium beam is twice as deep as the shallow beam, whereas the deep beam is twice as deep as the medium beam.
2. *Choose concrete cube strength:* The concrete compressive strength was taken as either the SANS minimum of 20 MPa or the maximum of 40 MPa, which are the limits defined by SANS.
3. *Choose an applied shear stress:* An applied shear stress  $v_u$  was chosen as 4.75, 3, 2, 1.5, 1 or  $v_{min}$  MPa. The minimum applied shear stress  $v_{min}$  was chosen such that the beam would require the exact amount of minimum shear reinforcement of the section, according to SANS clause 4.11.4.5.3. (See table 5.15).
4. *Choose  $a/d$  (maximum  $M/Vd$ ) ratio:* The  $a/d$  ratio was chosen as 2.5, 3.0, 4.0, 5.0 or 6.0, at the location of the inner support. The  $a/d$  ratio determines the amount of longitudinal tension steel required to resist bending, relative to the amount of shear reinforcement which depends on the

applied shear stress. Therefore if  $v_u$  is known the ultimate moment,  $M_u$  can be calculated from the  $a/d$  ratio from which the amount of required bending steel can be designed.

5. *Design steel:* Once a section, cube strength, applied shear stress and  $a/d$  ratio was chosen, the amount of shear reinforcement and longitudinal tension reinforcement required for the section was calculated according to SANS. Design situations where more than the maximum allowable longitudinal tension reinforcement or less than minimum shear reinforcement was required, were considered impractical and not included in the parametric study, as these are not allowed by SANS.
6. *Determine reliability:* The reliability of the particular design situation was calculated with the first order second moment method.

The process described in the six points above is represented graphically in figure 5.5. The design of steel for a beam with effective depth of 300 mm, 40 MPa cube strength, applied shear stress of 2.0 and  $M/Vd$  of 6.0 is highlighted. The design calculations for this section are shown in Appendix C.1. In table 5.16 an example of the Microsoft Excel spreadsheet used to calculate the reinforcement steel of the various design situations is shown. The particular table shows the design calculations of seven beams all with effective depth of 300 mm, 40 MPa cube strength and  $M/Vd$  of 6.0. Each beam has a different applied shear stress, ranging from 4.75 MPa to 0.5 MPa. First the applied shear force and applied moment is calculated from the applied shear stress, to determine the required amount of bending and shear steel. If the longitudinal tension steel exceeds 4% then the particular design situation is considered impractical and is not included in the parameter study. For example the beam in table 5.16 with applied shear stress of 3 MPa requires more than 5 % tension steel. The reliability index was therefore not calculated for this case. However the beam in table 5.16 with applied shear stress of 2.2 MPa requires exactly 4% of steel, the maximum allowed by SANS. It is therefore not possible to stress a beam with this section and concrete strength and  $a/d$  ratio of 6.0 to a shear stress of 4.75 MPa without exceeding the maximum allowable percentage of tension steel. The beams with applied shear stress of 1 MPa and 0.5 MPa require less than the minimum amount of shear reinforcement and therefore fall outside the range of the parameter study. The beam with applied shear stress of 1.15 MPa required the exact amount of minimum shear reinforcement. The columns of table 5.16 that are highlighted in grey represent beam designs that fall within the limits of SANS. The reliability of SANS was therefore determined for these cases. The results from the parameter study are reported in section 5.2.3.2 for SANS.

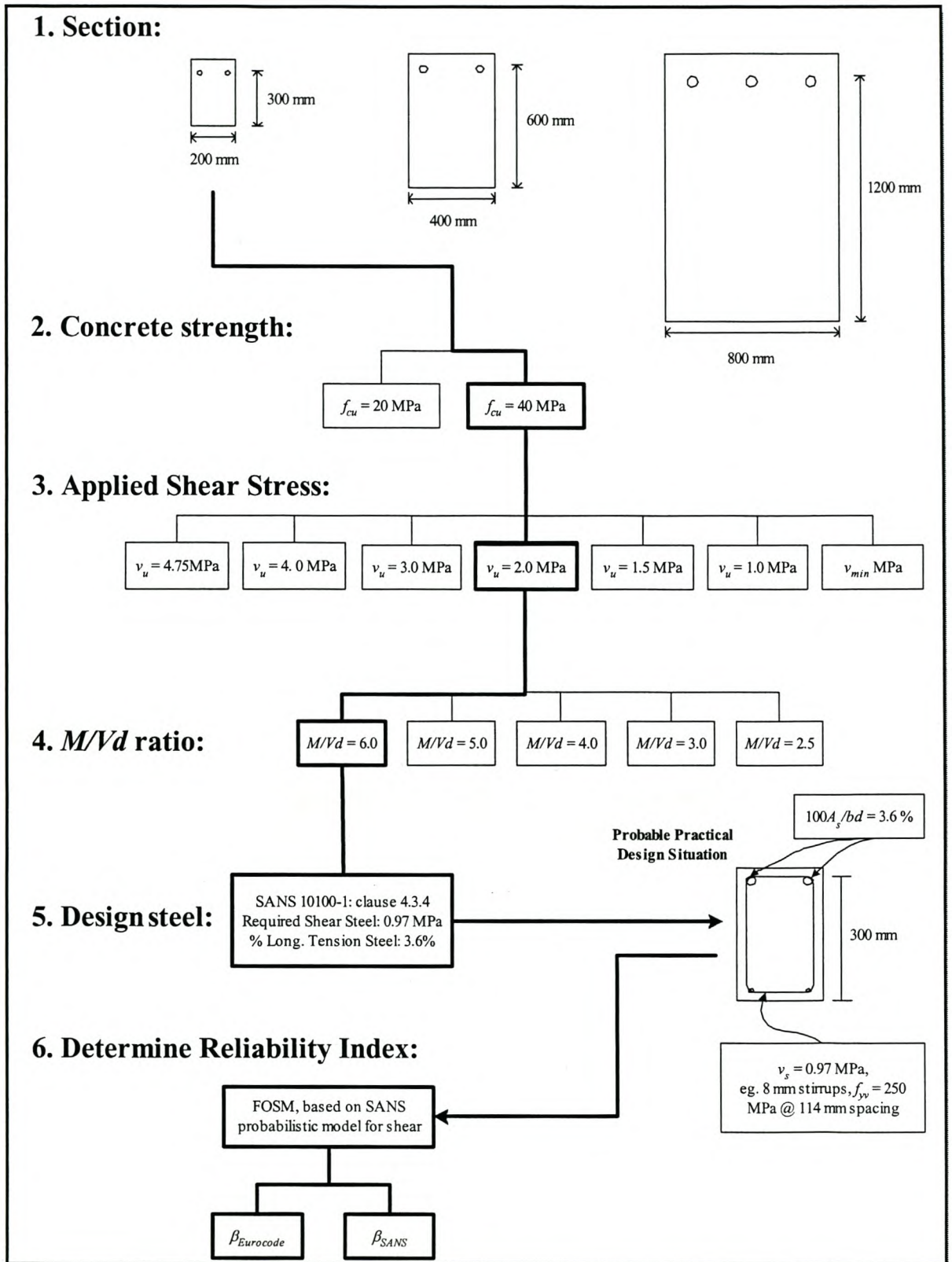


Figure 5.5: Schematic of process for determining probable design situations

		Calculate Forces						
$V_{inner\ support}$ (MPa)		3	2.2	2	1.5	1.15	1	0.5
$V_{inner\ support}$ (kN)		180	132	120	90	69	60	30
$M_{u,inner\ support}$ (kNm)		324	237.6	216	162	124.2	108	54

		Determine required amount of bending steel						
$K$		0.450	0.330	0.300	0.225	0.173	0.150	0.075
$K'$		0.156	0.156	0.156	0.156	0.156	0.156	0.156
$A_s'$ required ?		0	0	0	0	0	1	1
$z$ (mm <sup>2</sup> )		233	233	233	233	233	237	272
$A_s'$ (mm <sup>2</sup> )		2333	1381	1143	548	131	0	0
$A_s$ (mm <sup>2</sup> )		3162	2374	2177	1684	1339	1166	506
% Comp. Steel		3.9	2.3	1.9	0.9	0.2	0.0	0.0
% Tension Steel		5.3	4.0	3.6	2.8	2.2	1.9	0.8

		Check maximum tension steel of 4%						
Maximum Exceeded?		Yes	No	No	No	No	No	No

		Calculate Concrete Contribution to Shear Resistance						
$v_c$ SANS10100 (MPa)		1.2	1.1	1.03	0.9	0.9	0.8	0.6
$100v_c/v_u$ (%)		39.1	48.4	51.7	63.3	76.5	84.0	127.2*

\* For this beam  $v_c > v_u$  therefore only minimum stirrups required.

		Calculate Required amount of Stirrups						
$v_s$ (MPa)		1.83	1.14	0.97	0.55	0.26	0.16	-
Required $s$ for 8 mm bar		60	97	114	200	407	687	-
Less than nominal stirrups?		No	No	No	No	No	Yes	Yes

$\beta_{SANS}$ (MPa)		n.a.	2.6	2.5	2.3	2.2	n.a.	n.a.
----------------------	--	------	-----	-----	-----	-----	------	------

Table 5.16: Example design of reinforcement for beams of parameter study

## 5.2.2.2 Parametric Study: SANS 10100-1

### 5.2.2.2.1 Results of Parametric Study

The initial investigation of section 5.2.1.3 showed that the model factor of the SANS probabilistic model completely dominates the uncertainty in the shear design procedure as indicated by the direction cosines of greater than 0.9. The other basic variables,  $f_{cu}$ ,  $A_s$ ,  $d$ ,  $b$ ,  $A_{sv}$ ,  $s$  and  $f_{yv}$  have very small direction cosines and hence contribute very little to the overall uncertainty in the SANS shear design procedure. In chapter 4 it was shown that the SANS model factor displayed significant trends with  $\rho$ ,  $v_s$  and  $a/d$ . These trends indicate that SANS does not fully account for the effects of these parameters on the shear resistance. It was essential to model the model factor correctly to eliminate the shortcomings of the SANS method with respect to  $\rho$ ,  $v_s$  and  $a/d$ . The bias of a model factor for a specific design situation was determined from the following multi-parameter linear regression function, fitted to the experimental data (see section 4.2.3):

$$\text{Bias } MF_{SANS} = 1.28 - 0.052(a/d) + 0.040(\rho) + 0.035(v_s)$$

While the SANS method does not account for the effects of  $a/d$  and to a degree the effect of  $v_s$  and  $\rho$  in calculating the design shear resistance, which represents the demand side of the limit state function for a specific design situation for which the reliability is to be determined, the correct shear resistance is determined by the general probabilistic model on the supply side through accurate modelling of the bias of the model factor.

Therefore while  $\rho$  composed of the basic variables,  $A_s$ ,  $b$  and  $d$  makes little contribution to the uncertainty of the shear resistance model due to their small direction cosines,  $\rho$  does have a significant effect on the level of reliability in that it directly influences the bias of the model factor. The same applies for the amount of shear reinforcement  $v_s$ , which is made up of  $A_{sv}$ ,  $f_{yv}$ ,  $b$  and  $s$ . The  $a/d$  ratio does not affect the shear resistance according to the SANS model, but the trend in the model factor with  $a/d$  clearly indicates that this is incorrect. A calculation of the bias in the model factor for various combinations of  $a/d$ ,  $\rho$  and  $v_s$  shown in table 5.17 gives an indication of the trends in the reliability to be

expected from the parameter study. The bias increases with increased amount of shear reinforcement and longitudinal reinforcement but decreases with increasing  $a/d$  ratio.

	$a/d = 2.5$	$a/d = 6.0$
$\rho = 1\%, v_s = 1 \text{ MPa}$	1.22	<b>1.04</b>
$\rho = 3\%, v_s = 3 \text{ MPa}$	<b>1.34</b>	1.15

**Table 5.17: Bias of  $MF_{SANS}$  for various configurations of  $\rho$ ,  $v_s$  and  $a/d$**

Table 5.17 shows that the highest bias and hence the highest reliability is expected for a highly reinforced beam with a low  $a/d$  ratio, while the lowest bias and hence the lowest reliability is expected for a lightly reinforced beam with a high  $a/d$  ratio. This was confirmed to be the case by the parameter study.

While the trends in the level of reliability with  $a/d$ ,  $\rho$  and  $v_s$  were expected due to their influence on the model factor of the general probabilistic model used in the FOSM analysis, two other parameters that affect shear resistance namely  $f_{cu}$  and  $d$  were also found to affect the level of reliability. These two parameters do not affect the model factor of the general probabilistic model, and it was therefore not at first evident that changing these parameters would affect the level of reliability. However these two parameters affect the relative contribution of the concrete contribution term of the SANS shear design procedure to the overall shear design resistance thereby affecting the relative influence of the partial material factors for steel and concrete on the overall shear resistance and thereby influencing the reliability of SANS.

Therefore two main categories of trends in the reliability of SANS were observed from the parameter study:

1. The trend in reliability with  $a/d$ ,  $\rho$  and  $v_s$  because these factors are not adequately accounted for by the SANS shear design procedure.
2. The trend in reliability with  $f_{cu}$  and  $d$  as a result of their effect on the relative influence of the partial material factors.

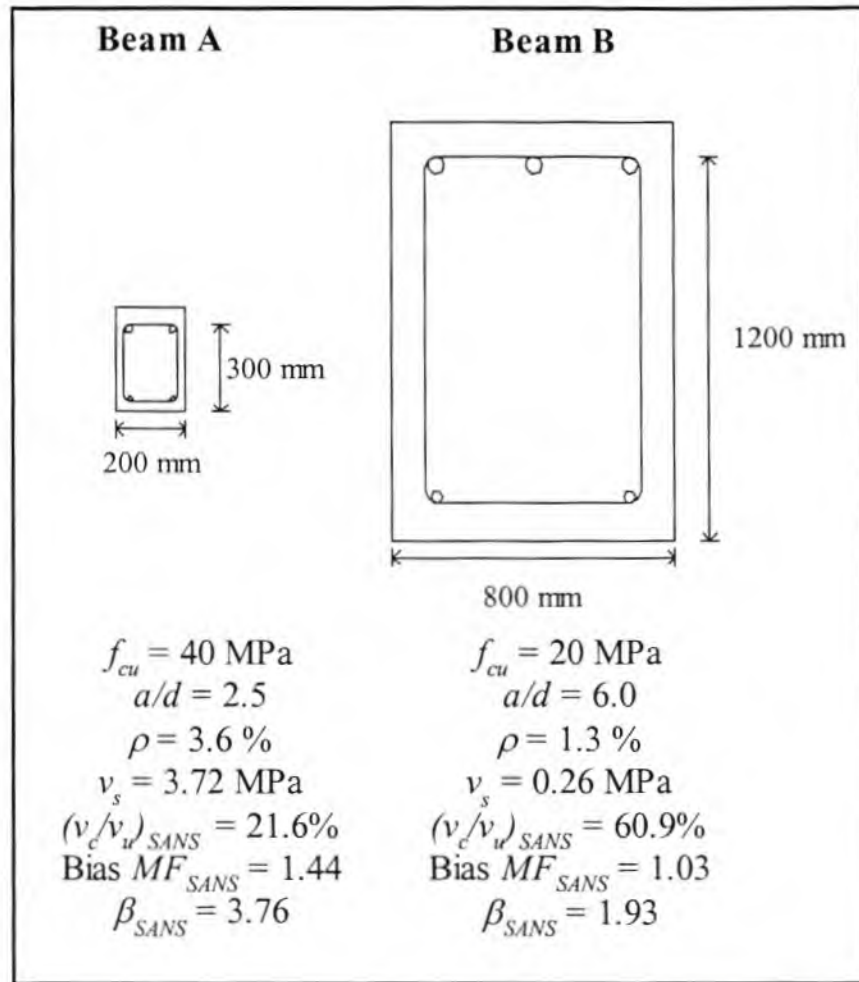
The results from the parameter study with the two main categories are reported in turn, but first some individual beam configurations from the parameter study are presented for the two cases.

### **Reliability from individual test from the parameter study**

Two beam configurations from the parameter study are illustrated in detail here. The design properties of the beams are shown in figure 5.6. The configurations are named Beam A and B for easy reference.

Beam A was found to have the highest reliability index of all the beams investigated in the parameter study at 3.76, while Beam B had the lowest reliability index in the parameter study at 1.93. The shear reinforcement of Beam A is designed to withstand the maximum allowable shear stress of 4.75 MPa according to SANS. The beam contains 3.6% of longitudinal bending reinforcement, which is close to the maximum of 4% allowed by SANS. The combination of a high amount of shear and longitudinal reinforcement and an  $a/d$  ratio of only 2.5 leads to a high conservative bias in the model factor of 44% which results in the high level of reliability. Beam B is a relatively lightly reinforced member with an  $a/d$  ratio of 6.0. The beam contained the minimum amount of stirrups. It had the lowest conservative bias in the model factor of all beams investigated in the parameter study at only 3%, leading to a low reliability index of only 1.93.

The first and final iteration of the FOSM analysis for Beam A are shown in table 5.18 and table 5.19 respectively, while the first and final iterations for Beam B are shown in table 5.20 and 5.22. The vector of basic variables  $X^*$  for the final iteration of beam A and B, given in the last column of Table 5.19 and 5.21 for Beam A and Beam B respectively represents the most likely failure point of each configuration. The value of  $\beta$  of 3.76 for Beam A and 1.93 for Beam B, represent the probability of failure corresponding to the respective failure points


 Figure 5.6: Beams from parameter study with lowest and highest  $\beta$  for SANS

SANS Iteration 1 Beam A						
Variable $X_i$	Design Value	Expected Value	Std Dev	dg/dX	Direction Cosines	$X^*$
$f_{cu}$ (MPa)	40	57.2	10.3	0.140	0.10	53
$A_s$ ( $mm^2$ )	2130	2130	42.6	0.016	0.01	2128
$b$ (mm)	200	202	4.0	-0.241	-0.16	205
$d$ (mm)	300	297	5.9	-0.027	-0.02	297
$A_v$ ( $mm^2$ )	101	101	2.0	0.146	0.10	100
$f_{yv}$ (MPa)	250	300.	30.0	0.731	0.49	243
$s$ (mm)	29	29.5	0.9	-0.219	-0.15	30
$MF$	1	1.44	0.183	1.228	0.83	0.86
				1.480	$\beta$	3.84
					$g(X)$	0.00

Table 5.18: FOSM first iteration for Beam A for SANS

<b>SANS Final Iteration Beam A</b>						
<b>Variable <math>X_i</math></b>	<b>Design Value</b>	<b>Expected Value</b>	<b>Std Dev</b>	<b>dg/dX</b>	<b>Direction Cosines</b>	<b>X*</b>
$f_{cu}$ (MPa)		54.5	10.3	0.080	0.07	55
$A_s$ (mm <sup>2</sup> )		2129	42.6	0.009	0.01	2129
$b$ (mm)		204	4.0	-0.127	-0.11	204
$d$ (mm)		297	5.9	-0.015	-0.01	297
$A_v$ (mm <sup>2</sup> )		101	2.0	0.070	0.06	101
$f_{yv}$ (MPa)		262	30.0	0.398	0.34	262
$s$ (mm)		30	0.9	-0.103	-0.09	30
$MF$		0.80	0.183	1.085	0.93	0.80
				1.172	$\beta$	3.76
					$g(X)$	0.00

**Table 5.19: FOSM final iteration for Beam A for SANS**

<b>SANS Final Iteration Beam B</b>						
<b>Variable <math>X_i</math></b>	<b>Design Value</b>	<b>Expected Value</b>	<b>Std Dev</b>	<b>dg/dX</b>	<b>Direction Cosines</b>	<b>X*</b>
$f_{cu}$ (MPa)	20	28.6	5.1	0.040	0.20	27
$A_s$ (mm <sup>2</sup> )	12092	12092	242	0.004	0.02	12081
$b$ (mm)	800	808	16.2	-0.054	-0.27	817
$d$ (mm)	1200	1188	23.8	-0.008	-0.04	1190
$A_v$ (mm <sup>2</sup> )	101	101	2.0	0.007	0.04	101
$f_{yv}$ (MPa)	250	300	30.0	0.037	0.18	289
$s$ (mm)	105	105	3.1	-0.011	-0.06	105
$MF$	1	1.03	0.18	0.184	0.92	0.69
				0.200	$\beta$	1.97
					$g(X)$	0.00

**Table 5.20: FOSM first iteration for Beam A for SANS**

<b>SANS Final Iteration Beam B</b>						
<b>Variable <math>X_i</math></b>	<b>Design Value</b>	<b>Expected Value</b>	<b>Std Dev</b>	<b>dg/dX</b>	<b>Direction Cosines</b>	<b><math>X^*</math></b>
$f_{cu}$ (MPa)	20	27.1	5.1	0.027	0.15	27
$A_s$ (mm <sup>2</sup> )	12092	12085	241.8	0.003	0.02	12085
$b$ (mm)	800	814	16.2	-0.034	-0.18	814
$d$ (mm)	1200	1189	23.8	-0.005	-0.03	1189
$A_v$ (mm <sup>2</sup> )	101	101	2.0	0.005	0.03	101
$f_{yv}$ (MPa)	250	292	30.0	0.024	0.13	292
$s$ (mm)	105	105	3.1	-0.007	-0.04	105
$MF$	1	0.69	0.18	0.179	0.96	0.69
				0.186	$\beta$	<b>1.93</b>
					$g(X)$	0.00

**Table 5.21: FOSM final iteration for Beam A for SANS**

Although the direction cosines indicate that the model factor dominates the uncertainty of the performance function, while the other basic variables have little influence due to their relatively small direction cosines, the vector of co-ordinates of the failure point,  $X^*$ , do indicate that the material properties,  $f_{cu}$  and  $f_{yv}$  contribute significantly to the conservative bias in the performance function. In table 5.22 the co-ordinates of the failure point of beam A and B have been extracted from table 5.19 and table 5.21 respectively. They are compared to the nominal design values in order to give an indication of contribution of each basic variable to the overall bias of the resistance side of the performance function.

	<b>Beam A</b>			<b>Beam B</b>		
	<b>Design Value</b>	<b>Failure Point</b>	<b>% Failure point/Design Value</b>	<b>Design Value</b>	<b>Failure Point</b>	<b>% Failure point/Design Value</b>
$f_{cu}$ (MPa)	40	55	138	20	27	135
$A_s$ (mm <sup>2</sup> )	2130	2129	100	12092	12085	100
$b$ (mm)	200	204	102	800	814	102
$d$ (mm)	300	297	99	1200	1189	99
$A_v$ (mm <sup>2</sup> )	101	101	100	101	101	100
$f_{yv}$ (MPa)	250	262	105	250	292	117
$s$ (mm)	29	30	103	105	105	100
$MF$	1	0.80	80	1	0.69	69

**Table 5.22: Contribution of basic variables to overall bias of performance function**

Table 5.22 clearly indicates that dimensional basic variables such as  $A_s$  and  $b$  make no significant contribution to the overall bias. However the steel yield strength,  $f_{yv}$  and to a greater extent the concrete strength,  $f_{cu}$  contribute to the overall conservative bias. At the failure point the conservative bias of the concrete is greater than 30%, for both Beam A and Beam B. This is mainly due to the use of 5% characteristic values of for  $f_{cu}$  and  $f_{yk}$ , which introduces additional safety to the performance function. Along with  $f_{cu}$  and  $f_{yv}$  the model factor contributes significantly to the conservative bias of the supply side of the performance function.

While the bias in the model factor changes with different design situations the standard deviation remains constant at 0.18. Therefore the uncertainty due to the variability of the model factor remains unchanged for different design situations. For this reason the direction cosines for the two very different design situations of Beam A and B are very similar at failure (0.92 for Beam A compared to 0.96 for Beam B). The failure coordinates of the model factor are very different (0.80 for Beam A and 0.69 for Beam B) reflecting the influence of the bias of the model factor on the level of reliability.

The strong effect of the bias of the model factor on the reliability is highlighted by these two cases. Beam configuration A represents a probable design situation with a specific combination of  $\rho$ ,  $v_s$  and  $a/d$  that would lead to the highest level of reliability for SANS in the parameter study, whereas Beam B represents a design situation where the specific combination of  $\rho$ ,  $v_s$  and  $a/d$  leads to the lowest level of reliability for SANS. Beams A and B therefore demonstrate the effect of  $\rho$ ,  $v_s$  and  $a/d$  on the reliability of SANS.

The second category of factor that affects reliability is the effect of  $f_{cu}$  and  $d$ . While the SANS shear design method fully accounts for the effects of these parameters on the shear resistance according to the general probabilistic model, they were found to affect the level of reliability none the less. The equation below represents the general performances function of SANS.

$$g(\mathbf{X}) = \underbrace{v(\mathbf{X})}_{\text{general probabilistic model}} - \underbrace{v_{SANS}}_{\text{code design shear resistance}} = v(\mathbf{X}) - \left( \frac{v_c}{\gamma_{m,c}} + \frac{v_s}{\gamma_{m,s}} \right)_{SANS}$$

The demand side of the performance function is represented by the general probabilistic model, which is a function of the basic variables represented by the vector  $\mathbf{X}$ . The supply side of performance

function is represented by the SANS shear design resistance of the case under investigation calculated from design values. The shear parameters  $f_{cu}$  and  $d$  do not affect the model factor which is the dominant basic variable in the general probabilistic model. However  $f_{cu}$  and  $d$  do affect the size of the concrete contribution term  $v_c$  on the demand side of the performance function. Beams with a low  $f_{cu}$  and high  $d$  have a relatively small concrete contribution term,  $v_c$  compared to beams with a high  $f_{cu}$  and low  $d$ . If the concrete contribution term is relatively small with respect to the overall design shear resistance  $v_{SANS}$ , the influence of the partial material factor for concrete is reduced while that of the partial material factor for steel is increased. The partial material factor for concrete has a value of 1.4 compared to 1.15 for steel and therefore has a greater influence on reliability. Beams with a high concrete contribution to overall shear resistance will have a higher level of reliability than similar beams that have a lower concrete contribution to overall shear resistance, because the increased influence of the partial material factor for concrete increases the safety margin between  $v(X)$  and  $v_{SANS}$  by reducing the value of  $v_{SANS}$ . The factors  $v_s$  and  $\rho$  also affect the relative influence of the partial material factors by influencing the relative contribution of the steel and concrete terms to the overall shear resistance. These factors also influence the model factor of the general probabilistic model. However the effect on the model factor dominates the effect on the relative influence of the partial material factor. This is demonstrated with the aid of table 5.23 below

SANS	Beam A	Beam B
Bias $MF$	1.44	1.03
$100v_c/v_u$ (%)	22	61
$\beta$	3.76	1.93

**Table 5.23: Effect of concrete contribution and bias in  $MF$  on reliability of SANS.**

Beam B has a relatively high concrete contribution to overall shear resistance of 61%. Therefore the influence of the partial material factor for concrete is high relative to the partial material factor for steel. Beam A has a relatively low concrete contribution at 22%, therefore the partial material factor for concrete has low influence on the design shear resistance compared to that of steel. Because the partial material factor for concrete is greater than that for steel, Beam B should have a higher level of reliability than Beam A, because it has the higher concrete contribution. However this is not the case because Beam A has a higher conservative bias in the model factor than beam B, which ultimately

dominates the level of reliability. Three beam configurations chosen from the parameter study are shown in figure 5.7 to demonstrate the effect of the partial material factor for concrete more clearly.

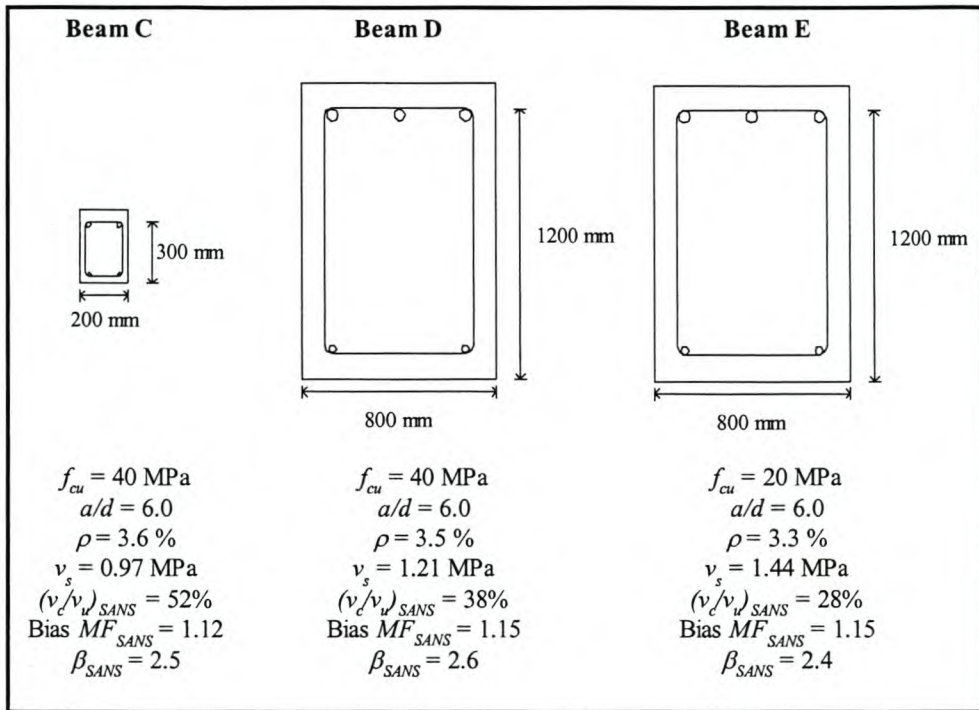


**Figure 5.7: Beam configurations for illustration of effect of concrete contribution on reliability.**

The three beam examples are similar in that the reinforcement for all three beams was designed to withstand a shear stress of 2 MPa according to SANS and the three beams have the same  $a/d$  ratio. Beam D and E differ in that Beam D is made from a 20 MPa concrete, whereas Beam E is made from a 40 MPa concrete. The reduced concrete strength in Beam E results in a reduced concrete contribution of 28% compared to 38% in Beam D. As a result Beam E requires slightly more shear reinforcement than Beam D in order to withstand the same applied shear stress of 2 MPa. Both Beam D and Beam E have the same bias in the model factor of 1.15. Therefore the difference in reliability index between the beams, namely 2.6 for Beam D and 2.4 for Beam E, is as a direct result of the difference in concrete contribution in the two beams. Because Beam D has a higher concrete contribution than Beam E the influence of the partial material factor for concrete is greater in Beam D than in Beam E.

When Beam C and Beam D are compared we see that the bias in the model factor of Beam C is slightly lower than that of Beam D, because Beam C requires slightly less shear reinforcement. Note that Beam

C is one of the beam configurations in table 5.16. Because Beam C is relatively shallow the size effect of shear is less pronounced than in Beam D hence leading to a concrete contribution of 52% in Beam C compared to 38% in Beam D. For this reason less shear reinforcement is required in Beam C. However since the model factor of Beam C is slightly lower than that of Beam D, the beam has a lower reliability compared to Beam D. The higher concrete contribution of Beam C counteracts the effect to some extent, resulting in a reliability index of 2.5 for beam C which would otherwise have been lower. Therefore changes in reliability with changes in  $f_{cu}$  and  $d$  result from the effect that these parameters have on the concrete contribution to overall shear resistance.

### **Trends in SANS reliability with $\rho$ , $v_s$ , $a/d$ and concrete contribution**

The section above illustrated the effect that the various shear parameters have on the reliability of the SANS shear design procedure through selected beam configurations from the parameter study. In this section the results from a number of beam configurations are represented graphically to illustrate these trends in reliability with respect to the various shear parameters more generally.

Figure 5.7 and 5.8 show the trends in SANS reliability with amount of shear reinforcement and percentage of longitudinal reinforcement for the 25 beam configurations from the parameter study that had an effective member depth of 300 mm and a concrete strength of 40 MPa. Each point in the plots indicates a single unique beam configuration. Beam configurations with the same  $a/d$  ratio are connected to highlight the trends in the level of reliability. Beam configurations A and C previously presented in detail is part of these 25 beam configurations and is indicated in the figures. The design data of the four beams in figures 5.8 and 5.9 with  $a/d$  of 6.0 where given previously in table 5.18.

The figures confirm the expected behaviour in the reliability with  $a/d$ ,  $v_s$  and  $\rho$ . Reliability increases with increasing  $v_s$  and  $\rho$ , as both  $v_s$  and  $\rho$  increase the conservative bias in the model factor of the general probabilistic model thereby increasing the level of reliability of SANS. The reliability decreases with increasing  $a/d$ , because the conservative bias in the model factor decreases with increasing  $a/d$ .

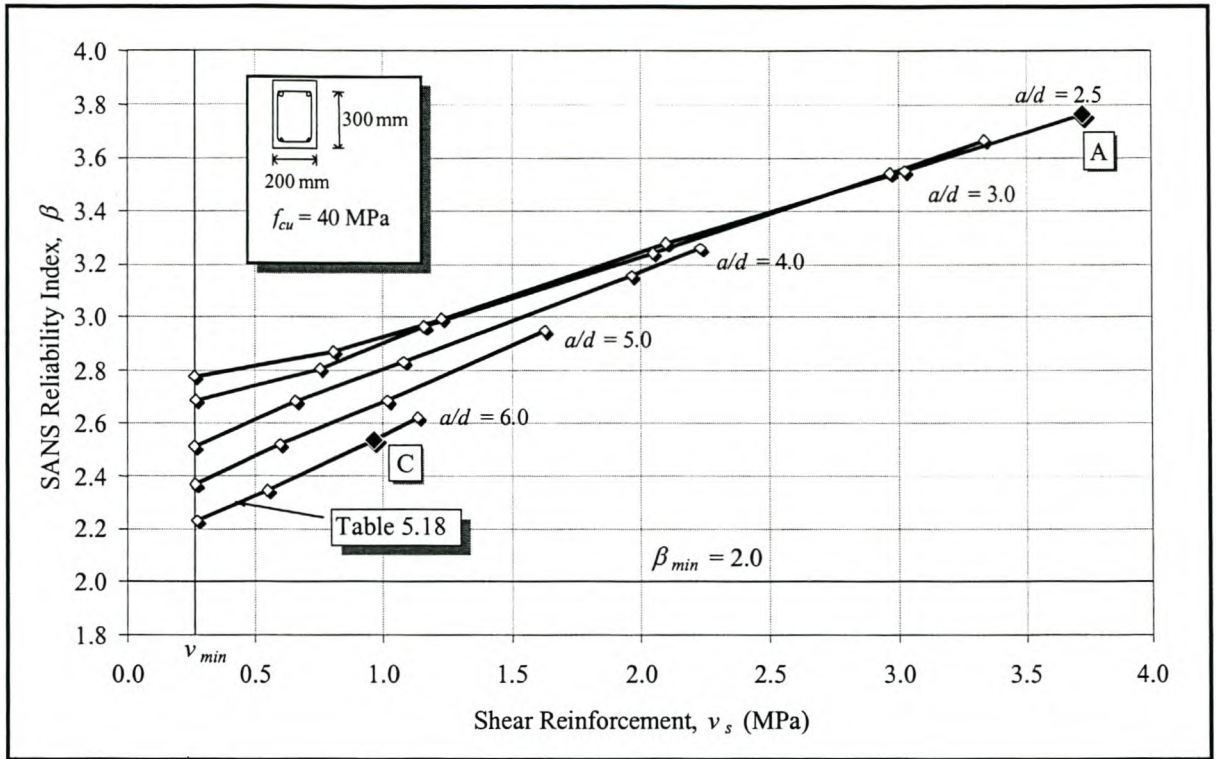


Figure 5.8: SANS Reliability Index vs. shear reinforcement (Set 1)

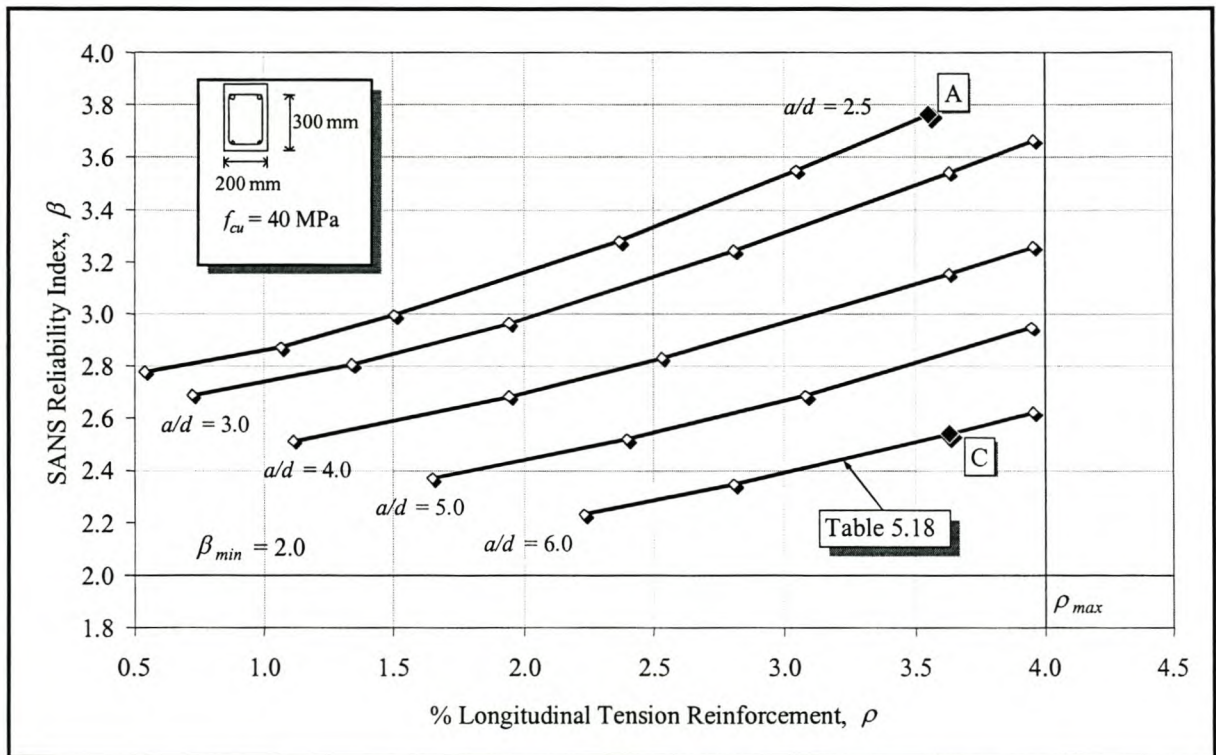


Figure 5.9: SANS Reliability Index vs. percentage longitudinal tension reinforcement (Set 1)

### Expected reliability relating to design situations

Figures 5.8 and 5.9 not only provide information on the trends in the reliability index with  $a/d$ ,  $\rho$  and  $v_s$ , but also on the probable combinations of these parameters in design, which helps in identifying probable design situations with relatively low levels of reliability and probable design situations with relatively high levels of reliability. Three general situations are distinguishable by comparing figures 5.8 and 5.9.

- *Combinations of high percentages of longitudinal reinforcement with low amounts of shear reinforcement.* Such cases are probable for beams with high  $a/d$  ratios. For beams with higher  $a/d$  ratios low percentages of longitudinal shear reinforcement in combination with low amounts of shear reinforcement are unlikely since this would result in too little longitudinal reinforcement against bending. For example the four beam configurations in figures 5.7 and 5.8 with  $a/d$  equal to 6.0 have longitudinal reinforcement ranging from 2.2% to 4.0% and shear reinforcement ranging from the minimum of 0.26 to 1.14 MPa. On figure 5.8 it can be seen that there are no test cases with  $a/d$  of 6.0 with shear reinforcement higher than 1.14 MPa. Higher amounts of shear reinforcement imply higher applied shear stresses which would require an increase in longitudinal reinforcement beyond the allowable 4%. Beam C is an example of a beam with a high amount of longitudinal reinforcement in combination with a relatively low amount of shear reinforcement. Because of the high  $a/d$  ratio and relatively low amount of shear reinforcement these beam configurations have a relatively low conservative bias in the model factor and therefore relatively low levels of reliability.
- *Relatively low percentages of longitudinal reinforcement with low amounts of shear reinforcement.* Such cases are probable for beams with low  $a/d$  ratios. The low  $a/d$  ratio ensures that the beam will not require high amounts of bending reinforcement at low shear stresses, because the bending moment remains small. The combination of low amounts of reinforcement in both directions leads to lower reliability but this is counteracted by the low values of  $a/d$  that are common for such cases.
- *Relatively high percentages of shear reinforcement with high amounts of longitudinal reinforcement.* Such cases are probable for beams with low  $a/d$  ratios that are highly stressed in

shear. The high shear stress requires a high amount of shear reinforcement in combination with a relatively high percentage of longitudinal reinforcement, without the maximum amount of longitudinal reinforcement being exceeded. Beam configuration A is an example of such a case. The combination of high amounts of reinforcement and a low  $a/d$  ratio leads to a relatively high conservative bias in the model factor and therefore to relatively high levels of reliability.

Combinations of high amounts of shear reinforcement and high amounts of longitudinal reinforcement at high  $a/d$  ratios have the highest levels of reliability while combinations of low shear reinforcement, high longitudinal reinforcement and high  $a/d$  have the lowest levels of reliability.

Apart from the increase in reliability with increasing  $\rho$ , increasing  $v_s$  and decreasing  $a/d$  another trend can be observed from figure 5.9. As the amount of shear reinforcement increases the effect of  $a/d$  on the level of reliability decreases. The flare-out in the  $a/d$  ratio is reduced and the reliability seems to converge with increasing shear reinforcement. The likely combination of parameters  $a/d$ ,  $\rho$  and  $v_s$  is such that the model factors for tests with high  $v_s$  is very similar despite the difference in  $a/d$ .

Figures 5.8 and 5.9 represented 25 beams with  $d$  of 300 mm and  $f_{cu}$  of 40 MPa. However reliability was tested for a set of similar beam configurations but where the  $f_{cu}$  was taken as 20 MPa. Similarly beams with sections of 600 mm and 1200 mm depth were tested, with  $f_{cu}$  taken as either 20 or 40 MPa. In addition to the set of beam configurations  $i$  from figures 5.8 and 5.9, this resulted in five additional sets of beam configurations. The 25 test from figure 5.8 and 5.9, named Set 1, displayed the highest levels of reliability compared to the other 5 sets, whereas the set of beam configurations with  $f_{cu}$  of 20 MPa and  $d$  of 1200 mm, namely Set 6, displayed the lowest levels of reliability of all the sets. The four intermediate sets, for example Set 3 with beam configurations with  $f_{cu}$  of 40 and  $d$  of 600 mm displayed levels of reliability somewhere in between those of Set 1 and Set 6. Figure 5.10 and 5.11 show the comparison of the levels of reliability for the two sets. Line  $a/d = 6.0$  from Set 6 represents the lower bound of reliability from the parameters study, while the line of  $a/d = 2.5$  from Set 1 represents the upper bound of reliability of the configurations tested in the parameter study. All tests conformed to the requirement of a minimum reliability index of 2.0 with exception of Beam configuration B from Set 6.

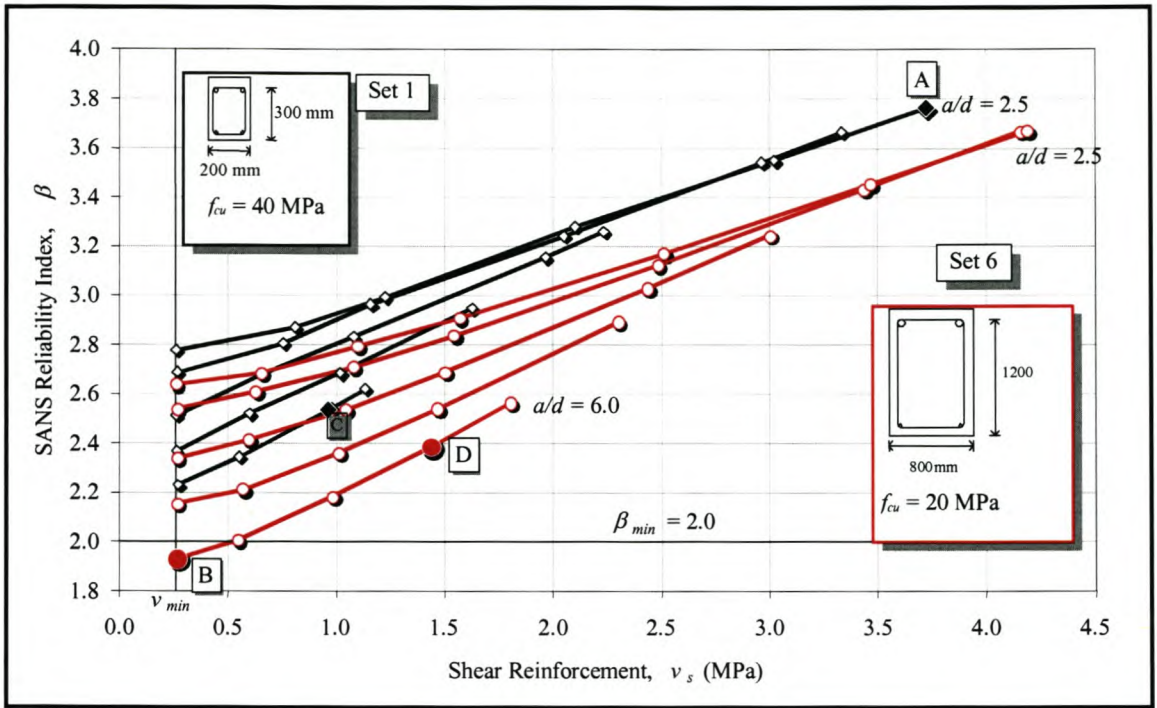


Figure 5.10: SANS Reliability vs. amount of shear reinforcement of Set 1 and Set 6 compared

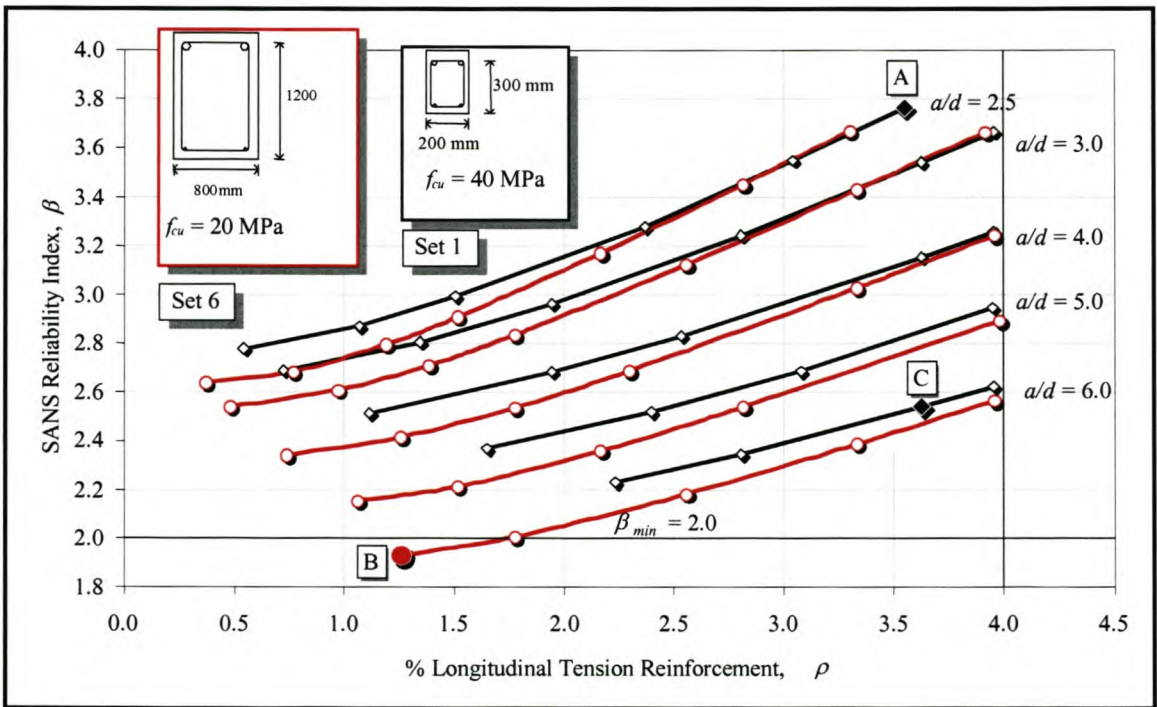
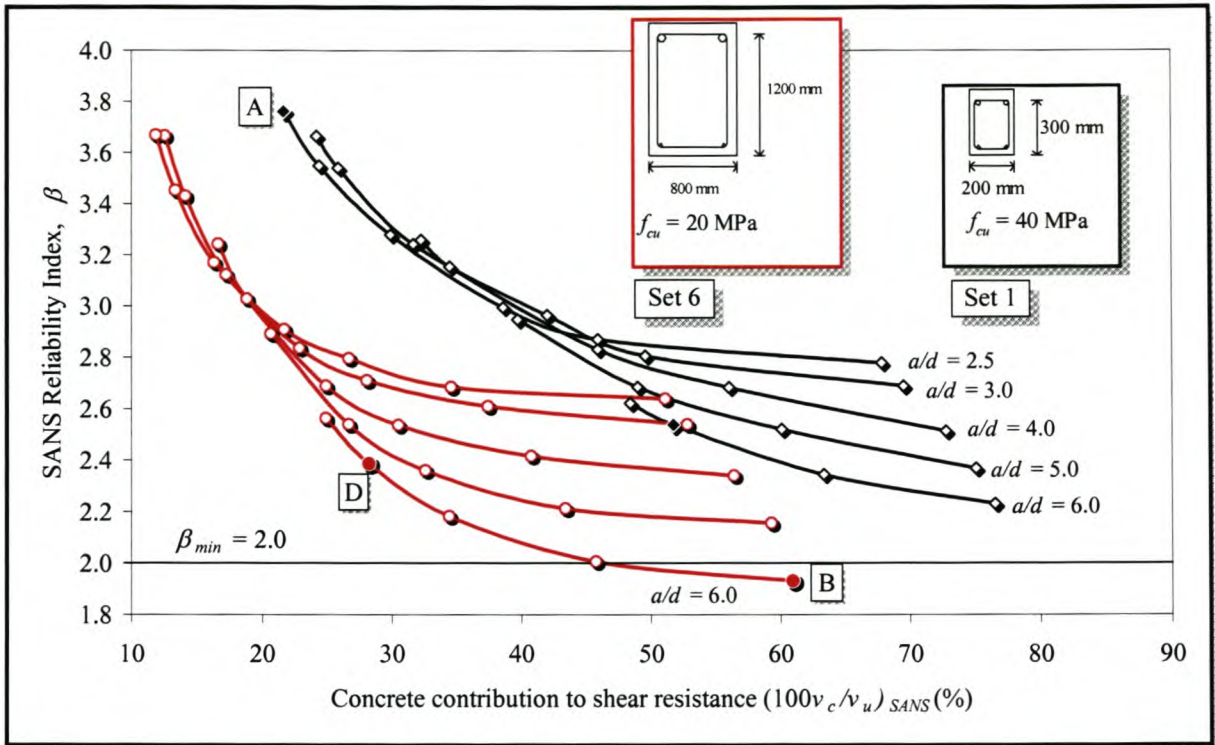
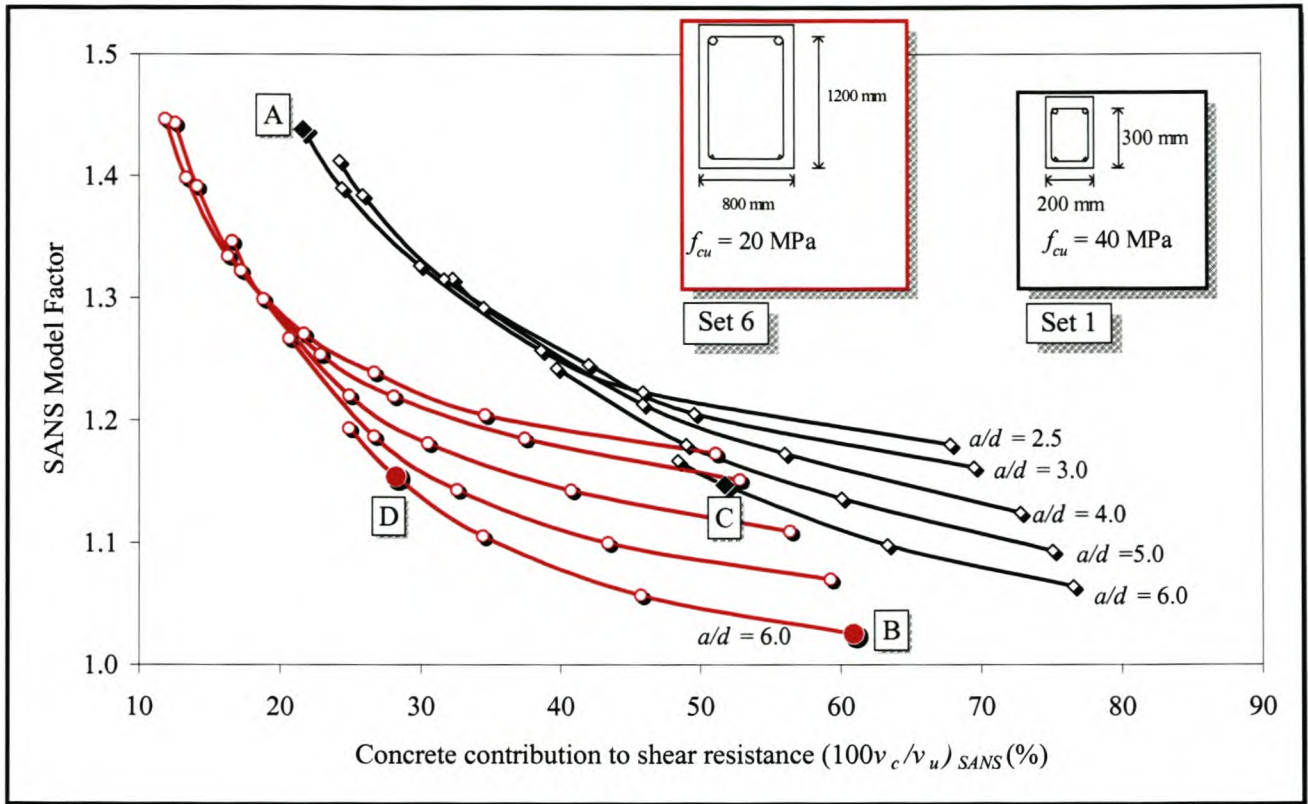


Figure 5.11: SANS Reliability vs. amount of longitudinal reinforcement of Set 1 and Set 6 compared



**Figure 5.12: SANS Reliability vs. amount of concrete contribution of Set 1 and Set 6 compared**

Figure 5.12 shows a plot of the reliability of each beam configuration from Set 1 and Set 6 against its corresponding percentage of concrete contribution to overall shear resistance. The concrete contribution term  $v_c$  is factored with the partial material factor for concrete of 1.4. The plot indicates that reliability decreases with decreasing concrete contribution. This behaviour is a result of the direct link between the model factor and the concrete contribution, as concrete contribution tends to increase with decreasing  $v_s$  and decreasing  $\rho$ . This means lightly reinforced members carry a greater part of the shear stress in the concrete rather than the steel. This behaviour is confirmed by a plot of the model factor of each beam configuration from Set 1 and Set 6 against the concrete contribution, shown in figure 5.13. The behaviour of the model factor versus concrete contribution is nearly identical to that of the reliability versus concrete contribution giving further proof of the dominance of the model factor on the reliability. The non-linear behaviour in reliability versus concrete contribution is as a result of the non-linear increase in the concrete contribution to the overall shear resistance.



**Figure 5.13: SANS model factor vs. amount of concrete contribution of Set 1 and Set 6 compared**

Figure 5.10 shows that the reliability of SANS is sensitive to the  $a/d$  ratio. The sensitivity increases with increasing concrete contribution. If SANS had not been sensitive to  $a/d$  all the cases of Set 1 and 6 would have followed the same trajectory. Set 6 had a lower concrete compressive strength and higher effective member depth than Set 1. Beam C from Set 1 and Beam D from Set 6 are both able to withstand 2 MPa of shear according to SANS but have different concrete contribution, because of their different values of  $f_{cu}$  and  $d$ . This results in a downward shift in reliability of Beam C from 2.5 to 2.4 for beam D. Note that the model factor of these two sets is the about the same in figure 5.13, so the difference in reliability is the result of the difference in concrete contribution.

Overall the decrease in concrete strength and increase in effective member depth therefore leads to an overall decrease in concrete contribution in Set 6 as compared to Set 1, resulting in an overall shift to the left. The influence of the partial material factor for concrete on the overall reduced values of concrete contribution for the beam configurations of Set 6, results in an overall downward shift in reliability. The downward shift becomes more pronounced for beams with a high concrete contribution

where the partial material factor for concrete has greater influence on the reliability. Figure 5.12 shows that the change in reliability from Set 1 to Set 6 (i.e. the downward shift) is more subtle compared to the change in reliability with increasing concrete contribution due to the effect of the model factor.

The reliability of SANS can be summarized as follows:

- The highest levels of reliability for SANS can be expected for highly stressed members. Such members are likely to be highly reinforced and have low percentages of concrete contribution to overall shear resistance.
- Relatively low levels of reliability are expected for lightly stressed members that are likely to contain little reinforcement. Such members tend to have a high percentage of concrete contribution. The reliability of these members is highly sensitive to the  $a/d$  ratio and decreases with increasing  $a/d$ , that is with higher moment across the section in addition to shear.
- Reliability decreases with increasing effective member depth and decreasing concrete strength. It is possible for very deep beams that are lightly reinforced in shear to display levels of reliability less than the target minimum of 2.0.

#### 5.2.2.2.2 Discussion of the results

The three main purposes of the parameter study were to determine the reliability of SANS over a range of probable design situations, to identify design cases where the reliability is less than the target minimum  $\beta$  of 2.0 and to assess the consistency of the reliability.

#### Reliability of SANS over a range of probable design situations

Figure 5.13 shows a plot of the reliability of SANS against concrete contribution for beam configurations from Set 1 and Set 6 from the parameter study. The plot is identical to figure 5.12 however the band of probable design situations is highlighted. The deep beam configurations with low concrete strength of Set 6 represent the lower bound of the band while the beam configurations of Set 6 represent the upper bound. The plots of the intermediate sets 2 to 5 fall within the highlighted area but are not shown for clarity. The area where at least the minimum level of reliability is achieved is

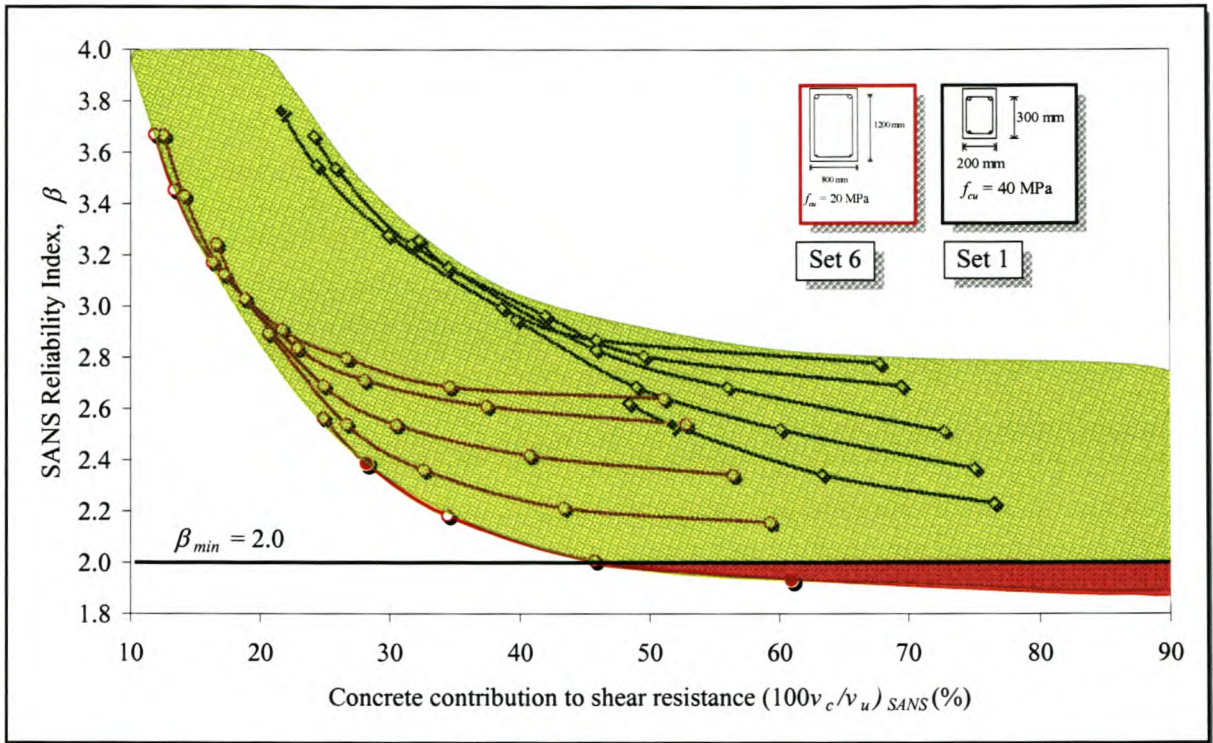


**Figure 5.14: Band of reliability for SANS for probable design situations.**

highlighted in green while the area where minimum level of reliability is not achieved is highlighted in red. The plot shows that the reliability decreases with increasing concrete contribution from a maximum of about 3.8 to a minimum of about 1.9. The minimum level of reliability is achieved for the majority of the band. Minimum reliability may not be achieved for very deep beams with a relatively high concrete contribution to overall shear resistance. This represents only a small part of the set of possible design situations.

Figure 5.13 is intended to represent the reliability of a range of possible design situations. It is however debatable if the upper and lower bounds of figure 5.13 is representative of practice. The upper bound represents a set of beam configurations with a relatively shallow section of 300 mm. However shallower members do occur in practice especially in the form of slabs, which would lead to a higher levels of reliability and therefore an increased upper bound. However slabs are generally designed without shear reinforcement for economy. Slabs with say an effective member depth of 200 mm containing shear reinforcement are therefore not very likely. In general punching shear is the governing shear failure mechanism for such slabs, in any case; therefore the upper bound of figure 5.13 is a

reasonable assumption. The lower bound represents very deep beams made from low strength concretes. Beams deeper than 1200 mm may occur in practice and these are not prohibited by SANS. However it is unlikely that such large beams would be made from 20 MPa concrete. In any case insufficient reliability for very deep beams is only likely where such a beam has a very high concrete contribution relative to the contribution of the shear reinforcement to overall shear resistance. Deep beams with high relative concrete contribution are those containing close to the minimum amount of stirrups. The problem of insufficient reliability in such beams could be solved by raising the minimum required amount of stirrups in such beams. The additional shear reinforcement would limit the maximum allowable concrete contribution resulting in sufficient reliability for such cases. A large  $a/d$  value for deep beams is also very unlikely. For  $a/d < 5$  reliability is sufficient, even for 20 MPa concrete.

### **Consistency of SANS reliability**

The broad band of reliability in figure 5.13 is testimony of the inconsistency of the reliability of SANS. Ideally reliability should be close to the minimum for all possible design situations. The reliability remains more or less consistent for beams with a concrete contribution of greater than 50%, in the sense that the gradient of the band remains fairly shallow. However when the concrete contribution falls below about 50% the reliability rises rapidly with decreasing concrete contribution. In this range the shear reinforcement is the main contributor to the shear resistance. As the amount of shear reinforcement increases it becomes increasingly likely that the spacing of the shear reinforcement is decreased. It is therefore more likely that the shear reinforcement will cross a shear crack, thereby improving the effectiveness of the shear reinforcement. It is likely that SANS does not fully account for this effect leading to higher levels of reliability for members with high amounts of shear reinforcement. Because SANS does not correctly account for the increased influence of shear reinforcement, the reliability increases rapidly. Reliability indices are greater than 3.0 for beam configurations with a high amount of shear reinforcement, leading to unnecessarily uneconomical designs. Consistency of reliability could be improved by improving the manner in which SANS takes shear reinforcement into account. However because the source of this uncertainty is not easily quantified it would probably be easier to adjust the partial material factors. Raising the partial material factor for concrete, while lowering that for steel, would raise the reliability of beams with a high relative concrete contribution, but lower the reliability of beams a very low concrete contribution. This would lower the curvature of

the band, thereby improving consistency over a range of concrete contribution. However the effect would probably be limited as the effect of the model factor dominates the effect of the partial material factors on reliability as was shown in section 5.2.3.2.1.

Because the SANS shear design procedure does not take moment shear interaction into account when designing the shear reinforcement, the reliability is sensitive to the  $a/d$  (or  $M/Vd$ ) ratio. For a section with a high moment to shear ratio the shear cracks are wider than in sections with low moment to shear ratio and as a result of the higher strains in the web of the beam due to bending. Wider cracks reduce the effectiveness of shear transfer mechanisms such as aggregate interlock at the crack interface thereby reducing the shear resistance. By ignoring these effects in design the reliability of SANS is reduced with increasing  $a/d$ . Since the  $a/d$  ratio affects the mechanisms that transmit shear in the concrete part of the beam, it is not surprising that the reliability of SANS becomes more sensitive to  $a/d$  as the concrete contribution is increased. Introducing a term to account for  $a/d$  in the empirical concrete contribution term could eliminate the sensitivity of SANS to this factor thereby improving consistency. The flare in the  $a/d$  lines of figure 5.13 would therefore be eliminated for beam configurations with a high concrete contribution term, and the reliability of beams with a similar section depth and concrete strength would follow the same trajectory regardless of  $a/d$  ratio.

Eliminating the effect of  $a/d$  would narrow the band of reliability to some extent. For example a beam with  $f_{cu}$  of 20 MPa and effective depth of 1200 mm,  $a/d$  of 6.0 and concrete contribution of 40% has reliability of 2.5 according to figure 5.13. For a beam with  $f_{cu}$  of 40 MPa, effective depth of 300 mm and  $a/d$  of 6.0 also with a concrete contribution of 40% has a higher reliability of about 3.0. Because both beams have the same concrete contribution the difference in reliability is due to a difference in the bias of the model factor of the two beams, and not due to the influence of the partial material factors. The difference in model factor derives from the fact that the two beams have different relative amounts of shear reinforcement and longitudinal reinforcement. Therefore the only way to improve consistency here would be to eliminate any trends in the code with these two shear parameters, which would require reformulation of the shear resistance procedure.

Although the reliability of SANS is subject to trends, these trends are uniform over the entire range of parameters. Therefore the reliability of SANS always decreases with increasing concrete contribution, but the rate of decrease also declines with increasing concrete contribution. Discontinuities in the

reliability where not observed. The suggested improvements in the consistency in reliability of SANS by adjustment of the partial material factors are demonstrated briefly the following section.

### **5.2.3 Recommendations for improving the reliability of the SANS shear design procedure**

In the previous section the reliability of members with shear reinforcement designed with SANS, was found to increase with increasingly reinforced members (both in bending and shear), while reliability decreased with increasing  $a/d$ . Most importantly reliability was found to increase with decreasing concrete contribution. Target minimum reliability of 2.0 was achieved for all cases in the parameter study except those with a relatively high concrete contribution. Such are typically very deep beams that are lightly reinforced in both directions with  $a/d$  close to 6.0. Because reliability increases with decreasing concrete contribution (which decreases with increasing shear reinforcement) minimum reliability can be achieved for such cases by increasing the nominal amount of stirrups.

Alternatively the partial material factors for steel and concrete can be adjusted. By raising the partial material factor for concrete the minimum level of reliability is achieved and by lowering the partial material factor for steel the reliability of highly reinforced members (with low concrete contribution) can be decreased. The combined effect also improves the consistency of the reliability of SANS. This is shown for the set of beam configurations from the parameter study with  $d = 1200$  mm and  $f_{cu} = 20$  MPa in figure 5.15 below. These were the test cases with the lowest levels of reliability in the parameter study. The material factors were adjusted to:  $\gamma_{m,c} = 1.6$  and  $\gamma_{m,s} = 1.05$ . Reliability is improved for members with high concrete contribution to overall shear resistance so that a target minimum reliability of 2.0 for lightly reinforced members with a very high concrete contribution. Economy of design is improved for highly stressed members where mainly the shear reinforcement contributes to shear resistance, through the lowering of the partial material factor for steel. Overall the reliability drops by 0.5 for such cases.

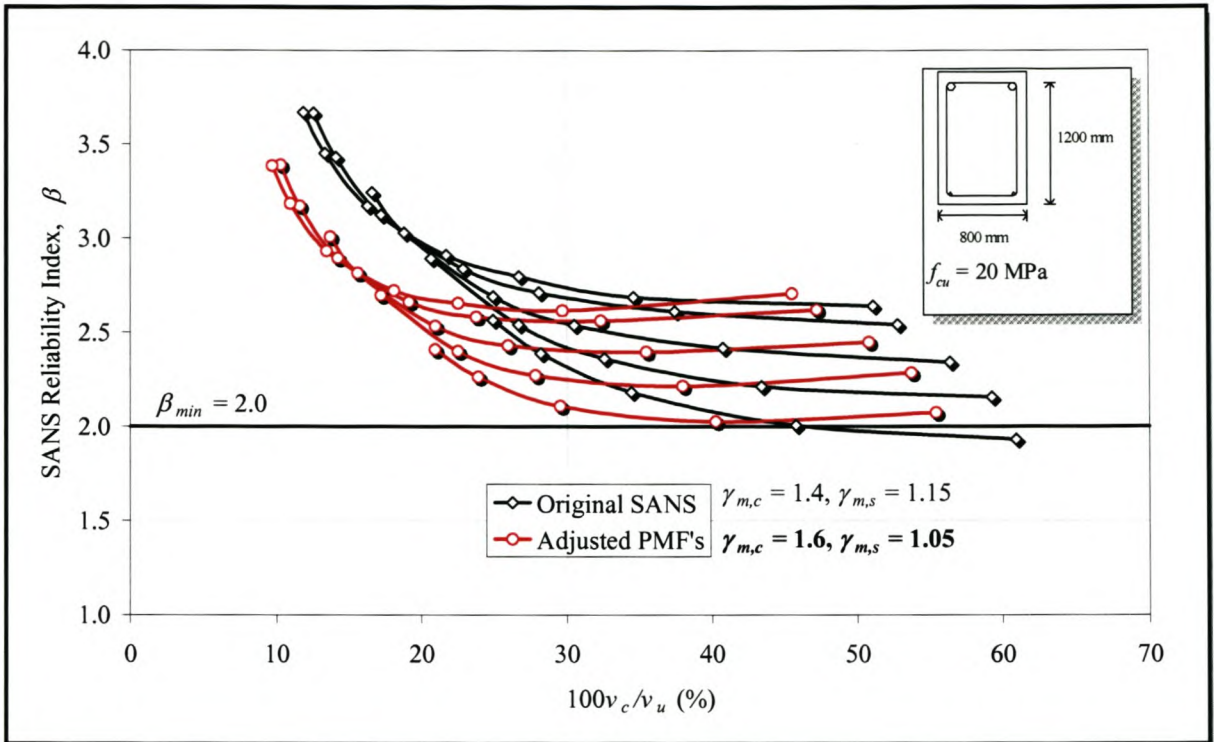


**Figure 5.15: Effect on reliability of SANS through adjustment of partial material factors**

The flare in the reliability for members with relatively high concrete contribution could decrease if a factor for  $a/d$  is included in the concrete contribution term of SANS. Members with similar concrete contribution but different values for  $a/d$  show significant differences in reliability. The inclusion of an  $a/d$  term in the concrete contribution would also improve the consistency of reliability for members without shear reinforcement were  $a/d$  was the only factor that caused decreasing trend in reliability with increasing  $a/d$ .

# Chapter 6

## Conclusions and Recommendations

The main objective of this thesis was to determine the level of reliability of the shear design procedure for beams with and without shear reinforcement of the South African concrete design code, SANS 10100-1:2003.

SANS follows the traditional empirical approach for designing reinforced concrete members in shear, which is still followed by most international design codes. The American Bridge Design Code (AASHTO LRFD, 2000) is an exception, amongst others, having adopted a more rational design procedure based on the Modified Compression Field Theory. The traditional approach as followed by SANS involves the discretion of the shear resistance of a concrete member with shear reinforcement into two parts, namely the shear resistance provided by the concrete matrix and the shear resistance provided by the shear reinforcement. This is based on the analogy that the beam behaves like a parallel cord truss, where the vertical tension ties are formed by the stirrups and the inclined compression struts are formed by the concrete. Failure is assumed when the shear reinforcement yields in tension.

The shear resistance of a beam is then given by:

$$v_R = v_c + v_s \cot \theta \quad [6.1]$$

where  $v_s$  is the amount of shear reinforcement per unit area and  $\theta$  is the angle of the compression struts assumed to be  $45^\circ$  in SANS. The concrete contribution to shear resistance,  $v_c$  is calculated from an empirical formula that is a function of parameters that are well known from experimental data to affect shear resistance. These parameters include concrete compressive strength, percentage of longitudinal reinforcement and effective member depth in the case of the SANS empirical formula. Other empirical formulations exist that include a wider range of shear parameters. In members without shear reinforcement resistance to shear is provided only by the concrete part and hence shear resistance for such members is calculated from the empirical formula.

## 6.1 Members without shear reinforcement

The empirical nature of the SANS shear design procedure for members without shear reinforcement proved, through comparison to experimental data, to provide a good prediction of shear resistance of such members. It was found that there were little or no trends in the reliability of this method with the important shear parameters, namely concrete compressive strength, percentage longitudinal reinforcement and effective member depth that are all taken to account by the method.

However the method does not account for the effect of moment-shear interaction on shear resistance. As beams become more slender (i.e. the ratio between length and effective depth increases) wider cracks form at the location of maximum moment due to increased longitudinal tensile stresses compared to less slender beams. Wider crack widths negatively impact on the shear resistance mechanisms attributed to the concrete contribution to overall shear resistance. In shear literature this effect is quantified by the maximum moment to shear to effective depth ratio ( $M/Vd$ ). For a simply supported beam with a point load at mid span this ratio is equivalent to the shear span to effective depth ratio ( $a/d$ ) where the shear span is the distance from the support to the location of the point load. The critical shear section in a beam is therefore at a section where the moment to shear ratio is at a maximum. In conjunction to this as beams become more slender, the shear resistance decreases proportionally at the location of maximum moment to shear ratio.

The SANS method does not account for this effect and as a result the reliability study showed that this lead to a very high reliability index of 3.5 for members with  $a/d$  (or  $M/Vd$ ) ratio close to 2.5 which decreased linearly to the target minimum of 2.0 for members with  $a/d$  ratio of 7.0. As members with  $a/d$  greater than 6.0 generally fail in bending provided that the longitudinal reinforcement does not exceed the maximum value of 4% required by the code, the target minimum reliability of 2.0 was found to be achieved for most probable design situations.

Beams without shear reinforcement are not commonly used in practice as the code only allows this provided the applied shear stress is less than half the calculated shear resistance. Shear resistance may govern the sizing of such members such as column bases and pile caps. Inclusion of a  $M/Vd$  term in the empirical formulation would improve consistency in reliability with  $a/d$  which would lead reliability

closer to the target minimum and thus potentially provide more economical designs in the sizing of members.

## 6.2 Members without shear reinforcement

The reliability of beams with shear reinforcement designed with SANS was found to

- Decrease with increasing  $a/d$ .
- Increase with decreasing concrete contribution to overall shear resistance.

The decreasing trend in reliability with increasing shear span to depth ratio, as for members without shear reinforcement, is attributed to the fact that SANS does not take the effect of slenderness on shear resistance into account. As concrete contribution to overall shear resistance decreases the shear reinforcement contribution increases proportionally. This means that reliability was found to increase with increasing shear reinforcement. Shear reinforcement increases, as a member becomes more stressed in shear, therefore reliability was found to increase for highly stressed members.

Combinations of high concrete contribution to overall shear resistance in a member (i.e. one that is lightly stressed in shear) and high a  $a/d$  ratio were therefore found to yield the lowest reliability in the parameter study. Target minimum reliability of 2.0 was achieved for all cases in the parameter study except for some isolated cases with a relatively high concrete contribution. Such beams are typically very deep beams that are lightly reinforced in both directions with  $a/d$  (or  $M/Vd$ ) close to 6.0. On the other hand the reliability index was found to be as much as twice the target minimum value for members that are relatively highly stressed in shear, which leads to potentially uneconomical designs.

The target minimum reliability could be achieved for lightly stressed members with a high concrete contribution relative to shear reinforcement contribution by increasing the limit on minimum required shear reinforcement. This would effectively place an upper limit on the concrete contribution to overall shear resistance

The two extremes for members with and without shear reinforcement overlap and target minimum reliability can be achieved by introducing a term for  $M/Vd$  to the empirical concrete contribution formulation which affects the design of both types of members. For continuous beams this ratio is at a maximum at the inner supports, while for simply supported beams with point loads it is at the location of the load. The ratio is difficult to quantify for simply supported beams with distributed loads where the maximum shear is at the supports where the moment is zero, and the maximum moment is at mid-span where the shear stress is zero. As the  $a/d$  ratio is in essence a slenderness ratio for the simply supported beam a similar slenderness ratio could be derived for such beams.

Comparison with experimental data indicated the increase in conservative bias in SANS as the relative contribution to shear reinforcement increased. This translates into a dramatic increase in reliability well above the target minimum reliability. From this it can be concluded that the SANS method underestimates the contribution of the shear reinforcement to shear resistance and this effect is amplified as the shear reinforcement increases. The source of this conservatism is the simplified assumption that the angle of inclination of compression struts in the truss analogy is  $45^\circ$  (equation 6.1). Shallower angles would lead to a greater shear reinforcement contribution. However calculation of the correct angle is complex and involves numerous parameters as outlined by the Modified Compression Field Theory. The conservatism in SANS is therefore a direct result of a simplifying assumption to facilitate the design process. To decrease the reliability of highly reinforced members the partial material factor for steel could be decreased as was shown in Chapter 5.

### **6.3 Recommendations for further studies**

The reliability analysis in this thesis demonstrated the major importance that the model factor plays in predicting the probabilistic shear resistance. The SANS model was shown to provide a good probabilistic model for shear.

However the modelling of the model factor can further be improved to yield more accurate results. Experimental error in the database from which the model factor was determined was not investigated. Furthermore the model factor was applied to the overall shear resistance of members with shear reinforcement. Given the importance of the concrete contribution, greater accuracy would be achieved by deriving separate model factors for concrete contribution and steel contribution.

The SANS model was shown to provide a good general probabilistic model for normal strength concrete. Currently SANS does not provide for the design of high strength concrete members. High strength concrete has smoother crack surfaces leading to decreased crack interface shearing capacity and therefore proportionally lower shear resistance compared to normal strength concrete. The increased use of high strength concrete in practice and its adoption into European and American codes warrants an investigation into whether the SANS shear design procedure can safely be applied to high strength concrete. Given the general conservatism of the SANS shear design procedure it may be safe to apply it to high strength concrete as well. The study can further be extended to shear in pre-stressed beams as well as beams subjected to axial forces.

# References

## Publications

- Collins, M.P., Mitchell, D., Adebar, P., Vecchio, F.J., "A General Shear Design Method", ACI Structural Journal, V.93, January-February 1996, pp. 36 – 45
- Holický, M., Retief, J.V., "Reliability Assessment of Alternative Load Combination Schemes for Structural Design", Journal SAICE, Volume 47, Number 1, pp 15-20, 2005
- Kani, G.N.J., "The Riddle of Shear Failure and its Solution", ACI Structural Journal, V. 61, April 1964, pp. 441 – 465
- Kani, G.N.J., "Basic Facts Concerning Shear Failure", ACI Structural Journal, V 63., June 1966, pp. 675 – 690.
- Mirza, S.A., MacGregor, J.G., "Variations in Dimensions of Reinforced Concrete Members", ASCE Journal of the Structural Division, V. 105, April 1979, pp. 751-766
- Mirza, S.A., MacGregor, J.G., "Variability of Mechanical Properties of Reinforcing Bars", ASCE Journal of the Structural Division, V. 105, May 1979, pp. 921-937
- Mirza, S.A., MacGregor, J.G., "Statistical Descriptions of Strength of Concrete", ASCE Journal of the Structural Division, V. 105, June 1979, pp. 1021-1037
- Moss, R., Webster, R., "Comparison of EC2 and BS8110", [www.Eurocode.info](http://www.Eurocode.info), January 2003
- Narayanan R.S., "EN 1992 Eurocode 2: Design of Concrete Structures", Proceedings of the ICE, Civil Engineering, V. 144, Paper 12643, November 2001, pp. 23 – 28
- Rahal, N., Collins, M.P., "Background to the General Method of Shear Design in the 1994 CSA-A23.3 standard", Canadian Journal of Civil Engineering, V. 26, July 1999, pp. 827 – 839
- Ritter, W., "Die Bauweise Hennebique", Schweizerische Bauzeitung, Zurich, 1899
- Ter Haar, T.R., Retief J.V., "Resistance factors for structural concrete design codes as derived from loading code calibration"
- Vecchio, F.J, Collins, M.P., "The Modified Compression Field Theory for Reinforced Concrete Elements Subjected to Shear", V.83, March-April 1986, pp. 219 – 231

Vecchio, F.J., Collins, M.P., “Predicting the Response of Reinforced Concrete Beams Subjected to Shear Using Modified Compression Field Theory”, ACI Structural Journal, V. 85, May-June 1998, pp. 258 – 268

### **Books**

Hsu, T.T.C, “Unified Theory of Reinforced Concrete”, 1<sup>st</sup> Edition, CRC Press, Florida, 1993

Kong, F.K., Evans, R.H, “Reinforced and Prestressed Concrete”, 3<sup>rd</sup> Edition, E & FN Spon, London, 1998

Melchers, R.E., “Structural Reliability analysis and prediction”, 2<sup>nd</sup> Edition, John Wiley & Sons, Brisbane, 1999

Narayanan R.S., “Concrete Structures: Eurocode EC2 & BS 8110 compared”, 1<sup>st</sup> Edition, Longman Scientific & Technical, Harlow England, 1994

### **Reports**

Report of ACI-ASCE Committee 445 on Shear and Torsion, “Recent Approaches to Shear Design of Structural Concrete, ACI Structural Journal, V.124, December 1998, pp. 1375 – 1416

Report of ACI-ASCE Committee 426 on Shear and Diagonal Tension “The Shear Strength of Reinforced Concrete Members”, V.99, June 1973, pp. 1091-1188

Holicky, M., “Conventional probabilistic models for basic variables”, Klokner Institute, CTU, Prague, 2002

### **National Standards**

“AASHTOO LRFD Bridge Design Specifications and Commentary”, American Association of State Highway and Transportation Officials, Washington D.C., 2000

“SABS 0100: Boubetonwerk Deel 1: Ontwerp”, Suid-Afrikaanse Buro van Standarde, Pretoria, 1992

“CEB-*fip* Model Code 1990”, Thomas Telford, London, 1990

“ENV 1992 Eurocode 2: Planung von Stahlbeton und Spannbetontragwerken: Teil 1 Grundregeln und Anwendungsregeln Deutsche Fassung”, Normenausschuss Bauwesen im DIN Deutsches Institut für Normung, Berlin, 1991

### **Theses**

Bohigas, A.C., "Shear Design of Reinforced High Strength Concrete Beams", Universitat Politecnica De Catalunya, Barcelona, 2002

## **Experimental Database**

### **Experiments without shear reinforcement**

Kuchma, D.A., Reineck, K., Kim, K.S., Marx, S., "Shear Databank for Reinforced Concrete members without shear reinforcement", ACI Structural Journal, V.100, March-April 2003, pp. 240 – 249. (Experimental Data listed in Appendix B, available from ACI Headquarters, Detroit) (Supplied in attached CD)

### **Experiments with shear reinforcement**

Placas, A., Regan P.E., "Shear Failure of Reinforced Concrete Beams", ACI Structural Journal, V. 68, October 1971, pp. 763 – 773

Bressler B., Scordelis, A.C., "Shear Strength of Reinforced Concrete Beams", ACI Structural Journal, V.60., September 1963, pp. 51 – 73

Elazanaty A.H., Nislon A.H., Slate F.O., "Shear Capacity of Reinforced Concrete Beams using High Strength Concrete", ACI Structural Journal ,V.83, March – April 1986, pp. 290-296

Yoon, Y., Cook, W.D., Mitchell, D., "Minimum Shear Reinforcement in Normal, Medium, and High Strength Concrete Beams", ACI Structural Journal, V. , September-October 1996, pp. 576-584

Johnson MK, Ramirez JA, Minimum Shear Reinforcement in Beams with High Strength Concrete, ACI Structural Journal, V.86, July-August 1989, pp. 376-382

Anderson, N.S., Ramirez, J.A., Detailing of Stirrup Reinforcement, ACI Structural Journal, V.86, September-October 1989, pp. 507-515

Thompos, E.J., Frosch, R., Influence of Beam Size, Longitudinal Reinforcement and Stirrup Effectiveness on Concrete Shear Strength, ACI Structural Journal, V.99, September – October 2002, pp. 559-567

Rodriguez, C.P., Darwin D., "Shear Strength of Lightly Reinforced T-Beams in Negative Bending", ACI Structural Journal, V., January-February 1987, pp. 77-85

Rajagopalan, K.S., Ferguson, P.M., Exploratory Shear Tests Emphasizing Percentage Longitudinal Steel, ACI Structural Journal, V.55, August 1968, pp. 634-638

Bressler, B., Scordelis, A.C., "Shear Strength of Reinforced Concrete Beams-Series III", Structures and Materials Research, V.65, 1966

Al-Musawi J.M.S., Sarsam, K.F., “Shear Design of High Strength Concrete, Normal Strength Concrete Reinforced Concrete Beams with Web Reinforcement”, ACI Structural Journal, V.89, November-December 1992, pp. 658-664.

Xie, Y., Shuaib, A.H., Tiejun, Y., Hino, S., Chung, W., “Shear Ductility of Reinforced concrete beams of NSC and HSC”, V.91, March –April 1994, pp. 140-149

Krefeld, W.J., Thurston W.T., “Studies of the Shear and Diagonal Tension Strength of Simply Supported Concrete Beams”, ACI Structural Journal, V.63, April 1966, pp.451 -476

Elstner, C., Moody, K.G., Viest, I.M., Hognestad, E., “Shear Strength of Reinforced Concrete Beams”, ACI Structural Journal, V.51, February 1955, pp. 525-539

Clark, A.P., “Diagonal Tension in RC Beams”, v. 48, October 1951, pp. 145 - 156

Zararis, P.D., “Shear Strength of Minimum Shear Reinforcement of Reinforced Concrete Slender Beams”, ACI Structural Journal, V.83, March-April 2003, pp. 203 – 214.

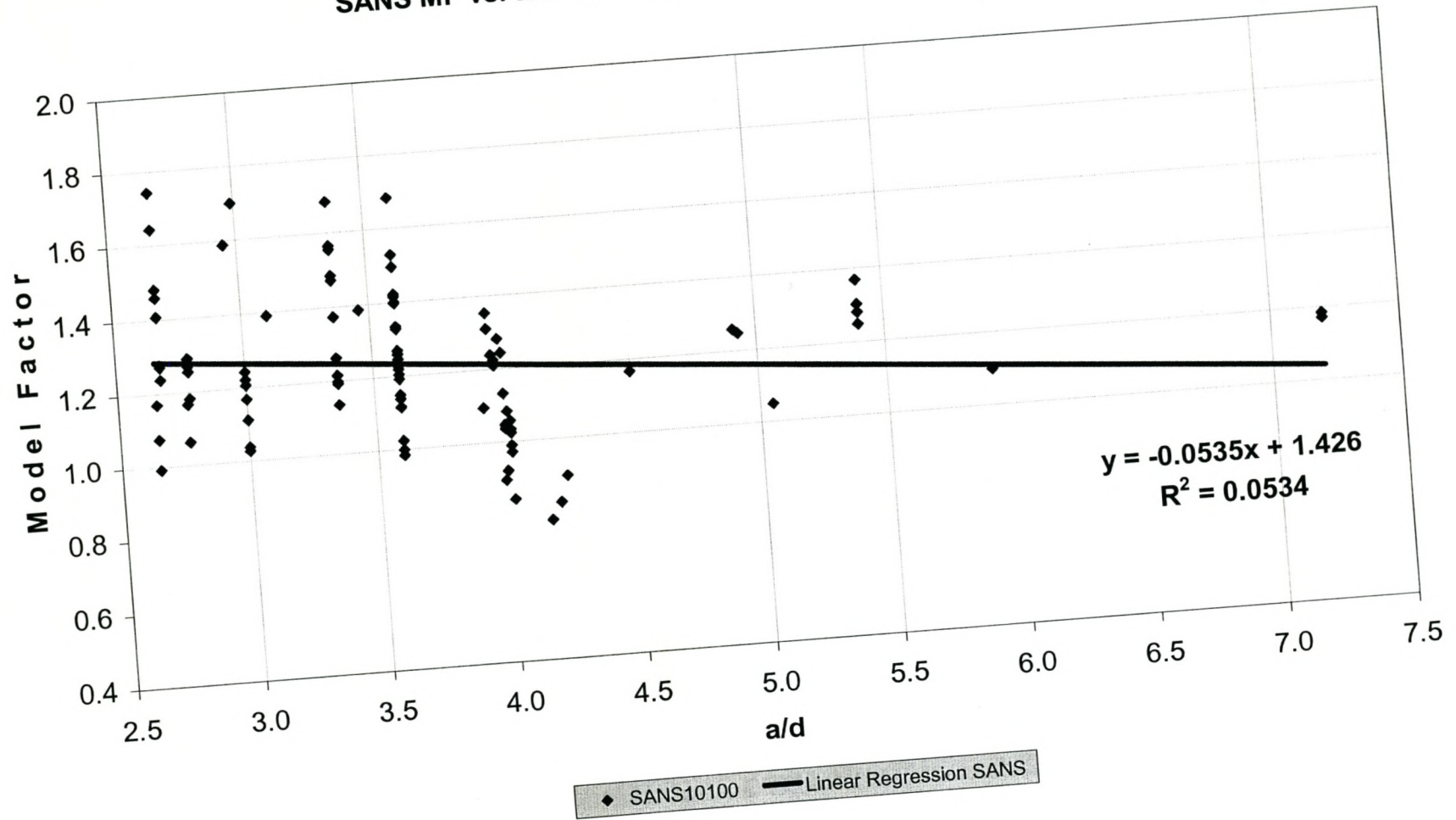
Guralnick, S.A., “High-Strength Deformed Bars for Concrete Reinforcement”, ACI Structural Journal, V.57, August 1960, pp. 241 - 279

# Appendix A

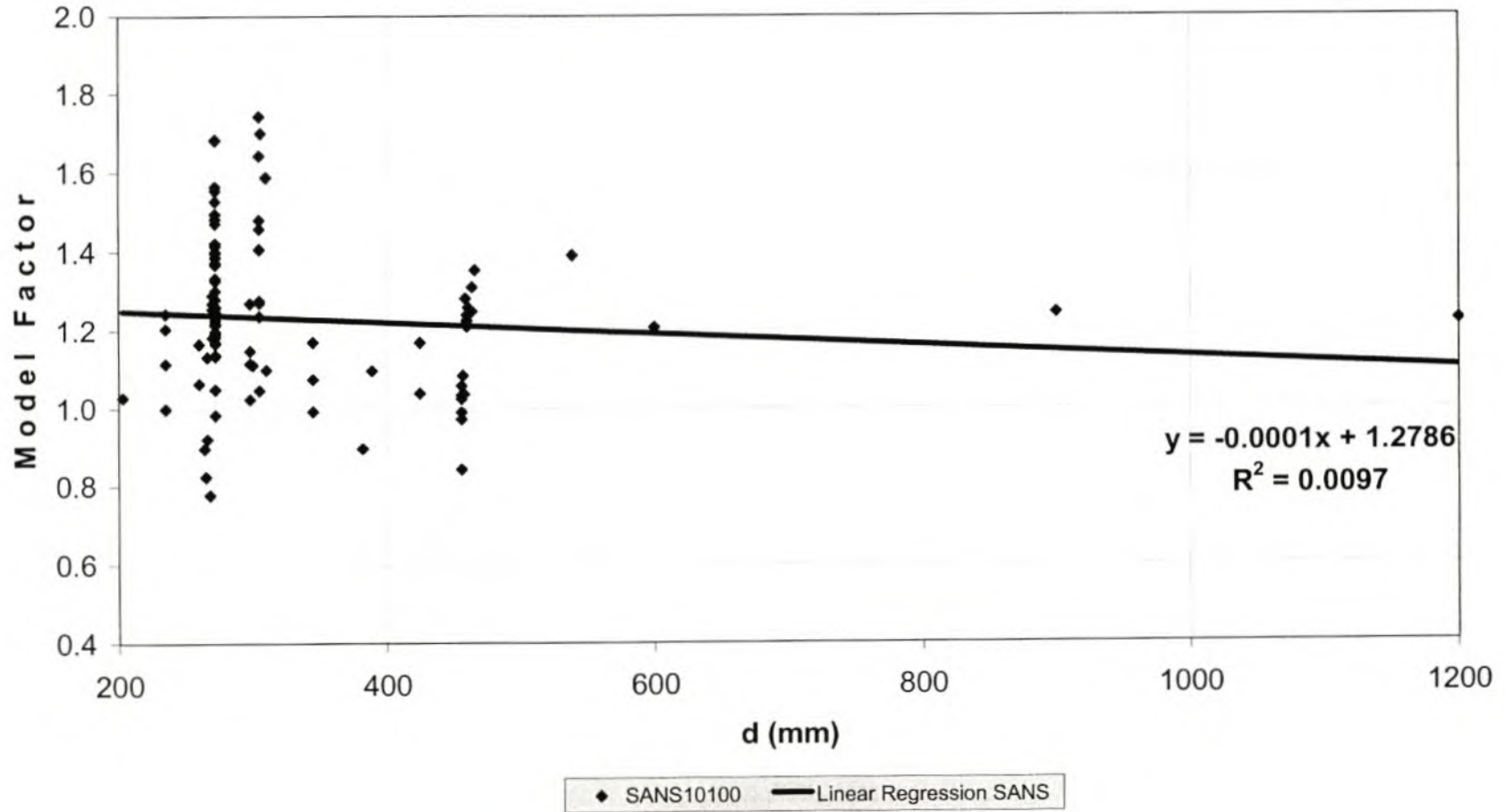
**Note: Refer to attached CD for Appendix A1 – A4.**

Appendix A.5 – Linear regression plots for SANS, Model factor for SDB\_WithSR Subset 1: 99 Tests

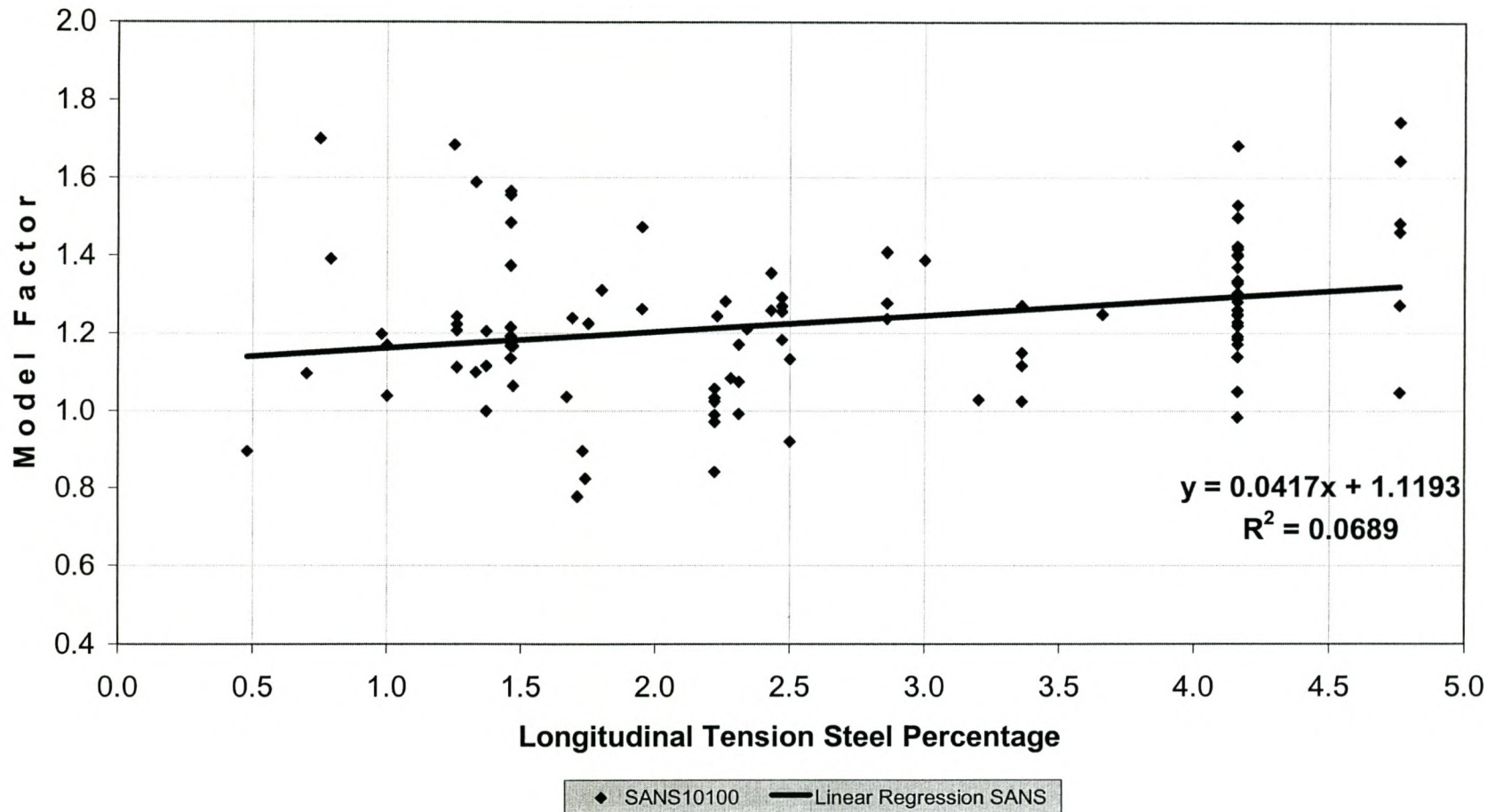
SANS MF vs. a/d for SDB\_WithSR Subset 1: 99 Tests



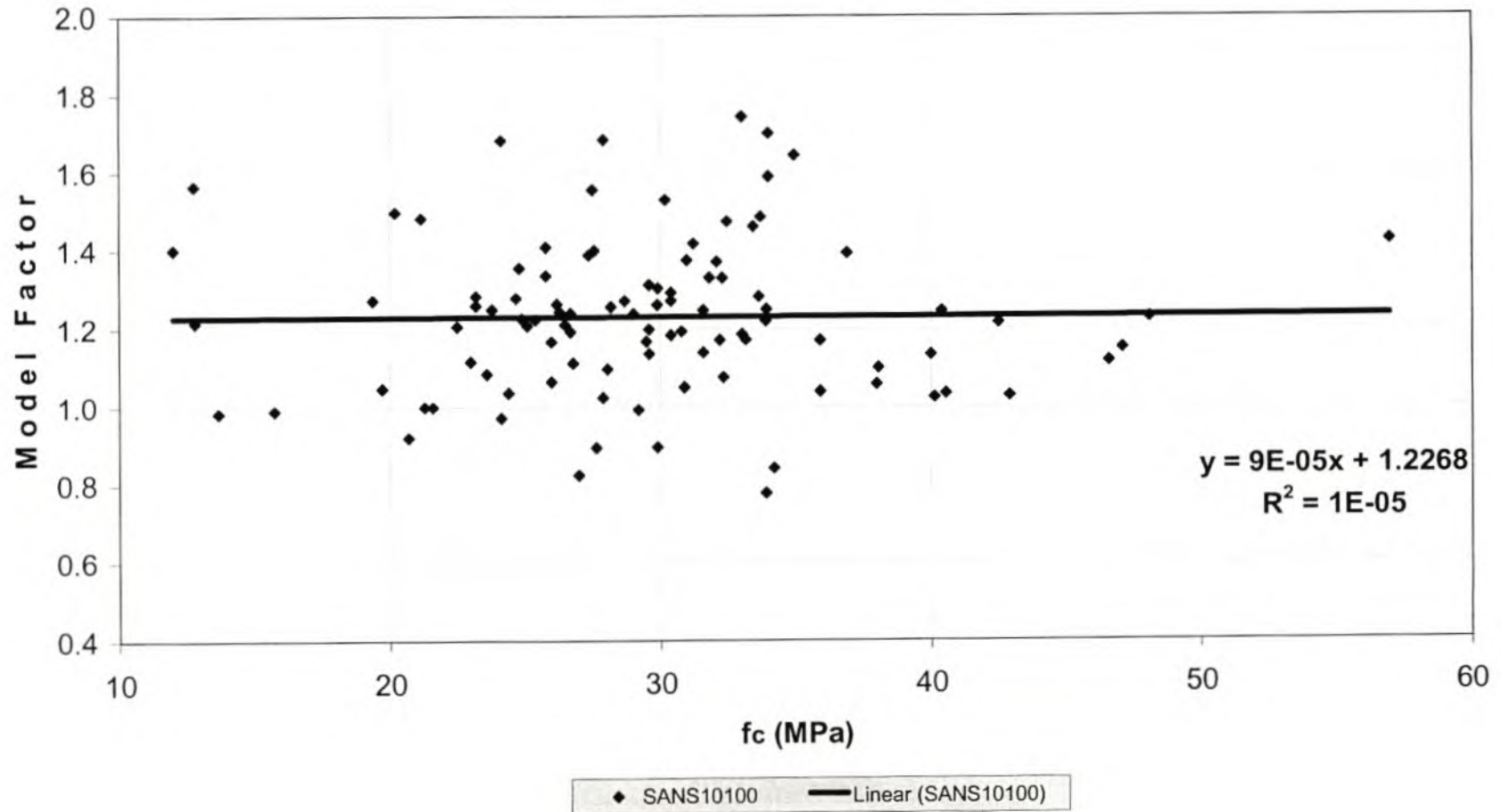
SANS MF vs. d for SDB\_WithSR Subset 1: 99 Tests



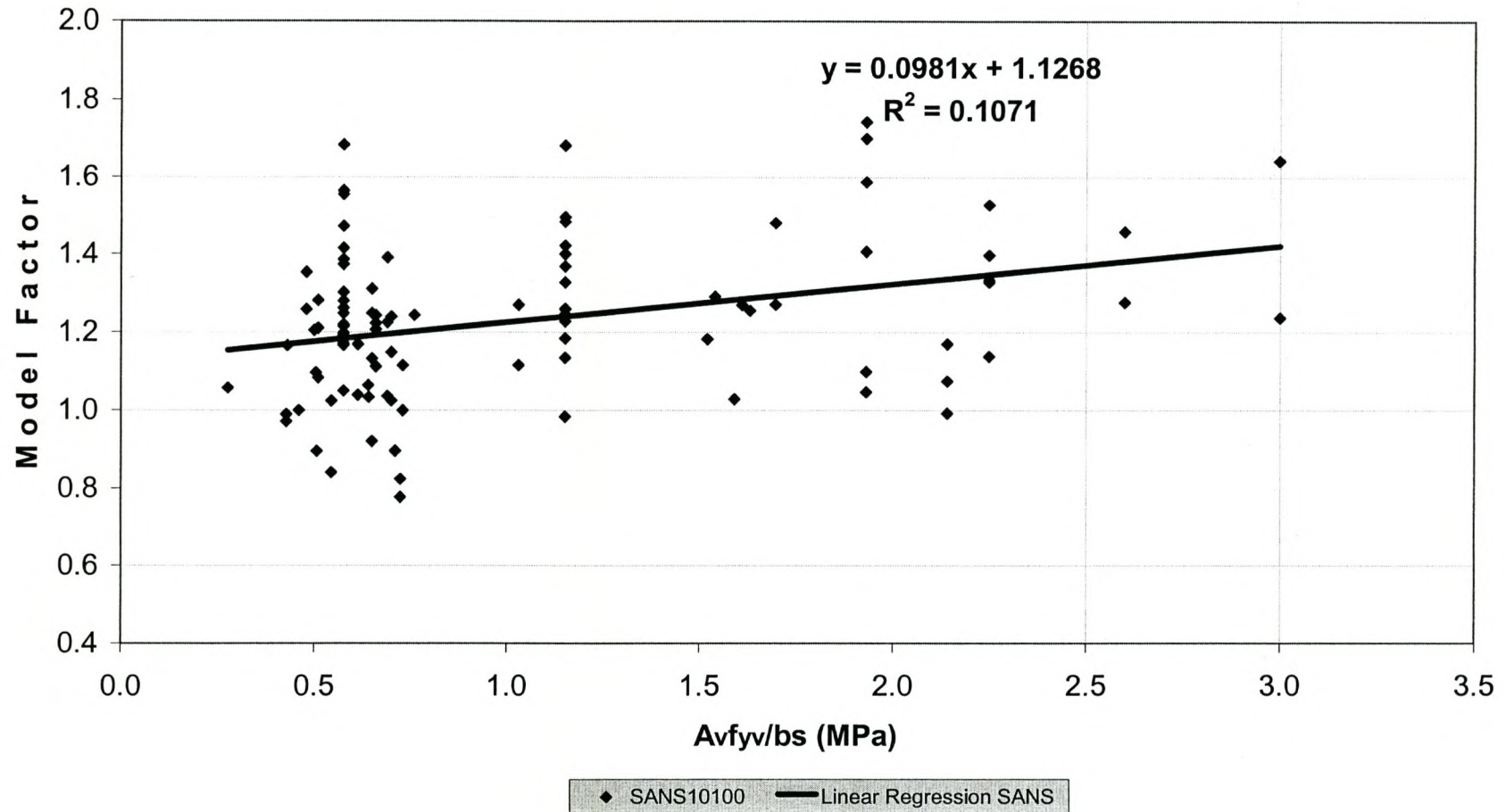
SANS MF vs.  $\rho$  for SDB\_WithSR Subset 1: 99 Tests



SANS MF vs.  $f_c$  for SDB\_WithSR Subset 1: 99 Tests



SANS MF vs. shear reinforcement for SDB\_WithSR Subset 1: 99 Tests



## Appendix B

### B.1 Example applying AASHTO LRFD 2000 for members with shear reinforcement

This appendix demonstrates an interpolation technique applied in Microsoft Excel to calculate the shear resistance of each experiment in the experimental database as predicted by AASHTO. The determination of shear resistance of a beam with the specifications as given in table B.1 1 is demonstrated. The example is test 163 of the database with shear reinforcement, SDB\_WithSR, designation AS3-N (Al-Musawi and Sarsam).

AASHTO Example		
Material Properties		
$f_c$	40.2	MPa
$f_{v-long}$	495	MPa
Section Geometry		
$d$	235	mm
$z$	211.5	mm
$b_w$	180	mm
$100A_s/bd$	2.23	%
$A_v f_{yv}/bs$	1.14	MPa
Loading		
$a/d$	2.5	
$M/V_{eff}$	0.376	m

**Table B.1: Example - Determining shear resistance with AASHTO LRFD 2000 for members with shear reinforcement**

The values of  $\beta$  and  $\theta$  where shown graphically in chapter 2, however AASHTO provides them in a tabulated form, as given in Table B.2 and B.3. The tables for  $\beta$  and  $\theta$  show that for a certain amount of applied shear stress,  $v_u$ , a number of possible values of  $\beta$  and  $\theta$  exist depending on the strain in the web of the beam. This represents one row in the  $\beta$  and  $\theta$  tables. However for a certain  $\epsilon_x$ ,  $\beta$  and  $\theta$  only one value of shear resistance is

possible. This means that for a beam with strain 0.5 and  $v/f_c$  of 0.1, the value of  $\theta$  is  $30.8^\circ$  and the value of  $\beta$  is 0.208 as shown in the tables for  $\beta$  and  $\theta$  (see Table B.2 and B.3). The required amount of shear reinforcement for a beam,  $v_s$ , with configuration  $ij$  where  $i$  is the value of  $v/f_c$  and  $j$  is the value of the strain,  $\epsilon_x$  can now be calculated from the following equation derived from the AASHTO equation for shear resistance: (from equation 2.60)

$$v_{s,ij} = \left[ (v/f_c)_{ij} f_c - \beta_{ij} \sqrt{f_c} \right] \tan \theta_{ij}$$

The values of  $v_{s,ij}$  are shown in table B.4.

AASHTO LRFD 2000: Values for $\theta$											
$v/f_c \setminus \epsilon_x$	-0.2	-0.1	-0.05	0	0.125	0.25	0.5	0.75	1	1.5	2
0.075	22.3	20.4	21	21.8	24.3	26.6	30.5	33.7	36.4	40.8	43.9
0.1	18.1	20.4	21.4	22.5	24.9	27.1	<b>30.8</b>	34	36.7	40.8	43.1
0.125	19.9	21.9	22.8	23.7	25.9	27.9	31.4	34.4	37	41	43.2
0.15	21.6	23.3	24.2	25	26.9	28.8	32.1	34.9	37.3	40.5	42.8
0.175	23.2	24.7	25.5	26.2	28	29.7	32.7	35.2	36.8	39.7	42.2
0.2	24.7	26.1	26.7	27.4	29	30.6	32.8	34.5	36.1	39.2	41.7
0.225	26.1	27.3	27.9	28.5	30	30.8	32.3	34	35.7	38.8	41.4
0.25	27.5	28.6	29.1	29.7	30.6	31.3	32.8	34.3	35.8	38.6	41.2

**Table B.2 –  $\theta$  Values for members with at least minimum amount of stirrups**

Values for $\beta$											
$v/f_c \setminus \epsilon_x$	-0.2	-0.1	-0.05	0	0.125	0.25	0.5	0.75	1	1.5	2
0.075	0.53	0.40	0.34	0.31	0.27	0.24	0.22	0.20	0.19	0.16	0.14
0.1	0.32	0.28	0.27	0.26	0.24	0.23	0.21	0.19	0.18	0.16	0.14
0.125	0.26	0.25	0.25	0.24	0.23	0.22	0.20	0.19	0.18	0.16	0.14
0.15	0.24	0.23	0.23	0.23	0.22	0.21	0.20	0.18	0.17	0.15	0.13
0.175	0.23	0.22	0.22	0.22	0.21	0.20	0.19	0.18	0.16	0.14	0.13
0.2	0.22	0.22	0.21	0.21	0.20	0.20	0.18	0.16	0.15	0.13	0.12
0.225	0.21	0.20	0.20	0.20	0.20	0.18	0.15	0.14	0.14	0.13	0.12
0.25	0.20	0.20	0.19	0.19	0.18	0.16	0.14	0.13	0.12	0.11	0.11

**Table B.3:  $\beta$  Values for members with a least minimum amount of stirrups**

Note the above tables are represented as graphs in Chapter 2.

$v_s \mid \epsilon_x$	-0.2	-0.1	-0.05	0	0.125	0.25	0.5	0.75	1	1.5	2
3.015	-0.13	0.19	0.32	0.41	0.59	0.73	0.97	1.17	1.35	1.71	2.05
4.020	0.66	0.83	0.91	0.98	1.15	1.31	1.61	1.88	2.14	2.59	2.92
5.025	1.21	1.38	1.46	1.54	1.74	1.93	2.29	2.62	2.94	3.49	3.89
6.030	1.79	1.96	2.05	2.14	2.36	2.58	3.00	3.39	3.75	4.33	4.79
7.035	2.40	2.59	2.69	2.79	3.03	3.28	3.74	4.17	4.49	5.09	5.64
8.040	3.06	3.27	3.37	3.48	3.75	4.01	4.45	4.82	5.17	5.86	6.47
9.045	3.78	4.00	4.11	4.22	4.51	4.72	5.10	5.48	5.88	6.63	7.33
10.050	4.57	4.79	4.91	5.03	5.28	5.49	5.90	6.29	6.68	7.44	8.20

**Table B.4: Required amount of stirrups**

Now for a specific experiment the amount of shear reinforcement  $v_s = A_v f_{yv} / b_s$  is known but the strain is not known. So from table B.4 the possible values of  $\theta$  and  $\beta$  for a certain amount of shear reinforcement,  $v_s$ , are found by linear interpolation. The values are shown in table B.5 and B.6. If the amount of stirrups supplied is less than the minimum shear stress then the minimum values for  $\beta$  and  $\theta$  are chosen. For the specific example the shear stress  $v_u / f_c$  has to lie somewhere between 0.075 and 0.1 according to table B.5 and B.6.

min	0	0	0	0	0	0	0	33.7	36.4	40.8	43.9
	0	0	0	0	24.9	27.0	30.6	0	0	0	0
	19.7	21.2	22.0	22.8	0	0	0	0	0	0	0
	0	0	0	0	0	0	0	0	0	0	0
	0	0	0	0	0	0	0	0	0	0	0
	0	0	0	0	0	0	0	0	0	0	0
	0	0	0	0	0	0	0	0	0	0	0
	0	0	0	0	0	0	0	0	0	0	0
final $\theta$	19.7	21.2	22.0	22.8	24.9	27.0	30.6	33.7	36.4	40.8	43.9

**Table B.5: Possible values of  $\theta$**

min	0	0	0	0	0	0	0	0.20	0.19	0.16	0.14
	0	0	0	0	0.24	0.23	0.21	0	0	0	0
	0.27	0.26	0.26	0.26	0	0	0	0	0	0	0
	0	0	0	0	0	0	0	0	0	0	0
	0	0	0	0	0	0	0	0	0	0	0
	0	0	0	0	0	0	0	0	0	0	0
	0	0	0	0	0	0	0	0	0	0	0
	0	0	0	0	0	0	0	0	0	0	0
	0	0	0	0	0	0	0	0	0	0	0
final $\beta$	0.27	0.26	0.26	0.26	0.24	0.23	0.21	0.20	0.19	0.16	0.14

**Table B.6: Possible values of  $\beta$**

Next the shear resistance  $V_u$  is calculated from equation 2.60 for a value of  $\beta$  and its corresponding value of  $\theta$ , for each possible  $\beta$  and its corresponding  $\theta$ , shown in table B.7. The bending moment is calculated for each possibility from the corresponding strain, by rearranging equation 2.61,

$$M = 0.9 \left[ (2\varepsilon_x E_s A_s) - 0.5V_u \cot \theta \right] d$$

The moment,  $M$ , may not exceed the value at which the longitudinal tension steel yields,

$$M_{u,max} = 0.9 \left[ A_s f_y - (V_u + 0.5V_s) \cot \theta_{max} \right] d$$

where  $\theta_{max}$  is the maximum value of  $\theta$  at the maximum strain of 0.002 at which the longitudinal reinforcement is assumed to yield. Therefore  $M_{final}$  is taken as the minimum of  $M$  and  $M_{u,max}$ . The maximum moment to shear ratio ( $M_{final}/V_u$ ) is determined for each strain value.

Variable	-0.2	-0.1	-0.05	0	0.125	0.25	0.5	0.75	1	1.5	2
$V_c$	65.5	63.6	62.6	61.6	58.7	56.4	51.6	48.0	44.8	39.2	33.7
$V_s$	121.5	111.7	107.5	103.1	93.6	85.4	73.5	65.1	58.9	50.3	45.1
$V_c+V_s$	187.0	175.3	170.1	164.7	152.3	141.8	125.1	113.1	103.7	89.5	78.8
$V_u$ (kN)	<b>187.0</b>	<b>175.3</b>	<b>170.1</b>	<b>164.7</b>	<b>152.3</b>	<b>141.8</b>	<b>125.1</b>	<b>113.1</b>	<b>103.7</b>	<b>89.5</b>	<b>78.8</b>
$M$ (kNm)	-74.1	-57.1	-49.2	-41.3	-23.0	-6.1	24.5	52.4	78.9	129.7	178.9
yield $\theta$	43.9	43.9	43.9	43.9	43.9	43.9	43.9	43.9	43.9	43.9	43.9
$M_{u,max}$	88.3	89.8	90.5	91.2	92.9	94.2	96.6	98.3	99.7	101.9	103.7
final $M$	<b>-74.1</b>	<b>-57.1</b>	<b>-49.2</b>	<b>-41.3</b>	<b>-23.0</b>	<b>-6.1</b>	<b>24.5</b>	<b>52.4</b>	<b>78.9</b>	<b>101.9</b>	<b>103.7</b>
$M/V$ (m)	-0.4	-0.3	-0.3	-0.3	-0.2	0.0	0.2	0.5	0.8	1.1	1.3

**Table B.7: Determining  $M/V$  for values of  $\epsilon_x$**

Now the range of possible  $M/V$  ratios is known for this particular example and the correct value of  $V_u$  can be interpolated from table B.7 if  $M_u/V_u$  for the beam example is known. Now the maximum moment to shear ratio of a beam is known even if the loads are not known. For a simply supported beam with a point load a mid-span  $M/V$  equals the  $a/d$  ratio. However AASHTO states the ratio for determining the shear resistance can be taken a distance  $0.9d$  away from the location of the maximum  $M/V$  ratio (or  $0.9d$  away from the load at mid-span), (Angelakos, Benz and Collins, 2001). Therefore the effective  $M/V$  ratio is calculated as  $(a-0.9d)$ .

Finally the ultimate value of shear force,  $V_u$  is found from row 5 and the last row of table 7 by linear interpolation for the effective value of  $M/V$ , which is 0.376 for this example. The corresponding value for  $M_u$  is calculated simply by multiplying  $V_u$  with  $(M/V)_{eff}$ .

$\epsilon_x$	-0.2	-0.1	-0.05	0	0.125	0.25	0.5	0.75	1	1.5	2	-0.2	-0.1
$M_u$	0	0	0	0	0	0	<b>44</b>	0	0	0	0	0	0
$V_u$	0	0	0	0	0	0	<b>116.7</b>	0	0	0	0	0	0

**Table B.8: Interpolation results for  $M_u$  and  $V_u$  for example.**

The beam with properties as shown in table B.1 therefore has a ultimate shear strength as of 117 kN and an ultimate moment capacity of 44 kNm, according to AASHTO. The results as shown have not been factored with the resistance (safety) factor of 0.9 required by AASHTO. Table B.7 can be used to plot a moment shear interaction diagram

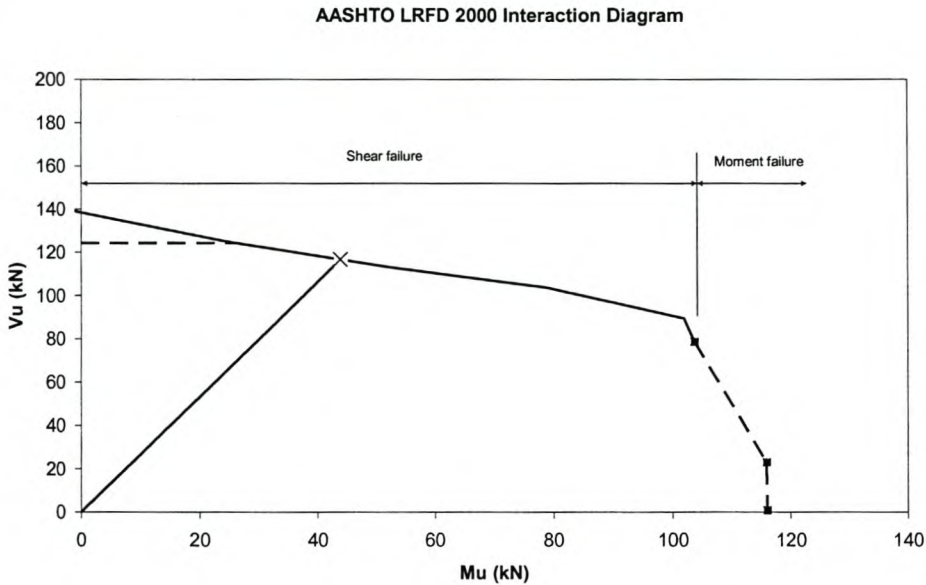


**Figure B.1: Moment Shear interaction for example.**

The dashed line on the right indicates the region for which the longitudinal steel experiences a strain higher than 0.002. Normally it is assumed that the longitudinal steel will have yielded at strains higher than 0.002 but for some steels this is not the case. This line indicates the effect that the shear force has on the moment capacity. As the shear force increases the moment capacity decreases. The AASHTO assumes that the ultimate moment capacity is at a point where the applied shear stress  $V_u$  equals half the stress in the steel  $V_s$  at a strain of 0.002. The dashed line to the right represents a requirement by AASHTO that the  $M$  not be taken more than  $0.9dV$ . The cross on the interaction line indicates the moment to shear ratio for the example.

## B2. Example applying AASHTO LRFD 2000 for members without shear reinforcement

An example of the interpolation technique using MS Excel for AASHTO members without shear reinforcement is shown in this section. The first experiment in the SDB\_WithoutSR Subset 1, by Angelakos, Bentz and Collins, designated DB230 is used for the demonstration.

AASHTO Example		
Material Properties		
$f_c$	32	MPa
$f_{y-long}$	550	MPa
Section Geometry		
$d$	925	mm
$z$	832.5	mm
$b_w$	300	mm
$100A_s/bd$	2.02	%
$agg$	10	mm
$s_{xe}$	1120.7	mm
Loading		
$a/d$	3.02	
$M/V_{eff}$	1.961	m

**Table B.9 – Example: Determining shear resistance with AASHTO LRFD 2000 for members with shear reinforcement**

For members without shear reinforcement the values of  $\beta$  and  $\theta$  are function of the effective crack spacing,  $s_{xe}$ . The crack spacing  $s_x$  is taken equal to the  $0.9d$  (or  $z$ ). However the tables for  $\beta$  and  $\theta$  (Table B.10 and B.11) were derived for 19 mm aggregate. The beam example shown has an aggregate size of 10 mm, so the effective crack spacing is calculated as follows:

$$s_{xe} = \frac{35}{agg + 16} s_x \quad [2.10]$$

Note for the beam example the smaller aggregate size leads to larger crack spacing and hence a lower shear capacity. The effective moment to shear ratio is calculated in the same manner as for members with shear reinforcement.

<b>AASTHO LRFD 2000: Values for <math>\theta</math></b>											
$v/f_c \mid \epsilon_x$	-0.2	-0.1	-0.05	0	0.125	0.25	0.5	0.75	1	1.5	2
127	25.4	25.5	25.9	26.4	27.7	28.9	30.9	32.4	33.7	35.6	37.2
254	27.6	27.6	28.3	29.3	31.6	33.5	36.3	38.4	40.1	42.7	44.7
381	29.5	29.5	29.7	31.1	34.1	36.5	39.9	42.4	44.4	47.4	49.7
508	31.2	31.2	31.2	32.3	36.0	38.8	42.7	45.5	47.6	50.9	53.4
762	34.1	34.1	34.1	34.2	38.9	42.3	46.9	50.1	52.6	56.2	59.0
1016	36.6	36.6	36.6	36.6	41.1	45.0	50.2	53.7	56.3	60.2	63.0
1524	40.8	40.8	40.8	40.8	44.5	49.2	55.1	58.9	61.8	65.8	68.6
2032	44.3	44.3	44.3	44.3	47.1	52.3	58.7	62.8	65.7	69.7	72.4

**Table B.10: Values for  $\theta$**

<b>AASTHO LRFD 2000: Values for <math>\beta</math></b>											
$s_{xe} \mid \epsilon_x$	-0.2	-0.1	-0.05	0	0.125	0.25	0.5	0.75	1	1.5	2
127	0.530	0.505	0.463	0.429	0.368	0.325	0.272	0.239	0.215	0.184	0.163
254	0.481	0.481	0.448	0.408	0.338	0.294	0.240	0.208	0.186	0.157	0.138
381	0.445	0.445	0.439	0.394	0.318	0.273	0.220	0.189	0.168	0.140	0.121
508	0.416	0.416	0.416	0.384	0.304	0.257	0.205	0.174	0.154	0.127	0.109
762	0.371	0.371	0.371	0.370	0.282	0.235	0.183	0.153	0.134	0.108	0.092
1016	0.338	0.338	0.338	0.338	0.266	0.218	0.167	0.138	0.119	0.095	0.079
1524	0.291	0.291	0.291	0.291	0.243	0.194	0.143	0.116	0.099	0.076	0.063
2032	0.258	0.258	0.258	0.258	0.226	0.176	0.127	0.101	0.084	0.064	0.051

**Table B.11: Values for  $\beta$**

$s_{xe} \setminus \epsilon_x$	-0.2	-0.1	-0.05	0	0.125	0.25	0.5	0.75	1	1.5	2
127	127	127	127	127	127	127	127	127	127	127	127
254	254	254	254	254	254	254	254	254	254	254	254
381	381	381	381	381	381	381	381	381	381	381	381
508	508	508	508	508	508	508	508	508	508	508	508
762	762	762	762	762	762	762	762	762	762	762	762
1016	1016	1016	1016	1016	1016	1016	1016	1016	1016	1016	1016
1524	1524	1524	1524	1524	1524	1524	1524	1524	1524	1524	1524
2032	2032	2032	2032	2032	2032	2032	2032	2032	2032	2032	2032

**Table B.12 – Interpolation table for  $s_{xe}$**

min	0	0	0	0	0	0	0	0	0	0	0
	0.0	0.0	0.0	0.0	0.0	0.0	0.0	0.0	0.0	0.0	0.0
	0.0	0.0	0.0	0.0	0.0	0.0	0.0	0.0	0.0	0.0	0.0
	0.0	0.0	0.0	0.0	0.0	0.0	0.0	0.0	0.0	0.0	0.0
	0.0	0.0	0.0	0.0	0.0	0.0	0.0	0.0	0.0	0.0	0.0
	0.0	0.0	0.0	0.0	0.0	0.0	0.0	0.0	0.0	0.0	0.0
	37.5	37.5	37.5	37.5	41.8	45.9	51.2	54.8	57.4	61.3	64.2
	0.0	0.0	0.0	0.0	0.0	0.0	0.0	0.0	0.0	0.0	0.0
	0.0	0.0	0.0	0.0	0.0	0.0	0.0	0.0	0.0	0.0	0.0
final $\theta$	37.5	37.5	37.5	37.5	41.8	45.9	51.2	54.8	57.4	61.3	64.2

**Table B.13: Possible values of  $\theta$**

min	0	0	0	0	0	0	0	0	0	0	0
	0.0	0.0	0.0	0.0	0.0	0.0	0.0	0.0	0.0	0.0	0.0
	0.0	0.0	0.0	0.0	0.0	0.0	0.0	0.0	0.0	0.0	0.0
	0.0	0.0	0.0	0.0	0.0	0.0	0.0	0.0	0.0	0.0	0.0
	0.0	0.0	0.0	0.0	0.0	0.0	0.0	0.0	0.0	0.0	0.0
	0.0	0.0	0.0	0.0	0.0	0.0	0.0	0.0	0.0	0.0	0.0
	0.329	0.329	0.329	0.329	0.262	0.213	0.162	0.134	0.115	0.091	0.076
	0.0	0.0	0.0	0.0	0.0	0.0	0.0	0.0	0.0	0.0	0.0
	0.0	0.0	0.0	0.0	0.0	0.0	0.0	0.0	0.0	0.0	0.0
final $\theta$	37.5	37.5	37.5	37.5	41.8	45.9	51.2	54.8	57.4	61.3	64.2

**Table B.14 - Possible values of  $\beta$**

Variable	-0.2	-0.1	-0.05	0	0.125	0.25	0.5	0.75	1	1.5	2
$V_c$	464.5	464.5	464.5	464.5	369.6	300.9	228.6	188.8	162.4	128.7	107.4
$V_u$ (kN)	<b>464.5</b>	<b>464.5</b>	<b>464.5</b>	<b>464.5</b>	<b>369.6</b>	<b>300.9</b>	<b>228.6</b>	<b>188.8</b>	<b>162.4</b>	<b>128.7</b>	<b>107.4</b>
$M$ (kNm)	-439	-345	-299	-252	-55	112	390	644	889	1369	1843
yield $\theta$	64.2	64.2	64.2	64.2	64.2	64.2	64.2	64.2	64.2	64.2	64.2
$M_{u,max}$	2377	2376.8	2376.8	2376.8	2415.0	2443	2473	2488	2499	2512	2521
final $M$	<b>-438.6</b>	<b>-345.3</b>	<b>-298.7</b>	<b>-252.1</b>	<b>-55.3</b>	<b>111.6</b>	<b>389.6</b>	<b>643.8</b>	<b>889</b>	<b>1369</b>	<b>1843</b>
$M/V$ (m)	-0.9	-0.7	-0.6	-0.5	-0.1	0.4	1.7	3.4	5.5	10.6	17.2

**Table B.15 - Determining  $M/V$  for values of  $\epsilon_x$**

The crack spacing in table B.12 is used to interpolate the possible values of  $\beta$  and  $\theta$  as shown in table B.13 and B.14. After that the shear resistance,  $V_c = \beta\sqrt{f_c}$  (equation 2.9) is calculated for each value of  $\beta$ , as shown in table B.15. As no shear reinforcement is provided,  $V_c$  equals the ultimate force  $V_u$ . The ultimate moment is calculated from the following expression for each value of  $\theta$  from table B.13, (from equation 2.11)

$$M = 0.9 \left[ (\epsilon_x E_s A_s) - 0.5 V_u \cot \theta \right] d$$

Note the equation differs for that of with shear reinforcement, because the strain is calculated at the level of the tension reinforcement instead of using the average strain distribution. The ultimate moment at yielding of the longitudinal reinforcement is calculated from:

$$M_{u,max} = 0.9 \left[ A_s f_y - V_u \cot \theta_{max} \right] d$$

Finally  $V_u$  for the specific example is interpolated from table B.15, with the known  $M/V$  of 1.961. The ultimate shear force is determined to be 221 kN.

$\epsilon_x$	-0.2	-0.1	-0.05	0	0.125	0.25	0.5	0.75	1	1.5	2	-0.2	-0.1
$M_u$	0	0	0	0	0	0	435	0	0	0	0	0	0
$V_u$	0	0	0	0	0	0	221	0	0	0	0	0	0

The shear resistance of the beam was tested at 257 kN. The AASTHO model factor for this experiment is therefore, 1.163.

# Appendix C

## Example: Design example of parameter study from Chapter 5.2.

Design reinforcement steel for beam section at the inner support in Table 5.16 with applied shear stress 2.0 MPa and  $a/d = 6.0$ .

Specifications	
$f_{cu}$ (MPa)	40
$b$ (mm)	200
$d$ (mm)	600
$f_{yv}$ (MPa)	250
$f_y$ (MPa)	450
$A_v$ (mm <sup>2</sup> )	101
$a/d$	6
$L$ (m)	18
$v_{inner\ support}$ (MPa)	2

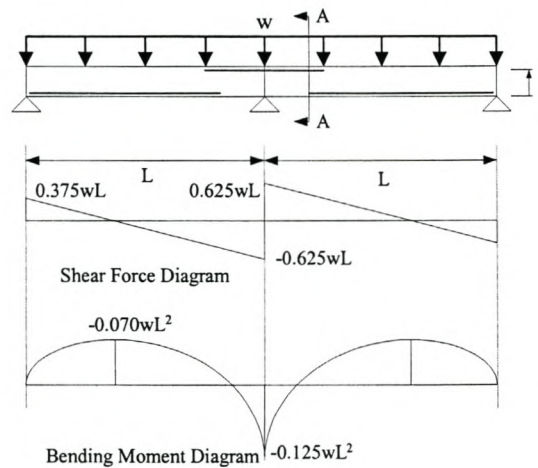


**Table C.1: Nominal design values for beam example**

**Figure C.1: Force diagrams for continuous beam**

### 1. Calculate Forces

$$v_u = v_{inner\_support} = 2.0 \text{ MPa}$$

$$\begin{aligned} \therefore V_{inner\_support} &= v_{inner\_support} bd \\ &= 2 \times 200 \times 600 / 1000 \\ &= 240 \text{ kN} \end{aligned}$$

$$w = \frac{V}{0.625l} = \frac{240}{0.625 \times 18} = 21.33 \text{ kN/m}$$

$$M = 0.125wl^2 = 0.125 \times 21.33 \times 18^2 = 864 \text{ kN/m}$$

**2. Determine required bending steel (SANS 10100-1, clause 4.3.3.4)**

$$K = \frac{M}{bd^2 f_{cu}} = \frac{864 \times 10^6}{200 \times 600^2 \times 40} = 0.3$$

$K > 0.156$   $\therefore$  compression reinforcement is required

$$\therefore z = d \left\{ 0.5 + \sqrt{0.25 - \frac{K'}{0.9}} \right\} = 600 \left\{ 0.5 + \sqrt{0.25 - \frac{0.156}{0.9}} \right\} = 466 \text{ mm}$$

$$A_s' = \frac{(K - K') f_{cu} b d^2}{f_{yc} (d - d')} = \frac{(0.3 - 0.156)(40 \times 200 \times 600^2)}{0.72 \times 450 \times (600 - 20)} = 2207 \text{ mm}^2$$

assuming 20mm cover

$$A_s = \frac{K' f_{cu} b d^2}{0.87 f_y z} + \frac{A_s' f_{yc}}{0.87 f_y} = \frac{0.156 \times 40 \times 200 \times 600^2}{0.87 \times 450 \times 466} + \frac{2207 \times 0.72 \times 450}{0.87 \times 450} = 4288 \text{ mm}^2$$

**3. Check maximum allowable longitudinal reinforcement, SANS 10100-1: Clause 4.11.5.1**

$$\rho_{tension} = \frac{100 A_s}{bd} = \frac{100 \times 4288}{200 \times 600} = 3.6\% < \rho_{max} = 4\%$$

$$\rho_{compression} = \frac{100 A_s'}{bd} = \frac{100 \times 2207}{200 \times 600} = 1.8\% < \rho_{max} = 4\%$$

**4. Design shear reinforcement, SANS 10100-1: Clause 4.3.4**

$$v_c = \frac{0.75}{\gamma_{m,c}} \left( \frac{f_{cu}}{25} \right)^{1/3} \left( \frac{100 A_s}{bd} \right)^{1/3} \left( \frac{400}{d} \right)^{1/4} = \frac{0.75}{1.4} \left( \frac{40}{25} \right)^{1/3} (3.6)^{1/3} \left( \frac{400}{600} \right)^{1/4} = 0.87 \text{ MPa}$$

$$\therefore \frac{100 v_c}{v_u} = \frac{100 \times 0.87}{2} = 43.5\%$$

$$v_s = v_u - v_c = 2.0 - 0.87 = 1.13 \text{ MPa}$$

$$\text{now } v_s = \frac{A_v f_{yv}}{\gamma_{m,s} b s}$$

$$\therefore \frac{A_v}{s} = \frac{\gamma_{m,s} v_s b}{f_{yv}} = \frac{1.15 \times 1.13 \times 200}{250} = 1.04$$

for 8mm stirrups,  $A_v = 101 \text{ mm}^2$

$$\therefore s = 101/1.04 = 97 \text{ mm}$$

### 5. Check for minimum shear reinforcement

$$\text{SANS clause 4.11.4.5.3: } v_{s,\min} = 0.0012 \times \frac{f_{yv}}{\gamma_{m,c}} = 0.26 \text{ MPa}$$

$$\text{Eurocode eqn. 2.58: } v_{s,\min} = 0.08 \sqrt{f_{ck}} = 0.08 \sqrt{40 \times 0.79 / 1.5} = 0.37 \text{ MPa}$$

$$\therefore v_s = 1.13 \text{ MPa} > 0.37 \text{ MPa} > 0.26 \Rightarrow \text{OK}$$